

A functional m⁶A- RNA methylation pathway in the oyster *Crassostrea gigas* assumes epitranscriptomic regulation of lophotrochozoan development

Le Franc Lorane ^{1,2}, Bernay Benoit ³, Petton Bruno ⁴, Since Marc ⁵, Favrel Pascal ^{1,2},
Rivière Guillaume ^{1,2,*}

¹ UNICAEN CNRS BOREA Normandie Univ Caen, France

² Laboratoire Biologie des organismes et Ecosystèmes aquatiques (BOREA) Muséum d'Histoire naturelle CNRS IRD Sorbonne Université, Université de Caen Normandie Université des Antilles Caen, France

³ UNICAEN, ICOREPROTEOGEN Core Facility Caen SF, France

⁴ Ifremer, Laboratoire des Sciences de l'Environnement Marin UMR 6539 CNRS/UBO/IRD/Ifremer Centre Bretagne Normandie Univ Plouzané, France

⁵ UNICAEN, Comprehensive Cancer Center F. Baclesse, SF ICORE PRISMM Core Facility Normandie Univ Caen, France

* Corresponding author : Guillaume Rivière, email address : guillaume.riviere@unicaen.fr

Abstract :

N⁶-methyladenosine (m⁶A) is a prevalent epitranscriptomic mark in eukaryotic RNA, with crucial roles for mammalian and ecdysozoan development. Indeed, m⁶A-RNA and the related protein machinery are important for splicing, translation, maternal-to-zygotic transition and cell differentiation. However, to date, the presence of an m⁶A-RNA pathway remains unknown in more distant animals, questioning the evolution and significance of the epitranscriptomic regulation. Therefore, we investigated the m⁶A-RNA pathway in the oyster *Crassostrea gigas*, a lophotrochozoan model whose development was demonstrated under strong epigenetic influence. Using mass spectrometry and dot blot assays, we demonstrated that m⁶A-RNA is actually present in the oyster and displays variations throughout early oyster development, with the lowest levels at the end of cleavage. In parallel, by in silico analyses, we were able to characterize at the molecular level a complete and conserved putative m⁶A machinery. The expression levels of the identified putative m⁶A writers, erasers and readers were strongly regulated across oyster development. Finally, RNA pull-down coupled to LC-MS/MS allowed us to prove the actual presence of readers able to bind m⁶A-RNA and exhibiting specific developmental patterns. Altogether, our results demonstrate the conservation of a complete m⁶A-RNA pathway in the oyster and strongly suggest its implication in early developmental processes including MZT. This first demonstration and characterization of an epitranscriptomic regulation in a lophotrochozoan model, potentially involved in the embryogenesis, bring new insights into our understanding of developmental epigenetic processes and their evolution.

Keywords : development, epitranscriptomics, methylation, oyster, RNA

Abbreviations

*N*⁶-methyladenosine (m⁶A), Methyltransferase like (METTL), Wilms' tumor 1-associated protein (WTAP), RNA-binding motif 15 (RBM15), Ring finger E3 ubiquitin ligase (HAKAI), Zinc finger CCCH-type containing 13 (ZC3H13), AlkB homologue 5 (ALKBH5), Fat mass and obesity associated protein (FTO), YTH domain family protein (YTHDF), YTH domain containing protein (YTHDC), Heterogeneous nuclear ribonucleoproteins A2 B1 (HNRNPA2B1), Proline rich coiled-coil 2a (Prcc2a), Eukaryotic initiation factor 3 (eIF3), Sterile sea water (SSW), Oocytes (E), Fertilized oocytes (F E), Two to eight cell embryos (2/8 C), Hours post fertilization (hpf), Morula (M), Blastula (B), Gastrula (G), D larvae (D), solid-phase reversible immobilization (SPRI), TPM (Transcripts Per Million), Gene ontology (GO), oyster m⁶A-interacting protein (Cg-m⁶A-BPs), S-adenosyl-methionine (SAM), maternal-to-zygotic transition (MZT), acetonitrile (ACN)

66 Introduction

67
68 The *N*⁶-methyladenosine (m⁶A) is the prevalent chemical RNA modification in all eukaryotic
69 coding and non-coding RNAs [1]. Messenger RNAs are the most heavily m⁶A methylated
70 RNAs, with m⁶A bases lying mostly in their 3' UTRs, at the vicinity of their stop codon [2–4]
71 and also in 5' UTRs and long internal exons [4,5]. *N*⁶-methylation of RNA adenosines is
72 responsible for RNA processing and, like DNA methylation or histone modifications,
73 contributes to the regulation of gene expression without changing the DNA or mRNA
74 sequence. Therefore m⁶A constitutes a new layer of post-transcriptional gene regulation, which
75 is emerging or has been proven critical in various biological processes, and referred to as
76 epitranscriptomic [2].

77
78 The dynamics and biological outcomes of m⁶A levels are the results of the activity of a complex
79 protein machinery comprising writers, erasers and readers. The addition of a methyl group to
80 the 6th nitrogen of RNA adenosines is catalysed by m⁶A writers with distinct properties.
81 Methyltransferase like 16 (METTL16) is a 'stand-alone' class I methyltransferase that
82 recognizes the UACA*GAGAA consensus sequence (with * indicating the target adenosine)
83 [6]. By contrast, METTL3 transfers methyl groups to adenosines within the RRA*CH motif
84 [2,3,7]. METTL3 is only active within a tripartite 'core complex' [8] comprising METTL3,
85 METTL14 which enhances the methyltransferase activity supported by the MTA-70 domain of
86 METTL3 [9,10] and the regulator protein Wilms' tumor 1-associated protein (WTAP) [4,9,11].
87 This core complex can interact with Virilizer-like (or KIAA1429) [12], ring finger E3 ubiquitin

1
2
3 88 ligase (HAKAI) [12,13], zinc finger CCCH-type containing 13 (ZC3H13) [12,14], RNA-binding
4
5
6 89 motif 15 (RBM15) and RBM15B [7,15] which are suspected to intervene in the core complex
7
8
9 90 activity and target specificity. The demethylation of adenosines has been demonstrated to be
10
11 91 an active process catalysed by eraser enzymes belonging to the Fe(II)/2-oxoglutarate
12
13 92 dioxygenase family: AlkB homologue 5 (ALKBH5) [16,17] and the fat mass and obesity
14
15 93 associated protein (FTO) [17,18].

16
17
18
19 94 A growing number of reader proteins which recognize the m⁶A-RNA mark is being described.
20
21 95 They may be divided into two classes depending on the presence of a YTH domain
22
23 96 (YTH) domain in their primary sequence. The YTH protein family includes YTH domain family
24
25 97 protein 1-3 (YTHDF1-3) and YTH domain containing protein 2 (YTHDC2), which are cytosolic
26
27 98 m⁶A readers involved in m⁶A-RNA stability and translation [19–22]. The fifth YTH member is
28
29
30
31
32 99 YTHDC1, which is present in the nucleus and controls splicing [23] and nuclear export [24] of
33
34
35 100 m⁶A-RNA. The second class of readers comprises proteins without YTH domain which are
36
37 101 involved in several molecular mechanisms. For example, the heterogeneous nuclear
38
39 102 ribonucleoprotein A2 B1 (HNRNPA2B1) is important for miRNA processing [25]. Insulin-like
40
41
42 103 growth factor 2 mRNA binding protein 1-3 (IGF2BP 1-3) [26] and proline-rich coiled-coil 2a
43
44 104 (Prcc2a) [27] participate in RNA stability while eukaryotic initiation factor 3 (eIF3) guides cap-
45
46
47 105 independent translation [5].

48
49
50 106
51
52
53 107 The m⁶A epitranscriptomes underlie important biological functions, most of which being related
54
55 108 to developmental processes, including the control of cell differentiation [27–32], maternal to
56
57
58 109 zygotic transition (MZT) [33], sex determination [7,34] and gametogenesis [16,21,35,36]. Such
59
60

1
2
3 110 critical epitranscriptomic outcomes are conserved in the animal evolution and were
4
5
6 111 characterized in both vertebrates and ecdysozoans, i.e. mammals and drosophila.

7
8 112 However, such conserved biological significance originates in diverse epitranscriptomic
9
10
11 113 mechanisms. Indeed, not all ecdysozoans bear a complete m⁶A-RNA machinery, such as *C.*
12
13 114 *elegans* whose genome is devoid of the related protein machinery with the exception of a
14
15
16 115 putative orthologue of METTL16 [37,38]. In addition, no m⁶A eraser has been described to
17
18
19 116 date in non-vertebrate models, and especially ecdysozoans such as the drosophila or *C.*
20
21 117 *elegans* [38–40], where it cannot be excluded that m⁶A-RNA methylation could be removed by
22
23
24 118 the activity of characterised 6mA-DNA demethylases [41,42]. This situation may illustrate a
25
26
27 119 growing complexity of epitranscriptomic mechanisms during the animal phylogeny and raises
28
29
30 120 fundamental questions about its evolution and its presence in organisms distant from
31
32 121 mammals and ecdysozoans. However, to date, no data about a possible epitranscriptomic
33
34
35 122 regulation is available to our knowledge in lophotrochozoans, the understudied sister group of
36
37 123 ecdysozoans within protostomes, although representing an important range of metazoan
38
39
40 124 biodiversity.

41
42
43 125 The Pacific oyster *Crassostrea gigas* (i.e. *Magallana gigas*) is a bivalve mollusc whose great
44
45 126 ecological and economical significance allowed its emergence as a model species within
46
47
48 127 lophotrochozoan organisms. As such, an important amount of genetic, transcriptomic and
49
50
51 128 epigenetic data have been generated in this model. Interestingly, the embryolarval
52
53 129 development of *C. gigas* is described to be under the strong epigenetic influence of DNA
54
55
56 130 methylation [43–47] and histone marks [48–50]. Besides, oyster development occurs exposed
57
58
59 131 to external environmental conditions, and in other models the m⁶A methylation of RNA and/or
60

1
2
3 132 the expression of its machinery can be induced by heat stress, UV exposure or endocrine
4
5
6 133 disruptors [5,51–54], questioning the presence of an m⁶A pathway in *C. gigas* and its
7
8 134 significance in oyster early development.

9
10
11 135 To investigate this, we measured m⁶A levels in RNA across the entire embryolarval life of the
12
13 136 oyster using mass spectrometry and dot-blot. We also searched the available *in silico*
14
15 137 resources for putative conserved m⁶A-related proteins in *C. gigas* genomic data as well as
16
17 138 their cognate expression kinetics using RNAseq assembly analyses. We also performed RNA-
18
19 139 pull-down with a synthetic m⁶A-RNA oligonucleotide coupled to liquid chromatography and
20
21 140 mass spectrometry (LC-MS/MS) to characterize potential oyster m⁶A-binding proteins. To our
22
23 141 knowledge, this study is the first report unravelling epitranscriptomic mechanisms outside
24
25 142 vertebrate and ecdysozoan animal models.
26
27
28
29
30
31

32 143

33 34 35 144 **Results:**

36
37
38 145

39
40
41 146 **m⁶A is present in oyster RNA, differentially affects distinct RNA populations and**
42
43 147 **displays variations during embryonic life.**

44
45
46 148 Mass spectrometry measurements revealed that m⁶A is present in oyster RNA, with global
47
48 149 m⁶A/A levels of ca. 0.3%, a value comparable to what has been found in the human and the
49
50 150 fruit fly (Figure 1A). Immunoblot assays indicate that total and polyA+ RNA present variable
51
52 151 amounts of m⁶A during oyster development and that these variations display distinct profiles
53
54 152 suggesting specific methylation patterns between RNA populations. Indeed, N⁶A-methylation
55
56 153 in total RNA is the highest in the early stages (oocytes and fertilized oocytes) then gradually
57
58
59
60

1
2
3 154 decreases until the morula stage before gradually increasing again up to the trochophore stage
4
5
6 155 when it recovers its maximum (Figure 1B). In contrast, m⁶A levels in polyA⁺ RNA are hardly
7
8 156 detected in early stages but display a peak in the gastrula and trochophore stages (Figure 1C).
9

10
11 157

12
13
14 158 **m⁶A machinery is conserved at the molecular level in the oyster.**

15
16 159 *In silico* analyses led to the identification of oyster sequences encoding putative orthologues
17
18
19 160 of m⁶A writers, erasers and readers that are present in the human and/or in the human and
20
21 161 the fruit fly.

22
23
24 162 All the eight m⁶A-RNA writers characterized in the human and/or drosophila at the time of the
25
26
27 163 study, namely METTL3, METTL14, WTAP, Virilizer-like, HAKAI, ZC3H13, RBM15/15B and
28
29
30 164 METTL16, were present in the oyster at the gene level. The encoded protein primary
31
32 165 sequences all display the specific domains required for enzymatic activity and/or binding. They
33
34
35 166 include MT-A70 and AdoMetMtases SF domains for METTL3, METTL14 and METTL16,
36
37 167 respectively, that bear the methyltransferase activity. Oyster WTAP and Virilizer-like
38
39
40 168 orthologues exhibit WTAP and VIR_N domains, respectively, that are required in their human
41
42
43 169 counterparts to bind and activate the catalytic subunit of the m⁶A-RNA methyltransferase
44
45
46 170 complex. Oyster Hakai and RBM15/15B present RHHL, RHF-Zn-BS and specific RRM
47
48 171 domains, respectively, similar to human and fruit fly orthologues. Besides, the oyster ZC3H13
49
50
51 172 bears the Rho SF domain present in the human, but not in the fruit fly orthologue (Figure 2A).
52
53 173 *C. gigas* also presents a putative m⁶A-RNA eraser, ALKBH5, which is present in the human
54
55
56 174 but has not been characterized in drosophila. The oyster ALKBH5 exhibits a 2OG-FeII_Oxy
57
58
59 175 domain suggestive of a presumably conserved catalytic functionality through fe²⁺-dependent
60

1
2
3 176 oxoglutarate oxidation. Of note, no orthologue of the human FTO eraser could be identified in
4
5
6 177 the oyster genomic or transcriptomic databases available to date (Figure 2B).

7
8 178 Many m⁶A reader orthologues have also been found in the oyster, including proteins containing
9
10
11 179 a YTH domain, such as YTHDF, YTHDC1 and YTHDC2. An oyster Prrc2a-like protein
12
13
14 180 produces homology with the human Prrc2a, especially within the m⁶A-binding GRE-rich
15
16
17 181 domain. Oyster readers also include a heterogeneous nuclear ribonucleoprotein-coding gene,
18
19 182 hnRNPA2B1 with greater sequence similarity with the drosophila counterpart than with the
20
21
22 183 human orthologue. Similarly, the IGF2BP-coding sequence has also been found in *C. gigas*
23
24 184 (Figure 2C). Five oyster sequences display homologies with eIF3a which is able to bind m⁶A-
25
26
27 185 RNA [5] but it was not possible to discriminate whether a unique oyster predicted protein was
28
29
30 186 an eIF3a orthologue.

31
32 187 Overall, these results indicate the conservation of a complete m⁶A-RNA machinery in the
33
34
35 188 oyster. The complete list of the identified genes encoding the conserved m⁶A machinery actors
36
37
38 189 and their isoforms, as well as the related information is given in the supplementary data (Data
39
40 190 S1).

41
42
43 191

44 45 192 **Oyster putative m⁶A actors display expression level variations across development.**

46
47
48 193 RNAseq data analyses showed that all the oyster m⁶A-related genes were expressed during
49
50
51 194 the early life (Figure 3). Their expression level displayed gene-specific profiles, most of them
52
53
54 195 being variable throughout oyster development.

55
56 196 The expression of writers belonging to the core methylation complex is weak overall. METTL3
57
58
59 197 and WTAP share similar profiles with little expression increasing up to the gastrulation and
60

1
2
3 198 remaining stable afterwards. In contrast METTL14 displays a weak expression level across
4
5
6 199 the embryo larval life. The expression profile of Virilizer-like resembles WTAP, while HAKAI,
7
8 200 RBM15/15B and METTL16 seem to have mRNA levels which decrease after cleavage,
9
10
11 201 whereas those of ZC3H13 transcript variants seem to drop at the D larva stage. Interestingly,
12
13
14 202 METTL16 mRNA levels display an opposite developmental profile when compared to METTL3
15
16 203 expression; with the highest values during cleavage which decrease later on (Figure 3A).
17
18
19 204 ALKBH5 transcripts are weakly represented within oyster early embryos and the higher TPM
20
21 205 values are found in gastrulas. However, maximum levels are observed after metamorphosis in
22
23
24 206 juveniles (Figure 3B).
25
26
27 207 Regarding m⁶A putative readers, the expression of YTH family genes during development
28
29 208 showed different patterns. In fact, YTHDF is the most represented YTH-domain bearing actor
30
31 209 and YTHDF TPM values are ca. 5-fold higher than all the other oyster YTH readers. YTHDF is
32
33
34 210 strongly expressed at the beginning of development until a peak at the morula stage. Prrc2a
35
36
37 211 is the most represented reader at the mRNA level in oyster embryos, and the sum of the TPM
38
39
40 212 of the two Prrc2a oyster isoforms are at most ca. 20-fold higher than those of YTH family.
41
42
43 213 However, Prrc2a and YTHDF transcript content profiles are similar across oyster development,
44
45
46 214 and also remind of the IGF2BP mRNA levels.
47
48
49 215 By contrast, the two isoforms of YTHDC1 identified by *in silico* analysis, YTHDC1.1 and
50
51 216 YTHDC1.2, display similar patterns together with YTHDC2, with a maximum representation in
52
53
54 217 gastrulas. The expression of hnRNPA2B1 isoforms has likewise patterns except for a marked
55
56 218 drop at the D larvae stage (Figure 3 C).
57
58
59 219
60

1
2
3 **220 Oyster orthologues of m⁶A-RNA interacting proteins bind m⁶A RNA *in vitro*.**
4

5
6 221 To determine whether oyster proteins can bind m⁶A-RNA, we performed RNA-pulldown of
7
8 222 cytoplasmic and nuclear embryonic cell extracts using a methylated versus a non-methylated
9
10
11 223 oligonucleotide, followed by LC/MS-MS characterisation and identification of the captured
12
13
14 224 proteins with the Mascot software.
15

16 225 In nuclear extracts, we detected 591 proteins able to bind both the methylated and
17
18 226 unmethylated oligos. We identified 43 proteins specific to unmethylated RNA while 131
19
20
21 227 proteins specifically bind the m⁶A-methylated oligo. In cytosolic extracts, there were
22
23
24 228 respectively 646, 436 and 36 of such proteins, respectively. Regardless of the methylation
25
26
27 229 status, more proteins in the cytoplasmic extracts can bind to the RNA oligonucleotides than in
28
29
30 230 the nuclear extracts (1118 proteins vs. 765, respectively). However, more nuclear proteins are
31
32 231 found exclusively bound to the m⁶A-containing oligo than cytoplasmic proteins (131 vs. 36, i.e.
33
34 232 17 % vs. 3 %, respectively). In addition, many nuclear and cytoplasmic proteins can bind both
35
36
37 233 the methylated and the non-methylated oligo (591 vs. 646, i.e. 77 % vs. 58 %). An important
38
39
40 234 number of proteins in the cytoplasmic extract were found exclusively bound to the non-
41
42
43 235 methylated oligo, whereas only a limited number of nuclear proteins display such a specificity
44
45 236 (436 vs. 43, i.e. 39 % vs. 6 %). Among the 167 m⁶A-specific proteins in oyster extracts, only 5
46
47
48 237 were found in both the nuclear and cytoplasmic extracts. These results show that oyster
49
50
51 238 proteins can directly or indirectly bind m⁶A-RNA, and suggest an important
52
53
54 239 compartmentalization of m⁶A-related processes.
55

56 240 Among the identified proteins in this assay, four of the putative oyster m⁶A readers are found,
57
58 241 YTHDC1, hnRNPA2B1, IGF2BP and eIF3. In the nuclear extracts YTHDC1 is uncovered as
59
60

1
2
3 242 m⁶A-specific whereas hnRNPA2B1 and IGF2BP were present complexed with both the m⁶A-
4
5
6 243 and A-oligos. In the cytoplasmic extracts, YTHDC1 and eIF3a are m⁶A-specific while
7
8 244 hnRNPA2B1, IGF2BP were pulled down by both methylated and unmethylated oligos (Figure
9
10
11 245 4A).

12
13 246 These results demonstrate that some proteins in the oyster can specifically bind m⁶A-RNA and
14
15
16 247 that the putative m⁶A reader orthologues in the oyster are conserved at the protein level and
17
18
19 248 are able to interact with m⁶A-RNA.

20
21
22 249

23
24 250 **The m⁶A-interacting protein-coding genes display clustered expression regulation and**
25
26
27 251 **functional annotation during oyster development.**

28
29 252 The mRNA expression level of the genes encoding the 162 oyster m⁶A-interacting protein (Cg-
30
31
32 253 m⁶A-BPs) was examined using RNAseq databases. Most of them display a specific and
33
34
35 254 regulated expression level across oyster developmental stages. However, three main
36
37
38 255 expression clusters could be distinguished according to their developmental mRNA expression
39
40
41 256 level profile. Cluster 1 includes genes that show high expression at the beginning of the embryo
42
43
44 257 life (i.e. cleavage) and strongly decrease after gastrulation; the second cluster contains weakly
45
46
47 258 expressed genes except in the latest examined larval phases, after gastrulation (i.e.
48
49
50 259 Trochophore and D Larvae); cluster 3 groups genes that show an expression peak during
51
52
53 260 gastrulation (Figure 4B).

54
55
56 261 The Gene Ontology annotation of the Cg-m⁶A-BP genes reveal that the distinct clusters are
57
58
59 262 related to distinct functional pathways as indicated by the little - if any - common GO terms
60
263 between them (Figure 4C). However, the functional pathways of all three gene clusters point

1
2
3 264 out to their implication in translation and its regulation, although the terms enriched in each
4
5
6 265 cluster illustrate different aspects of translation, such as translation initiation (cluster 1), splicing
7
8 266 and nuclear export (cluster 2) and ribosomal and mitochondrial processes (cluster 3)
9
10
11 267 respectively (Figure 4D).
12

13
14 26815
16 269 **Discussion**
17
18
19

20 270 This work demonstrates that m⁶A-RNA is present and variable during the embryo-larval life of
21
22
23 271 the oyster, and that *C. gigas* exhibits putative conserved and functional m⁶A-RNA writers,
24
25
26 272 eraser and readers. The dynamics of such mark and of its actors strongly suggest a biological
27
28 273 significance of the epitranscriptomic pathway in the control of development of a
29
30
31 274 lophotrochozoan species, which has, to date, never been demonstrated to our knowledge.
32

33
34 275 **m⁶A-RNA levels vary across oyster development.**
35

36 276 Using mass spectrometry and immunological measurements, we showed that oyster RNA is
37
38
39 277 m⁶A-methylated. The global proportion of N⁶-methyladenosine in RNA in the developing oyster
40
41
42 278 (0.28 %) is similar to those observed elsewhere in the animal kingdom, such as in the fruit fly
43
44 279 (0.24 %) [34] or the human (0.11- 0.23 %) [55] (Figure 1A), despite those values are difficult
45
46
47 280 to compare because they were not measured within the same developmental phase (adult flies
48
49 281 and human cell lines vs. oyster embryos). However, the comparable magnitude of m⁶A-RNA
50
51
52 282 amounts between taxa, in contrast to DNA methylation [46], may indicate conserved biological
53
54
55 283 significance of epitranscriptomic processes between groups. The amount of m⁶A in total RNA
56
57 284 displays a striking decrease during cleavage and then recovers its maximum levels at the end
58
59
60 285 of the gastrulation (Figure 1B). Therefore, the m⁶A decrease in total RNA during cleavage, i.e.

1
2
3 286 before the transcription of the zygotic genome starts, reflects a degradation of maternal m⁶A-
4
5
6 287 RNAs or their demethylation. However, all RNA populations do not exhibit the same pattern,
7
8 288 indeed polyA⁺ RNAs are m⁶A methylated only after cleavage. The extent of polyadenylation
9
10
11 289 of oyster maternal messenger RNAs accumulating during vitellogenesis is unknown.
12
13
14 290 Therefore, which maternal RNA population(s) is methylated in oyster oocytes is unclear.
15
16 291 Nevertheless, the observation that m⁶A-RNA levels are variable and affecting distinct RNA
17
18
19 292 populations across embryonic stages strongly favours an important biological significance of
20
21
22 293 m⁶A-RNA in oyster development. We hypothesize that oyster maternal messenger RNAs are
23
24 294 poorly polyadenylated, and that m⁶A, aside polyadenylation, might play a role in the stability of
25
26
27 295 quiescent maternal mRNAs. Alternatively, other maternal RNA populations such as snRNA,
28
29
30 296 miRNA, rRNA or lncRNA might be methylated [6,15,25,56], which become demethylated or
31
32 297 degraded up to the morula stage. The later increase in m⁶A RNA after cleavage could therefore
33
34
35 298 be the result of the methylation of the increasingly transcribed RNAs from the blastula stage,
36
37 299 including polyadenylated mRNAs.

38
39
40 300 **The m⁶A-RNA machinery is conserved in the oyster and regulated during development.**

41
42 301 The important regulation of m⁶A levels during oyster development assumes the presence of a
43
44
45 302 related protein machinery. We identified *in silico* cDNA sequences encoding conserved
46
47
48 303 putatively functional orthologues of m⁶A-RNA writers, eraser and readers in the oyster, with
49
50
51 304 great confidence (homologies ranging from ca. 30 to 65 % with their human counterpart, see
52
53
54 305 Data S1). The writers include all the members of the methylation complex (METTL3, METTL14,
55
56 306 WTAP, Virilizer-like, Hakai, ZC3H13, RBM15/15B) identified to date in the human and the fruit
57
58 307 fly [7,11,12,14,15,57]. We also identified an orthologue of the stand-alone METTL16 m⁶A
59
60

1
2
3 308 methyltransferase. Each orthologue bears the conserved domain(s) demonstrated to be
4
5
6 309 implicated in the catalytic and/or binding activity of their cognate counterpart in other species,
7
8
9 310 such as the MT-A70 domain which transfers methyl groups from the S-adenosyl-methionine
10
11 311 (SAM) to the N^6 nitrogen of RNA adenines [57]. Of the two proteins that can erase RNA
12
13
14 312 methylation, only ALKBH5, which is important for mouse spermatogenesis [16], was identified
15
16 313 at the cDNA level in the oyster. Indeed, no *C. gigas* sequence displayed significant homology
17
18
19 314 with the mammalian FTO protein, whose functional significance remains controversial [17].
20
21
22 315 Most the characterized m⁶A-RNA readers are also present at the molecular level in the oyster
23
24 316 and are putatively able to bind m⁶A regarding their primary sequence, such as the YTHDC and
25
26
27 317 YTHDF family members [19,21,23,58], Prrc2A [27], HnRNPA2B1 [25] and IGF2BP [26]. Of
28
29
30 318 note, some of these readers have not been characterized to date in *D. melanogaster* but
31
32 319 display strong homologies between humans and oysters. In mammals, eIF3a has important
33
34
35 320 functional outcomes in cap-independent translational stress response [5]. However, it was not
36
37
38 321 possible to ascribe a single oyster sequence as a unique eIF3a orthologue (Data S1), although
39
40 322 its presence was demonstrated by RNA pull down (see below) (see Data S2). Altogether, *in*
41
42
43 323 *silico* results show the conservation of a complete m⁶A-RNA machinery in the oyster. To date
44
45 324 to our knowledge, this is the first demonstration in a lophotrochozoan organism of an
46
47
48 325 epitranscriptomic pathway. Its presence suggests its ancestral origin, and questions its
49
50
51 326 biological significance in oyster development.
52
53 327 To investigate this, we analysed the expression level of the m⁶A machinery genes using RNA-
54
55
56 328 seq data. Our results indicate that the core methylation complex (METTL3, METTL14 and
57
58
59 329 WTAP) would not be active during cleavage because of the absence of METTL3 and little
60

1
2
3 330 WTAP expression. METTL16 catalyses the downregulation of SAM methyl donor availability
4
5
6 331 in mammals [59]. If METTL16 function is conserved in the oyster as suggested by the high
7
8 332 sequence homology, the peak in METTL16 expression, together with the weak expression of
9
10
11 333 the core complex in 2/8 cell embryos is consistent with an absence of m⁶A-RNA up to the
12
13
14 334 blastula stage. Then, the core complex would likely be active as soon as the end of cleavage
15
16 335 (i.e. since the blastula stage), in line with the increase in m⁶A levels observed at the same time.
17
18
19 336 The correlation between the increasing METTL3 expression and m⁶A-RNA levels after
20
21 337 cleavage strongly favours the conservation of the methyltransferase activity of the oyster MT-
22
23
24 338 A70 domain. Interpreting the regulation of the m⁶A activity by the other methyltransferase
25
26 339 complex members (i.e. Virilizer-like, HAKAI, ZC3H13 and RBM15/15B) is difficult because how
27
28 340 - or even if - oyster orthologues act within the complex is not known. Nevertheless, their specific
29
30 341 expression profiles may reflect their implication in the regulation of distinct biological contexts.
31
32
33 342 There might be little functional significance of active m⁶A-RNA erasure during oyster
34
35 343 development, consistent with the normal embryonic phenotype of ALKBH5 knockdown mice
36
37
38 344 [16]. Overall, the m⁶A readers display distinct developmental expression patterns. While
39
40 345 YTHDF and Prrc2a peak during cleavage, YTHDC1, YTHDC2, IGF2BP and hnRNPA2B1
41
42
43 346 mRNA levels gradually increase up to the gastrulation and remain mostly highly expressed
44
45
46 347 afterwards (except for hnRNPA2B1 and IGF2BP). These profiles evoke the mediation of
47
48
49 348 distinct biological functions depending on the reader and the developmental phases.
50
51
52 349 Therefore, we hypothesized that YTHDF and Prrc2a might participate in the blastulean
53
54
55 350 transition in the oyster. Indeed, in the zebrafish, a YTHDF reader triggers the maternal-to-
56
57
58 351 zygotic transition through the decay of the maternal m⁶A RNAs during cleavage [33]. The role
59
60

1
2
3 352 in the axon myelination and specification of mouse oligodendrocytes [27] is unlikely conserved
4
5
6 353 for *Prrc2a* because the oyster orthologue is expressed before the neurogenesis is detected in
7
8 354 trochophore stages [60]. Alternatively, the early expression of *Prrc2a* suggests that it might
9
10
11 355 rather compete with YTHDF for m⁶A-RNA targets [27], thereby possibly acting in oyster MZT,
12
13
14 356 bringing new perspectives into this process which remains poorly understood in
15
16 357 lophotrochozoans. In mammals m⁶A is implicated in the embryonic cell fate [30,31] notably via
17
18
19 358 the regulation of cell differentiation by YTHDC2 [32] or hnRNPA2B1 [29]. In the oyster,
20
21
22 359 YTHDC1, YTHDC2, IGF2BP and hnRNPA2B1 have their maximum expression during
23
24 360 gastrulation correlated to the second m⁶A peak, suggesting similar implications.

25
26
27 361 **Putative oyster m⁶A readers actually bind m⁶A-RNA *in vitro*.**

28
29 362 To better approach the developmental processes involving m⁶A in the oyster, we characterized
30
31
32 363 the proteins that can interact with m⁶A-RNA using a methylated-RNA-pulldown / mass
33
34
35 364 spectrometry assay. We identified 162 proteins able to specifically bind the m⁶A-RNA oligo in
36
37
38 365 embryonic cell extracts, demonstrating the actual presence of genuine m⁶A-readers in the
39
40
41 366 oyster. Most (ca. 75 %) of these proteins were found in nuclear extracts and only 5 were found
42
43
44 367 in both the cytoplasmic and nuclear fractions, showing an important compartmentalization of
45
46
47 368 the epitranscriptomic pathway. Regarding the little number of m⁶A readers in other animals,
48
49
50 369 and because the assay conditions do not discriminate between direct and indirect interactions,
51
52
53 370 we hypothesize that most these proteins indirectly bind m⁶A via a limited number of 'scaffold'
54
55
56 371 m⁶A readers. Such authentic readers that only bind the m⁶A-RNA oligo in our assay likely
57
58
59 372 include YTHDC1 and eIF3a, which have been demonstrated to directly bind m⁶A in other
60
373 species, demonstrating the conservation of the m⁶A-binding capacity and specificity of the YTH

1
2
3 374 domain in the oyster. Besides, YTHDC1 is found in both cell fractions, suggesting its
4
5
6 375 implication in the trafficking of m⁶A-RNA across the nuclear envelope [24], and reinforcing the
7
8 376 hypothesis that YTH proteins could participate in oyster MZT and cell differentiation. The
9
10
11 377 presence of the oyster eIF3a in the cytoplasm is consistent with a conserved role in m⁶A-
12
13
14 378 mediated translation processes, such as cap-independent translation [5].

15
16 379 **Possible functions of m⁶A-RNA in oyster development.**
17
18

19 380 We investigated the expression level and the functional annotation of the 162 genes encoding
20
21 381 the m⁶A-interacting proteins across oyster early life. These genes can be clustered into three
22
23
24 382 successive expression phases corresponding to three distinct functional pathways, which are
25
26
27 383 independent albeit all mostly related to translation regulation. The cluster 1 is mostly expressed
28
29 384 during the cleavage and the associated GO terms are related to the initiation of translation,
30
31
32 385 consistent with maternal RNA consumption before MZT is complete and the zygotic genome
33
34
35 386 becomes fully activated. The genes within cluster 3 show an expression peak during
36
37 387 gastrulation. Their ontology terms evoke ribosomal and mitochondrial processes, the latter
38
39
40 388 being required for energy supply and signalling integration during gastrulation [61–64]. The
41
42
43 389 cluster 2 contains genes that peak after gastrulation and which are related to splicing and
44
45
46 390 nuclear export. Such functional annotations are in line with a fine regulation of transcript variant
47
48 391 translation within the distinct cell lineages in the three cell layers of the late embryos.

49
50 392

51
52
53 393 Taken together, our findings bring to light a possible implication of m⁶A in oyster development.

54
55
56 394 First, during cleavage the decrease of m⁶A-RNA, the weak expression of methyltransferase
57
58 395 complex genes, the maximum of YTHDF gene expression and the expression of Cg-m⁶A-BPs
59
60

1
2
3 396 related to the initiation of the translation strongly suggest the implication of m⁶A in MZT in *C.*
4
5
6 397 *gigas*. Second, the increasing m⁶A level during gastrula stage is correlated to the increase of
7
8 398 methyltransferase complex gene expression. In addition, the increased RNA level of readers
9
10
11 399 putatively related to cell differentiation and the peak of gene expression of Cg-m⁶A-BPs
12
13 400 associated to ribosomal and mitochondrial processes, support the hypothesize of a m⁶A
14
15
16 401 implication in gastrulation. Finally, the highest m⁶A level at the trochophore stage, the gene
17
18
19 402 expression of the methyltransferase complex and of readers associated to cell differentiation,
20
21
22 403 as well as high RNA level of Cg-m⁶A-BPs related to splicing and nuclear export is correlated
23
24 404 with the fine cell differentiation taking place at this stage. However, inferring the biological
25
26
27 405 significance of m⁶A in development from the indirect and incomplete functional annotation of
28
29
30 406 the oyster genome is only limited. Characterization of the precise targets of m⁶A and how their
31
32
33 407 individual methylation is regulated across development, for example using high throughput
34
35
36 408 sequencing of precipitated m⁶A-RNA (MeRIP-seq), could be extremely relevant to better
37
38 409 understand this issue. In addition, despite sequence conservation and binding ability of oyster
39
40 410 actor orthologues strongly suggest functional conservation, future dedicated studies such as
41
42
43 411 biochemical inhibition or gene inactivation could help demonstrate their genuine biological
44
45
46 412 function. Besides, there seems to be an inverse correlation between m⁶A-RNA and 5mC-DNA
47
48
49 413 levels during the considered oyster developmental window [46]. This may suggest an interplay
50
51
52 414 between epigenetic and epitranscriptomic marks, possibly reflecting competition for methyl-
53
54
55 415 donor availability [59] or a link by histone epigenetic pathways [65,66].
56
57
58 416 Regarding the potential influence of the environment on m⁶A and the accumulation of RNA in
59
60 417 oocytes, we are at present investigating our hypothesis that m⁶A may convey intergenerational

1
2
3 418 epitranscriptomic inheritance of maternal life traits in the oyster. On an evolutionary
4
5
6 419 perspective, the presence of a putatively fully conserved epitranscriptomic pathway in the
7
8 420 oyster suggests that it was already present in the bilaterian common ancestor thereby in favour
9
10
11 421 of an important biological significance. Why *Drosophila* and *Caenorhabditis* seem to have lost
12
13 422 specific m⁶A-RNA erasers could be related to a sub-functionalization of the DMAD [41] and
14
15
16 423 NMAD-1 [42] N⁶-methyladenine DNA demethylase activity broadened towards RNA. However,
17
18
19 424 more work is required to better understand the evo-devo implications of our results.
20
21

425

22
23
24 426 To conclude, in this work we report the discovery and characterisation of a putatively complete
25
26
27 427 epitranscriptomic pathway in a lophotrochozoan organism, the oyster *Crassostrea gigas*. This
28
29
30 428 pathway includes the m⁶A mark in RNA and the actors of all the aspects of its regulation
31
32
33 429 (writers, eraser, readers) which are conserved at the molecular level and putatively functional.
34
35
36 430 We show that m⁶A levels are variable across oyster development and that m⁶A differentially
37
38
39 431 affects distinct RNA populations. Expression levels of the related enzymatic machinery is
40
41
42 432 consistent with the observed m⁶A level variations. We demonstrate the m⁶A binding capacity
43
44
45 433 and specificity of putative oyster m⁶A readers in the cytoplasm and nucleus of embryolarval
46
47
48 434 cells. These readers mediate distinct putative biological outcomes depending on the
49
50
51 435 development stage considered. From these results we hypothesize that early decay of
52
53
54 436 maternal m⁶A RNA participates in maternal-to-zygotic transition during cleavage and that later
55
56
57 437 *de novo* zygotic m⁶A methylation contributes to gastrulation and cell differentiation. This first
58
59
60 438 characterisation of an m⁶A-epitranscriptomic pathway in a lophotrochozoan organism, together
439 with its potential implication in development, opens new perspectives on the evolution of

1
2
3 440 epigenetic mechanisms and on the potential epitranscriptomic inheritance of environmentally-
4
5
6 441 induced life traits.
7
8
9 442

10
11
12 443 **Methods:**
13
14
15
16 444

17
18 445 **Animals:**
19
20

21 446 Broodstock oysters [67] and oyster embryos [46] were obtained at the IFREMER marine
22
23 447 facilities (Argenton, France) as previously described. Briefly, gametes of mature broodstock
24
25 448 oysters were obtained by stripping the gonads and filtering the recovered material on a 60 µm
26
27 449 mesh to remove large debris. Oocytes were collected as the remaining fraction on a 20 µm
28
29 450 mesh and spermatozoa as the passing fraction on a 20 µm mesh. Oocytes were pre-incubated
30
31 451 in 5 L of UV-treated and 1 µm filtered sterile sea water (SSW) at 21 °C until germinal vesicle
32
33 452 breakdown. Fertilization was triggered by the addition of ca. 10 spermatozooids per oocyte. After
34
35 453 the expulsion of the second polar body was assessed by light microscopy, embryos were
36
37 454 transferred in 150 L tanks of oxygenated SSW at 21 °C. The development stages were
38
39 455 determined by light microscopy observation. The stages collected were oocytes (E,
40
41 456 immediately before sperm addition), fertilized oocytes (F E, immediately before transfer to
42
43 457 150L tanks), two to eight cell embryos (2/8 C, ca. 1.5 hours post fertilization (hpf)), morula (M,
44
45 458 ca. 4 hpf), blastula (B, ca. 6 hpf), gastrula (G, ca. 10 hpf), trochophore (T, ca 16 hpf) and D
46
47 459 larvae (D, ca. 24 hpf). For each development stage, 3 million embryos were collected as the
48
49 460 remaining fraction on a 20 µm mesh and centrifuged at 123 g for 5min at room temperature.
50
51
52
53
54
55
56
57
58
59
60

1
2
3 461 Supernatant was discarded and samples of 1 million embryos were then snap-frozen in liquid
4
5
6 462 nitrogen directly of after resuspension in Tri-Reagent (Sigma-Aldrich, St Louis, MO, USA) (1
7
8 463 mL/10⁶ embryos) and stored at -80 °C. Three distinct experiments were realized (February to
9
10
11 464 May 2019) using the gametes of 126 to 140 broodstock animals, respectively.
12

13
14 465

15
16 466 **RNA extraction:**

- 17
18
19 467
 - total RNA extraction

20
21 468 RNA was extracted using phenol-chloroform followed by affinity chromatography as previously
22
23
24 469 described [68]. Briefly, embryos were ground in Tri-Reagent (Sigma-Aldrich) and RNA was
25
26
27 470 purified using affinity chromatography (Nucleospin RNA II kit, Macherey-Nagel, Duren,
28
29
30 471 Germany). Potential contaminating DNA was removed by digestion with rDNase (Macherey-
31
32 472 Nagel) according to the manufacturer's instructions for 15 min at 37 °C then RNA was purified
33
34
35 473 using Beckman Coulter's solid-phase reversible immobilization (SPRI) paramagnetic beads
36
37
38 474 (AgencourtAMPure XP, Beckman Coulter, Brea, CA, USA) according to the manufacturer's
39
40
41 475 instructions. Briefly, paramagnetic beads and RNAs were mixed slowly and incubated 5 min
42
43 476 at room temperature followed by 2 min on a magnetic rack. Cleared supernatant was removed,
44
45
46 477 and beads were washed three times with 70 % ethanol. After 4 min of drying at room
47
48
49 478 temperature, RNAs were mixed slowly with RNase free water and incubated for 1 min at room
50
51 479 temperature on the magnetic rack. Eluted total RNA was stored at -80 °C.

- 52
53
54 480
 - PolyA RNA enrichment

55
56
57 481 Poly-A RNA was extracted from total RNA by oligo-dT affinity chromatography (NucleoTrap
58
59 482 mRNA kit, Macherey-Nagel) according to the manufacturer's instructions. Briefly, up to 130 µg
60

1
2
3 483 of total RNAs were mixed with oligo-dT latex beads and incubated for 5 min at 68 °C then 10
4
5
6 484 min at room temperature. After centrifugation (2,000 g then 11,000 g), the pellets were washed
7
8 485 three times on the microfilter and dried by centrifugation at 11,000 g for 1 min. Finally, polyA+
9
10
11 486 RNA was incubated with RNase-free water for 7 min at 68 °C then centrifuged at 11,000 g for
12
13
14 487 1 min. Eluted polyA+ RNA was stored at -80 °C until needed.

15
16 488 Total and polyA-enriched RNA purity and concentrations were assayed by spectrophotometry
17
18
19 489 (Nanodrop, Thermo Scientific, Waltham, MA, USA).

20
21
22 490

23
24 491 **m⁶A quantification by LC-MS/MS:**

- 25
26
27 492
 - RNA hydrolysis

28
29 493 To generate nucleosides for quantification against standard curves, 5 µg of total RNA were
30
31
32 494 denatured for 10 min at 70 °C followed by 10 min on ice, and hydrolyzed with 100 U Nuclease
33
34
35 495 S1 (50 U/µL, Promega, Madison, WI, USA) in Nuclease S1 buffer (Promega) in a final reaction
36
37 496 volume of 25 µL for 2 h at 37 °C under gentle shaking. Samples were then incubated with
38
39
40 497 alkaline phosphatase buffer (Promega) for 5 min at room temperature, before 10 U alkaline
41
42
43 498 phosphatase (Promega) were added and incubated further for 2 h at 37 °C under gentle
44
45 499 shaking. Ten extra units of alkaline phosphatase were added after 1 hour of incubation to
46
47
48 500 complete the reaction. Finally, samples were centrifuged at 13,000 rpm for 10 min at 4 °C and
49
50
51 501 the supernatant containing digested total RNA was collected and kept at -20 °C before
52
53 502 quantification.

- 54
55
56
57 503
 - m⁶A quantification:

58
59
60

1
2
3 504 The apparatus was composed of a NexeraX² UHPLC system coupled with LCMS8030 Plus
4
5
6 505 (Shimadzu, Kyoto, Japan) mass spectrometer using an electrospray interface in positive mode.
7

8 506 The column (1.7 μm , 100x3 mm) was a HILIC Aquity[®] Amide (Waters, Millford, MA, USA)
9
10
11 507 maintained at 35 °C. The injection volume and run-to-run time were 3 μL and 10 min,
12
13
14 508 respectively. The flow rate was set to 1 mL/min. Mobile phase was initially composed of a
15
16
17 509 mixture of ammonium formate solution (10 mM) containing 0.2 % (v/v) formic acid and 95 %
18
19
20 510 acetonitrile (ACN) and it was maintained for 1 min. Then, a linear gradient was applied to reach
21
22
23 511 83 % ACN for 6 min. The composition returned to the initial conditions and the column was
24
25
26 512 equilibrated for 3 min.

27 513 The mass spectrometer was running in the Multiple Reaction Monitoring (MRM) acquisition
28
29
30 514 mode. LabSolutions 5.86 SP1 software was used to process the data. The desolvation
31
32
33 515 temperature was 230 °C, source temperature was 400 °C and nitrogen flows were 2.5 L/min
34
35
36 516 for the cone and 15 L/min for the desolvation. The capillary voltage was +4.5 kV. For each
37
38
39 517 compound, two transitions were monitored from the fragmentation of the $[\text{M}+\text{H}]^+$ ion. The first
40
41
42 518 transition (A in Table S1) was used for quantification and the second one (B in Table S1) for
43
44
45 519 confirmation of the compound according to European Commission Decision 2002/657/EC
46
47
48 520 (Table S1).

49
50
51 521 Blank plasma samples were analysed to check specificity. Calibrators were prepared using
52
53
54 522 diluted solutions of A (Toronto Research Chemical, Toronto, Canada) and m⁶A (Carbosynth,
55
56
57 523 Berkshire, UK) in water at 1, 2, 5, 10, 20 50, 100 ng/mL. The calibration curves were drawn by
58
59
60 524 plotting the ratio of the peak area of A and m⁶A. For both nucleosides, a quadratic regression
525 with 1/C weighting resulted in standard curves with $R^2 > 0.998$ and more than 75% of standards

1
2
3 526 with back-calculated concentrations within 15% of their nominal values as recommended for
4
5
6 527 by the European medicines agency for bioanalytical methods [69]. The limits of quantifications
7
8 528 for both compounds were considered as the lowest concentrations of the calibration curve.
9
10
11 529 m⁶A/A ratios were calculated for each single sample using the determined concentrations.
12
13
14 530 Final results are the average of three technical replicates.

15
16 531

17
18
19 532 **m⁶A quantification by immunoblotting:**

20
21 533 Immunological quantification of m⁶A was performed by dot-blot using total and polyA+ RNAs.
22
23
24 534 Dogfish total RNA (Dr. A. Gautier, personal communication) and a synthetic unmethylated
25
26
27 535 RNA oligo (Eurogentec, Liege, Belgium) were used as positive and negative controls,
28
29
30 536 respectively. RNA samples were denatured for 15 min at 55 °C with gentle shaking in
31
32
33 537 denaturing solution (2.2 M formaldehyde, 50 % formamide, 0.5X MOPS, DEPC water) followed
34
35
36 538 by 2 min on ice. Blotting was performed on a vacuum manifold as follows: a nylon membrane
37
38
39 539 (Amersham Hybond-N+, GE Healthcare life Sciences, Chicago, IL, USA) was pre-hydrated in
40
41
42 540 DEPC water for 5 min, then each well was washed twice with 10X SSC (Sigma-Aldrich) before
43
44
45 541 RNA was spotted onto the membrane and incubated for 15 min at room temperature. Then,
46
47
48 542 vacuum aspiration was applied and each well was washed twice with 10X SSC. After heat
49
50
51 543 crosslinking for 2 h at 70 °C, the membrane was rehydrated with DEPC water for 5 min, washed
52
53
54 544 with PBS then PBST (PBS, 0.1 % Tween-20) for 5 min each and blocked with two 5 min
55
56
57 545 incubations with blocking buffer (PBS, 0.1 % Tween-20, 10 % dry milk, 1 % BSA) at room
58
59
60 546 temperature. The blocked membrane was incubated overnight at 4 °C under gentle shaking
with the anti-m⁶A primary antibody (Total RNA: Millipore (Burlington, MA, USA) ABE572, 1 :

1
2
3 548 1,000 dilution in blocking buffer; polyA+ RNA: Diagenode (Liege, Belgium) C15200082, 1 : 500
4
5
6 549 dilution in blocking buffer) followed by four washes of PBST for 5 min. The secondary antibody
7
8 550 (Total RNA: Dako (Santa Clara, CA, USA) P0447 goat anti-mouse HRP antibody, 1 : 10,000
9
10
11 551 dilution; polyA+ RNA: Invitrogen (Carlsbad, CA, USA) A21202 donkey anti-mouse Alexa 488,
12
13 552 1 : 250 dilution) was diluted in PBST supplemented with 5 % dry milk and added onto the
14
15
16 553 membrane for 1 h 30 (total RNA) or 1 h (polyA+ RNA) at room temperature under gentle
17
18
19 554 shaking. Membranes were extensively washed in PBST (at least 4 washes of 5 min for total
20
21
22 555 RNA and 5 min then 1 h for polyA+ RNA) then total and polyA+ RNA immunoblots were
23
24 556 visualized using chemiluminescence (ECL kit, Promega) or fluorescence scanning at 480-530
25
26
27 557 nm (Pro Xpress, Perkin-Elmer, Waltham, MA, USA), respectively. The amount of m⁶A was
28
29
30 558 inferred from dot intensity measurements using ImageJ (v.1.49). Signal intensities were
31
32 559 determined as 'integrated densities as a percentage of the total' which corresponds to the area
33
34 560 under the curve of the signal of each dot after membrane background and negative control
35
36
37 561 signal subtraction.
38
39
40 562

41 42 563 ***In silico* analyses:**

43
44
45 564 All protein and RNA sequences of the m⁶A machinery of *Homo sapiens* and *Drosophila*
46
47
48 565 *melanogaster* (Data S1) were recovered by their published designation (i.e., 'METTL3' or
49
50 566 'YTHDF' etc.) and their identified protein sequence (ie. RefSeq accession number NP...)
51
52
53 567 collected from NCBI and used as query sequences to search for putative homologue
54
55
56 568 sequences in *Crassostrea gigas* databases. The presence of oyster orthologue RNA and
57
58
59 569 protein sequences were investigated by reciprocal
60

1
2
3 570 BLAST(<https://blast.ncbi.nlm.nih.gov/Blast.cgi>) on the *Crassostrea gigas* GigaTON [70] and
4
5
6 571 NCBI databases and results were compared between the two oyster databases. Domain
7
8 572 prediction was performed with CD-search software
9
10
11 573 (<https://www.ncbi.nlm.nih.gov/Structure/cdd/wrpsb.cgi>) with default settings on protein
12
13
14 574 sequences of *Homo sapiens*, *Drosophila melanogaster* and *Crassostrea gigas*. The GRE-rich
15
16 575 domain identified in vertebrate Prrc2a sequence [27] was performed with ProtParam
17
18
19 576 (<https://web.expasy.org/cgi-bin/protparam/protparam>).

20
21 577

22 23 24 578 **Protein machinery mRNA expression analyses:**

25
26
27 579 The transcriptome data of the different development stages are available on the GigaTON
28
29
30 580 database [70,71]. The correspondence between development stages in our study, and the
31
32
33 581 GigaTON database were assessed using light microscopy based on the morphological
34
35
36 582 description by Zhang et al., 2012 [71] (Table S2). Expression data was expressed in TPM
37
38
39 583 (Transcripts Per Million) [72] to provide a normalized comparison of gene expression between
40
41
42 584 all samples. The actual presence of some transcripts that display unclear or chimeric
43
44
45 585 sequences within available oyster databases was assessed using RT-PCR (Data S1).

46
47 586

48 587 **Protein m⁶A RNA pull down:**

- 49
50
51 588
 - Protein extraction and RNA affinity chromatography

52
53 589 Protein extraction and RNA affinity chromatography were performed as described previously
54
55
56 590 [27] with some modifications as follows. Equal amounts (1 million individuals) of each
57
58
59 591 developmental stage (oocyte to D larvae) were pooled together then homogenized in 3.5
60

1
2
3 592 volumes of buffer A (10 mM KCl, 1.5 mM MgCl₂, 10 mM HEPES, pH 7.9, DEPC water, 1X
4
5
6 593 Protease inhibitor cocktail, DTT 0.5 mM) by extensive pipetting (ca. 30 times) and incubated
7
8 594 10 min at 4 °C. Embryos were ground with 10 slow 23G-needle syringe strokes and centrifuged
9
10
11 595 at 2,000 rpm for 10 min at 4 °C. The supernatant was diluted in 0.11 volume of buffer B (1.4 M
12
13 596 KCl, 0.03 M MgCl₂, HEPES 0.3 M, pH 7.9, DEPC water), centrifuged at 10,000 g for 1 h at 4
14
15
16 597 °C and the supernatant containing cytosolic proteins was stored at -80 °C. The pellet of the
17
18
19 598 first centrifugation, containing nuclei, was re-suspended in two volumes of buffer C (0.42 M
20
21 599 NaCl, 1.5 mM MgCl₂, 0.2 mM EDTA, 25 % glycerol, 20 mM HEPES, pH 7.9, 0.5 mM PMSF,
22
23
24 600 0.5 mM DTT, water DEPC). Nuclei were then lysed with a 23 G needle (10 vigorous syringe
25
26
27 601 strokes) followed by centrifugation at 30,000 rpm for 30 min at 4 °C and the supernatant
28
29
30 602 containing nuclear proteins was stored at -80 °C.

31
32 603 To identify putative proteins able to bind m⁶A-RNA, the cytosolic and nuclear fractions were
33
34
35 604 submitted to affinity chromatography using 5'-biotin-labelled RNA oligonucleotides either
36
37
38 605 bearing N⁶-methylated adenosines or not. The methylated adenosines were designed to lie
39
40
41 606 within RRACH motifs, according to the conserved methylated consensus sequence in other
42
43 607 organisms [2,3,7,33,73] (oligo-m⁶A: 5'Biotin-AGAAAAGACAACCAACGAGRR-m⁶A-
44
45 608 CWCAUCAU-3', oligo-A: 5'Biotin-AGAAAAGACAACCAACGAGRRACWCAUCAU-3', R = A or
46
47
48 609 G, W = A or U, Eurogentec).

49
50 610 For RNA pull down, streptavidin-conjugated magnetic beads (Dynabeads Myone Streptavidin,
51
52
53 611 Invitrogen) were pre-blocked with 0.2 mg/mL tRNA (Sigma-Aldrich) and 0.2 mg/mL BSA for 1
54
55
56 612 h at 4 °C under gentle rotation followed by three washes with 0.1 M NaCl. To avoid the
57
58
59 613 identification of non-target proteins, cytosolic and nuclear protein extracts were cleared with
60

1
2
3 614 pre-blocked magnetic beads in binding buffer (50 mM Tris-HCl, 250 mM NaCl, 0.4 mM EDTA,
4
5
6 615 0.1 % NP-40, DEPC water, 1 mM DTT, 0.4 U/ μ L RNAsin) for 1 h at 4 °C under gentle rotation.
7
8 616 After incubation on magnetic rack, the supernatants containing putative target proteins were
9
10
11 617 collected and mixed with pre-blocked magnetic beads and oligo-m⁶A or oligo-A for 2 h at 4 °C
12
13
14 618 under gentle rotation. The beads binding putative target proteins were washed three times with
15
16 619 binding buffer and diluted in 50 mM ammonium bicarbonate.

17
18
19
20 620 • Identification of m⁶A-binding proteins by LC-MS/MS:

21
22 621 Protein samples were first reduced, alkylated and digested with trypsin then desalted and
23
24
25 622 concentrated onto a μ C18 Omix (Agilent, Santa Clara, CA, USA) before analysis.

26
27
28 623 The chromatography step was performed on a NanoElute (Bruker Daltonics, Billerica, MA,
29
30 624 USA) ultra-high pressure nano flow chromatography system. Peptides were concentrated onto
31
32
33 625 a C18 pepmap 100 (5 mm x 300 μ m i.d.) precolumn (Thermo Scientific) and separated at 50
34
35
36 626 °C onto a reversed phase Reprosil column (25 cm x 75 μ m i.d.) packed with 1.6 μ m C18 coated
37
38 627 porous silica beads (Ionopticks, Parkville, Victoria, Australia). Mobile phases consisted of 0.1
39
40
41 628 % formic acid, 99.9 % water (v/v) (A) and 0.1 % formic acid in 99.9 % ACN (v/v) (B). The
42
43
44 629 nanoflow rate was set at 400 nL/min, and the gradient profile was as follows: from 2 to 15 % B
45
46 630 within 60 min, followed by an increase to 25 % B within 30 min and further to 37 % within 10
47
48
49 631 min, followed by a washing step at 95 % B and re-equilibration.

50
51 632 MS experiments were carried out on an TIMS-TOF pro mass spectrometer (Bruker Daltonics)
52
53
54 633 with a modified nano-electrospray ion source (CaptiveSpray, Bruker Daltonics). The system
55
56
57 634 was calibrated each week and mass precision was better than 1 ppm. A 1600 spray voltage
58
59 635 with a capillary temperature of 180 °C was typically employed for ionizing. MS spectra were
60

1
2
3 636 acquired in the positive mode in the mass range from 100 to 1700 m/z. In the experiments
4
5
6 637 described here, the mass spectrometer was operated in PASEF mode with exclusion of single
7
8 638 charged peptides. A number of 10 PASEF MS/MS scans was performed during 1.16 seconds
9
10
11 639 from charge range 2-5.

12
13 640 The fragmentation pattern was used to determine the sequence of the peptide. Database
14
15
16 641 searching was performed using the Mascot 2.6.1 program (Matrix Science) with a *Crassostrea*
17
18 642 *gigas* Uniprot database (including 25,982 entries). The variable modifications allowed were as
19
20
21 643 follows: C-Carbamidomethyl, K-acetylation, methionine oxidation, and Deamidation (NQ). The
22
23
24 644 'Trypsin' parameter was set to 'Semispecific'. Mass accuracy was set to 30 ppm and 0.05 Da
25
26
27 645 for MS and MS/MS mode respectively. Mascot data were then transferred to Proline validation
28
29
30 646 software (<http://www.profiroteomics.fr/proline/>) for data filtering according to a significance
31
32 647 threshold of <0.05 and the elimination of protein redundancy on the basis of proteins being
33
34
35 648 evidenced by the same set or a subset of peptides (Data S2).

36
37
38 649 • Gene ontology analysis:

39
40
41 650 The mRNA sequences of the characterized m⁶A-binding proteins were identified using tBlastn
42
43 651 [74–76] against the GigaTON database [70] with default settings. Gene ontology (GO)
44
45
46 652 analyses were carried out with the GO annotations obtained from GigaTON database gene
47
48
49 653 universe [70]. GO term-enrichment tests were performed using the goseq (V1.22.0) R package
50
51 654 [77] with p-values calculated by the Wallenius method and filtered using REVIGO [78]. GO
52
53
54 655 terms with a p-value < 0.05 were considered significantly enriched (Data S3).

55
56 656

57
58
59 657 **Statistical analyses and graph production:**
60

1
2
3 658 Results are given as the mean \pm SD of three independent experiments unless otherwise stated.
4
5
6 659 They were analysed using one-way ANOVA or Kruskal-wallis tests when required, depending
7
8 660 on the normality of result distribution. The normality was tested using the Shapiro-Wilk's test
9
10
11 661 and homoscedasticity of variances with Bartlett's tests. Statistics and graphics were computed
12
13
14 662 with Prism v.6 (Graphpad), R (v.3.6.1) and RStudio (v.1.0.153) softwares. The R packages
15
16 663 *eulerr* [79] and *Complexheatmap* [80] were used for production of specific figures.
17
18
19 664
20
21
22 665
23
24

25 666 **Author contribution**

26
27
28 667 Experiment design: GR, LLF.

29
30 668 Benchwork and bioinformatics: LLF, GR, BB, BP, MS.

31
32
33 669 Data analysis: LLF, GR, BB, MS.

34
35
36 670 Manuscript writing and editing: LLF, GR, PF, BB, MS, BP.

37
38
39 671

40 41 672 **Acknowledgements**

42
43
44 673 The authors would like to acknowledge PRISMM core facility collaborators R. Delepée and S.
45
46 674 Lagadu for their expertise in m⁶A/A UHPLC-MS/MS quantification. We also thank J. Pontin for
47
48
49 675 technical assistance and J. Le Grand for help with sampling.
50
51
52 676

53 54 677 **Funding sources and disclosure of conflicts of interest**

55
56
57
58
59
60

1
2
3 678 This work was supported by the French National program CNRS EC2CO (Ecosphère
4
5
6 679 Continentale et Côtière 'HERITAGe' to G. Rivière) and the council of the Normandy Region
7
8 680 (RIN ECUME to P. Favrel). The authors declare they have no conflict of interest.
9

10
11 681
12
13
14
15
16
17
18
19
20
21
22
23
24
25
26
27
28
29
30
31
32
33
34
35
36
37
38
39
40
41
42
43
44
45
46
47
48
49
50
51
52
53
54
55
56
57
58
59
60

For Review Only

682 **References:**

- 683 1 Saletore Y, Meyer K, Korlach J, Vilfan ID, Jaffrey S & Mason CE (2012) The birth of the
684 Epitranscriptome: deciphering the function of RNA modifications. *Genome Biol.* **13**, 175.
- 685 2 Meyer KD, Saletore Y, Zumbo P, Elemento O, Mason CE & Jaffrey SR (2012)
686 Comprehensive analysis of mRNA methylation reveals enrichment in 3' UTRs and near
687 stop codons. *Cell* **149**, 1635–1646.
- 688 3 Dominissini D, Moshitch-moshkovitz S, Schwartz S, Salmon-Divon M, Ungar L, Osenberg
689 S, Cesarkas K, Jacob-hirsch J, Amariglio N, Kupiee M, Sorek R & Rechavi G (2012)
690 Topology of the human and mouse m⁶A RNAmethylomes revealed by m⁶A-seq.
691 *Nature* **485**, 201–206.
- 692 4 Ke S, Alemu EA, Mertens C, Gantman EC, Fak JJ, Mele A, Haripal B, Zucker-Scharff I,
693 Moore MJ, Park CY, Vågbø CB, Kusńnierczyk A, Klungland A, Darnell JE, Darnell RB,
694 Kuńnierczyk A, Klungland A, Darnell JE, Darnell RB, Kusńnierczyk A, Klungland A,
695 Darnell JE & Darnell RB (2015) A majority of m⁶A residues are in the last exons,
696 allowing the potential for 3' UTR regulation. *Genes Dev.* **29**, 2037–2053.
- 697 5 Meyer KD, Patil DP, Zhou J, Zinoviev A, Skabkin MA, Elemento O, Pestova T V., Qian SB
698 & Jaffrey SR (2015) 5' UTR m⁶A Promotes Cap-Independent Translation. *Cell* **163**,
699 999–1010.
- 700 6 Pendleton KE, Chen B, Liu K, Hunter O V., Xie Y, Tu BP & Conrad NK (2017) The U6
701 snRNA m⁶A Methyltransferase METTL16 Regulates SAM Synthetase Intron Retention.
702 *Cell* **169**, 824-835.e14.
- 703 7 Lence T, Akhtar J, Bayer M, Schmid K, Spindler L, Ho CH, Kreim N, Andrade-Navarro MA,
704 Poeck B, Helm M & Roignant JY (2016) M⁶A modulates neuronal functions and sex
705 determination in *Drosophila*. *Nature* **540**, 242–247.
- 706 8 Bokar JA, Shambaugh ME, Polayes D, Matera AG & Rottman FM (1997) Purification and
707 cDNA cloning of the AdoMet-binding subunit of the human mRNA (N⁶-adenosine)-
708 methyltransferase. *RNA* **3**, 1233–47.
- 709 9 Liu J, Yue Y, Han D, Wang X, Fu YY, Zhang L, Jia G, Yu M, Lu Z, Deng X, Dai Q, Chen W
710 & He C (2013) A METTL3–METTL14 complex mediates mammalian nuclear RNA N⁶-
711 adenosine methylation. *Nat. Chem. Biol.* **10**, 93–95.
- 712 10 Wang X, Feng J, Xue Y, Guan Z, Zhang D, Liu Z, Gong Z, Wang Q, Huang J, Tang C,
713 Zou T & Yin P (2016) Structural basis of N⁶-adenosine methylation by the METTL3-
714 METTL14 complex. *Nature* **534**, 575–578.
- 715 11 Ping X-LL, Sun B-FF, Wang L, Xiao W, Yang X, Wang W-JJ, Adhikari S, Shi Y, Lv Y,
716 Chen Y-SS, Zhao X, Li A, Yang YGYY-G, Dahal U, Lou X-MM, Liu X, Huang J, Yuan W-
717 PP, Zhu X-FF, Cheng T, Zhao Y-LL, Wang X, Danielsen JMRR, Liu F & Yang YGYY-G
718 (2014) Mammalian WTAP is a regulatory subunit of the RNA N⁶-methyladenosine
719 methyltransferase. *Cell Res.* **24**, 177–189.
- 720 12 Yue Y, Liu J, Cui X, Cao J, Luo G, Zhang Z, Cheng T, Gao M, Shu X, Ma H, Wang F,
721 Wang X, Shen B, Wang Y, Feng X, He C & Liu J (2018) VIRMA mediates preferential
722 m⁶A mRNA methylation in 3'UTR and near stop codon and associates with alternative
723 polyadenylation. *Cell Discov.* **4**, 10.
- 724 13 Růzička K, Zhang M, Campilho A, Bodi Z, Kashif M, Saleh M, Eeckhout D, El-Showk S, Li
725 H, Zhong S, Jaeger G De, Mongan NP, Hejátko J, Helariutta Y & Fray RG (2017)
726 Identification of factors required for m⁶A mRNA methylation in *Arabidopsis* reveals a

- 1
2
3 727 role for the conserved E3 ubiquitin ligase HAKAI. *New Phytol.* **215**, 157–172.
4
- 5 728 14 Knuckles P, Lence T, Haussmann IU, Jacob D, Kreim N, Carl SH, Masiello I, Hares T,
6 729 Villaseñor R, Hess D, Andrade-Navarro MA, Biggiogera M, Helm M, Soller M, Bühler M
7 730 & Roignant J-YY (2018) Zc3h13/Flacc is required for adenosine methylation by bridging
8 731 the mRNA-binding factor Rbm15/Spenito to the m⁶A machinery component
9 732 Wtap/Fl(2)d. *Genes Dev.* **32**, 1–15.
10
- 11 733 15 Patil DP, Chen CK, Pickering BF, Chow A, Jackson C, Guttman M & Jaffrey SR (2016)
12 734 m⁶A RNA methylation promotes XIST-mediated transcriptional repression. *Nature* **537**,
13 735 369–373.
14
- 15 736 16 Zheng G, Dahl JA, Niu Y, Fedorcsak P, Huang CM, Li CJ, Vågbo CB, Shi Y, Wang WL,
16 737 Song SH, Lu Z, Bosmans RPG, Dai Q, Hao YJ, Yang X, Zhao WM, Tong WM, Wang
17 738 XJ, Bogdan F, Furu K, Fu Y, Jia G, Zhao X, Liu J, Krokan HE, Klungland A, Yang YG &
18 739 He C (2013) ALKBH5 Is a Mammalian RNA Demethylase that Impacts RNA Metabolism
19 740 and Mouse Fertility. *Mol. Cell* **49**, 18–29.
20
- 21 741 17 Mauer J, Luo X, Blanjoie A, Jiao X, Grozhik A V, Patil DP, Linder B, Pickering BF,
22 742 Vasseur J-J, Chen Q, Gross SS, Elemento O, Debart F, Kiledjian M & Jaffrey SR (2017)
23 743 Reversible methylation of m⁶Am in the 5' cap controls mRNA stability. *Nature* **541**, 371–
24 744 375.
25
- 26 745 18 Jia G, Fu Y, Zhao X, Dai Q, Zheng G, Yang YGYG-GGYG-G, Yi C, Lindahl T, Pan T,
27 746 Yang YGYG-GGYG-G & He C (2011) N⁶-Methyladenosine in nuclear RNA is a major
28 747 substrate of the obesity-associated FTO. *Nat. Chem. Biol.* **7**, 885–887.
29
- 30 748 19 Wang X, Lu Z, Gomez A, Hon GC, Yue Y, Han D, Fu Y, Parisien M, Dai Q, Jia G, Ren B,
31 749 Pan T, He C, Zhike L, Gomez A, Hon GC, Yue Y, Han D, Fu Y, Årisien M, Dai Q, Jia G,
32 750 Ren B, Pan T & He C (2014) N⁶-methyladenosine-dependent regulation of messenger
33 751 RNA stability. *Nature* **505**, 117–120.
34
- 35 752 20 Wang X, Zhao BS, Roundtree IA, Lu Z, Han D, Ma H, Weng X, Chen K, Shi H & He C
36 753 (2015) N⁶-methyladenosine modulates messenger RNA translation efficiency. *Cell* **161**,
37 754 1388–1399.
38
- 39 755 21 Hsu PJ, Zhu Y, Ma H, Guo Y, Shi X, Liu Y, Qi M, Lu Z, Shi H, Wang J, Cheng Y, Luo G,
40 756 Dai Q, Liu M, Guo X, Sha J, Shen B & He C (2017) Ythdc2 is an N⁶-methyladenosine
41 757 binding protein that regulates mammalian spermatogenesis. *Cell Res.* **27**, 1115–1127.
42
- 43 758 22 Shi H, Wang X, Lu Z, Zhao BS, Ma H, Hsu PJ, Liu C & He C (2017) YTHDF3 facilitates
44 759 translation and decay of N⁶-methyladenosine-modified RNA. *Cell Res.* **27**, 315–328.
45
- 46 760 23 Xiao W, Adhikari S, Dahal U, Chen Y-S, Hao Y-J, Sun B-F, Sun H-Y, Li A, Ping X-L, Lai
47 761 W-Y, Wang XX-J, Ma H-L, Huang C-M, Yang YY-G, Huang N, Jiang G-B, Wang H-L,
48 762 Zhou Q, Wang XX-J, Zhao Y-L & Yang YY-G (2016) Nuclear m⁶A Reader YTHDC1
49 763 Regulates mRNA Splicing. *Mol. Cell* **61**, 507–519.
50
- 51 764 24 Roundtree IA, Luo G-ZZ, Zhang Z, Wang X, Zhou T, Cui Y, Sha J, Huang X, Guerrero L,
52 765 Xie P, He E, Shen B & He C (2017) YTHDC1 mediates nuclear export of N⁶-
53 766 methyladenosine methylated mRNAs. *Elife* **6**, 1–28.
54
- 55 767 25 Alarcón CR, Goodarzi H, Lee H, Liu X, Tavazoie SFSSF & Tavazoie SFSSF (2015)
56 768 HNRNPA2B1 Is a Mediator of m⁶A-Dependent Nuclear RNA Processing Events. *Cell*
57 769 **162**, 1299–1308.
58
- 59 770 26 Huang H, Weng H, Sun W, Qin X, Shi H, Wu H, Zhao BS, Mesquita A, Liu C, Yuan CL,
60 771 Hu YC, Hüttelmaier S, Skibbe JR, Su R, Deng X, Dong L, Sun M, Li C, Nachtergaele S,

- 1
2
3 772 Wang Y, Hu C, Ferchen K, Greis KD, Jiang X, Wei M, Qu L, Guan JL, He C, Yang J &
4 773 Chen J (2018) Recognition of RNA N6-methyladenosine by IGF2BP proteins enhances
5 774 mRNA stability and translation. *Nat. Cell Biol.* **20**, 285–295.
6
7 775 27 Wu R, Li A, Sun B, Sun J-GG, Zhang J, Zhang T, Chen Y, Xiao Y, Gao Y, Zhang Q, Ma J,
8 776 Yang X, Liao Y, Lai W-YY, Qi X, Wang S, Shu Y, Wang H-LL, Wang F, Yang Y-GG &
9 777 Yuan Z (2018) A novel m6A reader Prrc2a controls oligodendroglial specification and
10 778 myelination. *Cell Res.* **29**, 23–41.
11
12 779 28 Bertero A, Brown S, Madrigal P, Osnato A, Ortmann D, Yiangou L, Kadiwala J, Hubner
13 780 NC, De Los Mozos IR, Sadee C, Lenaerts A-SS, Nakanoh S, Grandy R, Farnell E, Ule
14 781 J, Stunnenberg HG, Mendjan S, Vallier L, Sadée C, Lenaerts A-SS, Nakanoh S, Grandy
15 782 R, Farnell E, Ule J, Stunnenberg HG, Mendjan S & Vallier L (2018) The SMAD2/3
16 783 interactome reveals that TGFβ controls m 6 A mRNA methylation in pluripotency.
17 784 *Nature* **555**, 256–259.
18
19 785 29 Kwon J, Jo YJ, Namgoong S & Kim NH (2019) Functional roles of hnRNPA2/B1 regulated
20 786 by METTL3 in mammalian embryonic development. *Sci. Rep.* **9**, 8640.
21
22 787 30 Geula S, Moshitch-Moshkovitz S, Dominissini D, Mansour AAF, Kol N, Salmon-Divon M,
23 788 Hershkovitz V, Peer E, Mor N, Manor YS, Ben-Haim MS, Eyal E, Yunger S, Pinto Y,
24 789 Jaitin DA, Viukov S, Rais Y, Krupalnik V, Chomsky E, Zerbib M, Maza I, Rechavi Y,
25 790 Massarwa R, Hanna S, Amit I, Levanon EY, Amariglio N, Stern-Ginossar N,
26 791 Novershtern N, Rechavi G & Hanna JH (2015) m6A mRNA methylation facilitates
27 792 resolution of naïve pluripotency toward differentiation. *Science (80-.).* **347**, 1002–1006.
28
29 793 31 Batista PJ, Molinie B, Wang J, Qu K, Zhang J, Li L, Bouley DM, Lujan E, Haddad B,
30 794 Daneshvar K, Carter AC, Flynn RA, Zhou C, Lim KS, Dedon P, Wernig M, Mullen AC,
31 795 Xing Y, Giallourakis CC, Chang HY, Howard Y, Batista PJ, Molinie B, Wang J, Qu K,
32 796 Zhang J, Li L, Bouley DM, Dedon P, Wernig M, Mullen AC, Xing Y, Giallourakis CC &
33 797 Chang HY (2014) M⁶A RNA modification controls cell fate transition in mammalian
34 798 embryonic stem cells. *Cell Stem Cell* **15**, 707–719.
35
36 799 32 Wojtas MN, Pandey RR, Mendel M, Homolka D, Sachidanandam R & Pillai RS (2017)
37 800 Regulation of m6A Transcripts by the 3'→5' RNA Helicase YTHDC2 Is Essential for a
38 801 Successful Meiotic Program in the Mammalian Germline. *Mol. Cell* **68**, 374-387.e12.
39
40 802 33 Zhao BS, Wang X, Beadell A V., Lu Z, Shi H, Kuuspalu A, Ho RK & He C (2017) M6A-
41 803 dependent maternal mRNA clearance facilitates zebrafish maternal-to-zygotic transition.
42 804 *Nature* **542**, 475–478.
43
44 805 34 Kan L, Grozhik A V., Vedanayagam J, Patil DP, Pang N, Lim K-S, Huang Y-C, Joseph B,
45 806 Lin C-J, Despic V, Guo J, Yan D, Kondo S, Deng W-M, Dedon PC, Jaffrey SR & Lai EC
46 807 (2017) The m6A pathway facilitates sex determination in *Drosophila*. *Nat. Commun.* **8**,
47 808 15737.
48
49 809 35 Kasowitz SD, Ma J, Anderson SJ, Leu NA, Xu Y, Gregory BD, Schultz RM & Wang PJ
50 810 (2018) Nuclear m 6 A reader YTHDC1 regulates alternative polyadenylation and splicing
51 811 during mouse oocyte development. *PLoS Genet.* **14**, 1–28.
52
53 812 36 Ivanova I, Much C, Di Giacomo M, Azzi C, Morgan M, Moreira PN, Monahan J, Carrieri C,
54 813 Enright AJ, O'Carroll D, Giacomo M Di, Azzi C, Morgan M, Moreira PN, Monahan J,
55 814 Carrieri C, Enright AJ, O'carroll D, Di Giacomo M, Azzi C, Morgan M, Moreira PN,
56 815 Monahan J, Carrieri C, Enright AJ & O'carroll D (2017) The RNA m 6 A Reader
57 816 YTHDF2 Is Essential for the Post-transcriptional Regulation of the Maternal
58 817 Transcriptome and Oocyte Competence. *Mol. Cell* **67**, 1059-1067.e4.
59
60

- 1
2
3 818 37 Lence T, Paolantoni C, Worpenberg L & Roignant JY (2019) Mechanistic insights into m⁶A
4 819 A RNA enzymes. *Biochim. Biophys. Acta - Gene Regul. Mech.* **1862**, 222–229.
5
6 820 38 Balacco DL & Soller M (2018) The m⁶A writer: Rise of a machine for growing tasks.
7 821 *Biochemistry* **58**, acs.biochem.8b01166.
8
9 822 39 Lence T, Soller M & Roignant JY (2017) A fly view on the roles and mechanisms of the
10 823 m⁶A mRNA modification and its players. *RNA Biol.* **14**, 1232–1240.
11
12 824 40 Robbens S, Rouzé P, Cock JM, Spring J, Worden AZ & Van De Peer Y (2008) The FTO
13 825 gene, implicated in human obesity, is found only in vertebrates and marine algae. *J.*
14 826 *Mol. Evol.* **66**, 80–84.
15
16 827 41 Zhang G, Huang H, Liu D, Cheng Y, Liu X, Zhang W, Yin R, Zhang D, Zhang P, Liu J, Li
17 828 C, Liu B, Luo Y, Zhu Y, Zhang N, He S, He C, Wang H & Chen D (2015) N⁶-
18 829 methyladenine DNA modification in *Drosophila*. *Cell* **161**, 893–906.
19
20 830 42 Greer EL, Blanco MA, Gu L, Sendinc E, Liu J, Aristizábal-Corrales D, Hsu CH, Aravind L,
21 831 He C & Shi Y (2015) DNA methylation on N⁶-adenine in *C. elegans*. *Cell* **161**, 868–878.
22
23 832 43 Riviere G, He Y, Tecchio S, Crowell E, Sourdain P, Guo X & Favrel P (2017) Dynamics
24 833 of DNA methylomes underlie oyster development. *PLOS Genet.* **13**, 1–16.
25
26 834 44 Sussarellu R, Lebreton M, Rouxel J, Akcha F, Riviere G & Rivière G (2018) Copper
27 835 induces expression and methylation changes of early development genes in
28 836 *Crassostrea gigas* embryos. *Aquat. Toxicol.* **196**, submitted.
29
30 837 45 Rondon R, Grunau C, Fallet M, Charlemagne N, Sussarellu R, Chaparro C, Montagnani
31 838 C, Mitta G, Bachère E, Akcha F & Cosseau C (2017) Effects of a parental exposure to
32 839 diuron on Pacific oyster spat methylome. *Environ. Epigenetics* **3**, 1–13.
33
34 840 46 Riviere G, Wu G-CC, Fellous A, Goux D, Sourdain P & Favrel P (2013) DNA Methylation
35 841 Is Crucial for the Early Development in the Oyster *C. gigas*. *Mar. Biotechnol.* **15**, 1–15.
36
37 842 47 Saint-Carlier E & Riviere G (2015) Regulation of Hox orthologues in the oyster
38 843 *Crassostrea gigas* evidences a functional role for promoter DNA methylation in an
39 844 invertebrate. *FEBS Lett.* **589**, 1459–1466.
40
41 845 48 Fellous A, Favrel P & Riviere G (2015) Temperature influences histone methylation and
42 846 mRNA expression of the Jmj-C histone-demethylase orthologues during the early
43 847 development of the oyster *Crassostrea gigas*. *Mar. Genomics* **19**, 23–30.
44
45 848 49 Fellous A, Favrel P, Guo X & Riviere G (2014) The Jumonji gene family in *Crassostrea*
46 849 *gigas* suggests evolutionary conservation of Jmj-C histone demethylases orthologues in
47 850 the oyster gametogenesis and development. *Gene* **538**, 164–175.
48
49 851 50 Fellous A, Le Franc L, Jouaux A, Goux D, Favrel P & Rivière G (2019) Histone
50 852 Methylation Participates in Gene Expression Control during the Early Development of
51 853 the Pacific Oyster *Crassostrea gigas*. *Genes (Basel)*. **10**, 695.
52
53 854 51 Zhou J, Wan J, Gao X, Zhang X, Jaffrey SR & Qian S-B (2015) Dynamic m⁶A mRNA
54 855 methylation directs translational control of heat shock response. *Nature* **526**, 591–594.
55
56 856 52 Lu Z, Ma Y, Li Q, Liu E, Jin M, Zhang L & Wei C (2019) The role of N⁶-methyladenosine
57 857 RNA methylation in the heat stress response of sheep (*Ovis aries*). *Cell Stress*
58 858 *Chaperones* **24**, 333–342.
59
60 859 53 Xiang Y, Laurent B, Hsu C, Nachtergaele S, Lu Z, Sheng W, Xu C, Chen H, Ouyang J,

- 1
2
3 860 Wang S, Ling D, Hsu P, Zou L, Jambhekar A & He C (2017) m6A RNA methylation
4 861 regulates the UV-induced DNA damage response. *Nature* **543**, 573–576.
5
6 862 54 Cayir A, Barrow TM, Guo L & Byun HM (2019) Exposure to environmental toxicants
7 863 reduces global N6-methyladenosine RNA methylation and alters expression of RNA
8 864 methylation modulator genes. *Environ. Res.* **175**, 228–234.
9
10 865 55 Liu J, Li K, Cai J, Zhang M, Zhang X, Xiong X, Meng H, Xu X, Huang Z, Fan J & Yi C
11 866 (2019) Landscape and Regulation of M⁶A and M⁶Am Methylome Across Human and
12 867 Mouse Tissues. *SSRN Electron. J.*, 1–56.
13
14 868 56 Ren W, Lu J, Huang M, Gao L, Li D, Greg Wang G & Song J (2019) Structure and
15 869 regulation of ZCCHC4 in m6A-methylation of 28S rRNA. *Nat. Commun.* **10**, 5042.
16
17 870 57 Bokar JA, Shambaugh ME, Polayes D, Matera AG & Rottman FM (1997) Purification and
18 871 cDNA cloning of the AdoMet-binding subunit of the human mRNA (N6-adenosine)-
19 872 methyltransferase. *RNA* **3**, 1233–1247.
20
21 873 58 Theler D, Dominguez C, Blatter M, Boudet J & Allain FHT (2014) Solution structure of the
22 874 YTH domain in complex with N6-methyladenosine RNA: A reader of methylated RNA.
23 875 *Nucleic Acids Res.* **42**, 13911–13919.
24
25 876 59 Shima H, Matsumoto M, Ishigami Y, Ebina M, Muto A, Sato Y, Kumagai S, Ochiai K,
26 877 Suzuki T & Igarashi K (2017) S-Adenosylmethionine Synthesis Is Regulated by
27 878 Selective N6-Adenosine Methylation and mRNA Degradation Involving METTL16 and
28 879 YTHDC1. *Cell Rep.* **21**, 3354–3363.
29
30 880 60 Yurchenko O V., Skiteva OI, Voronezhskaya EE & Dyachuk VA (2018) Nervous system
31 881 development in the Pacific oyster, *Crassostrea gigas* (Mollusca: Bivalvia). *Front. Zool.*
32 882 **15**, 1–21.
33
34 883 61 Ratnaparkhi A (2013) Signaling by folded gastrulation is modulated by mitochondrial
35 884 fusion and fission. *J. Cell Sci.* **126**, 5369–5376.
36
37 885 62 Ren L, Zhang C, Tao L, Hao J, Tan K, Miao K, Yu Y, Sui L, Wu Z, Tian J & An L (2017)
38 886 High-resolution profiles of gene expression and DNA methylation highlight mitochondrial
39 887 modifications during early embryonic development. *J. Reprod. Dev.* **63**, 247–261.
40
41 888 63 Prudent J, Popgeorgiev N, Bonneau B, Thibaut J, Gadet R, Lopez J, Gonzalo P, Rimokh
42 889 R, Manon S, Houart C, Herbomel P, Aouacheria A & Gillet G (2013) Bcl-wav and the
43 890 mitochondrial calcium uniporter drive gastrula morphogenesis in zebrafish. *Nat.*
44 891 *Commun.* **4**.
45
46 892 64 Dumollard R, Duchon M & Carroll J (2007) The Role of Mitochondrial Function in the
47 893 Oocyte and Embryo. *Curr. Top. Dev. Biol.* **77**, 21–49.
48
49 894 65 Huang H, Weng H, Zhou K, Wu T, Zhao BS, Sun MM, Chen Z, Deng X, Xiao G, Auer F,
50 895 Klemm L, Wu H, Zuo Z, Qin X, Dong Y, Zhou Y, Qin H, Tao S, Du J, Liu J, Lu Z, Yin H,
51 896 Mesquita A, Yuan CL, Hu Y-CC, Sun W, Su R, Dong L, Shen C, Li C, Qing Y, Jiang X,
52 897 Wu X, Sun MM, Guan J-LL, Qu L, Wei M, Müschen M, Huang G, He C, Yang J & Chen
53 898 J (2019) Histone H3 trimethylation at lysine 36 guides m6A RNA modification co-
54 899 transcriptionally. *Nature* **567**, 414–419.
55
56 900 66 Wang Y, Li Y, Yue M, Wang J, Kumar S, Wechsler-Reya RJ, Zhang Z, Ogawa Y, Kellis M,
57 901 Duyster G & Zhao JC (2018) N6-methyladenosine RNA modification regulates
58 902 embryonic neural stem cell self-renewal through histone modifications. *Nat. Neurosci.*
59 903 **21**, 195–206.
60

- 1
2
3 904 67 Petton B, Pernet F, Robert R & Boudry P (2013) Temperature influence on pathogen
4 905 transmission and subsequent mortalities in juvenile pacific oysters *Crassostrea gigas*.
5 906 *Aquac. Environ. Interact.* **3**, 257–273.
6
7 907 68 Riviere G, Fellous A, Franco A, Bernay B & Favrel P (2011) A crucial role in fertility for the
8 908 oyster angiotensin-converting enzyme orthologue CgACE. *PLoS One* **6**.
9
10 909 69 EMA (2011) *Guideline on bioanalytical method validation*.
11 910 *EMA/CHMP/EWP/192217/2009*.
12
13 911 70 Riviere G, Klopp C, Ibouniyamine N, Huvet A, Boudry P & Favrel P (2015) GigaTON: An
14 912 extensive publicly searchable database providing a new reference transcriptome in the
15 913 pacific oyster *Crassostrea gigas*. *BMC Bioinformatics* **16**, 1–12.
16
17 914 71 Zhang G, Fang X, Guo X, Li L, Luo R, Xu F, Yang P, Zhang L, Wu F, Chen Y, Wang J,
18 915 Peng C, Meng J, Yang L, Liu J, Wen B, Zhang N & Huang Z (2012) The oyster genome
19 916 reveals stress adaptation and complexity of shell formation. *Nature* **490**, 49–54.
20
21 917 72 Li B, Ruotti V, Stewart RM, Thomson JA & Dewey CN (2010) RNA-Seq gene expression
22 918 estimation with read mapping uncertainty. *Bioinformatics* **26**, 493–500.
23
24 919 73 Qi ST, Ma JY, Wang ZB, Guo L, Hou Y & Sun QY (2016) N6 -methyladenosine
25 920 sequencing highlights the involvement of mRNA methylation in oocyte meiotic
26 921 maturation and embryo development by regulating translation in *xenopus laevis*. *J. Biol.*
27 922 *Chem.* **291**, 23020–23026.
28
29 923 74 Altschul SF, Madden TL, Schäffer AA, Zhang J, Zhang Z, Miller W & Lipman DJ (1997)
30 924 Gapped BLAST and PSI-BLAST: a new generation of protein database search
31 925 programs. *Nucleic Acids Res.* **25**, 3389–3402.
32
33 926 75 Cock PJA, Chilton JM, Grüning B, Johnson JE & Soranzo N (2015) NCBI BLAST+
34 927 integrated into Galaxy. *Gigascience* **4**, 0–6.
35
36 928 76 Camacho C, Coulouris G, Avagyan V, Ma N, Papadopoulos J, Bealer K & Madden TL
37 929 (2009) BLAST+: Architecture and applications. *BMC Bioinformatics* **10**, 1–9.
38
39 930 77 Young MD, Wakefield MJ, Smyth GK & Oshlack A (2010) Gene ontology analysis for
40 931 RNA-seq: accounting for selection bias. *Genome Biol.* **11**, R14.
41
42 932 78 Supek F, Bošnjak M, Škunca N & Šmuc T (2011) Revigo summarizes and visualizes long
43 933 lists of gene ontology terms. *PLoS One* **6**.
44
45 934 79 Larsson J (2019) eulerr: Area-Proportional Euler and Venn Diagrams with Ellipses. .
46
47 935 80 Gu Z, Eils R & Schlesner M (2016) Complex heatmaps reveal patterns and correlations in
48 936 multidimensional genomic data. *Bioinformatics* **32**, 2847–2849.
49
50 937
51
52 938
53
54
55
56
57
58
59
60

1
2
3 939 **Figure legends**
4
5

6 940 Figure 1: m⁶A levels across oyster development.
7
8
9

10 941 **A.** m⁶A level quantified by LC-MS/MS in *Crassostrea gigas* embryo-larval stages pooled from
11
12 942 oocytes to D-larvae (n= 3) is compared to the m⁶A level in *Homo sapiens* and *Drosophila*
13
14 943 *melanogaster*; **B.** Dot blot quantification of m⁶A in total RNA throughout oyster development
15
16 944 (n=3); **C.** Dot blot quantification of m⁶A in polyA+ RNAs throughout oyster development (n=3)
17
18 945 Kruskal-Wallis test, $\alpha < 0,05$. E: Egg, F E: fertilized egg, 2/8C: two to eight cell embryos, M:
19
20 946 Morula, B: Blastula, G: Gastrula, T: Trochophore, D: D larvae. Chemiluminescence (B) and
21
22 947 fluorescence (C) are measured as a ratio between dot intensity of development stages and
23
24 948 their respective controls for each amount of RNA (120ng, 60ng and 30ng).
25
26
27
28
29
30
31
32
33
34
35

36 950 Figure 2: The putative conserved m⁶A machinery in *Crassostrea gigas*.
37
38
39

40 951 Domain architecture of actors of the m⁶A machinery identified by *in silico* analyses in the oyster
41
42 952 compared to the fruit fly and human, **A.** Writer proteins; **B.** Eraser protein; **C.** Reader proteins.
43
44 953 Putative domains involved in m⁶A processes are coloured (writers, green; eraser, red; readers,
45
46 954 blue). Other domains identified but not involved in m⁶A processes are indicated in grey. Only
47
48 955 one isoform is represented for each protein and each species for clarity (see supplementary
49
50 956 figure S2 for other isoforms).
51
52
53
54
55
56

57 958 Figure 3: Gene expression of the putative m⁶A machinery throughout oyster development
58
59
60

1
2
3 959 Expression levels of writers (**A**), eraser (**B**) and readers (**C**) identified by *in silico* analysis at
4
5
6 960 each development stage were inferred from the GigaTON database. Expression levels are
7
8 961 given in Transcripts Per kilobases per Million Reads (TPM) as the mean of the GigaTON values
9
10
11 962 according to the table S2. E: Egg, 2/8C: two to eight cell, M: Morula, B: Blastula, G: Gastrula,
12
13
14 963 T: Trochophore, D: D larvae, S: Spat, J: Juvenile.

15
16 964

17
18
19 965 Figure 4: Characterization of m⁶A-RNA binding proteins in oyster development.

20
21 966 **A.** Venn diagrams representation of proteins bound to the A- and/or m⁶A- oligos in nuclear and
22
23
24 967 cytosolic fractions of oyster embryo-larval stages. The number of proteins identified is
25
26
27 968 indicated. Some actors characterized in this study are highlighted: eIF3, YTHC1, hnRNPA2B1
28
29 969 and IGF2BP. **B.** Heatmap of gene expression levels of the proteins that bind specifically to the
30
31
32 970 m⁶A-oligo throughout oyster development. The expression level is normalized regarding the
33
34
35 971 maximum value for each gene according to the GigaTON database. **C.** GO term distribution
36
37 972 among the three expression clusters in B. **D.** Examples of GO term enrichment within the
38
39
40 973 expression clusters of the m⁶A-bound proteins. The $-\log_{10}(\text{p-value})$ associated to each term
41
42
43 974 is given. E: Egg, 2/8C: two to eight cells, M: Morula, B: Blastula, G: Gastrula, T: Trochophore,
44
45 975 D: D larvae, S: Spat, J: Juvenile.

46
47
48 976
49
50
51
52
53
54
55
56
57
58
59
60

1
2
3 977 **Supporting information:**

4
5 978 Data S1: Complete list of *in silico* identified putative m⁶A machinery proteins and their
6
7
8 979 respective BLAST results

9
10 980 Data S2: Identified proteins by RNA pull down coupled with mass spectrometry with m⁶A or
11
12
13 981 A-oligo, in nuclear or cytosolic protein extracts

14
15 982 Data S3: Complete list of GO terms of clustered genes of m⁶A interacting proteins (p-
16
17
18 983 value<0,05)

19
20 984 Table S1: Transitions used for each compound. A: first transition, B: second transition

21
22
23 985 Table S2: Table of correspondence between development stages in our study, and the
24
25
26 986 GigaTON database.

27
28
29 987
30
31
32
33
34
35
36
37
38
39
40
41
42
43
44
45
46
47
48
49
50
51
52
53
54
55
56
57
58
59
60

1
2
3 1 **A functional m⁶A-RNA methylation pathway in the oyster *Crassostrea gigas***
4
5
6 2 **assumes epitranscriptomic regulation of lophotrochozoan development**
7
8
9 3

10
11 4 **Authors**
12
13

14 5 Lorane LE FRANC¹, Benoit BERNAY², Bruno PETTON³, Marc SINCE⁴, Pascal FAVREL¹ and
15
16 6 Guillaume RIVIERE¹
17
18
19 7

20
21
22 8 **Addresses**
23
24

25 9 ¹Normandie Univ, UNICAEN, CNRS, BOREA, 14000 Caen, France.

26
27 10 Laboratoire Biologie des organismes et Ecosystèmes aquatiques (BOREA), Muséum
28
29 11 d'Histoire naturelle, Sorbonne Université, Université de Caen Normandie, Université des
30
31 12 Antilles, CNRS, IRD, Esplanade de la paix, 14032 Caen, France.
32
33

34
35 13 ²Normandie Univ, UNICAEN, SF ICORE, PROTEOGEN core facility, 14000 Caen, France
36
37

38 14 ³Ifremer, Laboratoire des Sciences de l'Environnement Marin, UMR 6539
39
40 15 CNRS/UBO/IRD/Ifremer, Centre Bretagne, 29280, Plouzané, France
41
42

43 16 ⁴ Normandie Univ, UNICAEN, Comprehensive Cancer Center F. Baclesse, SF ICORE,
44
45 17 PRISMM core facility, 14000 Caen, France.
46
47

48
49
50
51 19 **Corresponding author**
52

53 20 Guillaume Rivière (0033231565113 ; guillaume.riviere@unicaen.fr) , Normandie Univ,
54
55 21 UNICAEN, CNRS, BOREA, 14000 Caen, France (<https://borea.mnhn.fr/>). Tel :
56
57
58
59 22
60

1
2
3 **23 Running title**
4

5
6 **24** m⁶A-RNA methylation pathway in oyster development
7
8
9

10
11 **26 Abbreviations**
12

13
14 **27** N⁶-methyladenosine (m⁶A), Methyltransferase like (METTL), Wilms' tumor 1-associated
15
16 **28** protein (WTAP), RNA-binding motif 15 (RBM15), Ring finger E3 ubiquitin ligase (HAKAI), Zinc
17
18
19 **29** finger CCCH-type containing 13 (ZC3H13), AlkB homologue 5 (ALKBH5), Fat mass and
20
21 **30** obesity associated protein (FTO), YTH domain family protein (YTHDF), YTH domain
22
23
24 **31** containing protein (YTHDC), Heterogeneous nuclear ribonucleoproteins A2 B1
25
26
27 **32** (HNRNPA2B1), Proline rich coiled-coil 2a (Prcc2a), Eukaryotic initiation factor 3 (eIF3), Sterile
28
29 **33** sea water (SSW), Oocytes (E), Fertilized oocytes (F E), Two to eight cell embryos (2/8 C),
30
31
32 **34** Hours post fertilization (hpf), Morula (M), Blastula (B), Gastrula (G), D larvae (D), solid-phase
33
34
35 **35** reversible immobilization (SPRI), TPM (Transcripts Per Million), Gene ontology (GO), oyster
36
37 **36** m⁶A-interacting protein (Cg-m⁶A-BPs), S-adenosyl-methionine (SAM), maternal-to-zygotic
38
39
40 **37** transition (MZT), acetonitrile (ACN)
41
42
43

44
45 **39 Keywords**
46

47
48 **40** RNA, methylation, epitranscriptomics, oyster, development.
49
50

51
52
53
54 **42 Conflicts of interest**
55

56
57
58 **43** The authors declare they have no competing conflict of interest
59
60

Abstract

N^6 -methyladenosine (m^6A) is a prevalent epitranscriptomic mark in eukaryotic RNA, with crucial roles for mammalian and ecdysozoan development. Indeed, m^6A -RNA and the related protein machinery are important for splicing, translation, maternal-to-zygotic transition and cell differentiation. However, to date, the presence of an m^6A -RNA pathway remains unknown in more distant animals, questioning the evolution and significance of the epitranscriptomic regulation. Therefore, we investigated the m^6A -RNA pathway in the oyster *Crassostrea gigas*, a lophotrochozoan model whose development was demonstrated under strong epigenetic influence.

Using mass spectrometry and dot blot assays, we demonstrated that m^6A -RNA is actually present in the oyster and displays variations throughout early oyster development, with the lowest levels at the end of cleavage. In parallel, by *in silico* analyses, we were able to characterize at the molecular level a complete and conserved putative m^6A -machinery. The expression levels of the identified putative m^6A writers, erasers and readers were strongly regulated across oyster development. Finally, RNA pull-down coupled to LC-MS/MS allowed us to prove the actual presence of readers able to bind m^6A -RNA and exhibiting specific developmental patterns.

Altogether, our results demonstrate the conservation of a complete m^6A -RNA pathway in the oyster and strongly suggest its implication in early developmental processes including MZT.

This first demonstration and characterization of an epitranscriptomic regulation in a lophotrochozoan model, potentially involved in the embryogenesis, brings new insights into our understanding of developmental epigenetic processes and their evolution.

66 Introduction

67
68 The *N*⁶-methyladenosine (m⁶A) is the prevalent chemical RNA modification in all eukaryotic
69 coding and non-coding RNAs [1]. Messenger RNAs are the most heavily m⁶A methylated
70 RNAs, with m⁶A bases lying mostly in their 3' UTRs, at the vicinity of their stop codon [2–4]
71 and also in 5' UTRs and long internal exons [4,5]. *N*⁶-methylation of RNA adenosines is
72 responsible for RNA processing and, like DNA methylation or histone modifications,
73 contributes to the regulation of gene expression without changing the DNA or mRNA
74 sequence. Therefore m⁶A constitutes a new layer of post-transcriptional gene regulation, which
75 is emerging or has been proven critical in various biological processes, and referred to as
76 epitranscriptomic [2].

77
78 The dynamics and biological outcomes of m⁶A levels are the results of the activity of a complex
79 protein machinery comprising writers, erasers and readers. The addition of a methyl group to
80 the 6th nitrogen of RNA adenosines is catalysed by m⁶A writers with distinct properties.
81 Methyltransferase like 16 (METTL16) is a 'stand-alone' class I methyltransferase that
82 recognizes the UACA*GAGAA consensus sequence (with * indicating the target adenosine)
83 [6]. By contrast, METTL3 transfers methyl groups to adenosines within the RRA*CH motif
84 [2,3,7]. METTL3 is only active within a tripartite 'core complex' [8] comprising METTL3,
85 METTL14 which enhances the methyltransferase activity supported by the MTA-70 domain of
86 METTL3 [9,10] and the regulator protein Wilms' tumor 1-associated protein (WTAP) [4,9,11].
87 This core complex can interact with Virilizer-like (or KIAA1429) [12], ring finger E3 ubiquitin

1
2
3 88 ligase (HAKAI) [12,13], zinc finger CCCH-type containing 13 (ZC3H13) [12,14], RNA-binding
4
5 89 motif 15 (RBM15) and RBM15B [7,15] which are suspected to intervene in the core complex
6
7
8 90 activity and target specificity. The demethylation of adenosines has been demonstrated to be
9
10
11 91 an active process catalysed by eraser enzymes belonging to the Fe(II)/2-oxoglutarate
12
13 92 dioxygenase family: AlkB homologue 5 (ALKBH5) [16,17] and the fat mass and obesity
14
15 93 associated protein (FTO) [17,18].

16
17
18 94 A growing number of reader proteins which recognize the m⁶A-RNA mark is being described.
19
20
21 95 They may be divided into two classes depending on the presence of a YTH domain
22
23 96 (YTH) domain in their primary sequence. The YTH protein family includes YTH domain family
24
25 97 protein 1-3 (YTHDF1-3) and YTH domain containing protein 2 (YTHDC2), which are cytosolic
26
27 98 m⁶A readers involved in m⁶A-RNA stability and translation [19–22]. The fifth YTH member is
28
29 99 YTHDC1, which is present in the nucleus and controls splicing [23] and nuclear export [24] of
30
31
32 100 m⁶A-RNA. The second class of readers comprises proteins without YTH domain which are
33
34
35 101 involved in several molecular mechanisms. For example, the heterogeneous nuclear
36
37 102 ribonucleoprotein A2 B1 (HNRNPA2B1) is important for miRNA processing [25]. Insulin-like
38
39 103 growth factor 2 mRNA binding protein 1-3 (IGF2BP 1-3) [26] and proline-rich coiled-coil 2a
40
41 104 (Prcc2a) [27] participate in RNA stability while eukaryotic initiation factor 3 (eIF3) guides cap-
42
43 105 independent translation [5].
44
45
46
47
48
49
50
51
52

53 106
54
55 107 The m⁶A epitranscriptomes underlie important biological functions, most of which being related
56
57 108 to developmental processes, including the control of cell differentiation [27–32], maternal to
58
59 109 zygotic transition (MZT) [33], sex determination [7,34] and gametogenesis [16,21,35,36]. Such
60

1
2
3 110 critical epitranscriptomic outcomes are conserved in the animal evolution and were
4
5
6 111 characterized in both vertebrates and ecdysozoans, i.e. mammals and drosophila.

7
8 112 However, such conserved biological significance originates in diverse epitranscriptomic
9
10
11 113 mechanisms. Indeed, not all ecdysozoans bear a complete m⁶A-RNA machinery, such as *C.*
12
13 114 *elegans* whose genome is devoid of the related protein machinery with the exception of a
14
15
16 115 putative orthologue of METTL16 [37,38]. In addition, no m⁶A eraser has been described to
17
18
19 116 date in non-vertebrate models, and especially ecdysozoans such as the drosophila or *C.*
20
21 117 *elegans* [38–40], where it cannot be excluded that m⁶A-RNA methylation could be removed by
22
23
24 118 the activity of characterised 6mA-DNA demethylases [41,42]. This situation may illustrate a
25
26
27 119 growing complexity of epitranscriptomic mechanisms during the animal phylogeny and raises
28
29
30 120 fundamental questions about its evolution and its presence in organisms distant from
31
32 121 mammals and ecdysozoans. However, to date, no data about a possible epitranscriptomic
33
34
35 122 regulation is available to our knowledge in lophotrochozoans, the understudied sister group of
36
37 123 ecdysozoans within protostomes, although representing an important range of metazoan
38
39
40 124 biodiversity.

41
42 125 The Pacific oyster *Crassostrea gigas* (i.e. *Magallana gigas*) is a bivalve mollusc whose great
43
44
45 126 ecological and economical significance allowed its emergence as a model species within
46
47
48 127 lophotrochozoan organisms. As such, an important amount of genetic, transcriptomic and
49
50
51 128 epigenetic data have been generated in this model. Interestingly, the embryolarval
52
53 129 development of *C. gigas* is described to be under the strong epigenetic influence of DNA
54
55
56 130 methylation [43–47] and histone marks [48–50]. Besides, oyster development occurs exposed
57
58
59 131 to external environmental conditions, and in other models the m⁶A methylation of RNA and/or
60

1
2
3 132 the expression of its machinery can be induced by heat stress, UV exposure or endocrine
4
5
6 133 disruptors [5,51–54], questioning the presence of an m⁶A pathway in *C. gigas* and its
7
8 134 significance in oyster early development.

9
10
11 135 To investigate this, we measured m⁶A levels in RNA across the entire embryolarval life of the
12
13
14 136 oyster using mass spectrometry and dot-blot. We also searched the available *in silico*
15
16 137 resources for putative conserved m⁶A-related proteins in *C. gigas* genomic data as well as
17
18
19 138 their cognate expression kinetics using RNAseq assembly analyses. We also performed RNA-
20
21 139 pulldown with a synthetic m⁶A-RNA oligonucleotide coupled to liquid chromatography and
22
23
24 140 mass spectrometry (LC-MS/MS) to characterize potential oyster m⁶A-binding proteins. To our
25
26
27 141 knowledge, this study is the first report unravelling epitranscriptomic mechanisms outside
28
29 142 vertebrate and ecdysozoan animal models.

30
31
32 143

33 34 35 144 **Results:**

36
37
38 145

39
40
41 146 **m⁶A is present in oyster RNA, differentially affects distinct RNA populations and**
42
43 147 **displays variations during embryonic life.**

44
45
46 148 Mass spectrometry measurements revealed that m⁶A is present in oyster RNA, with global
47
48
49 149 m⁶A/A levels of ca. 0.3%, a value comparable to what has been found in the human and the
50
51 150 fruit fly (Figure 1A). Immunoblot assays indicate that total and polyA⁺ RNA present variable
52
53
54 151 amounts of m⁶A during oyster development and that these variations display distinct profiles
55
56
57 152 suggesting specific methylation patterns between RNA populations. Indeed, N⁶A-methylation
58
59 153 in total RNA is the highest in the early stages (oocytes and fertilized oocytes) then gradually
60

1
2
3 154 decreases until the morula stage before gradually increasing again up to the trochophore stage
4
5
6 155 when it recovers its maximum (Figure 1B). In contrast, m⁶A levels in polyA⁺ RNA are hardly
7
8 156 detected in early stages but display a peak in the gastrula and trochophore stages (Figure 1C).
9

10
11 157

12
13
14 158 **m⁶A machinery is conserved at the molecular level in the oyster.**

15
16 159 *In silico* analyses led to the identification of oyster sequences encoding putative orthologues
17
18
19 160 of m⁶A writers, erasers and readers that are present in the human and/or in the human and
20
21 161 the fruit fly.

22
23
24 162 All the eight m⁶A-RNA writers characterized in the human and/or drosophila at the time of the
25
26
27 163 study, namely METTL3, METTL14, WTAP, Virilizer-like, HAKAI, ZC3H13, RBM15/15B and
28
29
30 164 METTL16, were present in the oyster at the gene level. The encoded protein primary
31
32 165 sequences all display the specific domains required for enzymatic activity and/or binding. They
33
34
35 166 include MT-A70 and AdoMetMtases SF domains for METTL3, METTL14 and METTL16,
36
37 167 respectively, that bear the methyltransferase activity. Oyster WTAP and Virilizer-like
38
39
40 168 orthologues exhibit WTAP and VIR_N domains, respectively, that are required in their human
41
42
43 169 counterparts to bind and activate the catalytic subunit of the m⁶A-RNA methyltransferase
44
45
46 170 complex. Oyster Hakai and RBM15/15B present RHHL, RHF-Zn-BS and specific RRM
47
48 171 domains, respectively, similar to human and fruit fly orthologues. Besides, the oyster ZC3H13
49
50
51 172 bears the Rho SF domain present in the human, but not in the fruit fly orthologue (Figure 2A).
52
53 173 *C. gigas* also presents a putative m⁶A-RNA eraser, ALKBH5, which is present in the human
54
55
56 174 but has not been characterized in drosophila. The oyster ALKBH5 exhibits a 2OG-FeII_Oxy
57
58
59 175 domain suggestive of a presumably conserved catalytic functionality through fe²⁺-dependent
60

1
2
3 176 oxoglutarate oxidation. Of note, no orthologue of the human FTO eraser could be identified in
4
5
6 177 the oyster genomic or transcriptomic databases available to date (Figure 2B).

7
8 178 Many m⁶A reader orthologues have also been found in the oyster, including proteins containing
9
10
11 179 a YTH domain, such as YTHDF, YTHDC1 and YTHDC2. An oyster Prrc2a-like protein
12
13
14 180 produces homology with the human Prrc2a, especially within the m⁶A-binding GRE-rich
15
16
17 181 domain. Oyster readers also include a heterogeneous nuclear ribonucleoprotein-coding gene,
18
19 182 hnRNPA2B1 with greater sequence similarity with the drosophila counterpart than with the
20
21
22 183 human orthologue. Similarly, the IGF2BP-coding sequence has also been found in *C. gigas*
23
24 184 (Figure 2C). Five oyster sequences display homologies with eIF3a which is able to bind m⁶A-
25
26
27 185 RNA [5] but it was not possible to discriminate whether a unique oyster predicted protein was
28
29
30 186 an eIF3a orthologue.

31
32 187 Overall, these results indicate the conservation of a complete m⁶A-RNA machinery in the
33
34
35 188 oyster. The complete list of the identified genes encoding the conserved m⁶A machinery actors
36
37
38 189 and their isoforms, as well as the related information is given in the supplementary data (Data
39
40 190 S1).

41
42
43 191

44 45 192 **Oyster putative m⁶A actors display expression level variations across development.**

46
47
48 193 RNAseq data analyses showed that all the oyster m⁶A-related genes were expressed during
49
50
51 194 the early life (Figure 3). Their expression level displayed gene-specific profiles, most of them
52
53
54 195 being variable throughout oyster development.

55
56 196 The expression of writers belonging to the core methylation complex is weak overall. METTL3
57
58
59 197 and WTAP share similar profiles with little expression increasing up to the gastrulation and
60

1
2
3 198 remaining stable afterwards. In contrast METTL14 displays a weak expression level across
4
5
6 199 the embryo larval life. The expression profile of Virilizer-like resembles WTAP, while HAKAI,
7
8 200 RBM15/15B and METTL16 seem to have mRNA levels which decrease after cleavage,
9
10
11 201 whereas those of ZC3H13 transcript variants seem to drop at the D larva stage. Interestingly,
12
13
14 202 METTL16 mRNA levels display an opposite developmental profile when compared to METTL3
15
16 203 expression; with the highest values during cleavage which decrease later on (Figure 3A).
17
18
19 204 ALKBH5 transcripts are weakly represented within oyster early embryos and the higher TPM
20
21 205 values are found in gastrulas. However, maximum levels are observed after metamorphosis in
22
23
24 206 juveniles (Figure 3B).
25
26
27 207 Regarding m⁶A putative readers, the expression of YTH family genes during development
28
29 208 showed different patterns. In fact, YTHDF is the most represented YTH-domain bearing actor
30
31 209 and YTHDF TPM values are ca. 5-fold higher than all the other oyster YTH readers. YTHDF is
32
33
34 210 strongly expressed at the beginning of development until a peak at the morula stage. Prrc2a
35
36
37 211 is the most represented reader at the mRNA level in oyster embryos, and the sum of the TPM
38
39
40 212 of the two Prrc2a oyster isoforms are at most ca. 20-fold higher than those of YTH family.
41
42
43 213 However, Prrc2a and YTHDF transcript content profiles are similar across oyster development,
44
45
46 214 and also remind of the IGF2BP mRNA levels.
47
48
49 215 By contrast, the two isoforms of YTHDC1 identified by *in silico* analysis, YTHDC1.1 and
50
51 216 YTHDC1.2, display similar patterns together with YTHDC2, with a maximum representation in
52
53
54 217 gastrulas. The expression of hnRNPA2B1 isoforms has likewise patterns except for a marked
55
56 218 drop at the D larvae stage (Figure 3 C).
57
58
59 219
60

1
2
3 **220 Oyster orthologues of m⁶A-RNA interacting proteins bind m⁶A RNA *in vitro*.**
4

5
6 221 To determine whether oyster proteins can bind m⁶A-RNA, we performed RNA-pulldown of
7
8 222 cytoplasmic and nuclear embryonic cell extracts using a methylated versus a non-methylated
9
10
11 223 oligonucleotide, followed by LC/MS-MS characterisation and identification of the captured
12
13
14 224 proteins with the Mascot software.
15

16 225 In nuclear extracts, we detected 591 proteins able to bind both the methylated and
17
18 226 unmethylated oligos. We identified 43 proteins specific to unmethylated RNA while 131
19
20
21 227 proteins specifically bind the m⁶A-methylated oligo. In cytosolic extracts, there were
22
23
24 228 respectively 646, 436 and 36 of such proteins, respectively. Regardless of the methylation
25
26
27 229 status, more proteins in the cytoplasmic extracts can bind to the RNA oligonucleotides than in
28
29
30 230 the nuclear extracts (1118 proteins vs. 765, respectively). However, more nuclear proteins are
31
32 231 found exclusively bound to the m⁶A-containing oligo than cytoplasmic proteins (131 vs. 36, i.e.
33
34 232 17 % vs. 3 %, respectively). In addition, many nuclear and cytoplasmic proteins can bind both
35
36
37 233 the methylated and the non-methylated oligo (591 vs. 646, i.e. 77 % vs. 58 %). An important
38
39
40 234 number of proteins in the cytoplasmic extract were found exclusively bound to the non-
41
42
43 235 methylated oligo, whereas only a limited number of nuclear proteins display such a specificity
44
45 236 (436 vs. 43, i.e. 39 % vs. 6 %). Among the 167 m⁶A-specific proteins in oyster extracts, only 5
46
47
48 237 were found in both the nuclear and cytoplasmic extracts. These results show that oyster
49
50
51 238 proteins can directly or indirectly bind m⁶A-RNA, and suggest an important
52
53 239 compartmentalization of m⁶A-related processes.
54

55
56 240 Among the identified proteins in this assay, four of the putative oyster m⁶A readers are found,
57
58 241 YTHDC1, hnRNPA2B1, IGF2BP and eIF3. In the nuclear extracts YTHDC1 is uncovered as
59
60

1
2
3 242 m⁶A-specific whereas hnRNPA2B1 and IGF2BP were present complexed with both the m⁶A-
4
5
6 243 and A-oligos. In the cytoplasmic extracts, YTHDC1 and eIF3a are m⁶A-specific while
7
8 244 hnRNPA2B1, IGF2BP were pulled down by both methylated and unmethylated oligos (Figure
9
10
11 245 4A).

12
13 246 These results demonstrate that some proteins in the oyster can specifically bind m⁶A-RNA and
14
15
16 247 that the putative m⁶A reader orthologues in the oyster are conserved at the protein level and
17
18
19 248 are able to interact with m⁶A-RNA.

20
21
22 249

23
24 250 **The m⁶A-interacting protein-coding genes display clustered expression regulation and**
25
26
27 251 **functional annotation during oyster development.**

28
29 252 The mRNA expression level of the genes encoding the 162 oyster m⁶A-interacting protein (Cg-
30
31
32 253 m⁶A-BPs) was examined using RNAseq databases. Most of them display a specific and
33
34
35 254 regulated expression level across oyster developmental stages. However, three main
36
37
38 255 expression clusters could be distinguished according to their developmental mRNA expression
39
40
41 256 level profile. Cluster 1 includes genes that show high expression at the beginning of the embryo
42
43
44 257 life (i.e. cleavage) and strongly decrease after gastrulation; the second cluster contains weakly
45
46
47 258 expressed genes except in the latest examined larval phases, after gastrulation (i.e.
48
49
50 259 Trochophore and D Larvae); cluster 3 groups genes that show an expression peak during
51
52
53 260 gastrulation (Figure 4B).

54
55
56 261 The Gene Ontology annotation of the Cg-m⁶A-BP genes reveal that the distinct clusters are
57
58
59 262 related to distinct functional pathways as indicated by the little - if any - common GO terms
60
263 between them (Figure 4C). However, the functional pathways of all three gene clusters point

1
2
3 264 out to their implication in translation and its regulation, although the terms enriched in each
4
5
6 265 cluster illustrate different aspects of translation, such as translation initiation (cluster 1), splicing
7
8 266 and nuclear export (cluster 2) and ribosomal and mitochondrial processes (cluster 3)
9
10
11 267 respectively (Figure 4D).
12

13
14 268

16 269 **Discussion**

17
18
19
20 270 This work demonstrates that m⁶A-RNA is present and variable during the embryo-larval life of
21
22
23 271 the oyster, and that *C. gigas* exhibits putative conserved and functional m⁶A-RNA writers,
24
25
26 272 eraser and readers. The dynamics of such mark and of its actors strongly suggest a biological
27
28 273 significance of the epitranscriptomic pathway in the control of development of a
29
30
31 274 lophotrochozoan species, which has, to date, never been demonstrated to our knowledge.
32

33 275 **m⁶A-RNA levels vary across oyster development.**

34
35
36 276 Using mass spectrometry and immunological measurements, we showed that oyster RNA is
37
38
39 277 m⁶A-methylated. The global proportion of N⁶-methyladenosine in RNA in the developing oyster
40
41
42 278 (0.28 %) is similar to those observed elsewhere in the animal kingdom, such as in the fruit fly
43
44 279 (0.24 %) [34] or the human (0.11- 0.23 %) [55] (Figure 1A), despite those values are difficult
45
46
47 280 to compare because they were not measured within the same developmental phase (adult flies
48
49 281 and human cell lines vs. oyster embryos). However, the comparable magnitude of m⁶A-RNA
50
51
52 282 amounts between taxa, in contrast to DNA methylation [46], may indicate conserved biological
53
54
55 283 significance of epitranscriptomic processes between groups. The amount of m⁶A in total RNA
56
57 284 displays a striking decrease during cleavage and then recovers its maximum levels at the end
58
59
60 285 of the gastrulation (Figure 1B). Therefore, the m⁶A decrease in total RNA during cleavage, i.e.

1
2
3 286 before the transcription of the zygotic genome starts, reflects a degradation of maternal m⁶A-
4
5
6 287 RNAs or their demethylation. However, all RNA populations do not exhibit the same pattern,
7
8 288 indeed polyA⁺ RNAs are m⁶A methylated only after cleavage. The extent of polyadenylation
9
10
11 289 of oyster maternal messenger RNAs accumulating during vitellogenesis is unknown.
12
13
14 290 Therefore, which maternal RNA population(s) is methylated in oyster oocytes is unclear.
15
16 291 Nevertheless, the observation that m⁶A-RNA levels are variable and affecting distinct RNA
17
18
19 292 populations across embryonic stages strongly favours an important biological significance of
20
21
22 293 m⁶A-RNA in oyster development. We hypothesize that oyster maternal messenger RNAs are
23
24 294 poorly polyadenylated, and that m⁶A, aside polyadenylation, might play a role in the stability of
25
26
27 295 quiescent maternal mRNAs. Alternatively, other maternal RNA populations such as snRNA,
28
29
30 296 miRNA, rRNA or lncRNA might be methylated [6,15,25,56], which become demethylated or
31
32 297 degraded up to the morula stage. The later increase in m⁶A RNA after cleavage could therefore
33
34
35 298 be the result of the methylation of the increasingly transcribed RNAs from the blastula stage,
36
37
38 299 including polyadenylated mRNAs.

300 **The m⁶A-RNA machinery is conserved in the oyster and regulated during development.**

301 The important regulation of m⁶A levels during oyster development assumes the presence of a
302 related protein machinery. We identified *in silico* cDNA sequences encoding conserved
303 putatively functional orthologues of m⁶A-RNA writers, eraser and readers in the oyster, with
304 great confidence (homologies ranging from ca. 30 to 65 % with their human counterpart, see
305 Data S1). The writers include all the members of the methylation complex (METTL3, METTL14,
306 WTAP, Virilizer-like, Hakai, ZC3H13, RBM15/15B) identified to date in the human and the fruit
307 fly [7,11,12,14,15,57]. We also identified an orthologue of the stand-alone METTL16 m⁶A
308
309
310

1
2
3 308 methyltransferase. Each orthologue bears the conserved domain(s) demonstrated to be
4
5
6 309 implicated in the catalytic and/or binding activity of their cognate counterpart in other species,
7
8
9 310 such as the MT-A70 domain which transfers methyl groups from the S-adenosyl-methionine
10
11 311 (SAM) to the N^6 nitrogen of RNA adenines [57]. Of the two proteins that can erase RNA
12
13
14 312 methylation, only ALKBH5, which is important for mouse spermatogenesis [16], was identified
15
16 313 at the cDNA level in the oyster. Indeed, no *C. gigas* sequence displayed significant homology
17
18
19 314 with the mammalian FTO protein, whose functional significance remains controversial [17].
20
21
22 315 Most the characterized m^6A -RNA readers are also present at the molecular level in the oyster
23
24 316 and are putatively able to bind m^6A regarding their primary sequence, such as the YTHDC and
25
26
27 317 YTHDF family members [19,21,23,58], Prrc2A [27], HnRNPA2B1 [25] and IGF2BP [26]. Of
28
29
30 318 note, some of these readers have not been characterized to date in *D. melanogaster* but
31
32 319 display strong homologies between humans and oysters. In mammals, eIF3a has important
33
34
35 320 functional outcomes in cap-independent translational stress response [5]. However, it was not
36
37
38 321 possible to ascribe a single oyster sequence as a unique eIF3a orthologue (Data S1), although
39
40 322 its presence was demonstrated by RNA pull down (see below) (see Data S2). Altogether, *in*
41
42
43 323 *silico* results show the conservation of a complete m^6A -RNA machinery in the oyster. To date
44
45 324 to our knowledge, this is the first demonstration in a lophotrochozoan organism of an
46
47
48 325 epitranscriptomic pathway. Its presence suggests its ancestral origin, and questions its
49
50
51 326 biological significance in oyster development.

52
53 327 To investigate this, we analysed the expression level of the m^6A machinery genes using RNA-
54
55
56 328 seq data. Our results indicate that the core methylation complex (METTL3, METTL14 and
57
58
59 329 WTAP) would not be active during cleavage because of the absence of METTL3 and little
60

1
2
3 330 WTAP expression. METTL16 catalyses the downregulation of SAM methyl donor availability
4
5
6 331 in mammals [59]. If METTL16 function is conserved in the oyster as suggested by the high
7
8 332 sequence homology, the peak in METTL16 expression, together with the weak expression of
9
10
11 333 the core complex in 2/8 cell embryos is consistent with an absence of m⁶A-RNA up to the
12
13
14 334 blastula stage. Then, the core complex would likely be active as soon as the end of cleavage
15
16 335 (i.e. since the blastula stage), in line with the increase in m⁶A levels observed at the same time.
17
18
19 336 The correlation between the increasing METTL3 expression and m⁶A-RNA levels after
20
21 337 cleavage strongly favours the conservation of the methyltransferase activity of the oyster MT-
22
23
24 338 A70 domain. Interpreting the regulation of the m⁶A activity by the other methyltransferase
25
26 339 complex members (i.e. Virilizer-like, HAKAI, ZC3H13 and RBM15/15B) is difficult because how
27
28 340 - or even if - oyster orthologues act within the complex is not known. Nevertheless, their specific
29
30 341 expression profiles may reflect their implication in the regulation of distinct biological contexts.
31
32
33 342 There might be little functional significance of active m⁶A-RNA erasure during oyster
34
35 343 development, consistent with the normal embryonic phenotype of ALKBH5 knockdown mice
36
37 344 [16]. Overall, the m⁶A readers display distinct developmental expression patterns. While
38
39 345 YTHDF and Prrc2a peak during cleavage, YTHDC1, YTHDC2, IGF2BP and hnRNPA2B1
40
41 346 mRNA levels gradually increase up to the gastrulation and remain mostly highly expressed
42
43 347 afterwards (except for hnRNPA2B1 and IGF2BP). These profiles evoke the mediation of
44
45 348 distinct biological functions depending on the reader and the developmental phases.
46
47 349 Therefore, we hypothesized that YTHDF and Prrc2a might participate in the blastulean
48
49 350 transition in the oyster. Indeed, in the zebrafish, a YTHDF reader triggers the maternal-to-
50
51 351 zygotic transition through the decay of the maternal m⁶A RNAs during cleavage [33]. The role
52
53
54
55
56
57
58
59
60

1
2
3 352 in the axon myelination and specification of mouse oligodendrocytes [27] is unlikely conserved
4
5
6 353 for *Prrc2a* because the oyster orthologue is expressed before the neurogenesis is detected in
7
8 354 trochophore stages [60]. Alternatively, the early expression of *Prrc2a* suggests that it might
9
10
11 355 rather compete with YTHDF for m⁶A-RNA targets [27], thereby possibly acting in oyster MZT,
12
13
14 356 bringing new perspectives into this process which remains poorly understood in
15
16 357 lophotrochozoans. In mammals m⁶A is implicated in the embryonic cell fate [30,31] notably via
17
18
19 358 the regulation of cell differentiation by YTHDC2 [32] or hnRNPA2B1 [29]. In the oyster,
20
21
22 359 YTHDC1, YTHDC2, IGF2BP and hnRNPA2B1 have their maximum expression during
23
24 360 gastrulation correlated to the second m⁶A peak, suggesting similar implications.
25
26

27 361 **Putative oyster m⁶A readers actually bind m⁶A-RNA *in vitro*.**

28
29 362 To better approach the developmental processes involving m⁶A in the oyster, we characterized
30
31
32 363 the proteins that can interact with m⁶A-RNA using a methylated-RNA-pulldown / mass
33
34
35 364 spectrometry assay. We identified 162 proteins able to specifically bind the m⁶A-RNA oligo in
36
37
38 365 embryonic cell extracts, demonstrating the actual presence of genuine m⁶A-readers in the
39
40 366 oyster. Most (ca. 75 %) of these proteins were found in nuclear extracts and only 5 were found
41
42
43 367 in both the cytoplasmic and nuclear fractions, showing an important compartmentalization of
44
45
46 368 the epitranscriptomic pathway. Regarding the little number of m⁶A readers in other animals,
47
48 369 and because the assay conditions do not discriminate between direct and indirect interactions,
49
50
51 370 we hypothesize that most these proteins indirectly bind m⁶A via a limited number of 'scaffold'
52
53
54 371 m⁶A readers. Such authentic readers that only bind the m⁶A-RNA oligo in our assay likely
55
56 372 include YTHDC1 and eIF3a, which have been demonstrated to directly bind m⁶A in other
57
58 373 species, demonstrating the conservation of the m⁶A-binding capacity and specificity of the YTH
59
60

1
2
3 374 domain in the oyster. Besides, YTHDC1 is found in both cell fractions, suggesting its
4
5
6 375 implication in the trafficking of m⁶A-RNA across the nuclear envelope [24], and reinforcing the
7
8 376 hypothesis that YTH proteins could participate in oyster MZT and cell differentiation. The
9
10
11 377 presence of the oyster eIF3a in the cytoplasm is consistent with a conserved role in m⁶A-
12
13
14 378 mediated translation processes, such as cap-independent translation [5].

16 379 **Possible functions of m⁶A-RNA in oyster development.**

18
19 380 We investigated the expression level and the functional annotation of the 162 genes encoding
20
21 381 the m⁶A-interacting proteins across oyster early life. These genes can be clustered into three
22
23
24 382 successive expression phases corresponding to three distinct functional pathways, which are
25
26
27 383 independent albeit all mostly related to translation regulation. The cluster 1 is mostly expressed
28
29 384 during the cleavage and the associated GO terms are related to the initiation of translation,
30
31
32 385 consistent with maternal RNA consumption before MZT is complete and the zygotic genome
33
34
35 386 becomes fully activated. The genes within cluster 3 show an expression peak during
36
37 387 gastrulation. Their ontology terms evoke ribosomal and mitochondrial processes, the latter
38
39
40 388 being required for energy supply and signalling integration during gastrulation [61–64]. The
41
42
43 389 cluster 2 contains genes that peak after gastrulation and which are related to splicing and
44
45
46 390 nuclear export. Such functional annotations are in line with a fine regulation of transcript variant
47
48 391 translation within the distinct cell lineages in the three cell layers of the late embryos.

49
50 392
51
52
53 393 Taken together, our findings bring to light a possible implication of m⁶A in oyster development.
54
55
56 394 First, during cleavage the decrease of m⁶A-RNA, the weak expression of methyltransferase
57
58 395 complex genes, the maximum of YTHDF gene expression and the expression of Cg-m⁶A-BPs
59
60

1
2
3 396 related to the initiation of the translation strongly suggest the implication of m⁶A in MZT in *C.*
4
5
6 397 *gigas*. Second, the increasing m⁶A level during gastrula stage is correlated to the increase of
7
8 398 methyltransferase complex gene expression. In addition, the increased RNA level of readers
9
10
11 399 putatively related to cell differentiation and the peak of gene expression of *Cg*-m⁶A-BPs
12
13 400 associated to ribosomal and mitochondrial processes, support the hypothesize of a m⁶A
14
15
16 401 implication in gastrulation. Finally, the highest m⁶A level at the trochophore stage, the gene
17
18
19 402 expression of the methyltransferase complex and of readers associated to cell differentiation,
20
21
22 403 as well as high RNA level of *Cg*-m⁶A-BPs related to splicing and nuclear export is correlated
23
24 404 with the fine cell differentiation taking place at this stage. However, inferring the biological
25
26
27 405 significance of m⁶A in development from the indirect and incomplete functional annotation of
28
29
30 406 the oyster genome is only limited. Characterization of the precise targets of m⁶A and how their
31
32
33 407 individual methylation is regulated across development, for example using high throughput
34
35
36 408 sequencing of precipitated m⁶A-RNA (MeRIP-seq), could be extremely relevant to better
37
38
39 409 understand this issue. In addition, despite sequence conservation and binding ability of oyster
40
41
42 410 actor orthologues strongly suggest functional conservation, future dedicated studies such as
43
44
45 411 biochemical inhibition or gene inactivation could help demonstrate their genuine biological
46
47
48 412 function. Besides, there seems to be an inverse correlation between m⁶A-RNA and 5mC-DNA
49
50
51 413 levels during the considered oyster developmental window [46]. This may suggest an interplay
52
53
54 414 between epigenetic and epitranscriptomic marks, possibly reflecting competition for methyl-
55
56
57 415 donor availability [59] or a link by histone epigenetic pathways [65,66].
58
59
60 416 Regarding the potential influence of the environment on m⁶A and the accumulation of RNA in
61
62
63 417 oocytes, we are at present investigating our hypothesis that m⁶A may convey intergenerational

1
2
3 418 epitranscriptomic inheritance of maternal life traits in the oyster. On an evolutionary
4
5
6 419 perspective, the presence of a putatively fully conserved epitranscriptomic pathway in the
7
8
9 420 oyster suggests that it was already present in the bilaterian common ancestor thereby in favour
10
11 421 of an important biological significance. Why *Drosophila* and *Caenorhabditis* seem to have lost
12
13 422 specific m⁶A-RNA erasers could be related to a sub-functionalization of the DMAD [41] and
14
15
16 423 NMAD-1 [42] N⁶-methyladenine DNA demethylase activity broadened towards RNA. However,
17
18
19 424 more work is required to better understand the evo-devo implications of our results.
20

21 425
22
23
24 426 To conclude, in this work we report the discovery and characterisation of a putatively complete
25
26
27 427 epitranscriptomic pathway in a lophotrochozoan organism, the oyster *Crassostrea gigas*. This
28
29
30 428 pathway includes the m⁶A mark in RNA and the actors of all the aspects of its regulation
31
32 429 (writers, eraser, readers) which are conserved at the molecular level and putatively functional.
33

34
35 430 We show that m⁶A levels are variable across oyster development and that m⁶A differentially
36
37
38 431 affects distinct RNA populations. Expression levels of the related enzymatic machinery is
39
40 432 consistent with the observed m⁶A level variations. We demonstrate the m⁶A binding capacity
41
42
43 433 and specificity of putative oyster m⁶A readers in the cytoplasm and nucleus of embryolarval
44
45
46 434 cells. These readers mediate distinct putative biological outcomes depending on the
47
48 435 development stage considered. From these results we hypothesize that early decay of
49
50
51 436 maternal m⁶A RNA participates in maternal-to-zygotic transition during cleavage and that later
52
53
54 437 *de novo* zygotic m⁶A methylation contributes to gastrulation and cell differentiation. This first
55
56 438 characterisation of an m⁶A-epitranscriptomic pathway in a lophotrochozoan organism, together
57
58
59 439 with its potential implication in development, opens new perspectives on the evolution of
60

1
2
3 440 epigenetic mechanisms and on the potential epitranscriptomic inheritance of environmentally-
4
5
6 441 induced life traits.

7
8 442

9
10
11
12 443 **Methods:**

13
14
15 444

16
17
18 445 **Animals:**

19
20
21 446 Broodstock oysters [67] and oyster embryos [46] were obtained at the IFREMER marine
22
23 447 facilities (Argenton, France) as previously described. Briefly, gametes of mature broodstock
24
25 448 oysters were obtained by stripping the gonads and filtering the recovered material on a 60 µm
26
27 449 mesh to remove large debris. Oocytes were collected as the remaining fraction on a 20 µm
28
29 450 mesh and spermatozoa as the passing fraction on a 20 µm mesh. Oocytes were pre-incubated
30
31 451 in 5 L of UV-treated and 1 µm filtered sterile sea water (SSW) at 21 °C until germinal vesicle
32
33 452 breakdown. Fertilization was triggered by the addition of ca. 10 spermatozooids per oocyte. After
34
35 453 the expulsion of the second polar body was assessed by light microscopy, embryos were
36
37 454 transferred in 150 L tanks of oxygenated SSW at 21 °C. The development stages were
38
39 455 determined by light microscopy observation. The stages collected were oocytes (E,
40
41 456 immediately before sperm addition), fertilized oocytes (F E, immediately before transfer to
42
43 457 150L tanks), two to eight cell embryos (2/8 C, ca. 1.5 hours post fertilization (hpf)), morula (M,
44
45 458 ca. 4 hpf), blastula (B, ca. 6 hpf), gastrula (G, ca. 10 hpf), trochophore (T, ca 16 hpf) and D
46
47 459 larvae (D, ca. 24 hpf). For each development stage, 3 million embryos were collected as the
48
49 460 remaining fraction on a 20 µm mesh and centrifuged at 123 g for 5min at room temperature.
50
51
52
53
54
55
56
57
58
59
60

1
2
3 461 Supernatant was discarded and samples of 1 million embryos were then snap-frozen in liquid
4
5
6 462 nitrogen directly of after resuspension in Tri-Reagent (Sigma-Aldrich, St Louis, MO, USA) (1
7
8 463 mL/10⁶ embryos) and stored at -80 °C. Three distinct experiments were realized (February to
9
10
11 464 May 2019) using the gametes of 126 to 140 broodstock animals, respectively.
12

13
14 46515
16 466 **RNA extraction:**

- 17
-
- 18
-
- 19 467
- total RNA extraction

20
21 468 RNA was extracted using phenol-chloroform followed by affinity chromatography as previously
22
23
24 469 described [68]. Briefly, embryos were ground in Tri-Reagent (Sigma-Aldrich) and RNA was
25
26
27 470 purified using affinity chromatography (Nucleospin RNA II kit, Macherey-Nagel, Duren,
28
29
30 471 Germany). Potential contaminating DNA was removed by digestion with rDNase (Macherey-
31
32 472 Nagel) according to the manufacturer's instructions for 15 min at 37 °C then RNA was purified
33
34
35 473 using Beckman Coulter's solid-phase reversible immobilization (SPRI) paramagnetic beads
36
37 474 (AgencourtAMPure XP, Beckman Coulter, Brea, CA, USA) according to the manufacturer's
38
39
40 475 instructions. Briefly, paramagnetic beads and RNAs were mixed slowly and incubated 5 min
41
42
43 476 at room temperature followed by 2 min on a magnetic rack. Cleared supernatant was removed,
44
45
46 477 and beads were washed three times with 70 % ethanol. After 4 min of drying at room
47
48
49 478 temperature, RNAs were mixed slowly with RNase free water and incubated for 1 min at room
50
51 479 temperature on the magnetic rack. Eluted total RNA was stored at -80 °C.
52

- 53
-
- 54 480
- PolyA RNA enrichment

55
56 481 Poly-A RNA was extracted from total RNA by oligo-dT affinity chromatography (NucleoTrap
57
58
59 482 mRNA kit, Macherey-Nagel) according to the manufacturer's instructions. Briefly, up to 130 µg
60

1
2
3 483 of total RNAs were mixed with oligo-dT latex beads and incubated for 5 min at 68 °C then 10
4
5
6 484 min at room temperature. After centrifugation (2,000 g then 11,000 g), the pellets were washed
7
8 485 three times on the microfilter and dried by centrifugation at 11,000 g for 1 min. Finally, polyA+
9
10
11 486 RNA was incubated with RNase-free water for 7 min at 68 °C then centrifuged at 11,000 g for
12
13
14 487 1 min. Eluted polyA+ RNA was stored at -80 °C until needed.

15
16 488 Total and polyA-enriched RNA purity and concentrations were assayed by spectrophotometry
17
18
19 489 (Nanodrop, Thermo Scientific, Waltham, MA, USA).

20
21
22 490

23
24 491 **m⁶A quantification by LC-MS/MS:**

- 25
26
27 492
 - RNA hydrolysis

28
29 493 To generate nucleosides for quantification against standard curves, 5 µg of total RNA were
30
31
32 494 denatured for 10 min at 70 °C followed by 10 min on ice, and hydrolyzed with 100 U Nuclease
33
34
35 495 S1 (50 U/µL, Promega, Madison, WI, USA) in Nuclease S1 buffer (Promega) in a final reaction
36
37 496 volume of 25 µL for 2 h at 37 °C under gentle shaking. Samples were then incubated with
38
39
40 497 alkaline phosphatase buffer (Promega) for 5 min at room temperature, before 10 U alkaline
41
42
43 498 phosphatase (Promega) were added and incubated further for 2 h at 37 °C under gentle
44
45 499 shaking. Ten extra units of alkaline phosphatase were added after 1 hour of incubation to
46
47
48 500 complete the reaction. Finally, samples were centrifuged at 13,000 rpm for 10 min at 4 °C and
49
50
51 501 the supernatant containing digested total RNA was collected and kept at -20 °C before
52
53 502 quantification.

- 54
55
56
57 503
 - m⁶A quantification:
- 58
59
60

1
2
3 504 The apparatus was composed of a NexeraX² UHPLC system coupled with LCMS8030 Plus
4
5 505 (Shimadzu, Kyoto, Japan) mass spectrometer using an electrospray interface in positive mode.

6
7
8 506 The column (1.7 μ m, 100x3 mm) was a HILIC Aquity[®] Amide (Waters, Millford, MA, USA)
9
10
11 507 maintained at 35 °C. The injection volume and run-to-run time were 3 μ L and 10 min,
12
13
14 508 respectively. The flow rate was set to 1 mL/min. Mobile phase was initially composed of a
15
16
17 509 mixture of ammonium formate solution (10 mM) containing 0.2 % (v/v) formic acid and 95 %
18
19
20 510 acetonitrile (ACN) and it was maintained for 1 min. Then, a linear gradient was applied to reach
21
22
23 511 83 % ACN for 6 min. The composition returned to the initial conditions and the column was
24
25
26 512 equilibrated for 3 min.

27 513 The mass spectrometer was running in the Multiple Reaction Monitoring (MRM) acquisition
28
29
30 514 mode. LabSolutions 5.86 SP1 software was used to process the data. The desolvation
31
32
33 515 temperature was 230 °C, source temperature was 400 °C and nitrogen flows were 2.5 L/min
34
35
36 516 for the cone and 15 L/min for the desolvation. The capillary voltage was +4.5 kV. For each
37
38
39 517 compound, two transitions were monitored from the fragmentation of the [M+H]⁺ ion. The first
40
41
42 518 transition (A in Table S1) was used for quantification and the second one (B in Table S1) for
43
44
45 519 confirmation of the compound according to European Commission Decision 2002/657/EC
46
47
48 520 (Table S1).

49
50
51 521 Blank plasma samples were analysed to check specificity. Calibrators were prepared using
52
53
54 522 diluted solutions of A (Toronto Research Chemical, Toronto, Canada) and m⁶A (Carbosynth,
55
56
57 523 Berkshire, UK) in water at 1, 2, 5, 10, 20 50, 100 ng/mL. The calibration curves were drawn by
58
59
60 524 plotting the ratio of the peak area of A and m⁶A. For both nucleosides, a quadratic regression
525
with 1/C weighting resulted in standard curves with R²>0.998 and more than 75% of standards

1
2
3 526 with back-calculated concentrations within 15% of their nominal values as recommended for
4
5
6 527 by the European medicines agency for bioanalytical methods [69]. The limits of quantifications
7
8 528 for both compounds were considered as the lowest concentrations of the calibration curve.
9
10
11 529 m⁶A/A ratios were calculated for each single sample using the determined concentrations.
12
13
14 530 Final results are the average of three technical replicates.
15

16 531

17
18
19 532 **m⁶A quantification by immunoblotting:**

20
21 533 Immunological quantification of m⁶A was performed by dot-blot using total and polyA+ RNAs.
22
23
24 534 Dogfish total RNA (Dr. A. Gautier, personal communication) and a synthetic unmethylated
25
26
27 535 RNA oligo (Eurogentec, Liege, Belgium) were used as positive and negative controls,
28
29
30 536 respectively. RNA samples were denatured for 15 min at 55 °C with gentle shaking in
31
32
33 537 denaturing solution (2.2 M formaldehyde, 50 % formamide, 0.5X MOPS, DEPC water) followed
34
35
36 538 by 2 min on ice. Blotting was performed on a vacuum manifold as follows: a nylon membrane
37
38
39 539 (Amersham Hybond-N+, GE Healthcare life Sciences, Chicago, IL, USA) was pre-hydrated in
40
41
42 540 DEPC water for 5 min, then each well was washed twice with 10X SSC (Sigma-Aldrich) before
43
44
45 541 RNA was spotted onto the membrane and incubated for 15 min at room temperature. Then,
46
47
48 542 vacuum aspiration was applied and each well was washed twice with 10X SSC. After heat
49
50
51 543 crosslinking for 2 h at 70 °C, the membrane was rehydrated with DEPC water for 5 min, washed
52
53
54 544 with PBS then PBST (PBS, 0.1 % Tween-20) for 5 min each and blocked with two 5 min
55
56
57 545 incubations with blocking buffer (PBS, 0.1 % Tween-20, 10 % dry milk, 1 % BSA) at room
58
59
60 546 temperature. The blocked membrane was incubated overnight at 4 °C under gentle shaking
with the anti-m⁶A primary antibody (Total RNA: Millipore (Burlington, MA, USA) ABE572, 1 :

1
2
3 548 1,000 dilution in blocking buffer; polyA+ RNA: Diagenode (Liege, Belgium) C15200082, 1 : 500
4
5
6 549 dilution in blocking buffer) followed by four washes of PBST for 5 min. The secondary antibody
7
8 550 (Total RNA: Dako (Santa Clara, CA, USA) P0447 goat anti-mouse HRP antibody, 1 : 10,000
9
10
11 551 dilution; polyA+ RNA: Invitrogen (Carlsbad, CA, USA) A21202 donkey anti-mouse Alexa 488,
12
13
14 552 1 : 250 dilution) was diluted in PBST supplemented with 5 % dry milk and added onto the
15
16 553 membrane for 1 h 30 (total RNA) or 1 h (polyA+ RNA) at room temperature under gentle
17
18
19 554 shaking. Membranes were extensively washed in PBST (at least 4 washes of 5 min for total
20
21
22 555 RNA and 5 min then 1 h for polyA+ RNA) then total and polyA+ RNA immunoblots were
23
24 556 visualized using chemiluminescence (ECL kit, Promega) or fluorescence scanning at 480-530
25
26
27 557 nm (Pro Xpress, Perkin-Elmer, Waltham, MA, USA), respectively. The amount of m⁶A was
28
29
30 558 inferred from dot intensity measurements using ImageJ (v.1.49). Signal intensities were
31
32
33 559 determined as 'integrated densities as a percentage of the total' which corresponds to the area
34
35 560 under the curve of the signal of each dot after membrane background and negative control
36
37 561 signal subtraction.
38
39
40 562

563 ***In silico* analyses:**

44
45 564 All protein and RNA sequences of the m⁶A machinery of *Homo sapiens* and *Drosophila*
46
47
48 565 *melanogaster* (Data S1) were recovered by their published designation (i.e., 'METTL3' or
49
50
51 566 'YTHDF' etc.) and their identified protein sequence (ie. RefSeq accession number NP...)
52
53
54 567 collected from NCBI and used as query sequences to search for putative homologue
55
56
57 568 sequences in *Crassostrea gigas* databases. The presence of oyster orthologue RNA and
58
59 569 protein sequences were investigated by reciprocal
60

1
2
3 570 BLAST(<https://blast.ncbi.nlm.nih.gov/Blast.cgi>) on the *Crassostrea gigas* GigaTON [70] and
4
5
6 571 NCBI databases and results were compared between the two oyster databases. Domain
7
8 572 prediction was performed with CD-search software
9
10
11 573 (<https://www.ncbi.nlm.nih.gov/Structure/cdd/wrpsb.cgi>) with default settings on protein
12
13
14 574 sequences of *Homo sapiens*, *Drosophila melanogaster* and *Crassostrea gigas*. The GRE-rich
15
16 575 domain identified in vertebrate Prrc2a sequence [27] was performed with ProtParam
17
18
19 576 (<https://web.expasy.org/cgi-bin/protparam/protparam>).

20
21
22 577

23 24 578 **Protein machinery mRNA expression analyses:**

25
26
27 579 The transcriptome data of the different development stages are available on the GigaTON
28
29
30 580 database [70,71]. The correspondence between development stages in our study, and the
31
32
33 581 GigaTON database were assessed using light microscopy based on the morphological
34
35
36 582 description by Zhang et al., 2012 [71] (Table S2). Expression data was expressed in TPM
37
38
39 583 (Transcripts Per Million) [72] to provide a normalized comparison of gene expression between
40
41
42 584 all samples. The actual presence of some transcripts that display unclear or chimeric
43
44
45 585 sequences within available oyster databases was assessed using RT-PCR (Data S1).

46
47
48 586

49 50 587 **Protein m⁶A RNA pull down:**

- 51 588 • Protein extraction and RNA affinity chromatography

52
53 589 Protein extraction and RNA affinity chromatography were performed as described previously
54
55
56 590 [27] with some modifications as follows. Equal amounts (1 million individuals) of each
57
58
59 591 developmental stage (oocyte to D larvae) were pooled together then homogenized in 3.5
60

1
2
3 592 volumes of buffer A (10 mM KCl, 1.5 mM MgCl₂, 10 mM HEPES, pH 7.9, DEPC water, 1X
4
5
6 593 Protease inhibitor cocktail, DTT 0.5 mM) by extensive pipetting (ca. 30 times) and incubated
7
8 594 10 min at 4 °C. Embryos were ground with 10 slow 23G-needle syringe strokes and centrifuged
9
10
11 595 at 2,000 rpm for 10 min at 4 °C. The supernatant was diluted in 0.11 volume of buffer B (1.4 M
12
13 596 KCl, 0.03 M MgCl₂, HEPES 0.3 M, pH 7.9, DEPC water), centrifuged at 10,000 g for 1 h at 4
14
15
16 597 °C and the supernatant containing cytosolic proteins was stored at -80 °C. The pellet of the
17
18
19 598 first centrifugation, containing nuclei, was re-suspended in two volumes of buffer C (0.42 M
20
21 599 NaCl, 1.5 mM MgCl₂, 0.2 mM EDTA, 25 % glycerol, 20 mM HEPES, pH 7.9, 0.5 mM PMSF,
22
23
24 600 0.5 mM DTT, water DEPC). Nuclei were then lysed with a 23 G needle (10 vigorous syringe
25
26
27 601 strokes) followed by centrifugation at 30,000 rpm for 30 min at 4 °C and the supernatant
28
29
30 602 containing nuclear proteins was stored at -80 °C.

31
32 603 To identify putative proteins able to bind m⁶A-RNA, the cytosolic and nuclear fractions were
33
34
35 604 submitted to affinity chromatography using 5'-biotin-labelled RNA oligonucleotides either
36
37
38 605 bearing N⁶-methylated adenosines or not. The methylated adenosines were designed to lie
39
40
41 606 within RRACH motifs, according to the conserved methylated consensus sequence in other
42
43 607 organisms [2,3,7,33,73] (oligo-m⁶A: 5'Biotin-AGAAAAGACAACCAACGAGRR-m⁶A-
44
45 608 CWCAUCAU-3', oligo-A: 5'Biotin-AGAAAAGACAACCAACGAGRRACWCAUCAU-3', R = A or
46
47
48 609 G, W = A or U, Eurogentec).

49
50 610 For RNA pull down, streptavidin-conjugated magnetic beads (Dynabeads Myone Streptavidin,
51
52
53 611 Invitrogen) were pre-blocked with 0.2 mg/mL tRNA (Sigma-Aldrich) and 0.2 mg/mL BSA for 1
54
55
56 612 h at 4 °C under gentle rotation followed by three washes with 0.1 M NaCl. To avoid the
57
58
59 613 identification of non-target proteins, cytosolic and nuclear protein extracts were cleared with
60

1
2
3 614 pre-blocked magnetic beads in binding buffer (50 mM Tris-HCl, 250 mM NaCl, 0.4 mM EDTA,
4
5
6 615 0.1 % NP-40, DEPC water, 1 mM DTT, 0.4 U/ μ L RNasin) for 1 h at 4 °C under gentle rotation.
7
8 616 After incubation on magnetic rack, the supernatants containing putative target proteins were
9
10
11 617 collected and mixed with pre-blocked magnetic beads and oligo-m⁶A or oligo-A for 2 h at 4 °C
12
13
14 618 under gentle rotation. The beads binding putative target proteins were washed three times with
15
16 619 binding buffer and diluted in 50 mM ammonium bicarbonate.

17
18
19
20 620 • Identification of m⁶A-binding proteins by LC-MS/MS:

21
22 621 Protein samples were first reduced, alkylated and digested with trypsin then desalted and
23
24
25 622 concentrated onto a μ C18 Omix (Agilent, Santa Clara, CA, USA) before analysis.

26
27
28 623 The chromatography step was performed on a NanoElute (Bruker Daltonics, Billerica, MA,
29
30 624 USA) ultra-high pressure nano flow chromatography system. Peptides were concentrated onto
31
32
33 625 a C18 pepmap 100 (5 mm x 300 μ m i.d.) precolumn (Thermo Scientific) and separated at 50
34
35
36 626 °C onto a reversed phase Reprosil column (25 cm x 75 μ m i.d.) packed with 1.6 μ m C18 coated
37
38 627 porous silica beads (Ionopticks, Parkville, Victoria, Australia). Mobile phases consisted of 0.1
39
40
41 628 % formic acid, 99.9 % water (v/v) (A) and 0.1 % formic acid in 99.9 % ACN (v/v) (B). The
42
43
44 629 nanoflow rate was set at 400 nL/min, and the gradient profile was as follows: from 2 to 15 % B
45
46 630 within 60 min, followed by an increase to 25 % B within 30 min and further to 37 % within 10
47
48
49 631 min, followed by a washing step at 95 % B and re-equilibration.

50
51 632 MS experiments were carried out on an TIMS-TOF pro mass spectrometer (Bruker Daltonics)
52
53
54 633 with a modified nano-electrospray ion source (CaptiveSpray, Bruker Daltonics). The system
55
56
57 634 was calibrated each week and mass precision was better than 1 ppm. A 1600 spray voltage
58
59 635 with a capillary temperature of 180 °C was typically employed for ionizing. MS spectra were
60

1
2
3 636 acquired in the positive mode in the mass range from 100 to 1700 m/z. In the experiments
4
5
6 637 described here, the mass spectrometer was operated in PASEF mode with exclusion of single
7
8 638 charged peptides. A number of 10 PASEF MS/MS scans was performed during 1.16 seconds
9
10
11 639 from charge range 2-5.

12
13 640 The fragmentation pattern was used to determine the sequence of the peptide. Database
14
15
16 641 searching was performed using the Mascot 2.6.1 program (Matrix Science) with a *Crassostrea*
17
18 642 *gigas* Uniprot database (including 25,982 entries). The variable modifications allowed were as
19
20
21 643 follows: C-Carbamidomethyl, K-acetylation, methionine oxidation, and Deamidation (NQ). The
22
23
24 644 'Trypsin' parameter was set to 'Semispecific'. Mass accuracy was set to 30 ppm and 0.05 Da
25
26
27 645 for MS and MS/MS mode respectively. Mascot data were then transferred to Proline validation
28
29
30 646 software (<http://www.profiroteomics.fr/proline/>) for data filtering according to a significance
31
32 647 threshold of <0.05 and the elimination of protein redundancy on the basis of proteins being
33
34
35 648 evidenced by the same set or a subset of peptides (Data S2).

36
37
38 649 • Gene ontology analysis:

39
40
41 650 The mRNA sequences of the characterized m⁶A-binding proteins were identified using tBlastn
42
43 651 [74–76] against the GigaTON database [70] with default settings. Gene ontology (GO)
44
45
46 652 analyses were carried out with the GO annotations obtained from GigaTON database gene
47
48
49 653 universe [70]. GO term-enrichment tests were performed using the goseq (V1.22.0) R package
50
51 654 [77] with p-values calculated by the Wallenius method and filtered using REVIGO [78]. GO
52
53
54 655 terms with a p-value < 0.05 were considered significantly enriched (Data S3).

55
56 656

57
58
59 657 **Statistical analyses and graph production:**
60

1
2
3 658 Results are given as the mean \pm SD of three independent experiments unless otherwise stated.
4
5
6 659 They were analysed using one-way ANOVA or Kruskal-wallis tests when required, depending
7
8 660 on the normality of result distribution. The normality was tested using the Shapiro-Wilk's test
9
10
11 661 and homoscedasticity of variances with Bartlett's tests. Statistics and graphics were computed
12
13
14 662 with Prism v.6 (Graphpad), R (v.3.6.1) and RStudio (v.1.0.153) softwares. The R packages
15
16 663 *eulerr* [79] and *Complexheatmap* [80] were used for production of specific figures.
17
18
19 664
20
21
22 665
23
24
25
26 666 **Author contribution**
27
28 667 Experiment design: GR, LLF.
29
30
31 668 Benchwork and bioinformatics: LLF, GR, BB, BP, MS.
32
33
34 669 Data analysis: LLF, GR, BB, MS.
35
36 670 Manuscript writing and editing: LLF, GR, PF, BB, MS, BP.
37
38
39 671
40
41 672 **Acknowledgements**
42
43
44 673 The authors would like to acknowledge PRISMM core facility collaborators R. Delepée and S.
45
46 674 Lagadu for their expertise in m⁶A/A UHPLC-MS/MS quantification. We also thank J. Pontin for
47
48
49 675 technical assistance and J. Le Grand for help with sampling.
50
51
52 676
53
54 677 **Funding sources and disclosure of conflicts of interest**
55
56
57
58
59
60

1
2
3 678 This work was supported by the French National program CNRS EC2CO (Ecosphère
4
5
6 679 Continentale et Côtière 'HERITAGE' to G. Rivière) and the council of the Normandy Region
7
8 680 (RIN ECUME to P. Favrel). The authors declare they have no conflict of interest.
9

10
11 681
12
13
14
15
16
17
18
19
20
21
22
23
24
25
26
27
28
29
30
31
32
33
34
35
36
37
38
39
40
41
42
43
44
45
46
47
48
49
50
51
52
53
54
55
56
57
58
59
60

For Review Only

682 **References:**

- 683 1 Saletore Y, Meyer K, Korlach J, Vilfan ID, Jaffrey S & Mason CE (2012) The birth of the
684 Epitranscriptome: deciphering the function of RNA modifications. *Genome Biol.* **13**, 175.
- 685 2 Meyer KD, Saletore Y, Zumbo P, Elemento O, Mason CE & Jaffrey SR (2012)
686 Comprehensive analysis of mRNA methylation reveals enrichment in 3' UTRs and near
687 stop codons. *Cell* **149**, 1635–1646.
- 688 3 Dominissini D, Moshitch-moshkovitz S, Schwartz S, Salmon-Divon M, Ungar L, Osenberg
689 S, Cesarkas K, Jacob-hirsch J, Amariglio N, Kupiee M, Sorek R & Rechavi G (2012)
690 Topology of the human and mouse m⁶A RNAmethylomes revealed by m⁶A-seq.
691 *Nature* **485**, 201–206.
- 692 4 Ke S, Alemu EA, Mertens C, Gantman EC, Fak JJ, Mele A, Haripal B, Zucker-Scharff I,
693 Moore MJ, Park CY, Vågbø CB, Kusńierczyk A, Klungland A, Darnell JE, Darnell RB,
694 Kuńierczyk A, Klungland A, Darnell JE, Darnell RB, Kusńierczyk A, Klungland A,
695 Darnell JE & Darnell RB (2015) A majority of m⁶A residues are in the last exons,
696 allowing the potential for 3' UTR regulation. *Genes Dev.* **29**, 2037–2053.
- 697 5 Meyer KD, Patil DP, Zhou J, Zinoviev A, Skabkin MA, Elemento O, Pestova T V., Qian SB
698 & Jaffrey SR (2015) 5' UTR m⁶A Promotes Cap-Independent Translation. *Cell* **163**,
699 999–1010.
- 700 6 Pendleton KE, Chen B, Liu K, Hunter O V., Xie Y, Tu BP & Conrad NK (2017) The U6
701 snRNA m⁶A Methyltransferase METTL16 Regulates SAM Synthetase Intron Retention.
702 *Cell* **169**, 824-835.e14.
- 703 7 Lence T, Akhtar J, Bayer M, Schmid K, Spindler L, Ho CH, Kreim N, Andrade-Navarro MA,
704 Poeck B, Helm M & Roignant JY (2016) M⁶A modulates neuronal functions and sex
705 determination in *Drosophila*. *Nature* **540**, 242–247.
- 706 8 Bokar JA, Shambaugh ME, Polayes D, Matera AG & Rottman FM (1997) Purification and
707 cDNA cloning of the AdoMet-binding subunit of the human mRNA (N⁶-adenosine)-
708 methyltransferase. *RNA* **3**, 1233–47.
- 709 9 Liu J, Yue Y, Han D, Wang X, Fu YY, Zhang L, Jia G, Yu M, Lu Z, Deng X, Dai Q, Chen W
710 & He C (2013) A METTL3–METTL14 complex mediates mammalian nuclear RNA N⁶-
711 adenosine methylation. *Nat. Chem. Biol.* **10**, 93–95.
- 712 10 Wang X, Feng J, Xue Y, Guan Z, Zhang D, Liu Z, Gong Z, Wang Q, Huang J, Tang C,
713 Zou T & Yin P (2016) Structural basis of N⁶-adenosine methylation by the METTL3-
714 METTL14 complex. *Nature* **534**, 575–578.
- 715 11 Ping X-LL, Sun B-FF, Wang L, Xiao W, Yang X, Wang W-JJ, Adhikari S, Shi Y, Lv Y,
716 Chen Y-SS, Zhao X, Li A, Yang YGYY-G, Dahal U, Lou X-MM, Liu X, Huang J, Yuan W-
717 PP, Zhu X-FF, Cheng T, Zhao Y-LL, Wang X, Danielsen JMRR, Liu F & Yang YGYY-G
718 (2014) Mammalian WTAP is a regulatory subunit of the RNA N⁶-methyladenosine
719 methyltransferase. *Cell Res.* **24**, 177–189.
- 720 12 Yue Y, Liu J, Cui X, Cao J, Luo G, Zhang Z, Cheng T, Gao M, Shu X, Ma H, Wang F,
721 Wang X, Shen B, Wang Y, Feng X, He C & Liu J (2018) VIRMA mediates preferential
722 m⁶A mRNA methylation in 3'UTR and near stop codon and associates with alternative
723 polyadenylation. *Cell Discov.* **4**, 10.
- 724 13 Růzička K, Zhang M, Campilho A, Bodi Z, Kashif M, Saleh M, Eeckhout D, El-Showk S, Li
725 H, Zhong S, Jaeger G De, Mongan NP, Hejátko J, Helariutta Y & Fray RG (2017)
726 Identification of factors required for m⁶A mRNA methylation in *Arabidopsis* reveals a

- 1
2
3 727 role for the conserved E3 ubiquitin ligase HAKAI. *New Phytol.* **215**, 157–172.
4
- 5 728 14 Knuckles P, Lence T, Haussmann IU, Jacob D, Kreim N, Carl SH, Masiello I, Hares T,
6 729 Villaseñor R, Hess D, Andrade-Navarro MA, Biggiogera M, Helm M, Soller M, Bühler M
7 730 & Roignant J-YY (2018) Zc3h13/Flacc is required for adenosine methylation by bridging
8 731 the mRNA-binding factor Rbm15/Spenito to the m⁶A machinery component
9 732 Wtap/Fl(2)d. *Genes Dev.* **32**, 1–15.
- 10
11 733 15 Patil DP, Chen CK, Pickering BF, Chow A, Jackson C, Guttman M & Jaffrey SR (2016)
12 734 m⁶A RNA methylation promotes XIST-mediated transcriptional repression. *Nature* **537**,
13 735 369–373.
- 14
15 736 16 Zheng G, Dahl JA, Niu Y, Fedorcsak P, Huang CM, Li CJ, Vågbo CB, Shi Y, Wang WL,
16 737 Song SH, Lu Z, Bosmans RPG, Dai Q, Hao YJ, Yang X, Zhao WM, Tong WM, Wang
17 738 XJ, Bogdan F, Furu K, Fu Y, Jia G, Zhao X, Liu J, Krokan HE, Klungland A, Yang YG &
18 739 He C (2013) ALKBH5 Is a Mammalian RNA Demethylase that Impacts RNA Metabolism
19 740 and Mouse Fertility. *Mol. Cell* **49**, 18–29.
- 20
21 741 17 Mauer J, Luo X, Blanjoie A, Jiao X, Grozhik A V, Patil DP, Linder B, Pickering BF,
22 742 Vasseur J-J, Chen Q, Gross SS, Elemento O, Debart F, Kiledjian M & Jaffrey SR (2017)
23 743 Reversible methylation of m⁶Am in the 5' cap controls mRNA stability. *Nature* **541**, 371–
24 744 375.
- 25
26 745 18 Jia G, Fu Y, Zhao X, Dai Q, Zheng G, Yang YGYG-GGYG-G, Yi C, Lindahl T, Pan T,
27 746 Yang YGYG-GGYG-G & He C (2011) N⁶-Methyladenosine in nuclear RNA is a major
28 747 substrate of the obesity-associated FTO. *Nat. Chem. Biol.* **7**, 885–887.
- 29
30 748 19 Wang X, Lu Z, Gomez A, Hon GC, Yue Y, Han D, Fu Y, Parisien M, Dai Q, Jia G, Ren B,
31 749 Pan T, He C, Zhike L, Gomez A, Hon GC, Yue Y, Han D, Fu Y, Årisien M, Dai Q, Jia G,
32 750 Ren B, Pan T & He C (2014) N⁶-methyladenosine-dependent regulation of messenger
33 751 RNA stability. *Nature* **505**, 117–120.
- 34
35 752 20 Wang X, Zhao BS, Roundtree IA, Lu Z, Han D, Ma H, Weng X, Chen K, Shi H & He C
36 753 (2015) N⁶-methyladenosine modulates messenger RNA translation efficiency. *Cell* **161**,
37 754 1388–1399.
- 38
39 755 21 Hsu PJ, Zhu Y, Ma H, Guo Y, Shi X, Liu Y, Qi M, Lu Z, Shi H, Wang J, Cheng Y, Luo G,
40 756 Dai Q, Liu M, Guo X, Sha J, Shen B & He C (2017) Ythdc2 is an N⁶-methyladenosine
41 757 binding protein that regulates mammalian spermatogenesis. *Cell Res.* **27**, 1115–1127.
- 42
43 758 22 Shi H, Wang X, Lu Z, Zhao BS, Ma H, Hsu PJ, Liu C & He C (2017) YTHDF3 facilitates
44 759 translation and decay of N⁶-methyladenosine-modified RNA. *Cell Res.* **27**, 315–328.
- 45
46 760 23 Xiao W, Adhikari S, Dahal U, Chen Y-S, Hao Y-J, Sun B-F, Sun H-Y, Li A, Ping X-L, Lai
47 761 W-Y, Wang XX-J, Ma H-L, Huang C-M, Yang YY-G, Huang N, Jiang G-B, Wang H-L,
48 762 Zhou Q, Wang XX-J, Zhao Y-L & Yang YY-G (2016) Nuclear m⁶A Reader YTHDC1
49 763 Regulates mRNA Splicing. *Mol. Cell* **61**, 507–519.
- 50
51 764 24 Roundtree IA, Luo G-ZZ, Zhang Z, Wang X, Zhou T, Cui Y, Sha J, Huang X, Guerrero L,
52 765 Xie P, He E, Shen B & He C (2017) YTHDC1 mediates nuclear export of N⁶-
53 766 methyladenosine methylated mRNAs. *Elife* **6**, 1–28.
- 54
55 767 25 Alarcón CR, Goodarzi H, Lee H, Liu X, Tavazoie SFSSF & Tavazoie SFSSF (2015)
56 768 HNRNPA2B1 Is a Mediator of m⁶A-Dependent Nuclear RNA Processing Events. *Cell*
57 769 **162**, 1299–1308.
- 58
59 770 26 Huang H, Weng H, Sun W, Qin X, Shi H, Wu H, Zhao BS, Mesquita A, Liu C, Yuan CL,
60 771 Hu YC, Hüttelmaier S, Skibbe JR, Su R, Deng X, Dong L, Sun M, Li C, Nachtergaele S,

- 1
2
3 772 Wang Y, Hu C, Ferchen K, Greis KD, Jiang X, Wei M, Qu L, Guan JL, He C, Yang J &
4 773 Chen J (2018) Recognition of RNA N6-methyladenosine by IGF2BP proteins enhances
5 774 mRNA stability and translation. *Nat. Cell Biol.* **20**, 285–295.
- 6
7 775 27 Wu R, Li A, Sun B, Sun J-GG, Zhang J, Zhang T, Chen Y, Xiao Y, Gao Y, Zhang Q, Ma J,
8 776 Yang X, Liao Y, Lai W-YY, Qi X, Wang S, Shu Y, Wang H-LL, Wang F, Yang Y-GG &
9 777 Yuan Z (2018) A novel m6A reader Prrc2a controls oligodendroglial specification and
10 778 myelination. *Cell Res.* **29**, 23–41.
- 11
12 779 28 Bertero A, Brown S, Madrigal P, Osnato A, Ortmann D, Yiangou L, Kadiwala J, Hubner
13 780 NC, De Los Mozos IR, Sadee C, Lenaerts A-SS, Nakanoh S, Grandy R, Farnell E, Ule
14 781 J, Stunnenberg HG, Mendjan S, Vallier L, Sadée C, Lenaerts A-SS, Nakanoh S, Grandy
15 782 R, Farnell E, Ule J, Stunnenberg HG, Mendjan S & Vallier L (2018) The SMAD2/3
16 783 interactome reveals that TGF β controls m 6 A mRNA methylation in pluripotency.
17 784 *Nature* **555**, 256–259.
- 18
19 785 29 Kwon J, Jo YJ, Namgoong S & Kim NH (2019) Functional roles of hnRNPA2/B1 regulated
20 786 by METTL3 in mammalian embryonic development. *Sci. Rep.* **9**, 8640.
- 21
22 787 30 Geula S, Moshitch-Moshkovitz S, Dominissini D, Mansour AAF, Kol N, Salmon-Divon M,
23 788 Hershkovitz V, Peer E, Mor N, Manor YS, Ben-Haim MS, Eyal E, Yunger S, Pinto Y,
24 789 Jaitin DA, Viukov S, Rais Y, Krupalnik V, Chomsky E, Zerbib M, Maza I, Rechavi Y,
25 790 Massarwa R, Hanna S, Amit I, Levanon EY, Amariglio N, Stern-Ginossar N,
26 791 Novershtern N, Rechavi G & Hanna JH (2015) m6A mRNA methylation facilitates
27 792 resolution of naïve pluripotency toward differentiation. *Science (80-.).* **347**, 1002–1006.
- 28
29 793 31 Batista PJ, Molinie B, Wang J, Qu K, Zhang J, Li L, Bouley DM, Lujan E, Haddad B,
30 794 Daneshvar K, Carter AC, Flynn RA, Zhou C, Lim KS, Dedon P, Wernig M, Mullen AC,
31 795 Xing Y, Giallourakis CC, Chang HY, Howard Y, Batista PJ, Molinie B, Wang J, Qu K,
32 796 Zhang J, Li L, Bouley DM, Dedon P, Wernig M, Mullen AC, Xing Y, Giallourakis CC &
33 797 Chang HY (2014) M⁶A RNA modification controls cell fate transition in mammalian
34 798 embryonic stem cells. *Cell Stem Cell* **15**, 707–719.
- 35
36 799 32 Wojtas MN, Pandey RR, Mendel M, Homolka D, Sachidanandam R & Pillai RS (2017)
37 800 Regulation of m6A Transcripts by the 3'→5' RNA Helicase YTHDC2 Is Essential for a
38 801 Successful Meiotic Program in the Mammalian Germline. *Mol. Cell* **68**, 374-387.e12.
- 39
40 802 33 Zhao BS, Wang X, Beadell A V., Lu Z, Shi H, Kuuspalu A, Ho RK & He C (2017) M6A-
41 803 dependent maternal mRNA clearance facilitates zebrafish maternal-to-zygotic transition.
42 804 *Nature* **542**, 475–478.
- 43
44 805 34 Kan L, Grozhik A V., Vedanayagam J, Patil DP, Pang N, Lim K-S, Huang Y-C, Joseph B,
45 806 Lin C-J, Despic V, Guo J, Yan D, Kondo S, Deng W-M, Dedon PC, Jaffrey SR & Lai EC
46 807 (2017) The m6A pathway facilitates sex determination in *Drosophila*. *Nat. Commun.* **8**,
47 808 15737.
- 48
49 809 35 Kasowitz SD, Ma J, Anderson SJ, Leu NA, Xu Y, Gregory BD, Schultz RM & Wang PJ
50 810 (2018) Nuclear m 6 A reader YTHDC1 regulates alternative polyadenylation and splicing
51 811 during mouse oocyte development. *PLoS Genet.* **14**, 1–28.
- 52
53 812 36 Ivanova I, Much C, Di Giacomo M, Azzi C, Morgan M, Moreira PN, Monahan J, Carrieri C,
54 813 Enright AJ, O'Carroll D, Giacomo M Di, Azzi C, Morgan M, Moreira PN, Monahan J,
55 814 Carrieri C, Enright AJ, O'carroll D, Di Giacomo M, Azzi C, Morgan M, Moreira PN,
56 815 Monahan J, Carrieri C, Enright AJ & O'carroll D (2017) The RNA m 6 A Reader
57 816 YTHDF2 Is Essential for the Post-transcriptional Regulation of the Maternal
58 817 Transcriptome and Oocyte Competence. *Mol. Cell* **67**, 1059-1067.e4.
- 59
60

- 1
2
3 818 37 Lence T, Paolantoni C, Worpenberg L & Roignant JY (2019) Mechanistic insights into m⁶A
4 819 RNA enzymes. *Biochim. Biophys. Acta - Gene Regul. Mech.* **1862**, 222–229.
5
6 820 38 Balacco DL & Soller M (2018) The m⁶A writer: Rise of a machine for growing tasks.
7 821 *Biochemistry* **58**, acs.biochem.8b01166.
8
9 822 39 Lence T, Soller M & Roignant JY (2017) A fly view on the roles and mechanisms of the
10 823 m⁶A mRNA modification and its players. *RNA Biol.* **14**, 1232–1240.
11
12 824 40 Robbens S, Rouzé P, Cock JM, Spring J, Worden AZ & Van De Peer Y (2008) The FTO
13 825 gene, implicated in human obesity, is found only in vertebrates and marine algae. *J.*
14 826 *Mol. Evol.* **66**, 80–84.
15
16 827 41 Zhang G, Huang H, Liu D, Cheng Y, Liu X, Zhang W, Yin R, Zhang D, Zhang P, Liu J, Li
17 828 C, Liu B, Luo Y, Zhu Y, Zhang N, He S, He C, Wang H & Chen D (2015) N⁶-
18 829 methyladenine DNA modification in *Drosophila*. *Cell* **161**, 893–906.
19
20 830 42 Greer EL, Blanco MA, Gu L, Sendinc E, Liu J, Aristizábal-Corrales D, Hsu CH, Aravind L,
21 831 He C & Shi Y (2015) DNA methylation on N⁶-adenine in *C. elegans*. *Cell* **161**, 868–878.
22
23 832 43 Riviere G, He Y, Tecchio S, Crowell E, Sourdain P, Guo X & Favrel P (2017) Dynamics
24 833 of DNA methylomes underlie oyster development. *PLOS Genet.* **13**, 1–16.
25
26 834 44 Sussarellu R, Lebreton M, Rouxel J, Akcha F, Riviere G & Rivière G (2018) Copper
27 835 induces expression and methylation changes of early development genes in
28 836 *Crassostrea gigas* embryos. *Aquat. Toxicol.* **196**, submitted.
29
30 837 45 Rondon R, Grunau C, Fallet M, Charlemagne N, Sussarellu R, Chaparro C, Montagnani
31 838 C, Mitta G, Bachère E, Akcha F & Cosseau C (2017) Effects of a parental exposure to
32 839 diuron on Pacific oyster spat methylome. *Environ. Epigenetics* **3**, 1–13.
33
34 840 46 Riviere G, Wu G-CC, Fellous A, Goux D, Sourdain P & Favrel P (2013) DNA Methylation
35 841 Is Crucial for the Early Development in the Oyster *C. gigas*. *Mar. Biotechnol.* **15**, 1–15.
36
37 842 47 Saint-Carlier E & Riviere G (2015) Regulation of Hox orthologues in the oyster
38 843 *Crassostrea gigas* evidences a functional role for promoter DNA methylation in an
39 844 invertebrate. *FEBS Lett.* **589**, 1459–1466.
40
41 845 48 Fellous A, Favrel P & Riviere G (2015) Temperature influences histone methylation and
42 846 mRNA expression of the Jmj-C histone-demethylase orthologues during the early
43 847 development of the oyster *Crassostrea gigas*. *Mar. Genomics* **19**, 23–30.
44
45 848 49 Fellous A, Favrel P, Guo X & Riviere G (2014) The Jumonji gene family in *Crassostrea*
46 849 *gigas* suggests evolutionary conservation of Jmj-C histone demethylases orthologues in
47 850 the oyster gametogenesis and development. *Gene* **538**, 164–175.
48
49 851 50 Fellous A, Le Franc L, Jouaux A, Goux D, Favrel P & Rivière G (2019) Histone
50 852 Methylation Participates in Gene Expression Control during the Early Development of
51 853 the Pacific Oyster *Crassostrea gigas*. *Genes (Basel)*. **10**, 695.
52
53 854 51 Zhou J, Wan J, Gao X, Zhang X, Jaffrey SR & Qian S-B (2015) Dynamic m⁶A mRNA
54 855 methylation directs translational control of heat shock response. *Nature* **526**, 591–594.
55
56 856 52 Lu Z, Ma Y, Li Q, Liu E, Jin M, Zhang L & Wei C (2019) The role of N⁶-methyladenosine
57 857 RNA methylation in the heat stress response of sheep (*Ovis aries*). *Cell Stress*
58 858 *Chaperones* **24**, 333–342.
59
60 859 53 Xiang Y, Laurent B, Hsu C, Nachtergaele S, Lu Z, Sheng W, Xu C, Chen H, Ouyang J,

- 1
2
3 860 Wang S, Ling D, Hsu P, Zou L, Jambhekar A & He C (2017) m6A RNA methylation
4 861 regulates the UV-induced DNA damage response. *Nature* **543**, 573–576.
5
6 862 54 Cayir A, Barrow TM, Guo L & Byun HM (2019) Exposure to environmental toxicants
7 863 reduces global N6-methyladenosine RNA methylation and alters expression of RNA
8 864 methylation modulator genes. *Environ. Res.* **175**, 228–234.
9
10 865 55 Liu J, Li K, Cai J, Zhang M, Zhang X, Xiong X, Meng H, Xu X, Huang Z, Fan J & Yi C
11 866 (2019) Landscape and Regulation of M⁶A and M⁶Am Methylome Across Human and
12 867 Mouse Tissues. *SSRN Electron. J.*, 1–56.
13
14 868 56 Ren W, Lu J, Huang M, Gao L, Li D, Greg Wang G & Song J (2019) Structure and
15 869 regulation of ZCCHC4 in m6A-methylation of 28S rRNA. *Nat. Commun.* **10**, 5042.
16
17 870 57 Bokar JA, Shambaugh ME, Polayes D, Matera AG & Rottman FM (1997) Purification and
18 871 cDNA cloning of the AdoMet-binding subunit of the human mRNA (N6-adenosine)-
19 872 methyltransferase. *RNA* **3**, 1233–1247.
20
21 873 58 Theler D, Dominguez C, Blatter M, Boudet J & Allain FHT (2014) Solution structure of the
22 874 YTH domain in complex with N6-methyladenosine RNA: A reader of methylated RNA.
23 875 *Nucleic Acids Res.* **42**, 13911–13919.
24
25 876 59 Shima H, Matsumoto M, Ishigami Y, Ebina M, Muto A, Sato Y, Kumagai S, Ochiai K,
26 877 Suzuki T & Igarashi K (2017) S-Adenosylmethionine Synthesis Is Regulated by
27 878 Selective N6-Adenosine Methylation and mRNA Degradation Involving METTL16 and
28 879 YTHDC1. *Cell Rep.* **21**, 3354–3363.
29
30 880 60 Yurchenko O V., Skiteva OI, Voronezhskaya EE & Dyachuk VA (2018) Nervous system
31 881 development in the Pacific oyster, *Crassostrea gigas* (Mollusca: Bivalvia). *Front. Zool.*
32 882 **15**, 1–21.
33
34 883 61 Ratnaparkhi A (2013) Signaling by folded gastrulation is modulated by mitochondrial
35 884 fusion and fission. *J. Cell Sci.* **126**, 5369–5376.
36
37 885 62 Ren L, Zhang C, Tao L, Hao J, Tan K, Miao K, Yu Y, Sui L, Wu Z, Tian J & An L (2017)
38 886 High-resolution profiles of gene expression and DNA methylation highlight mitochondrial
39 887 modifications during early embryonic development. *J. Reprod. Dev.* **63**, 247–261.
40
41 888 63 Prudent J, Popgeorgiev N, Bonneau B, Thibaut J, Gadet R, Lopez J, Gonzalo P, Rimokh
42 889 R, Manon S, Houart C, Herbomel P, Aouacheria A & Gillet G (2013) Bcl-wav and the
43 890 mitochondrial calcium uniporter drive gastrula morphogenesis in zebrafish. *Nat.*
44 891 *Commun.* **4**.
45
46 892 64 Dumollard R, Duchon M & Carroll J (2007) The Role of Mitochondrial Function in the
47 893 Oocyte and Embryo. *Curr. Top. Dev. Biol.* **77**, 21–49.
48
49 894 65 Huang H, Weng H, Zhou K, Wu T, Zhao BS, Sun MM, Chen Z, Deng X, Xiao G, Auer F,
50 895 Klemm L, Wu H, Zuo Z, Qin X, Dong Y, Zhou Y, Qin H, Tao S, Du J, Liu J, Lu Z, Yin H,
51 896 Mesquita A, Yuan CL, Hu Y-CC, Sun W, Su R, Dong L, Shen C, Li C, Qing Y, Jiang X,
52 897 Wu X, Sun MM, Guan J-LL, Qu L, Wei M, Müschen M, Huang G, He C, Yang J & Chen
53 898 J (2019) Histone H3 trimethylation at lysine 36 guides m6A RNA modification co-
54 899 transcriptionally. *Nature* **567**, 414–419.
55
56 900 66 Wang Y, Li Y, Yue M, Wang J, Kumar S, Wechsler-Reya RJ, Zhang Z, Ogawa Y, Kellis M,
57 901 Duyster G & Zhao JC (2018) N6-methyladenosine RNA modification regulates
58 902 embryonic neural stem cell self-renewal through histone modifications. *Nat. Neurosci.*
59 903 **21**, 195–206.

- 1
2
3 904 67 Petton B, Pernet F, Robert R & Boudry P (2013) Temperature influence on pathogen
4 905 transmission and subsequent mortalities in juvenile pacific oysters *Crassostrea gigas*.
5 906 *Aquac. Environ. Interact.* **3**, 257–273.
6
7 907 68 Riviere G, Fellous A, Franco A, Bernay B & Favrel P (2011) A crucial role in fertility for the
8 908 oyster angiotensin-converting enzyme orthologue CgACE. *PLoS One* **6**.
9
10 909 69 EMA (2011) *Guideline on bioanalytical method validation*.
11 910 *EMA/CHMP/EWP/192217/2009*.
12
13 911 70 Riviere G, Klopp C, Ibouniyamine N, Huvet A, Boudry P & Favrel P (2015) GigaTON: An
14 912 extensive publicly searchable database providing a new reference transcriptome in the
15 913 pacific oyster *Crassostrea gigas*. *BMC Bioinformatics* **16**, 1–12.
16
17 914 71 Zhang G, Fang X, Guo X, Li L, Luo R, Xu F, Yang P, Zhang L, Wu F, Chen Y, Wang J,
18 915 Peng C, Meng J, Yang L, Liu J, Wen B, Zhang N & Huang Z (2012) The oyster genome
19 916 reveals stress adaptation and complexity of shell formation. *Nature* **490**, 49–54.
20
21 917 72 Li B, Ruotti V, Stewart RM, Thomson JA & Dewey CN (2010) RNA-Seq gene expression
22 918 estimation with read mapping uncertainty. *Bioinformatics* **26**, 493–500.
23
24 919 73 Qi ST, Ma JY, Wang ZB, Guo L, Hou Y & Sun QY (2016) N6 -methyladenosine
25 920 sequencing highlights the involvement of mRNA methylation in oocyte meiotic
26 921 maturation and embryo development by regulating translation in *xenopus laevis*. *J. Biol.*
27 922 *Chem.* **291**, 23020–23026.
28
29 923 74 Altschul SF, Madden TL, Schäffer AA, Zhang J, Zhang Z, Miller W & Lipman DJ (1997)
30 924 Gapped BLAST and PSI-BLAST: a new generation of protein database search
31 925 programs. *Nucleic Acids Res.* **25**, 3389–3402.
32
33 926 75 Cock PJA, Chilton JM, Grüning B, Johnson JE & Soranzo N (2015) NCBI BLAST+
34 927 integrated into Galaxy. *Gigascience* **4**, 0–6.
35
36 928 76 Camacho C, Coulouris G, Avagyan V, Ma N, Papadopoulos J, Bealer K & Madden TL
37 929 (2009) BLAST+: Architecture and applications. *BMC Bioinformatics* **10**, 1–9.
38
39 930 77 Young MD, Wakefield MJ, Smyth GK & Oshlack A (2010) Gene ontology analysis for
40 931 RNA-seq: accounting for selection bias. *Genome Biol.* **11**, R14.
41
42 932 78 Supek F, Bošnjak M, Škunca N & Šmuc T (2011) Revigo summarizes and visualizes long
43 933 lists of gene ontology terms. *PLoS One* **6**.
44
45 934 79 Larsson J (2019) eulerr: Area-Proportional Euler and Venn Diagrams with Ellipses. .
46
47 935 80 Gu Z, Eils R & Schlesner M (2016) Complex heatmaps reveal patterns and correlations in
48 936 multidimensional genomic data. *Bioinformatics* **32**, 2847–2849.
49
50 937
51
52 938
53
54
55
56
57
58
59
60

1
2
3 939 **Figure legends**
4
5

6 940 Figure 1: m⁶A levels across oyster development.
7
8

9
10 941 **A.** m⁶A level quantified by LC-MS/MS in *Crassostrea gigas* embryo-larval stages pooled from
11
12 942 oocytes to D-larvae (n= 3) is compared to the m⁶A level in *Homo sapiens* and *Drosophila*
13
14 943 *melanogaster*; **B.** Dot blot quantification of m⁶A in total RNA throughout oyster development
15
16 944 (n=3); **C.** Dot blot quantification of m⁶A in polyA+ RNAs throughout oyster development (n=3)
17
18 945 Kruskal-Wallis test, $\alpha < 0,05$. E: Egg, F E: fertilized egg, 2/8C: two to eight cell embryos, M:
19
20 946 Morula, B: Blastula, G: Gastrula, T: Trochophore, D: D larvae. Chemiluminescence (B) and
21
22 947 fluorescence (C) are measured as a ratio between dot intensity of development stages and
23
24 948 their respective controls for each amount of RNA (120ng, 60ng and 30ng).
25
26
27
28
29
30

31
32 949

33
34 950 Figure 2: The putative conserved m⁶A machinery in *Crassostrea gigas*.
35

36
37 951 Domain architecture of actors of the m⁶A machinery identified by *in silico* analyses in the oyster
38
39 952 compared to the fruit fly and human, **A.** Writer proteins; **B.** Eraser protein; **C.** Reader proteins.
40
41 953 Putative domains involved in m⁶A processes are coloured (writers, green; eraser, red; readers,
42
43 954 blue). Other domains identified but not involved in m⁶A processes are indicated in grey. Only
44
45 955 one isoform is represented for each protein and each species for clarity (see supplementary
46
47 956 figure S2 for other isoforms).
48
49
50
51

52
53 957

54
55 958 Figure 3: Gene expression of the putative m⁶A machinery throughout oyster development
56
57
58
59
60

1
2
3 959 Expression levels of writers (**A**), eraser (**B**) and readers (**C**) identified by *in silico* analysis at
4
5
6 960 each development stage were inferred from the GigaTON database. Expression levels are
7
8 961 given in Transcripts Per kilobases per Million Reads (TPM) as the mean of the GigaTON values
9
10
11 962 according to the table S2. E: Egg, 2/8C: two to eight cell, M: Morula, B: Blastula, G: Gastrula,
12
13
14 963 T: Trochophore, D: D larvae, S: Spat, J: Juvenile.

15
16 964

17
18
19 965 Figure 4: Characterization of m⁶A-RNA binding proteins in oyster development.

20
21 966 **A.** Venn diagrams representation of proteins bound to the A- and/or m⁶A- oligos in nuclear and
22
23
24 967 cytosolic fractions of oyster embryo-larval stages. The number of proteins identified is
25
26
27 968 indicated. Some actors characterized in this study are highlighted: eIF3, YTHC1, hnRNPA2B1
28
29 969 and IGF2BP. **B.** Heatmap of gene expression levels of the proteins that bind specifically to the
30
31
32 970 m⁶A-oligo throughout oyster development. The expression level is normalized regarding the
33
34
35 971 maximum value for each gene according to the GigaTON database. **C.** GO term distribution
36
37 972 among the three expression clusters in B. **D.** Examples of GO term enrichment within the
38
39
40 973 expression clusters of the m⁶A-bound proteins. The $-\log_{10}(\text{p-value})$ associated to each term
41
42
43 974 is given. E: Egg, 2/8C: two to eight cells, M: Morula, B: Blastula, G: Gastrula, T: Trochophore,
44
45 975 D: D larvae, S: Spat, J: Juvenile.

46
47
48 976 **Supporting information:**

49 977 Data S1: Complete list of *in silico* identified putative m⁶A machinery proteins and their
50
51
52 978 respective BLAST results

53
54
55 979 Data S2: Identified proteins by RNA pull down coupled with mass spectrometry with m⁶A or
56
57
58 980 A-oligo, in nuclear or cytosolic protein extracts

59
60

1
2
3 981 Data S3: Complete list of GO terms of clustered genes of m⁶A interacting proteins (p-
4
5
6 982 value<0,05)
7

8 983 Table S1: Transitions used for each compound. A: first transition, B: second transition
9

10
11 984 Table S2: Table of correspondence between development stages in our study, and the
12
13
14 985 GigaTON database.
15

16 986
17
18
19
20
21
22
23
24
25
26
27
28
29
30
31
32
33
34
35
36
37
38
39
40
41
42
43
44
45
46
47
48
49
50
51
52
53
54
55
56
57
58
59
60

For Review Only

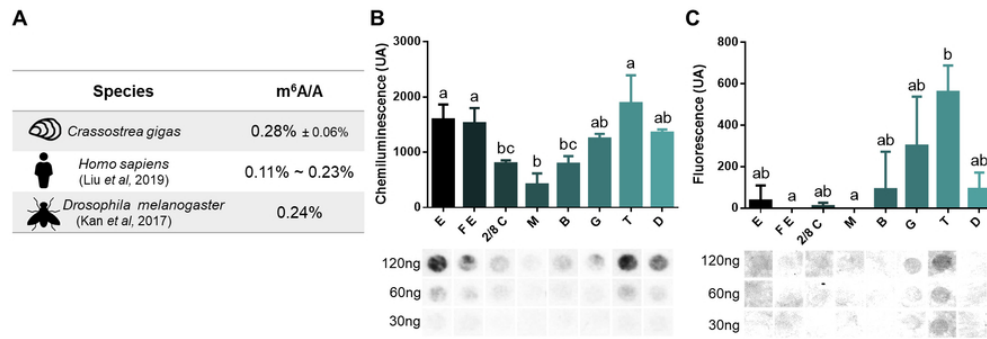


Figure 1: m⁶A levels across oyster development.

A. m⁶A level quantified by LC-MS/MS in *Crassostrea gigas* embryo-larval stages pooled from oocytes to D-larvae (n= 3) is compared to the m⁶A level in *Homo sapiens* and *Drosophila melanogaster*; B. Dot blot quantification of m⁶A in total RNA throughout oyster development (n=3); C. Dot blot quantification of m⁶A in polyA+ RNAs throughout oyster development (n=3) Kruskal-Wallis test, $\alpha < 0,05$. E: Egg, F E: fertilized egg, 2/8C: two to eight cell embryos, M: Morula, B: Blastula, G: Gastrula, T: Trochophore, D: D larvae. Chemiluminescence (B) and fluorescence (C) are measured as a ratio between dot intensity of development stages and their respective controls for each amount of RNA (120ng, 60ng and 30ng).

75x25mm (300 x 300 DPI)

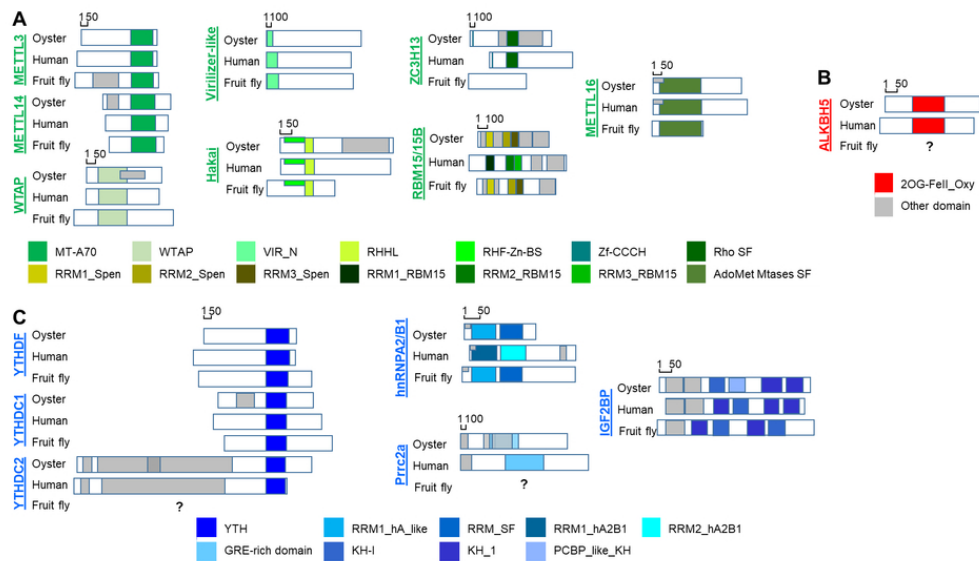


Figure 2: The putative conserved m6A machinery in *Crassostrea gigas*. Domain architecture of actors of the m6A machinery identified by in silico analyses in the oyster compared to the fruit fly and human, A. Writer proteins; B. Eraser protein; C. Reader proteins. Putative domains involved in m6A processes are coloured (writers, green; eraser, red; readers, blue). Other domains identified but not involved in m6A processes are indicated in grey. Only one isoform is represented for each protein and each species for clarity (see supplementary figure S2 for other isoforms).

80x47mm (300 x 300 DPI)

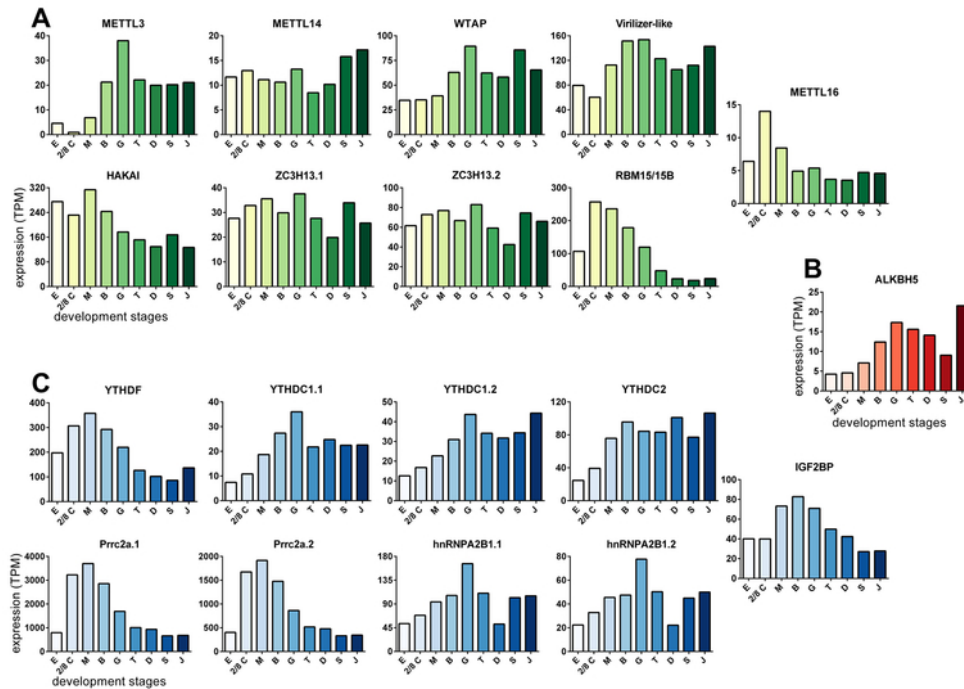


Figure 3: Gene expression of the putative m6A machinery throughout oyster development
 Expression levels of writers (A), eraser (B) and readers (C) identified by in silico analysis at each development stage were inferred from the GigaTON database. Expression levels are given in Transcripts Per kilobases per Million Reads (TPM) as the mean of the GigaTON values according to the table S2. E: Egg, 2/8C: two to eight cell, M: Morula, B: Blastula, G: Gastrula, T: Trochophore, D: D larvae, S: Spat, J: Juvenile.

65x46mm (300 x 300 DPI)

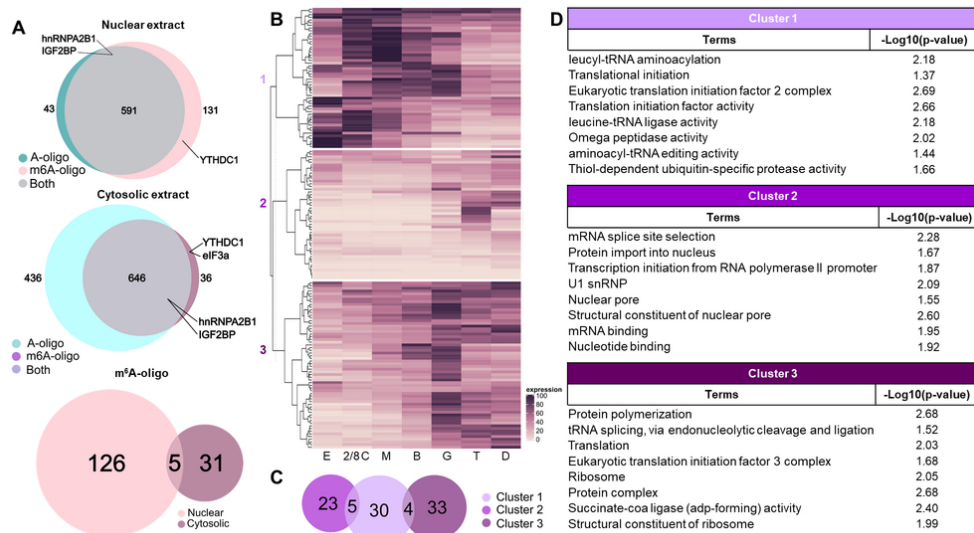


Figure 4: Characterization of m6A-RNA binding proteins in oyster development. A. Venn diagrams representation of proteins bound to the A- and/or m6A- oligos in nuclear and cytosolic fractions of oyster embryo-larval stages. The number of proteins identified is indicated. Some actors characterized in this study are highlighted: eIF3, YTHC1, hnRNPA2B1 and IGF2BP. B. Heatmap of gene expression levels of the proteins that bind specifically to the m6A-oligo throughout oyster development. The expression level is normalized regarding the maximum value for each gene according to the GigaTON database. C. GO term distribution among the three expression clusters in B. D. Examples of GO term enrichment within the expression clusters of the m6A-bound proteins. The $-\log_{10}(p\text{-value})$ associated to each term is given. E: Egg, 2/8C: two to eight cells, M: Morula, B: Blastula, G: Gastrula, T: Trochophore, D: D larvae, S: Spat, J: Juvenile.

85x49mm (300 x 300 DPI)

Data S1: Complete list of in silico identified putative m6A machinery proteins and their respective BLAST results

Probable assembly artefact highlighted in grey

| Specie | database | sequence accession number | length | conserved domain |
|---|----------|-------------------------------|--------|-----------------------------------|
| <u>METTL3</u> | | | | |
| <i>Homo sapiens</i> | NCBI | gi 21361827 (NP_062826.2) | 580 | MT-A70 |
| <i>Drosophila melanogaster</i> (IME4) | NCBI | gi 21355141 (NP_651204.1) | 608 | MT-A70 MDN1 |
| <i>Crassostrea gigas</i> | GIGATON | CHOYP_PHUM_PHUM423190.1.1 | 554 | MT-A70 |
| | NCBI | gi 762092209 (XP_011428532.1) | 555 | MT-A70 |
| <u>METTL14</u> | | | | |
| <i>Homo sapiens</i> | NCBI | gi 24308265 (NP_066012.1) | 456 | MT-A70 |
| <i>Drosophila melanogaster</i> (CG7818) | NCBI | gi 19920926 (NP_609205.1) | 397 | MT-A70 |
| <i>Crassostrea gigas</i> | GIGATON | CHOYP_MET14.1.1 | 495 | MT-A70 MttA_Hfc106 |
| | | CHOYP_LOC100743733.1.1 | 723 | MT-A70 7tmA_NPR-like_invertebrate |
| | NCBI | gi 762082967 (XP_011424173.1) | 470 | MT-A70 MttA_Hfc106 |
| <u>WTAP</u> | | | | |
| <i>Homo sapiens</i> | NCBI | gi 395455090 (NP_001257460.1) | 396 | WTAP |
| | | gi 23199974 (NP_690596.1) | 151 | WTAP |
| | | gi 395455092 (NP_001257461.1) | 170 | WTAP |
| <i>Drosophila melanogaster</i> (FL(2)D) | NCBI | gi 24653459 (NP_523732.2) | 536 | WTAP |
| | | gi 24653461 (NP_725327.1) | 412 | WTAP |
| <i>Crassostrea gigas</i> | GIGATON | CHOYP_FL2D.1.1 | 406 | WTAP IncA |
| | | CHOYP_SODM.1.2 | 252 | WTAP IncA |
| | | CHOYP_LOC100121674.1.1 | 290 | WTAP IncA |
| | NCBI | gi 762078268 (XP_011453082.1) | 406 | WTAP IncA |

VIRILIZER-LIKE

| | | | | | |
|---|---------|--------------------------------|-----------------------|-------|--|
| <i>Homo sapiens</i> (Virilizer-like, VIRMA) | NCBI | gi 33946282 (NP_056311.2) | 1812 | VIR_N | |
| | | gi 33946280 (NP_892121.1) | 1147 | VIR_N | |
| <i>Drosophila melanogaster</i> (Virilizer) | NCBI | gi 17864576 (NP_524900.1) | 1854 | VIR_N | |
| <i>Crassostrea gigas</i> | GIGATON | CHOYP_VIR.1.1 | 2021 | VIR_N | |
| | NCBI | gi 762120202 (XP_011443024.1) | 2023 | VIR_N | |
| | | gi 762120200 (XP_011443023.1) | 2023 | VIR_N | |
| | | gi 1139822239 (XP_019927346.1) | 2022 | VIR_N | |
| | | gi 1139822241 (XP_019927347.1) | 2021 | VIR_N | |
| gi 1139822243 (XP_019927348.1) | 1717 | VIR_N | PTZ00249 super family | | |

HAKAI

| | | | | | | |
|--------------------------------|---------|-------------------------------|-----|-----------|------|-----------------------|
| <i>Homo sapiens</i> | NCBI | gi 209180481 (NP_079090.2) | 491 | RHF-Zn-BS | RHHL | |
| | | gi 546230945 (NP_001271220.1) | 490 | RHF-Zn-BS | RHHL | |
| <i>Drosophila melanogaster</i> | NCBI | gi 19921556 (NP_609993.1) | 302 | RHF-Zn-BS | RHHL | |
| | | gi 24585301 (NP_724217.1) | 311 | RHF-Zn-BS | RHHL | |
| | | gi 442628448 (NP_788075.2) | 464 | RHF-Zn-BS | RHHL | |
| | | gi 442628450 (NP_001260593.1) | 473 | RHF-Zn-BS | RHHL | |
| <i>Crassostrea gigas</i> | GIGATON | CHOYP_LOC100864501.1.1 | 504 | RHF-Zn-BS | RHHL | PHA03247 super family |
| | NCBI | gi 762140345 (XP_011453340.1) | 498 | RHF-Zn-BS | RHHL | PHA03247 super family |
| | | gi 762140347 (XP_011453341.1) | 497 | RHF-Zn-BS | RHHL | PHA03247 super family |

ZC3H13

| | | | | | | |
|---------------------|------|--------------------------------|------|---------|--------|--|
| <i>Homo sapiens</i> | NCBI | gi 1060099240 (NP_001317493.1) | 1669 | Zf-CCCH | Rho SF | |
| | | gi 1060099108 (NP_001317496.1) | 1668 | Zf-CCCH | Rho SF | |

| | | | | | | | |
|---|---------|-------------------------------|------|---------|-------------------|-------------------|----------|
| | | gi 116008442 (NP_055885.3) | 1564 | Zf-CCCH | Rho SF | | |
| <i>Drosophila melanogaster</i> (CG7358) | NCBI | gi 24643154 (NP_573339.1) | 1150 | | | | |
| | | gi 665392303 (NP_001285418.1) | 1139 | | | | |
| | | gi 665392305 (NP_001285419.1) | 842 | | | | |
| <i>Crassostrea gigas</i> | GIGATON | CHOYP_BRAFLDRAFT_120702.1.1 | 1631 | Zf-CCCH | Rho SF | dnaA super family | PTZ00121 |
| | | CHOYP_LOC100568158.1.1 | 1611 | Zf-CCCH | Rho SF | dnaA super family | PTZ00121 |
| | NCBI | gi 762096734 (XP_011430912.1) | 1400 | Rho SF | dnaA super family | PTZ00121 | |
| | | gi 762096736 (XP_011430913.1) | 1400 | Rho SF | dnaA super family | PTZ00121 | |
| | | gi 762096738 (XP_011430914.1) | 1380 | Rho SF | PHA03307 | PTZ00121 | |
| | | gi 762096740 (XP_011430915.1) | 1329 | Rho SF | PTZ00121 | | |

RBM15/15B

| | | | | | | | | | |
|---|---------|-----------------------------|-----|------------|------------|------------|------------|------|-------------|
| <i>Homo sapiens</i> | NCBI | gi 47933339 (NP_073605) | 977 | RRM1_RBM15 | RRM2_RBM15 | RRM3_RBM15 | SF-CC1 | SPOC | |
| | | gi 319996623 (NP_001188474) | 969 | RRM1_RBM15 | RRM2_RBM15 | RRM3_RBM15 | SF-CC1 | SPOC | |
| | | gi 54607124 (NP_037418) | 890 | RRM1_RBM15 | RRM2_RBM15 | RRM3_RBM15 | U2AF_lg SF | SPOC | |
| <i>Drosophila melanogaster</i> (SPENITO/NITO) | NCBI | gi 24586450 (NP_724633) | 793 | RRM1_Spen | RRM2_Spen | RRM3_Spen | RRM | SPOC | |
| | | gi 19921778 (NP_610339) | 793 | RRM1_Spen | RRM2_Spen | RRM3_Spen | RRM | SPOC | |
| | | gi 665399388 (NP_001286174) | 793 | RRM1_Spen | RRM2_Spen | RRM3_Spen | RRM | SPOC | |
| <i>Crassostrea gigas</i> | GIGATON | CHOYP_LOC663518.1.1 | 717 | RRM1_Spen | RRM2_Spen | RRM3_Spen | RRM | SPOC | PTZ00449 SF |
| | NCBI | gi 762129377 (XP_011447812) | 717 | RRM1_Spen | RRM2_Spen | RRM3_Spen | RRM | SPOC | PTZ00449 SF |

METTL16

| | | | | | |
|---|---------|----------------------------|-----|------------------|-----------------------------------|
| <i>Homo sapiens</i> | NCBI | gi 122114654 (NP_076991.3) | 562 | AdoMet Mtases SF | S-adenosylmethionine binding site |
| <i>Drosophila melanogaster</i> (CG7544) | NCBI | gi 19922302 (NP_611015.1) | 305 | AdoMet Mtases SF | |
| | GIGATON | CHOYP_LOC100561572.1.1 | 527 | AdoMet Mtases SF | S-adenosylmethionine binding site |

| | | | | | |
|--------------------------|------|-------------------------------|-----|------------------|-----------------------------------|
| <i>Crassostrea gigas</i> | NCBI | gi 762141911 (XP_011454156.1) | 538 | AdoMet Mtases SF | S-adenosylmethionine binding site |
| | | gi 762141913 (XP_011454157.1) | 527 | AdoMet Mtases SF | S-adenosylmethionine binding site |

ALKBH5

| | | | | |
|--------------------------------|---------|-------------------------------|-----|--------------|
| <i>Homo sapiens</i> | NCBI | gi 148539642 (NP_060228.3) | 394 | 2OG-FelI_Oxy |
| <i>Drosophila melanogaster</i> | | | | |
| <i>Crassostrea gigas</i> | GIGATON | CHOYP_BRAFLDRAFT_126925.1.1 | 403 | 2OG-FelI_Oxy |
| | NCBI | gi 762097205 (XP_011431161.1) | 374 | 2OG-FelI_Oxy |

YTHDC1

| | | | | |
|--|---------|--------------------------------|-----|-----------|
| <i>Homo sapiens</i> | NCBI | gi 72534750 (NP_001026902.1) | 727 | YTH |
| | | gi 94536805 (NP_588611.2) | 709 | YTH |
| | | gi 1061213987 (NP_001317627.1) | 735 | YTH |
| <i>Drosophila melanogaster</i> (YT521) | NCBI | gi 24656811 (NP_647811.2) | 721 | YTH |
| | | gi 24656816 (NP_728876.1) | 710 | YTH |
| <i>Crassostrea gigas</i> | GIGATON | CHOYP_YTDC1.2.2 | 636 | YTH CDC27 |
| | | CHOYP_LOC586835.1.1 | 545 | YTH CDC27 |
| | NCBI | gi 762070401 (XP_011447601.1) | 636 | YTH CDC27 |

YTHDC2

| | | | | | | | | |
|--------------------------------|---------|--------------------------------|------|-----|------|-------------------------|--------------|-------------|
| <i>Homo sapiens</i> | NCBI | gi 269847874 (NP_073739.3) | 1430 | YTH | HrpA | R3H_DEXH_helicase | DEXHc_YTHDC2 | OB_NTP_bind |
| | | gi 1066536696 (NP_001332904.1) | 1268 | YTH | HrpA | DEXHc_YTHDC2 | OB_NTP_bind | |
| | | gi 1066546270 (NP_001332905.1) | 1130 | YTH | HrpA | DEAD-like_helicase_N SF | ANKYR | OB_NTP_bind |
| <i>Drosophila melanogaster</i> | | | | | | | | |
| <i>Crassostrea gigas</i> | GIGATON | CHOYP_YTDC2.1.1 | 1572 | YTH | HrpA | R3H super family | Ank_2 | |
| | NCBI | gi 762086858 (XP_011425711.1) | 1572 | YTH | HrpA | R3H super family | Ank_2 | |

YTHDF

| | | | | | | |
|---|---------|----------------------------------|-----|-----|-----------------------|-----------------------|
| <i>Homo sapiens</i> | NCBI | gi 29791407 (AAH50284.1) | 559 | YTH | RPA_2b-aaRSs_OBF_like | PHA03247 super family |
| | | gi 12803469 (AAH02559.1) | 579 | YTH | | |
| | | gi 31419299 (AAH52970.1) | 585 | YTH | | |
| <i>Drosophila melanogaster</i> (CG6422) | | gi 21356147 (NP_651322.1) | 700 | YTH | | |
| | | gi 24649883 (NP_733067.1) | 699 | YTH | | |
| | | gi 161078590 (NP_001097905.1) | 694 | YTH | | |
| <i>Crassostrea gigas</i> | GIGATON | CHOYP_COX1.6.15 | 532 | YTH | | |
| | | CHOYP_LOC100371022.1.1 | 531 | YTH | | |
| | NCBI | gi 762146089 (XP_011456337.1) | 522 | YTH | | |

hnRNPA2B1

| | | | | | | | |
|--|---------|----------------------------------|-----|--------------|------------|---------------------------|---------|
| <i>Homo sapiens</i> | NCBI | gi 4504447 (NP_002128.1) | 341 | RRM1_hA2B1 | RRM2_hA2B1 | Putative DNA binding site | hnRNPA1 |
| | | gi 14043072 (NP_112533.1) | 353 | RRM1_hA2B1 | RRM2_hA2B1 | Putative DNA binding site | hnRNPA1 |
| <i>Drosophila melanogaster</i> (hrb98DE) | NCBI | gi 24650831 (NP_733249.1) | 364 | RRM1_hA_like | RRM_SF | Putative DNA binding site | |
| | | gi 17738267 (NP_524543.1) | 365 | RRM1_hA_like | RRM_SF | Putative DNA binding site | |
| | | gi 24650838 (NP_733252.1) | 361 | RRM1_hA_like | RRM_SF | Putative DNA binding site | |
| | | gi 24650833 (NP_733250.1) | 360 | RRM1_hA_like | RRM_SF | Putative DNA binding site | |
| <i>Crassostrea gigas</i> | GIGATON | CHOYP_LOC100748395.1.7 | 229 | RRM1_hA_like | RRM_SF | Putative DNA binding site | |
| | | CHOYP_LOC100748395.2.7 | 394 | RRM1_hA_like | RRM_SF | Putative DNA binding site | |
| | | CHOYP_LOC100748395.3.7 | 315 | RRM1_hA_like | RRM_SF | Putative DNA binding site | |
| | | CHOYP_LOC100748395.4.7 | 372 | RRM1_hA_like | RRM_SF | Putative DNA binding site | |
| | | CHOYP_LOC100748395.6.7 | 315 | RRM1_hA_like | RRM_SF | Putative DNA binding site | |
| | | CHOYP_AGAP_AGAP002374.1.1 | 236 | RRM_SF | | | |

| | | | | | |
|--|------|-------------------------------|-----|--------------|----------------------------------|
| | | CHOYP_LOC100748395.5.7 | 205 | RRM_SF | |
| | NCBI | gi 762104361 (XP_011434715.1) | 370 | RRM1_hA_like | RRM_SF Putative DNA binding site |
| | | gi 762104364 (XP_011434716.1) | 369 | RRM1_hA_like | RRM_SF Putative DNA binding site |
| | | gi 762104366 (XP_011434717.1) | 363 | RRM1_hA_like | RRM_SF Putative DNA binding site |
| | | gi 762104368 (XP_011434718.1) | 353 | RRM1_hA_like | RRM_SF Putative DNA binding site |

Prrc2a

| | | | | | |
|--------------------------------|---------|--------------------------------|------|-----------------|--------------------------|
| <i>Homo sapiens</i> | NCBI | gi 314122241 (NP_004629.3) | 2157 | GRE-rich domain | BAT2_N |
| <i>Drosophila melanogaster</i> | | | | | |
| <i>Crassostrea gigas</i> | GIGATON | CHOYP_LOC100559941.1.2 | 2578 | GRE-rich domain | BAT2_N PTZ00121 PTZ00449 |
| | | CHOYP_LOC100559941.2.2 | 2554 | GRE-rich domain | BAT2_N PTZ00121 PTZ00449 |
| | | gi 1139830093 (XP_019928978.1) | 2922 | GRE-rich domain | BAT2_N PTZ00121 PTZ00449 |

IGF2BP

| | | | | | | | | |
|---------------------|------|-------------------------------|-----|-------------------------------|------|--------------|---------------------|---------------------|
| <i>Homo sapiens</i> | NCBI | gi 56237027 (NP_006537.3) | 577 | KH-I | KH-1 | RRM1_IGF2BP1 | RRM2_IGF2BP1 | |
| | | gi 238624257 (NP_001153895.1) | 438 | KH-I | KH-1 | RRM1_IGF2BP1 | RRM_SF super family | |
| | | gi 64085377 (NP_006539.3) | 599 | KH-I | KH-1 | PCBP_like_KH | RRM1_IGF2BP2 | RRM2_IGF2BP2 |
| | | gi 56118219 (NP_001007226.1) | 556 | KH-I | KH-1 | PCBP_like_KH | RRM1_IGF2BP2 | RRM2_IGF2BP2 |
| | | gi 631226390 (NP_001278798.1) | 605 | KH-I | KH-1 | PCBP_like_KH | RRM1_IGF2BP2 | RRM_SF super family |
| | | gi 631226392 (NP_001278801.1) | 542 | KH-I | KH-1 | PCBP_like_KH | RRM_SF super family | |
| | | gi 631226396 (NP_001278802.1) | 536 | KH-I | KH-1 | PCBP_like_KH | RRM2_IGF2BP2 | |
| | | gi 631226394 (NP_001278803.1) | 493 | KH-I | KH-1 | PCBP_like_KH | RRM2_IGF2BP2 | |
| | | gi 631226398 (NP_001278804.1) | 463 | KH-I | KH-1 | PCBP_like_KH | RRM_SF super family | |
| | | gi 30795212 (NP_006538.2) | 579 | KH-I | KH-1 | PCBP_like_KH | RRM1_IGF2BP3 | RRM2_IGF2BP3 |
| | | | | gi 386764188 (NP_001036268.2) | 631 | KH-I | KH-1 | RRM2_VICKZ |

| | | | | | | |
|---|---------|-------------------------------|-----|------|------|---|
| <i>Drosophila melanogaster</i> (IGF-II binding protein) | NCBI | gi 386764191 (NP_001245616.1) | 638 | KH-I | KH-1 | RRM2_VICKZ |
| | | gi 17530887 (NP_511111.1) | 566 | KH-I | KH-1 | |
| | | gi 24641097 (NP_727451.1) | 573 | KH-I | KH-1 | |
| | | gi 281360685 (NP_001162717.1) | 580 | KH-I | KH-1 | |
| <i>Crassostrea gigas</i> | GIGATON | CHOYP_LOC100114171.1.1 | 607 | KH-I | KH-1 | PCBP_like_KH RRM1_VICKZ RRM_SF super family |
| | NCBI | gi 762079091 (XP_011412002.1) | 611 | KH-I | KH-1 | PCBP_like_KH RRM1_VICKZ RRM_SF super family |
| | | gi 762079093 (XP_011412008.1) | 607 | KH-I | KH-1 | PCBP_like_KH RRM1_VICKZ RRM_SF super family |
| | | gi 762079095 (XP_011412017.1) | 590 | KH-I | KH-1 | PCBP_like_KH RRM1_VICKZ RRM_SF super family |

eIF3a

| | | | | | | | | |
|---|---------|-------------------------------|------|------|------------------|----------------------|-------------------|--------|
| <i>Homo sapiens</i> | NCBI | gi 4503509(NP_003741.1) | 1382 | PINT | Smc super family | U2AF_Ig super family | dnaA super family | Rho SF |
| <i>Drosophila melanogaster</i> (IGF-II binding protein) | NCBI | gi 665393171 (NP_730838.3) | 1140 | PINT | DUF5401 | Rho SF | | |
| | | gi 24643988 (NP_649470.2) | 1140 | PINT | DUF5401 | Rho SF | | |
| <i>Crassostrea gigas</i> | GIGATON | CHOYP_BRAFLDRAFT_75590.1.1 | 155 | | | | | |
| | | CHOYP_UBP47.2.2 | 1253 | PAM | DUF5401 | | | |
| | | CHOYP_MROH1.1.1 | 1046 | PAM | DUF5401 | | | |
| | NCBI | gi 762160635 (XP_011418535.1) | 759 | PAM | DUF5401 | | | |
| | | gi 762122193 (XP_011444042.1) | 1252 | PAM | DUF5401 | | | |

Data S1: Complete list of in silico identified putative m6A machinery proteins and their respective BLAST results

| | <i>Crassostrea gigas</i> | <i>Homo sapiens</i> | <i>Drosophila melanogaster</i> |
|----------------------|---|--|---|
| METTL3 | CHOYP_PHUM_PHUM423190.1.1 gi 762092209 (XP_011428532.1) | gi 21361827 (NP_062826.2) | gi 21355141 (NP_651204.1) 73.26% 73.96% |
| METTL14 | CHOYP_MET14.1.1 CHOYP_LOC100743733.1.1 gi 762092967 (XP_01142473.1) | gi 24308269 (NP_066012.1) 62.03% 60.88% 61.58% | gi 19920926 (NP_609205.1) 58.05% 57.76% 58.05% |
| WTAP | CHOYP_FLJD.1.1 CHOYP_SODM1.2 CHOYP_LOC100121674.1.1 gi 762078268 (XP_011453082.1) | gi 395455090 (NP_001257460.1) 52.68% 47.55% 52.68% 51.06% | gi 23199974 (NP_690596.1) 47.55% 47.52% 47.55% 47.55% |
| VRILIZER-like | CHOYP_VIR.1.1 gi 762120202 (XP_011443024.1) gi 762120203 (XP_011443023.1) gi 1139822239 (XP_019927346.1) gi 1139822241 (XP_019927347.1) gi 1139822243 (XP_019927348.1) | gi 33946282 (NP_056311.2) 30.70% 30.85% 30.85% 30.89% 30.95% 30.62% | gi 395455092 (NP_001257461.1) 47.55% 47.55% 47.55% 47.55% |
| HAKAI | CHOYP_LOC100864501.1.1 gi 762140343 (XP_011453340.1) gi 762140347 (XP_011453341.1) | gi 209180481 (NP_079090.2) 43.27% 29.43% 29.28% | gi 546230945 (NP_001271220.1) 43.96% 29.69% 29.68% |
| ZC3H13 | CHOYP_BRALDRAFT_120702.1.1 CHOYP_LOC100568158.1.1 gi 762096734 (XP_011430912.1) gi 762096736 (XP_011430913.1) gi 762096738 (XP_011430914.1) gi 762096740 (XP_011430915.1) | gi 1060099240 (NP_001317493.1) 37.11% 37.11% 31.48% 31.48% 31.48% 31.69% | gi 1060099108 (NP_001317496.1) 37.11% 37.11% 31.48% 31.48% 31.48% 40.58% |
| RBM15/15B | CHOYP_LOC663518.1.1 gi 762129377 (XP_011447812) | gi 47933339 (NP_073605) 56.73% 41.64% | gi 319996623 (NP_001188474) 56.73% 41.64% |
| METTL16 | CHOYP_LOC100561572.1.1 gi 762141911 (XP_011454156.1) gi 762141913 (XP_011454157.1) | gi 122114654 (NP_076991.3) 38.05% 37.68% 37.68% | gi 54607124 (NP_037418) 61.59% 34.94% |
| ALKBH5 | CHOYP_BRALDRAFT_126925.1.1 gi 762097205 (XP_011431161.1) | gi 148539642 (NP_060228.3) 72.43% 72.43% | |
| YTHDC1 | CHOYP_YTDC1.2.2 CHOYP_LOC358935.1.1 gi 762070401 (XP_011447601.1) | gi 72534750 (NP_001026902.1) 46.61% 51.52% 43.92% | gi 94536805 (NP_588611.2) 45.30% 52.27% 42.86% |
| YTHDC2 | CHOYP_YTDC2.1.1 gi 762086858 (XP_011425711.1) | gi 269847874 (NP_073739.3) 52.99% 53.09% 43.49% | gi 106653696 (NP_001332904.1) 51.83% 52.05% 71.72% |
| YTHDF | CHOYP_COX1.6.15 CHOYP_LOC100371022.1.1 gi 762146089 (XP_011456337.1) | gi 29791407 (AAH0284.1) 53.09% 53.09% 43.49% | gi 12803469 (AAH02559.1) 53.77% 52.05% 71.72% |
| hmRNP2B1 | CHOYP_LOC100748395.1.7 CHOYP_LOC100748395.2.7 CHOYP_LOC100748395.3.7 CHOYP_LOC100748395.4.7 CHOYP_LOC100748395.5.7 CHOYP_AGAP_AGAP002374.1.1 CHOYP_LOC100748395.6.7 gi 762104361 (XP_011434715.1) gi 762104364 (XP_011434716.1) gi 762104366 (XP_011434717.1) gi 762104368 (XP_011434718.1) | gi 4504447 (NP_002128.1) 55.37% 55.37% 55.37% 55.37% 54.24% 55.37% 55.37% 54.80% 55.37% 55.37% | gi 14043072 (NP_112533.1) 54.71% 54.71% 54.71% 54.71% 53.53% 54.71% 55.37% 54.80% 55.37% 55.37% |
| Prrc2a | CHOYP_LOC100559941.1.2 CHOYP_LOC100559941.2.2 gi 1139830093 (XP_019928978.1) | gi 314122241 (NP_004629.3) 46.02% 34.66% | |
| IGF2BP | CHOYP_LOC100114171.1.1 gi 762079091 (XP_011412002.1) gi 762079093 (XP_011412003.1) gi 762079095 (XP_011412017.1) | gi 56237027 (NP_006537.3) 34.87% 34.80% 35.04% 34.80% | gi 238624257 (NP_001153895.1) 35.71% 36.39% 36.39% 35.86% |
| eIF3a | CHOYP_BRALDRAFT_75690.1.1 CHOYP_UBP47.2.2 CHOYP_MIRCH1.1.1 gi 762160835 (XP_011418535.1) gi 762122193 (XP_011444042.1) | gi 45035096 (NP_003741.1) 40.86% 63.71% 54.20% 58.13% | gi 56118219 (NP_001007226.1) N/A 35.50% 35.61% 35.11% 35.88% |
| | | gi 631226390 (NP_001278798.1) 35.50% 35.61% 35.11% 35.88% | gi 631226392 (NP_001278801.1) 34.93% 35.53% 35.83% 35.53% |
| | | gi 631226396 (NP_001278802.1) 35.34% 35.93% 36.77% 36.24% | gi 631226394 (NP_001278803.1) 35.85% 36.38% 36.77% 36.38% |
| | | gi 631226398 (NP_001278804.1) 38.61% 39.76% 34.01% 39.76% | gi 30795212 (NP_006538.2) 33.16% 33.78% 34.01% 33.78% |
| | | gi 386764188 (NP_001036268.2) 42.72% 42.83% 42.77% 42.83% | gi 386764191 (NP_001245616.1) 42.26% 42.83% 42.45% 42.83% |
| | | gi 17530887 (NP_511111.1) 44.89% 45.07% 45.07% 45.07% | gi 24641097 (NP_727451.1) 44.89% 45.07% 45.07% 45.07% |
| | | gi 281360665 (NP_001162717.1) 44.20% 44.37% 44.52% 44.37% | |
| | | gi 665393171 (NP_730838.3) 45.97% 50.89% 50.89% 44.89% 48.45% | gi 24643988 (NP_649470.2) 45.97% 50.89% 50.89% 44.89% 48.45% |

Data S2: Identified proteins by RNA pull down coupled with mass spectrometry with m6A or A-oligo, in nuclear or cytosolic protein extracts

Proteins identified in nuclear extracts

| Oligo | Accession | Description |
|--------------|------------------|--|
| m6A | K1PTY5_CRAGI | Protocadherin Fat 4 |
| m6A | K1QNA2_CRAGI | Vitellogenin-6 |
| m6A | K1QBR5_CRAGI | Uncharacterized protein |
| m6A | K1PFG1_CRAGI | Uncharacterized protein |
| m6A | K1P9A4_CRAGI | Beta-1,3-glucan-binding protein |
| m6A | K1QHI5_CRAGI | Pyruvate carboxylase, mitochondrial |
| m6A | K1QQ94_CRAGI | Uncharacterized protein |
| m6A | K1R5B4_CRAGI | Proteasome activator complex subunit 4 |
| m6A | K1R164_CRAGI | Galectin-4 |
| m6A | K1PNI6_CRAGI | Heterogeneous nuclear ribonucleoprotein A/B |
| m6A | K1QMX5_CRAGI | Uncharacterized protein |
| m6A | K1PQP2_CRAGI | Nucleolin |
| m6A | K1QXR4_CRAGI | Pancreatic lipase-related protein 2 |
| m6A | K1R7V7_CRAGI | Tubulin beta chain |
| m6A | K1RGT5_CRAGI | Metalloendopeptidase |
| m6A | K1QSX8_CRAGI | ATPase family AAA domain-containing protein 2B |
| m6A | K1R9B6_CRAGI | H/ACA ribonucleoprotein complex subunit 4 |
| m6A | K1RWS2_CRAGI | Transcriptional activator protein Pur-alpha |
| m6A | K1RLF8_CRAGI | Splicing factor 3B subunit 3 |
| m6A | K1R3U2_CRAGI | Uncharacterized protein |
| m6A | K1QQ68_CRAGI | Tubulin alpha chain |
| m6A | K1QVJ8_CRAGI | Piwi-like protein 1 |
| m6A | K1PVA1_CRAGI | Transitional endoplasmic reticulum ATPase |
| m6A | K1QKB5_CRAGI | Uncharacterized protein |
| m6A | K1QHM2_CRAGI | Dolichyl-diphosphooligosaccharide--protein glycosyltransferase subunit 2 |
| m6A | K1QII6_CRAGI | Tubulin alpha chain |
| m6A | K1QSQ9_CRAGI | Putative ATP-dependent RNA helicase an3 |
| m6A | K1QQ27_CRAGI | Pancreatic lipase-related protein 2 |
| m6A | K1QMA4_CRAGI | RRP5-like protein |
| m6A | K1PEP0_CRAGI | 40S ribosomal protein S8 |
| m6A | K1QXX7_CRAGI | Myosin heavy chain, non-muscle (Fragment) |
| m6A | K1QK56_CRAGI | Uncharacterized protein |
| m6A | K1PNR3_CRAGI | Clathrin heavy chain |
| m6A | K1PN21_CRAGI | Tubulin beta chain |
| m6A | K1RG73_CRAGI | Acetyl-CoA carboxylase |
| m6A | K1RD58_CRAGI | Uncharacterized protein |
| m6A | K1QU53_CRAGI | NAD(P) transhydrogenase, mitochondrial |
| m6A | K1R473_CRAGI | Tubulin alpha chain |
| m6A | K1PH76_CRAGI | Y-box factor-like protein (Fragment) |
| m6A | K1PE00_CRAGI | Tubulin alpha chain |
| m6A | K1PJC1_CRAGI | Adipophilin |
| m6A | K1R6Z7_CRAGI | ATP synthase subunit alpha |
| m6A | K1R545_CRAGI | Pre-mRNA-processing-splicing factor 8 (Fragment) |
| m6A | K1RI55_CRAGI | Insulin-like growth factor 2 mRNA-binding protein 3 |
| m6A | K1QGS8_CRAGI | Elongation factor 1-alpha |
| m6A | K1QFM6_CRAGI | Vitellogenin |
| m6A | K1R6Q7_CRAGI | DNA topoisomerase I |
| m6A | K1Q988_CRAGI | Band 4.1-like protein 3 |
| m6A | K1QLS3_CRAGI | Cytochrome b-c1 complex subunit 2, mitochondrial |
| m6A | K1RWW5_CRAGI | ATP synthase subunit beta |
| m6A | K1S2N7_CRAGI | Innexin |
| m6A | K1P421_CRAGI | Histone H2A |
| m6A | K1RK12_CRAGI | 40S ribosomal protein S23 |
| m6A | K1QKD6_CRAGI | Uncharacterized protein |
| m6A | K1QWZ6_CRAGI | Dolichyl-diphosphooligosaccharide--protein glycosyltransferase subunit 1 |
| m6A | K1QFN2_CRAGI | Uncharacterized protein |
| m6A | K1PHW2_CRAGI | Uncharacterized protein |

| | | | |
|----|-----|--------------|---|
| 1 | | | |
| 2 | | | |
| 3 | m6A | K1PJ06_CRAGI | Importin subunit alpha-1 |
| 4 | m6A | K1QA13_CRAGI | Calcium-transporting ATPase |
| 5 | m6A | K1R0L4_CRAGI | Sodium/potassium-transporting ATPase subunit alpha |
| 6 | m6A | K1R115_CRAGI | Succinate dehydrogenase [ubiquinone] flavoprotein subunit, mitochondrial |
| 7 | m6A | K1QB61_CRAGI | Protocadherin Fat 4 |
| 8 | m6A | K1Q4H2_CRAGI | Nodal modulator 3 |
| 9 | | | |
| 10 | m6A | K1QWK2_CRAGI | MAM domain-containing glycosylphosphatidylinositol anchor protein 2 |
| 11 | m6A | K1R466_CRAGI | T-complex protein 1 subunit gamma |
| 12 | m6A | K1QFW9_CRAGI | Uncharacterized protein |
| 13 | m6A | K1R5U4_CRAGI | Acetyl-CoA carboxylase 1 |
| 14 | m6A | A5LGH1_CRAGI | Voltage-dependent anion channel |
| 15 | m6A | K1S4Q2_CRAGI | T-complex protein 1 subunit delta (Fragment) |
| 16 | m6A | K1REG6_CRAGI | DNA helicase |
| 17 | m6A | K1PUL2_CRAGI | Long-chain-fatty-acid--CoA ligase 1 |
| 18 | m6A | K1R294_CRAGI | T-complex protein 1 subunit beta |
| 19 | m6A | K1PMT6_CRAGI | Heterogeneous nuclear ribonucleoprotein U-like protein 1 |
| 20 | | | |
| 21 | m6A | K1RGB7_CRAGI | Epidermal retinal dehydrogenase 2 |
| 22 | m6A | K1R435_CRAGI | Splicing factor, arginine/serine-rich 4 |
| 23 | m6A | K1R252_CRAGI | Putative methylmalonate-semialdehyde dehydrogenase [acylating], mitochondrial |
| 24 | m6A | K1QAE5_CRAGI | Uncharacterized protein |
| 25 | m6A | K1QIR8_CRAGI | 78 kDa glucose-regulated protein |
| 26 | m6A | K1QYB3_CRAGI | Ig-like and fibronectin type-III domain-containing protein C25G4.10 |
| 27 | m6A | K1QJ14_CRAGI | 40S ribosomal protein S3a |
| 28 | m6A | K1PNQ5_CRAGI | Heat shock protein HSP 90-alpha 1 |
| 29 | m6A | K1S1S1_CRAGI | Insulin-like growth factor 2 mRNA-binding protein 1 |
| 30 | m6A | K1QM19_CRAGI | Uncharacterized protein |
| 31 | m6A | K1R420_CRAGI | Non-specific serine/threonine protein kinase |
| 32 | m6A | K1R4R9_CRAGI | Mitotic apparatus protein p62 |
| 33 | m6A | K1R0S3_CRAGI | T-complex protein 1 subunit theta |
| 34 | m6A | K1RAJ1_CRAGI | T-complex protein 1 subunit alpha |
| 35 | m6A | K1QH74_CRAGI | Splicing factor, arginine/serine-rich 1 |
| 36 | m6A | K1QRL6_CRAGI | Methenyltetrahydrofolate synthetase domain-containing protein |
| 37 | m6A | K1QUC6_CRAGI | Uncharacterized protein |
| 38 | m6A | K1RIT6_CRAGI | NADH-ubiquinone oxidoreductase 75 kDa subunit, mitochondrial |
| 39 | m6A | K1RBF6_CRAGI | Uncharacterized protein yfeX |
| 40 | m6A | K1PCS4_CRAGI | Eukaryotic translation initiation factor 2 subunit 3, Y-linked |
| 41 | m6A | K1Q620_CRAGI | Uncharacterized protein |
| 42 | m6A | K1QWX2_CRAGI | 60S acidic ribosomal protein P0 |
| 43 | m6A | K1PD57_CRAGI | Constitutive coactivator of PPAR-gamma-like protein 1-like protein |
| 44 | m6A | K1Q4S5_CRAGI | Cadherin-87A |
| 45 | m6A | K1RQA0_CRAGI | Dolichyl-diphosphooligosaccharide--protein glycosyltransferase subunit 2 |
| 46 | m6A | K1QMX8_CRAGI | DNA replication licensing factor MCM7 |
| 47 | m6A | K1QPX8_CRAGI | Alkyl/aryl-sulfatase BDS1 |
| 48 | m6A | K1QZW0_CRAGI | Polyadenylate-binding protein 2 |
| 49 | m6A | K1RWX7_CRAGI | Metabotropic glutamate receptor 3 |
| 50 | m6A | K1RFT1_CRAGI | Band 4.1-like protein 3 |
| 51 | m6A | K1RNB5_CRAGI | Propionyl-CoA carboxylase beta chain, mitochondrial |
| 52 | m6A | K1QBK6_CRAGI | Splicing factor 3B subunit 1 |
| 53 | m6A | K1Q0Z3_CRAGI | Estradiol 17-beta-dehydrogenase 11 |
| 54 | m6A | K1R953_CRAGI | Acetyl-CoA carboxylase |
| 55 | m6A | K1QNN9_CRAGI | MICOS complex subunit MIC60 |
| 56 | m6A | K1QXS6_CRAGI | Heterogeneous nuclear ribonucleoprotein A2-like protein 1 |
| 57 | m6A | K1RJH5_CRAGI | Polyadenylate-binding protein |
| 58 | m6A | K1R0Y9_CRAGI | ADP,ATP carrier protein |
| 59 | m6A | K1R4D4_CRAGI | 40S ribosomal protein SA |
| 60 | m6A | K1QWT8_CRAGI | Uncharacterized protein |
| | m6A | K1Q0L1_CRAGI | 60S ribosomal protein L23a |
| | m6A | K1Q260_CRAGI | Nucleolar protein 58 |
| | m6A | K1QT04_CRAGI | Uncharacterized protein |
| | m6A | K1Q9K6_CRAGI | Histone H3 |

| | | | |
|----|-----|--------------|---|
| 1 | | | |
| 2 | | | |
| 3 | m6A | K1QT21_CRAGI | Putative ATP-dependent RNA helicase DDX5 |
| 4 | m6A | K1QBN0_CRAGI | Methylcrotonoyl-CoA carboxylase beta chain, mitochondrial |
| 5 | m6A | K1PLY1_CRAGI | DNA polymerase |
| 6 | m6A | K1QBH0_CRAGI | Uncharacterized protein |
| 7 | m6A | K1Q923_CRAGI | Putative ATP-dependent RNA helicase DDX4 |
| 8 | m6A | K1QG58_CRAGI | Actin |
| 9 | m6A | K1QQB6_CRAGI | 40S ribosomal protein S14 |
| 10 | m6A | K1QDX9_CRAGI | Ribosome biogenesis protein BMS1-like protein |
| 11 | m6A | K1QF01_CRAGI | 40S ribosomal protein S4 |
| 12 | m6A | K1QLC5_CRAGI | T-complex protein 1 subunit epsilon |
| 13 | m6A | K1QY12_CRAGI | Dynamin-1-like protein |
| 14 | m6A | K1R0W4_CRAGI | Signal recognition particle subunit SRP72 |
| 15 | m6A | K1QX26_CRAGI | Endoplasmic |
| 16 | m6A | K1QHS8_CRAGI | Ribonucleoside-diphosphate reductase |
| 17 | m6A | K1QQ05_CRAGI | Insulin-like growth factor-binding protein complex acid labile chain |
| 18 | m6A | K1QFP5_CRAGI | NADH dehydrogenase [ubiquinone] flavoprotein 1, mitochondrial |
| 19 | m6A | K1QP17_CRAGI | Caprin-1 |
| 20 | m6A | K1R7A2_CRAGI | Uncharacterized protein |
| 21 | m6A | K1R4L8_CRAGI | Electron transfer flavoprotein-ubiquinone oxidoreductase, mitochondrial |
| 22 | m6A | K1R591_CRAGI | Inter-alpha-trypsin inhibitor heavy chain H4 |
| 23 | m6A | K1R7I9_CRAGI | Heterogeneous nuclear ribonucleoprotein Q |
| 24 | m6A | K1QBW8_CRAGI | Uncharacterized protein |
| 25 | m6A | K1RSZ6_CRAGI | 40S ribosomal protein S7 |
| 26 | m6A | K1QDZ5_CRAGI | Cytochrome c1, heme protein, mitochondrial |
| 27 | m6A | K1PGW7_CRAGI | Transmembrane protein 2 |
| 28 | m6A | K1QMB9_CRAGI | Eukaryotic translation initiation factor 3 subunit A |
| 29 | m6A | K1RNZ6_CRAGI | Eukaryotic translation initiation factor 3 subunit D |
| 30 | m6A | K1Q9W5_CRAGI | T-complex protein 1 subunit eta |
| 31 | m6A | K1Q404_CRAGI | DNA topoisomerase 2 |
| 32 | m6A | K1R7J6_CRAGI | Putative sodium/potassium-transporting ATPase subunit beta-2 |
| 33 | m6A | K1P8W6_CRAGI | 60S ribosomal protein L4 |
| 34 | m6A | K1RSA6_CRAGI | Methylcrotonoyl-CoA carboxylase subunit alpha, mitochondrial |
| 35 | m6A | K1RW85_CRAGI | Adenosylhomocysteinase |
| 36 | m6A | K1PS27_CRAGI | DNA helicase |
| 37 | m6A | K1RH18_CRAGI | Sarcalumenin |
| 38 | m6A | K1Q5H6_CRAGI | FACT complex subunit SSRP1 |
| 39 | m6A | K1PH66_CRAGI | Fibrinolytic enzyme, isozyme C |
| 40 | m6A | K1PF10_CRAGI | PAN2-PAN3 deadenylation complex catalytic subunit PAN2 |
| 41 | m6A | K1Q358_CRAGI | 60S acidic ribosomal protein P2 |
| 42 | m6A | K1PXH5_CRAGI | Putative saccharopine dehydrogenase |
| 43 | m6A | K1Q8S0_CRAGI | Nucleolar complex protein 3 homolog |
| 44 | m6A | K1QYB6_CRAGI | Delta-1-pyrroline-5-carboxylate synthetase |
| 45 | m6A | K1PV79_CRAGI | Importin subunit alpha |
| 46 | m6A | K1PV49_CRAGI | RuvB-like helicase |
| 47 | m6A | K1PRL4_CRAGI | 60S ribosomal protein L38 (Fragment) |
| 48 | m6A | K1QL67_CRAGI | 60S ribosomal protein L7a |
| 49 | m6A | K1PAY7_CRAGI | Propionyl-CoA carboxylase alpha chain, mitochondrial |
| 50 | m6A | K1R6L5_CRAGI | NADH-cytochrome b5 reductase |
| 51 | m6A | K1R1B1_CRAGI | 35 kDa SR repressor protein |
| 52 | m6A | K1QHQ6_CRAGI | Acyl-CoA dehydrogenase family member 9, mitochondrial |
| 53 | m6A | K1QZU8_CRAGI | Calcium-transporting ATPase |
| 54 | m6A | K1RN77_CRAGI | Nuclear autoantigenic sperm protein |
| 55 | m6A | K1PZ23_CRAGI | DnaJ-like protein subfamily C member 3 |
| 56 | m6A | K1R005_CRAGI | Filamin-C (Fragment) |
| 57 | m6A | K1RA35_CRAGI | Splicing factor, arginine/serine-rich 7 |
| 58 | m6A | K1R2V1_CRAGI | Importin subunit beta-1 |
| 59 | m6A | K1QAH9_CRAGI | H/ACA ribonucleoprotein complex subunit |
| 60 | m6A | K1QET2_CRAGI | Coatomer subunit alpha |
| | m6A | K1RAB9_CRAGI | Epoxide hydrolase 4 |
| | m6A | K1QGK2_CRAGI | Coatomer subunit beta |

| | | | |
|----|-----|--------------|---|
| 1 | | | |
| 2 | | | |
| 3 | m6A | K1PXN5_CRAGI | T-complex protein 1 subunit zeta |
| 4 | m6A | K1QHX2_CRAGI | La-related protein 7 |
| 5 | m6A | K1PZ08_CRAGI | Ras-related protein Rab-7a |
| 6 | m6A | K1RK68_CRAGI | Uncharacterized protein |
| 7 | m6A | K1Q0R4_CRAGI | ATP-binding cassette sub-family F member 2 |
| 8 | m6A | K1QW72_CRAGI | Catalase |
| 9 | m6A | K1PPP8_CRAGI | Vigilin |
| 10 | m6A | K1QVW3_CRAGI | Alkylglycerone-phosphate synthase |
| 11 | m6A | K1PBZ4_CRAGI | Regulator of nonsense transcripts 1 |
| 12 | m6A | K1Q6W5_CRAGI | FACT complex subunit spt16 |
| 13 | m6A | K1R5F2_CRAGI | 14-3-3 protein epsilon |
| 14 | m6A | K1R5F2_CRAGI | 14-3-3 protein epsilon |
| 15 | m6A | K1R5F2_CRAGI | 14-3-3 protein epsilon |
| 16 | m6A | K1RLT4_CRAGI | Signal recognition particle subunit SRP68 |
| 17 | m6A | K1RSS3_CRAGI | Myosin heavy chain, striated muscle |
| 18 | m6A | K1RNN9_CRAGI | Cytoskeleton-associated protein 5 |
| 19 | m6A | K1QN11_CRAGI | Pre-mRNA-processing-splicing factor 8 |
| 20 | m6A | K1PA54_CRAGI | Replication factor C subunit 3 |
| 21 | m6A | K1PA54_CRAGI | Replication factor C subunit 3 |
| 22 | m6A | K1QC78_CRAGI | Ras-related protein Rab-14 |
| 23 | m6A | K1QW36_CRAGI | 60S ribosomal protein L6 |
| 24 | m6A | K1Q9P5_CRAGI | Mitochondrial-processing peptidase subunit beta |
| 25 | m6A | K1Q253_CRAGI | Neutral and basic amino acid transport protein rBAT |
| 26 | m6A | K1Q253_CRAGI | Neutral and basic amino acid transport protein rBAT |
| 27 | m6A | K1QHK9_CRAGI | Dynein heavy chain, cytoplasmic |
| 28 | m6A | K1QFN1_CRAGI | 60S ribosomal protein L23 |
| 29 | m6A | K1P112_CRAGI | ATP synthase subunit gamma, mitochondrial |
| 30 | m6A | K1QE71_CRAGI | DNA helicase |
| 31 | m6A | K1QE71_CRAGI | DNA helicase |
| 32 | m6A | K1PK85_CRAGI | Cullin-associated NEDD8-dissociated protein 1 |
| 33 | m6A | K1QTD9_CRAGI | Nucleolar protein 56 |
| 34 | m6A | K1P9N7_CRAGI | 14-3-3 protein zeta |
| 35 | m6A | K1RG19_CRAGI | Protein FAM98A |
| 36 | m6A | K1PMP3_CRAGI | Protoporphyrinogen oxidase |
| 37 | m6A | K1PMP3_CRAGI | Protoporphyrinogen oxidase |
| 38 | m6A | K1QVN9_CRAGI | T-complex protein 1 subunit eta |
| 39 | m6A | K1QG65_CRAGI | rRNA 2'-O-methyltransferase fibrillarin |
| 40 | m6A | K1PM76_CRAGI | NADH dehydrogenase [ubiquinone] 1 alpha subcomplex subunit 9, mitochondrial |
| 41 | m6A | K1PM50_CRAGI | 40S ribosomal protein S16 |
| 42 | m6A | K1QEF9_CRAGI | Protein-glutamine gamma-glutamyltransferase K |
| 43 | m6A | K1RKC1_CRAGI | Far upstream element-binding protein 3 |
| 44 | m6A | K1RKC1_CRAGI | Far upstream element-binding protein 3 |
| 45 | m6A | K1PY89_CRAGI | Extracellular superoxide dismutase [Cu-Zn] |
| 46 | m6A | K1RIZ3_CRAGI | Bone morphogenetic protein 7 |
| 47 | m6A | K1RA95_CRAGI | Filamin-A |
| 48 | m6A | K1PWZ3_CRAGI | Guanine nucleotide-binding protein subunit beta |
| 49 | m6A | K1Q812_CRAGI | NADH dehydrogenase [ubiquinone] iron-sulfur protein 2, mitochondrial |
| 50 | m6A | K1Q812_CRAGI | NADH dehydrogenase [ubiquinone] iron-sulfur protein 2, mitochondrial |
| 51 | m6A | K1PFS5_CRAGI | Elongation factor 1-gamma |
| 52 | m6A | K1PX23_CRAGI | Eukaryotic peptide chain release factor subunit 1 |
| 53 | m6A | K1QSV1_CRAGI | Uncharacterized protein |
| 54 | m6A | K1Q6X5_CRAGI | Protein disulfide-isomerase |
| 55 | m6A | K1Q6X5_CRAGI | Protein disulfide-isomerase |
| 56 | m6A | K1RAU3_CRAGI | DNA ligase |
| 57 | m6A | K1PXG6_CRAGI | Serine/threonine-protein phosphatase |
| 58 | m6A | K1RIG6_CRAGI | LSM14-like protein A |
| 59 | m6A | K1QWK6_CRAGI | Metalloendopeptidase |
| 60 | m6A | K1RCW3_CRAGI | Elongation factor 1-beta |
| | m6A | K1QK18_CRAGI | Cytochrome b5 |
| | m6A | K1Q056_CRAGI | Calpain-A |
| | m6A | K1Q9M7_CRAGI | Histone H1-delta |
| | m6A | K1P7L5_CRAGI | Transmembrane 9 superfamily member |
| | m6A | K1QSU3_CRAGI | Protein I(2)37Cc |
| | m6A | K1PLF9_CRAGI | Arginine kinase |
| | m6A | K1Q1F4_CRAGI | 60S ribosomal protein L3 (Fragment) |
| | m6A | K1R1T8_CRAGI | Nucleolar protein 56 |
| | m6A | K1QGB4_CRAGI | 40S ribosomal protein S17 |
| | m6A | K1QJ08_CRAGI | 60S ribosomal protein L26 |
| | m6A | K1Q4Y8_CRAGI | Histone H1oo |

| | | | |
|----|-----|--------------|---|
| 1 | | | |
| 2 | | | |
| 3 | m6A | K1PKF5_CRAGI | Protein-glutamine gamma-glutamyltransferase 4 |
| 4 | m6A | K1QYT5_CRAGI | Phosphate carrier protein, mitochondrial |
| 5 | m6A | K1RHB2_CRAGI | Nucleolar RNA helicase 2 |
| 6 | m6A | K1RJJ7_CRAGI | Histone H5 |
| 7 | m6A | K1PS84_CRAGI | Alpha-crystallin B chain |
| 8 | m6A | K1R2N0_CRAGI | Histone H4 |
| 9 | m6A | K1R2N0_CRAGI | Histone H4 |
| 10 | m6A | K1PZP6_CRAGI | Coatomer subunit gamma |
| 11 | m6A | K1RGJ7_CRAGI | Neogenin |
| 12 | m6A | K1R9P5_CRAGI | Mitochondrial import receptor subunit TOM70 |
| 13 | m6A | K1RUM2_CRAGI | Uncharacterized protein |
| 14 | m6A | K1RUM2_CRAGI | Uncharacterized protein |
| 15 | m6A | K1RJ97_CRAGI | Multifunctional protein ADE2 |
| 16 | m6A | K1RJS5_CRAGI | Uncharacterized protein |
| 17 | m6A | K1QW41_CRAGI | Leucine-zipper-like transcriptional regulator 1 |
| 18 | m6A | K1R834_CRAGI | 60S ribosomal protein L9 |
| 19 | m6A | K1QLK8_CRAGI | GTP-binding protein SAR1b |
| 20 | m6A | K1QLK8_CRAGI | GTP-binding protein SAR1b |
| 21 | m6A | K1QDH9_CRAGI | Myosin-11 |
| 22 | m6A | K1QEF2_CRAGI | ADP-ribosylation factor-like protein 15 |
| 23 | m6A | K1PUX5_CRAGI | Casein kinase II subunit alpha |
| 24 | m6A | K1QLU6_CRAGI | Poly [ADP-ribose] polymerase |
| 25 | m6A | K1QLU6_CRAGI | Poly [ADP-ribose] polymerase |
| 26 | m6A | K1QUK3_CRAGI | Putative ATP-dependent RNA helicase DDX41 |
| 27 | m6A | K1S2S8_CRAGI | Signal recognition particle 54 kDa protein |
| 28 | m6A | K1PY73_CRAGI | Basic leucine zipper and W2 domain-containing protein 1 |
| 29 | m6A | K1S6V7_CRAGI | Serine/threonine-protein phosphatase 2A 65 kDa regulatory subunit A alpha isoform |
| 30 | m6A | K1QPC6_CRAGI | Nucleolar complex protein 2-like protein |
| 31 | m6A | K1QPC6_CRAGI | Nucleolar complex protein 2-like protein |
| 32 | m6A | K1QPP2_CRAGI | Elongation factor Tu, mitochondrial |
| 33 | m6A | K1QDN1_CRAGI | Heat shock protein 75 kDa, mitochondrial (Fragment) |
| 34 | m6A | K1R996_CRAGI | Long-chain-fatty-acid--CoA ligase 4 |
| 35 | m6A | K1RDW8_CRAGI | Golgi apparatus protein 1 |
| 36 | m6A | K1S3G2_CRAGI | HMGB1 |
| 37 | m6A | K1S3G2_CRAGI | HMGB1 |
| 38 | m6A | K1QR48_CRAGI | Calcium-binding mitochondrial carrier protein SCaMC-2 |
| 39 | m6A | K1P5V7_CRAGI | Eukaryotic translation initiation factor 3 subunit C |
| 40 | m6A | K1PV86_CRAGI | Phosphoglycerate mutase family member 5 |
| 41 | m6A | K1QWC3_CRAGI | 40S ribosomal protein S3 |
| 42 | m6A | K1PZ70_CRAGI | NADH dehydrogenase [ubiquinone] iron-sulfur protein 6, mitochondrial |
| 43 | m6A | K1PZ70_CRAGI | NADH dehydrogenase [ubiquinone] iron-sulfur protein 6, mitochondrial |
| 44 | m6A | K1PTL4_CRAGI | Odr-4-like protein |
| 45 | m6A | K1QRM1_CRAGI | Nuclear pore protein |
| 46 | m6A | K1PVD7_CRAGI | Cytochrome c oxidase subunit 5A, mitochondrial |
| 47 | m6A | K1QFR2_CRAGI | Calnexin |
| 48 | m6A | K1Q273_CRAGI | 60S ribosomal protein L14 |
| 49 | m6A | K1Q273_CRAGI | 60S ribosomal protein L14 |
| 50 | m6A | K1R0M2_CRAGI | Uncharacterized protein |
| 51 | m6A | K1R5W3_CRAGI | Uncharacterized protein |
| 52 | m6A | K1QXQ8_CRAGI | DNA helicase |
| 53 | m6A | K1QPY8_CRAGI | Extracellular superoxide dismutase [Cu-Zn] |
| 54 | m6A | K1Q6V6_CRAGI | Replication factor C subunit 4 |
| 55 | m6A | K1Q6V6_CRAGI | Replication factor C subunit 4 |
| 56 | m6A | K1QMS2_CRAGI | Cadherin EGF LAG seven-pass G-type receptor 3 |
| 57 | m6A | K1Q7T5_CRAGI | Protein disulfide-isomerase |
| 58 | m6A | K1QRZ3_CRAGI | 40S ribosomal protein S13 |
| 59 | m6A | K1R4Z3_CRAGI | Malate dehydrogenase, mitochondrial |
| 60 | m6A | K1PJ85_CRAGI | 26S protease regulatory subunit 6A |
| | m6A | K1PB87_CRAGI | Uncharacterized protein |
| | m6A | K1PXU6_CRAGI | 60S ribosomal protein L24 |
| | m6A | K1R6S5_CRAGI | 40S ribosomal protein S9 |
| | m6A | K1PVH5_CRAGI | Centromere/kinetochore protein zw10-like protein |
| | m6A | K1R512_CRAGI | Uncharacterized protein |
| | m6A | K1QK68_CRAGI | Myosin-2 essential light chain |
| | m6A | K1PUV4_CRAGI | 40S ribosomal protein S24 |
| | m6A | K1R5U8_CRAGI | UBX domain-containing protein 4 |
| | m6A | K1PW39_CRAGI | Glycerol-3-phosphate dehydrogenase, mitochondrial |
| | m6A | K1R790_CRAGI | Retinol dehydrogenase 13 |
| | m6A | K1QT61_CRAGI | NADH dehydrogenase [ubiquinone] flavoprotein 2, mitochondrial (Fragment) |

| | | | |
|----|-----|--------------|---|
| 1 | | | |
| 2 | | | |
| 3 | m6A | K1RG28_CRAGI | Kinase C and casein kinase substrate in neurons protein 2 |
| 4 | m6A | K1QKV1_CRAGI | Cytochrome b-c1 complex subunit 6 |
| 5 | m6A | K1P9S7_CRAGI | Brix domain-containing protein 2 |
| 6 | m6A | K1QN79_CRAGI | 40S ribosomal protein S11 |
| 7 | m6A | K1QEJ0_CRAGI | Ras GTPase-activating protein-binding protein 2 |
| 8 | m6A | K1S1X3_CRAGI | SWI/SNF-related matrix-associated actin-dependent regulator of chromatin subfamily A member 5 |
| 9 | m6A | K1R9T2_CRAGI | Eukaryotic translation initiation factor 3 subunit B |
| 10 | m6A | K1QED7_CRAGI | Replication protein A subunit |
| 11 | m6A | K1QK5_CRAGI | Metabotropic glutamate receptor 2 |
| 12 | m6A | K1RN97_CRAGI | Hemagglutinin/amebocyte aggregation factor |
| 13 | m6A | K1PJS7_CRAGI | Poly [ADP-ribose] polymerase |
| 14 | m6A | K1R6F5_CRAGI | Putative ATP-dependent RNA helicase DDX23 |
| 15 | m6A | K1R8R6_CRAGI | Fructose-bisphosphate aldolase |
| 16 | m6A | K1QY85_CRAGI | Transport protein Sec31A |
| 17 | m6A | K1QF31_CRAGI | Serine/threonine-protein kinase PLK |
| 18 | m6A | K1Q5J7_CRAGI | Uncharacterized protein |
| 19 | m6A | K1QPF0_CRAGI | Uncharacterized protein |
| 20 | m6A | K1P6Y1_CRAGI | Uncharacterized protein |
| 21 | m6A | K1QJM1_CRAGI | 60S ribosomal protein L30 |
| 22 | m6A | K1PXD4_CRAGI | Putative ATP-dependent RNA helicase DDX6 |
| 23 | m6A | K1PH31_CRAGI | Protein arginine N-methyltransferase 1 |
| 24 | m6A | K1PAM6_CRAGI | Uncharacterized protein |
| 25 | m6A | K1RFU6_CRAGI | Proteasome activator complex subunit 3 |
| 26 | m6A | K1Q324_CRAGI | Heterogeneous nuclear ribonucleoprotein K |
| 27 | m6A | K1QRG9_CRAGI | Uncharacterized protein |
| 28 | m6A | K1S6H7_CRAGI | Vacuolar protein sorting-associated protein 13C |
| 29 | m6A | K1QE94_CRAGI | Alpha-galactosidase |
| 30 | m6A | K1Q7Q2_CRAGI | CCAAT/enhancer-binding protein zeta |
| 31 | m6A | K1Q7G8_CRAGI | Fatty acid synthase |
| 32 | m6A | K1QXH3_CRAGI | Translational activator GCN1 |
| 33 | m6A | K1P8G1_CRAGI | Heterogeneous nuclear ribonucleoprotein H |
| 34 | m6A | K1QKQ8_CRAGI | THO complex subunit 4-A |
| 35 | m6A | K1RA63_CRAGI | Transmembrane protein 2 |
| 36 | m6A | K1QAA2_CRAGI | Uncharacterized protein |
| 37 | m6A | K1PLA7_CRAGI | Eukaryotic initiation factor 4A-II (Fragment) |
| 38 | m6A | K1QIV3_CRAGI | Uncharacterized protein |
| 39 | m6A | K1RAH2_CRAGI | Superoxide dismutase [Cu-Zn] |
| 40 | m6A | K1QXA9_CRAGI | Sortilin-related receptor |
| 41 | m6A | K1QSD9_CRAGI | Uncharacterized protein |
| 42 | m6A | K1Q3W3_CRAGI | NADH dehydrogenase [ubiquinone] iron-sulfur protein 3, mitochondrial |
| 43 | m6A | K1R3T3_CRAGI | Transcription factor BTF3 |
| 44 | m6A | K1QMH5_CRAGI | Small nuclear ribonucleoprotein Sm D1 |
| 45 | m6A | K1R1R9_CRAGI | Pre-mRNA-processing factor 6 |
| 46 | m6A | K1PM66_CRAGI | 60S ribosomal protein L12 |
| 47 | m6A | K1Q3W9_CRAGI | FAS-associated factor 2-B |
| 48 | m6A | K1P9D0_CRAGI | Stress-70 protein, mitochondrial |
| 49 | m6A | K1R4F7_CRAGI | Ras-related protein Rab-6B |
| 50 | m6A | K1QGP7_CRAGI | Uncharacterized protein |
| 51 | m6A | K1REY2_CRAGI | Dysferlin |
| 52 | m6A | K1QSB2_CRAGI | 26S protease regulatory subunit 6B |
| 53 | m6A | K1RAU8_CRAGI | Eukaryotic translation initiation factor 3 subunit E |
| 54 | m6A | K1QAB1_CRAGI | AP-2 complex subunit alpha |
| 55 | m6A | K1RFU8_CRAGI | High mobility group protein DSP1 |
| 56 | m6A | K1QAA8_CRAGI | CAAX prenyl protease 1-like protein |
| 57 | m6A | K1PXS8_CRAGI | Calreticulin |
| 58 | m6A | K1RV41_CRAGI | Guanine nucleotide-binding protein subunit beta-2-like 1 |
| 59 | m6A | K1Q5Z6_CRAGI | Eukaryotic translation initiation factor 2 subunit 2 |
| 60 | m6A | K1QYQ9_CRAGI | Uncharacterized protein |
| | m6A | K1RCL2_CRAGI | Mitochondrial import inner membrane translocase subunit Tim13-B |
| | m6A | K1PI50_CRAGI | 40S ribosomal protein S26 |

| | | | |
|----|-----|--------------|--|
| 1 | | | |
| 2 | | | |
| 3 | m6A | K1QGP1_CRAGI | Replication factor C subunit 2 |
| 4 | m6A | K1P541_CRAGI | Alpha-soluble NSF attachment protein |
| 5 | m6A | K1Q667_CRAGI | tRNA-splicing ligase RtcB homolog |
| 6 | m6A | K1QBM3_CRAGI | Ras-related protein Rab-2 |
| 7 | m6A | K1R7L4_CRAGI | Neural cell adhesion molecule 1 |
| 8 | m6A | K1PH13_CRAGI | Dolichyl-diphosphooligosaccharide--protein glycosyltransferase subunit STT3B |
| 9 | m6A | K1PH13_CRAGI | Dolichyl-diphosphooligosaccharide--protein glycosyltransferase subunit STT3B |
| 10 | m6A | K1QAI2_CRAGI | Ufm1-specific protease 2 |
| 11 | m6A | K1RJW8_CRAGI | Protein DEK |
| 12 | m6A | K1QKG8_CRAGI | Upstream activation factor subunit spp27 |
| 13 | m6A | K1R150_CRAGI | Ras-related protein Rab-1A |
| 14 | m6A | K1PI40_CRAGI | Uncharacterized protein |
| 15 | m6A | K1PI40_CRAGI | Uncharacterized protein |
| 16 | m6A | K1PZT2_CRAGI | Cytochrome c oxidase subunit 5B, mitochondrial |
| 17 | m6A | K1PJB0_CRAGI | Heat shock protein 70 B2 |
| 18 | m6A | K1PR25_CRAGI | Regulator of differentiation 1 |
| 19 | m6A | K1QMV5_CRAGI | Annexin |
| 20 | m6A | K1QMV5_CRAGI | Annexin |
| 21 | m6A | K1Q0N6_CRAGI | Dolichyl-diphosphooligosaccharide--protein glycosyltransferase subunit STT3A |
| 22 | m6A | K1QY58_CRAGI | Eukaryotic translation initiation factor 3 subunit I (Fragment) |
| 23 | m6A | K1RIJ1_CRAGI | Synaptobrevin (Fragment) |
| 24 | m6A | K1PNC7_CRAGI | AFG3-like protein 2 |
| 25 | m6A | K1QQR1_CRAGI | Major vault protein |
| 26 | m6A | K1QQR1_CRAGI | Major vault protein |
| 27 | m6A | K1R5V4_CRAGI | GTP-binding nuclear protein |
| 28 | m6A | K1QGA7_CRAGI | Kynurenine formamidase |
| 29 | m6A | K1PTV1_CRAGI | Splicing factor 3B subunit 4 |
| 30 | m6A | K1P3Q5_CRAGI | Programmed cell death 6-interacting protein |
| 31 | m6A | K1P3Q5_CRAGI | Programmed cell death 6-interacting protein |
| 32 | m6A | K1R2G9_CRAGI | SEC13-like protein |
| 33 | m6A | K1PF96_CRAGI | Spliceosome RNA helicase BAT1 |
| 34 | m6A | K1R1F0_CRAGI | ATP-dependent DNA helicase 2 subunit 1 |
| 35 | m6A | K1Q5Z1_CRAGI | Uncharacterized protein |
| 36 | m6A | K1Q880_CRAGI | Transportin-1 |
| 37 | m6A | K1PDF8_CRAGI | Splicing factor, arginine/serine-rich 6 |
| 38 | m6A | K1PDF8_CRAGI | Splicing factor, arginine/serine-rich 6 |
| 39 | m6A | K1PMY9_CRAGI | Calmodulin |
| 40 | m6A | K1PPW8_CRAGI | Coatomer subunit beta |
| 41 | m6A | K1QZQ8_CRAGI | Low-density lipoprotein receptor-related protein 8 |
| 42 | m6A | K1QE43_CRAGI | Uncharacterized protein |
| 43 | m6A | K1QE43_CRAGI | Uncharacterized protein |
| 44 | m6A | K1RDS1_CRAGI | Splicing factor, arginine/serine-rich 2 |
| 45 | m6A | K1RAI3_CRAGI | Annexin |
| 46 | m6A | K1PCR5_CRAGI | KH domain-containing, RNA-binding, signal transduction-associated protein 2 |
| 47 | m6A | K1QWP1_CRAGI | Nucleoporin seh1 |
| 48 | m6A | K1QAL1_CRAGI | Transmembrane emp24 domain-containing protein 7 |
| 49 | m6A | K1QAL1_CRAGI | Transmembrane emp24 domain-containing protein 7 |
| 50 | m6A | K1Q2H5_CRAGI | Uncharacterized protein |
| 51 | m6A | K1REPO_CRAGI | Uncharacterized protein |
| 52 | m6A | K1PKI9_CRAGI | Uncharacterized protein |
| 53 | m6A | K1RG79_CRAGI | Neuronal acetylcholine receptor subunit alpha-6 |
| 54 | m6A | K1Q1L4_CRAGI | Uncharacterized protein |
| 55 | m6A | K1Q1L4_CRAGI | Uncharacterized protein |
| 56 | m6A | K1QTP6_CRAGI | Cation-transporting ATPase |
| 57 | m6A | K1Q615_CRAGI | Peroxiredoxin-1 |
| 58 | m6A | K1QIZ7_CRAGI | Programmed cell death protein 6 |
| 59 | m6A | K1R0D7_CRAGI | Eukaryotic translation initiation factor 3 subunit M (Fragment) |
| 60 | m6A | K1QTV3_CRAGI | Murinoglobulin-2 |
| | m6A | K1PDL3_CRAGI | Ribosomal protein L19 |
| | m6A | K1QW21_CRAGI | 39S ribosomal protein L40, mitochondrial |
| | m6A | K1Q317_CRAGI | Serine/threonine-protein kinase SRPK1 |
| | m6A | K1QKG9_CRAGI | Cysteine desulfurase, mitochondrial |
| | m6A | K1PS77_CRAGI | Prostaglandin G/H synthase 1 |
| | m6A | K1QJW6_CRAGI | Translocon-associated protein subunit gamma |
| | m6A | K1QTV1_CRAGI | Uncharacterized protein |
| | m6A | K1QTV6_CRAGI | Eukaryotic translation initiation factor 3 subunit F |
| | m6A | K1PNY5_CRAGI | Splicing factor, proline-and glutamine-rich |
| | m6A | K1R100_CRAGI | Metaxin-2 |
| | m6A | K1R8L1_CRAGI | Exportin-2 |

| | | | |
|----|-----|--------------|--|
| 1 | | | |
| 2 | | | |
| 3 | m6A | K1QZ64_CRAGI | Nuclear pore complex protein Nup98-Nup96 |
| 4 | m6A | K1QWZ8_CRAGI | Catenin beta |
| 5 | m6A | K1QAT9_CRAGI | ATP-dependent RNA helicase DDX1 |
| 6 | m6A | K1P8Y9_CRAGI | Cytochrome b-c1 complex subunit 7 |
| 7 | m6A | K1PIC5_CRAGI | Transmembrane protein 85 |
| 8 | m6A | K1QMV7_CRAGI | V-type proton ATPase subunit D |
| 9 | m6A | K1RC37_CRAGI | Uncharacterized protein |
| 10 | m6A | K1PEY4_CRAGI | 26S proteasome non-ATPase regulatory subunit 2 |
| 11 | m6A | K1RG04_CRAGI | ALK tyrosine kinase receptor |
| 12 | m6A | K1QG72_CRAGI | Hemagglutinin/amebocyte aggregation factor |
| 13 | m6A | K1RK83_CRAGI | Tyrosine-protein kinase BAZ1B |
| 14 | m6A | K1QMT1_CRAGI | DnaJ-like protein subfamily B member 4 |
| 15 | m6A | K1P811_CRAGI | Pleckstrin-like protein domain-containing family F member 2 (Fragment) |
| 16 | m6A | K1R316_CRAGI | Nucleolar complex protein 2-like protein (Fragment) |
| 17 | m6A | K1QDB9_CRAGI | Transport protein Sec61 subunit alpha isoform 2 (Fragment) |
| 18 | m6A | K1QMJ8_CRAGI | Transcription initiation factor IIA subunit 1 |
| 19 | m6A | K1R5G4_CRAGI | 60S ribosomal protein L31 |
| 20 | m6A | K1R1W9_CRAGI | Nicalin-1 |
| 21 | m6A | K1QDA7_CRAGI | Uracil phosphoribosyltransferase |
| 22 | m6A | K1QI02_CRAGI | Vesicle-trafficking protein SEC22b |
| 23 | m6A | K1QFZ8_CRAGI | Ceramide kinase-like protein |
| 24 | m6A | K1Q151_CRAGI | 60S ribosomal protein L32 |
| 25 | m6A | K1QNS4_CRAGI | DnaJ-like protein subfamily C member 9 |
| 26 | m6A | K1REQ4_CRAGI | Cytochrome c oxidase subunit 6B |
| 27 | m6A | K1R4B8_CRAGI | Plexin domain-containing protein 2 |
| 28 | m6A | K1QC10_CRAGI | GTP-binding protein 1 |
| 29 | m6A | K1PJY2_CRAGI | Inositol polyphosphate 1-phosphatase |
| 30 | m6A | K1R983_CRAGI | Protein transport protein SEC23 |
| 31 | m6A | K1Q5Y3_CRAGI | Annexin |
| 32 | m6A | K1Q1N1_CRAGI | Alpha-mannosidase |
| 33 | m6A | K1QNU0_CRAGI | Non-specific serine/threonine protein kinase |
| 34 | m6A | K1R1Q8_CRAGI | Ras-related protein Rab-5C |
| 35 | m6A | K1RH95_CRAGI | Myosin-IIIB |
| 36 | m6A | K1QWE5_CRAGI | Ras-related protein Rab-18-B |
| 37 | m6A | K1QCB0_CRAGI | 40S ribosomal protein S5 |
| 38 | m6A | K1Q0I8_CRAGI | Putative splicing factor, arginine/serine-rich 7 |
| 39 | m6A | K1QXF5_CRAGI | Calcyphosin-like protein |
| 40 | m6A | K1R8C6_CRAGI | 40S ribosomal protein S12 |
| 41 | m6A | K1QFA9_CRAGI | Low-density lipoprotein receptor-related protein 2 |
| 42 | m6A | K1QYF5_CRAGI | Apoptosis-inducing factor 1, mitochondrial |
| 43 | m6A | K1QA50_CRAGI | V-type proton ATPase subunit H |
| 44 | m6A | K1PY39_CRAGI | Protocadherin Fat 4 |
| 45 | m6A | K1Q330_CRAGI | Dihydrolipoyl dehydrogenase |
| 46 | m6A | K1Q350_CRAGI | Glyceraldehyde-3-phosphate dehydrogenase |
| 47 | m6A | K1Q6U7_CRAGI | 78 kDa glucose-regulated protein |
| 48 | m6A | K1RBI9_CRAGI | Small nuclear ribonucleoprotein Sm D2 |
| 49 | m6A | K1P0H0_CRAGI | Aspartyl/asparaginyl beta-hydroxylase |
| 50 | m6A | K1QSR2_CRAGI | Apoptosis inhibitor 5 |
| 51 | m6A | K1RDV7_CRAGI | Cell division control protein 2-like protein (Fragment) |
| 52 | m6A | K1PD30_CRAGI | Putative histone-binding protein Caf1 |
| 53 | m6A | K1P7K8_CRAGI | Vesicle-fusing ATPase 1 |
| 54 | m6A | K1PVZ3_CRAGI | Cold shock domain-containing protein E1 |
| 55 | m6A | K1RKZ5_CRAGI | DNA damage-binding protein 1 |
| 56 | m6A | K1R0Z4_CRAGI | Uncharacterized protein |
| 57 | m6A | K1Q947_CRAGI | Dynein light chain |
| 58 | m6A | K1PU46_CRAGI | Lethal(2) giant larvae-like protein 1 |
| 59 | m6A | K1Q8K9_CRAGI | KRR1 small subunit processome component-like protein |
| 60 | m6A | K1PQZ3_CRAGI | Armadillo repeat-containing protein 4 |
| | m6A | K1QL00_CRAGI | Microsomal glutathione S-transferase 1 |
| | m6A | K1RDM2_CRAGI | 60S ribosomal protein L18a |

| | | | |
|----|-----|--------------|--|
| 1 | | | |
| 2 | | | |
| 3 | m6A | K1Q3V9_CRAGI | Mitochondrial carnitine/acylcarnitine carrier protein |
| 4 | m6A | K1QN55_CRAGI | 60S acidic ribosomal protein P1 |
| 5 | m6A | K1R3G0_CRAGI | Transformer-2-like protein beta |
| 6 | m6A | K1PWM3_CRAGI | MICOS complex subunit MIC13 |
| 7 | m6A | K1QKL8_CRAGI | V-type proton ATPase subunit a |
| 8 | m6A | K1S6T6_CRAGI | UPF0480 protein C15orf24-like protein |
| 9 | m6A | K1R0W0_CRAGI | Ferritin |
| 10 | m6A | K1PGK7_CRAGI | Uncharacterized protein |
| 11 | m6A | K1QY71_CRAGI | Histone H2B |
| 12 | m6A | K1QNT7_CRAGI | Aldehyde dehydrogenase, mitochondrial |
| 13 | m6A | K1RJ96_CRAGI | Sphere organelles protein SPH-1 |
| 14 | m6A | K1RZE2_CRAGI | Isocitrate dehydrogenase [NADP] |
| 15 | m6A | K1PPV1_CRAGI | Atlastin-2 |
| 16 | m6A | K1P9F1_CRAGI | Insulin-like growth factor-binding protein complex acid labile chain |
| 17 | m6A | K1QVU0_CRAGI | Synaptojanin-2-binding protein |
| 18 | m6A | K1QX44_CRAGI | Ras-related protein Rab-11B |
| 19 | m6A | K1QKU6_CRAGI | mRNA export factor |
| 20 | m6A | K1QDV6_CRAGI | Protein argonaute-2 |
| 21 | m6A | K1R5B9_CRAGI | DNA-directed RNA polymerase, mitochondrial |
| 22 | m6A | K1RCT2_CRAGI | Translocon-associated protein subunit delta |
| 23 | m6A | K1PKD4_CRAGI | 40S ribosomal protein S30 |
| 24 | m6A | K1PP50_CRAGI | Golgi integral membrane protein 4 |
| 25 | m6A | K1PG60_CRAGI | 60S ribosomal protein L17 |
| 26 | m6A | K1QWJ4_CRAGI | Splicing factor 3B subunit 5 |
| 27 | m6A | K1RB91_CRAGI | Neutral alpha-glucosidase AB |
| 28 | m6A | K1RD12_CRAGI | Uncharacterized protein |
| 29 | m6A | K1PQE3_CRAGI | RNA-binding protein Raly |
| 30 | m6A | K1Q2Y1_CRAGI | 40S ribosomal protein S15 |
| 31 | m6A | K1PQF1_CRAGI | Neural cell adhesion molecule L1 |
| 32 | m6A | K1QKJ0_CRAGI | Aldehyde dehydrogenase family 3 member B1 |
| 33 | m6A | K1PUQ5_CRAGI | Histone H2B |
| 34 | m6A | K1Q2W7_CRAGI | Uncharacterized protein |
| 35 | m6A | K1Q412_CRAGI | Uncharacterized protein |
| 36 | m6A | K1RNH1_CRAGI | 60S ribosomal protein L18 (Fragment) |
| 37 | m6A | K1QNT4_CRAGI | Anoctamin |
| 38 | m6A | K1P8B7_CRAGI | Ubiquitin-conjugating enzyme E2-17 kDa (Fragment) |
| 39 | m6A | K1Q1D7_CRAGI | Putative rRNA-processing protein EBP2 |
| 40 | m6A | K1PY30_CRAGI | Septin-2 |
| 41 | m6A | K1Q1R1_CRAGI | Exostosin-3 |
| 42 | m6A | K1RHP3_CRAGI | Proliferation-associated protein 2G4 |
| 43 | m6A | K1PZI3_CRAGI | SWI/SNF complex subunit SMARCC2 |
| 44 | m6A | K1QT97_CRAGI | N(G),N(G)-dimethylarginine dimethylaminohydrolase 1 |
| 45 | m6A | K1QQQ5_CRAGI | Replication factor C subunit 5 |
| 46 | m6A | K1PA61_CRAGI | Actin-like protein 6A |
| 47 | m6A | K1PNL0_CRAGI | Microtubule-associated protein futsch |
| 48 | m6A | K1QI28_CRAGI | V-type proton ATPase subunit B |
| 49 | m6A | K1PYL5_CRAGI | Uncharacterized protein |
| 50 | m6A | K1PJ65_CRAGI | Dual specificity mitogen-activated protein kinase kinase 7 |
| 51 | m6A | K1QMD8_CRAGI | Proteasome subunit alpha type |
| 52 | m6A | K1Q2L4_CRAGI | Transmembrane emp24 domain-containing protein 9 |
| 53 | m6A | K1Q8C1_CRAGI | Putative RNA-binding protein Luc7-like 2 |
| 54 | m6A | K1PS71_CRAGI | Uncharacterized protein |
| 55 | m6A | K1Q900_CRAGI | Galectin |
| 56 | m6A | K1RKR8_CRAGI | Pumilio-like protein 2 |
| 57 | m6A | K1RKE5_CRAGI | IQ and AAA domain-containing protein 1 |
| 58 | m6A | K1QRL4_CRAGI | Importin-5 |
| 59 | m6A | K1PGN0_CRAGI | Fatty-acid amide hydrolase 2 |
| 60 | m6A | K1RD83_CRAGI | Serine hydroxymethyltransferase |
| | m6A | K1RFA3_CRAGI | Lamin Dm0 |
| | m6A | K1QAG7_CRAGI | Phosphatidylinositide phosphatase SAC1 |

| | | | |
|----|-----|--------------|---|
| 1 | | | |
| 2 | | | |
| 3 | m6A | K1PJP7_CRAGI | Surfeit locus protein 4 |
| 4 | m6A | K1PG07_CRAGI | Lupus La-like protein |
| 5 | m6A | K1QVS0_CRAGI | Ras-like GTP-binding protein Rho1 |
| 6 | m6A | K1PWC3_CRAGI | Tetratricopeptide repeat protein 35 |
| 7 | m6A | K1QZK9_CRAGI | Uncharacterized protein |
| 8 | m6A | K1QAG9_CRAGI | Ferritin |
| 9 | m6A | K1QAG9_CRAGI | Ferritin |
| 10 | m6A | K1QHW8_CRAGI | Ferritin |
| 11 | m6A | K1PZF2_CRAGI | Exportin-7 |
| 12 | m6A | K1RCF4_CRAGI | Translocon-associated protein subunit alpha |
| 13 | m6A | K1QVIO_CRAGI | Isocitrate dehydrogenase [NAD] subunit, mitochondrial |
| 14 | m6A | K1PX47_CRAGI | Ubiquitin carboxyl-terminal hydrolase |
| 15 | m6A | K1P8G6_CRAGI | Vesicular integral-membrane protein VIP36 |
| 16 | m6A | K1PNZ8_CRAGI | Ribosomal protein L37 |
| 17 | m6A | K1Q373_CRAGI | Splicing factor, arginine/serine-rich 7 |
| 18 | m6A | K1R0U6_CRAGI | Uncharacterized protein |
| 19 | m6A | K1QAV0_CRAGI | Guanine nucleotide-binding protein G(Q) subunit alpha |
| 20 | m6A | K1R8Y1_CRAGI | Obg-like ATPase 1 |
| 21 | m6A | K1R8Y1_CRAGI | Obg-like ATPase 1 |
| 22 | m6A | K1QBY6_CRAGI | Transmembrane protein Tmp21 |
| 23 | m6A | K1QBY6_CRAGI | Transmembrane protein Tmp21 |
| 24 | m6A | K1QZ58_CRAGI | Splicing factor U2AF 26 kDa subunit |
| 25 | m6A | K1RAE9_CRAGI | ADP-ribosylation factor-like protein 8A |
| 26 | m6A | K1RAE9_CRAGI | ADP-ribosylation factor-like protein 8A |
| 27 | m6A | K1RCW5_CRAGI | Eukaryotic translation initiation factor 4 gamma 3 |
| 28 | m6A | K1PZ89_CRAGI | Mannosyl-oligosaccharide glucosidase |
| 29 | m6A | K1PBG6_CRAGI | Uncharacterized protein |
| 30 | m6A | K1QPS1_CRAGI | Poly [ADP-ribose] polymerase |
| 31 | m6A | K1R1C5_CRAGI | Signal recognition particle receptor subunit beta |
| 32 | m6A | K1R1C5_CRAGI | Signal recognition particle receptor subunit beta |
| 33 | m6A | K1PVG0_CRAGI | Long-chain fatty acid transport protein 4 |
| 34 | m6A | K1QXA1_CRAGI | Retinol dehydrogenase 12 |
| 35 | m6A | K1R481_CRAGI | Epimerase family protein SDR39U1 |
| 36 | m6A | K1QVP6_CRAGI | Developmentally-regulated GTP-binding protein 1 |
| 37 | m6A | K1QVP6_CRAGI | Developmentally-regulated GTP-binding protein 1 |
| 38 | m6A | K1PWB7_CRAGI | Uncharacterized protein |
| 39 | m6A | K1PNQ1_CRAGI | Ankyrin repeat domain-containing protein 5 |
| 40 | m6A | K1Q8C5_CRAGI | Putative ATP-dependent RNA helicase DDX47 |
| 41 | m6A | K1PR38_CRAGI | TAR DNA-binding protein 43 |
| 42 | m6A | K1P7Q6_CRAGI | 40S ribosomal protein S19 |
| 43 | m6A | K1P7Q6_CRAGI | 40S ribosomal protein S19 |
| 44 | m6A | K1RFD2_CRAGI | Adenylate kinase |
| 45 | m6A | K1PQJ9_CRAGI | ATP synthase subunit delta, mitochondrial |
| 46 | m6A | K1Q4U7_CRAGI | AP-3 complex subunit delta-1 |
| 47 | m6A | K1QM06_CRAGI | Prohibitin |
| 48 | m6A | K1QUW5_CRAGI | U2 snRNP auxiliary factor large subunit |
| 49 | m6A | K1QUW5_CRAGI | U2 snRNP auxiliary factor large subunit |
| 50 | m6A | K1PD36_CRAGI | Ubiquitin |
| 51 | m6A | K1PBL2_CRAGI | Eukaryotic initiation factor 4A-III |
| 52 | m6A | K1R3V8_CRAGI | COP9 signalosome complex subunit 4 |
| 53 | m6A | K1PII4_CRAGI | YTH domain-containing protein 1 |
| 54 | m6A | K1PZL0_CRAGI | B-box type zinc finger protein ncl-1 |
| 55 | m6A | K1PZL0_CRAGI | B-box type zinc finger protein ncl-1 |
| 56 | m6A | K1REW8_CRAGI | Ribosomal protein L15 |
| 57 | m6A | K1R9V5_CRAGI | Tetraspanin |
| 58 | m6A | K1QPX1_CRAGI | ATPase family AAA domain-containing protein 3 |
| 59 | m6A | K1QHI2_CRAGI | Heterogeneous nuclear ribonucleoprotein L |
| 60 | m6A | K1QZ95_CRAGI | Nuclear pore complex protein |
| | m6A | K1R401_CRAGI | Spectrin alpha chain |
| | m6A | K1PSA1_CRAGI | Transmembrane 9 superfamily member |
| | m6A | K1Q486_CRAGI | Uncharacterized protein |
| | m6A | K1PYA0_CRAGI | Cytoplasmic dynein 2 heavy chain 1 |
| | m6A | K1QLC6_CRAGI | JmjC domain-containing protein 8 |
| | m6A | K1RDG4_CRAGI | DNA helicase |
| | m6A | K1PQY0_CRAGI | Protein quiver |
| | m6A | K1QTD5_CRAGI | Low-density lipoprotein receptor-related protein 12 |
| | m6A | K1PSP7_CRAGI | Uncharacterized protein |
| | m6A | K1QAL3_CRAGI | RNA-binding protein 28 |
| | m6A | K1QND2_CRAGI | Septin-2 |

| | | | |
|----|-----|--------------|---|
| 1 | | | |
| 2 | | | |
| 3 | m6A | K1RMM6_CRAGI | Centromere protein J |
| 4 | m6A | K1R1K6_CRAGI | Heat shock protein beta-1 |
| 5 | m6A | K1R3Z4_CRAGI | 5'-3' exoribonuclease 1 |
| 6 | m6A | K1RB56_CRAGI | Ferritin |
| 7 | m6A | K1RIZ9_CRAGI | Band 4.1-like protein 5 |
| 8 | m6A | K1RFB1_CRAGI | Stomatin-like protein 2 (Fragment) |
| 9 | m6A | K1RNI9_CRAGI | Leucine-rich repeat-containing protein 59 |
| 10 | m6A | K1Q7U7_CRAGI | Basigin |
| 11 | m6A | K1RNX0_CRAGI | Small nuclear ribonucleoprotein E |
| 12 | m6A | K1P5F7_CRAGI | Metastasis-associated protein MTA1 |
| 13 | m6A | K1P5F7_CRAGI | Metastasis-associated protein MTA1 |
| 14 | m6A | K1PVG9_CRAGI | Malectin |
| 15 | m6A | K1R247_CRAGI | Condensin complex subunit 1 |
| 16 | m6A | K1PSN0_CRAGI | Pre-mRNA-processing factor 40-like protein A |
| 17 | m6A | K1PZV3_CRAGI | Guanine nucleotide-binding protein-like 3-like protein (Fragment) |
| 18 | m6A | K1RWP3_CRAGI | Peptidyl-tRNA hydrolase 2, mitochondrial |
| 19 | m6A | K1Q7E4_CRAGI | Ubiquitin-conjugating enzyme E2 N |
| 20 | m6A | K1R7E4_CRAGI | Ubiquitin-conjugating enzyme E2 N |
| 21 | m6A | K1R7E4_CRAGI | Ubiquitin-conjugating enzyme E2 N |
| 22 | m6A | K1RK33_CRAGI | Exportin-1 |
| 23 | m6A | K1RPP1_CRAGI | Synaptophysin |
| 24 | m6A | K1Q5P0_CRAGI | 60S ribosomal protein L17 |
| 25 | m6A | K1PND7_CRAGI | Fatty acid synthase |
| 26 | m6A | K1PND7_CRAGI | Fatty acid synthase |
| 27 | m6A | K1R0R7_CRAGI | Putative ATP-dependent RNA helicase DHX36 |
| 28 | m6A | K1QJL6_CRAGI | Microtubule-associated protein RP/EB family member 3 |
| 29 | m6A | K1QKZ6_CRAGI | Inosine-5'-monophosphate dehydrogenase |
| 30 | m6A | Q70MT4_CRAGI | 40S ribosomal protein S10 |
| 31 | m6A | K1RP91_CRAGI | Putative RNA exonuclease NEF-sp |
| 32 | m6A | K1PKK7_CRAGI | AP-2 complex subunit mu-1 |
| 33 | m6A | K1PKK7_CRAGI | AP-2 complex subunit mu-1 |
| 34 | m6A | K1PLR8_CRAGI | Chromosome transmission fidelity protein 18-like protein (Fragment) |
| 35 | m6A | K1PH10_CRAGI | Polyadenylate-binding protein-interacting protein 1 |
| 36 | m6A | K1P2G0_CRAGI | Strawberry notch-like protein 1 |
| 37 | m6A | K1P2G0_CRAGI | Strawberry notch-like protein 1 |
| 38 | m6A | K1PNU2_CRAGI | Histone-arginine methyltransferase CARM1 |
| 39 | m6A | K1QZJ6_CRAGI | Uncharacterized protein (Fragment) |
| 40 | m6A | K1PXB6_CRAGI | Cadherin-23 |
| 41 | m6A | K1QCK4_CRAGI | CLIP-associating protein 1 |
| 42 | m6A | K1PPH0_CRAGI | Gamma-tubulin complex component |
| 43 | m6A | K1Q105_CRAGI | Ferrochelatase |
| 44 | m6A | K1Q105_CRAGI | Ferrochelatase |
| 45 | m6A | K1QF52_CRAGI | Uncharacterized protein |
| 46 | m6A | K1Q2Z5_CRAGI | Putative ATP-dependent RNA helicase DDX46 |
| 47 | m6A | K1PXI0_CRAGI | Angiopoietin-4 |
| 48 | m6A | K1RPF7_CRAGI | 60S ribosomal protein L5 |
| 49 | m6A | K1QV25_CRAGI | Transcription elongation factor B polypeptide 2 |
| 50 | m6A | K1QV25_CRAGI | Transcription elongation factor B polypeptide 2 |
| 51 | m6A | K1PUJ1_CRAGI | Radixin |
| 52 | m6A | K1QHT0_CRAGI | Deoxyuridine 5'-triphosphate nucleotidohydrolase, mitochondrial |
| 53 | m6A | K1QMK5_CRAGI | Kinesin-associated protein 3 |
| 54 | m6A | K1QQ16_CRAGI | AP complex subunit beta |
| 55 | m6A | K1QQ16_CRAGI | AP complex subunit beta |
| 56 | m6A | K1QZ49_CRAGI | Adipocyte plasma membrane-associated protein |
| 57 | m6A | K1QIB2_CRAGI | Mitogen-activated protein kinase |
| 58 | m6A | K1QXH7_CRAGI | DNA replication licensing factor mcm4-B |
| 59 | m6A | K1QQV0_CRAGI | Histone H1.2 |
| 60 | m6A | K1Q61_CRAGI | Acetolactate synthase-like protein |
| | m6A | K1R5R4_CRAGI | Dynein heavy chain 10, axonemal |
| | m6A | K1R4J0_CRAGI | MAGUK p55 subfamily member 2 |
| | m6A | K1RR98_CRAGI | NADH dehydrogenase [ubiquinone] 1 alpha subcomplex subunit 4-like 2 |
| | m6A | K1Q5E0_CRAGI | Dual specificity protein kinase CLK2 |
| | m6A | K1R275_CRAGI | Putative ATP-dependent RNA helicase DDX52 |
| | m6A | K1RFV5_CRAGI | ATP-dependent RNA helicase DDX1 |
| | m6A | K1QNZ7_CRAGI | Ubiquilin-1 |
| | m6A | K1QZ50_CRAGI | RNA-dependent RNA polymerase |
| | m6A | K1QH4_CRAGI | Uncharacterized protein |
| | m6A | K1Q455_CRAGI | Netrin-3 |
| | m6A | K1QQL6_CRAGI | Leucyl-tRNA synthetase, cytoplasmic |

| | | | |
|----|-----|--------------|--|
| 1 | | | |
| 2 | | | |
| 3 | m6A | K1RZM3_CRAGI | Cartilage acidic protein 1 |
| 4 | m6A | K1R065_CRAGI | Golgi membrane protein 1 |
| 5 | m6A | K1RD19_CRAGI | RNA-binding protein 4 |
| 6 | m6A | K1R969_CRAGI | Uncharacterized protein |
| 7 | m6A | K1RE19_CRAGI | V-type proton ATPase subunit S1 |
| 8 | m6A | K1QGW5_CRAGI | WD repeat and SOF domain-containing protein 1 |
| 9 | m6A | K1QKI1_CRAGI | Tudor domain-containing protein 1 |
| 10 | m6A | K1PSH2_CRAGI | 28S ribosomal protein S12, mitochondrial |
| 11 | m6A | K1QMT2_CRAGI | Signal peptidase complex catalytic subunit SEC11 |
| 12 | m6A | K1QDI0_CRAGI | Transmembrane protein 49 |
| 13 | m6A | K1Q8T3_CRAGI | Importin subunit alpha |
| 14 | m6A | K1Q525_CRAGI | Mechanosensory protein 2 (Fragment) |
| 15 | m6A | K1Q5G6_CRAGI | 60 kDa heat shock protein, mitochondrial |
| 16 | m6A | K1QHF0_CRAGI | 40S ribosomal protein S27 |
| 17 | m6A | K1Q7X3_CRAGI | Pre-mRNA-splicing factor SYF1 |
| 18 | m6A | K1RRH1_CRAGI | Chromodomain-helicase-DNA-binding protein Mi-2-like protein |
| 19 | m6A | K1Q435_CRAGI | Eukaryotic translation initiation factor 2 subunit 1 |
| 20 | m6A | K1RNS1_CRAGI | NADH dehydrogenase [ubiquinone] 1 alpha subcomplex subunit 8 |
| 21 | m6A | K1QGF9_CRAGI | Rootletin |
| 22 | m6A | K1QJ36_CRAGI | Muscle, skeletal receptor tyrosine protein kinase |
| 23 | m6A | K1RNU5_CRAGI | Pre-mRNA-splicing factor RBM22 |
| 24 | m6A | K1R916_CRAGI | Structural maintenance of chromosomes protein |
| 25 | m6A | K1RUC9_CRAGI | Uncharacterized protein |
| 26 | m6A | K1QR54_CRAGI | Zinc finger RNA-binding protein |
| 27 | m6A | K1P9Q2_CRAGI | Signal peptidase complex subunit 3 |
| 28 | m6A | K1RTR1_CRAGI | ATP-citrate synthase |
| 29 | m6A | K1Q050_CRAGI | Centrin-3 |
| 30 | m6A | K1QPA5_CRAGI | Uncharacterized protein C16orf61-like protein |
| 31 | m6A | K1PSY2_CRAGI | Fragile X mental retardation syndrome-related protein 1 |
| 32 | m6A | K1R7G0_CRAGI | Chromobox-like protein 5 |
| 33 | m6A | K1QFG2_CRAGI | Telomere-associated protein RIF1 |
| 34 | m6A | K1QYV5_CRAGI | Cytoplasmic polyadenylation element-binding protein 1-B |
| 35 | m6A | K1R1I2_CRAGI | Cation-independent mannose-6-phosphate receptor |
| 36 | m6A | K1R255_CRAGI | Heterogeneous nuclear ribonucleoprotein L |
| 37 | m6A | K1RB07_CRAGI | 60S ribosomal protein L27a |
| 38 | m6A | K1RYF2_CRAGI | Enoyl-CoA hydratase domain-containing protein 3, mitochondrial |
| 39 | m6A | K1RJ53_CRAGI | Tetratricopeptide repeat protein 12 |
| 40 | m6A | K1QW73_CRAGI | Glycoprotein 3-alpha-L-fucosyltransferase A |
| 41 | m6A | K1RBC9_CRAGI | Transketolase-like protein 2 |
| 42 | m6A | K1QJ46_CRAGI | Putative methylcrotonoyl-CoA carboxylase beta chain, mitochondrial |
| 43 | m6A | K1Q9V2_CRAGI | Antigen KI-67 |
| 44 | m6A | K1PWQ2_CRAGI | 60 kDa neurofilament protein |
| 45 | m6A | K1QGF1_CRAGI | Splicing factor 3B subunit 2 |
| 46 | m6A | K1QTE0_CRAGI | Epidermal retinal dehydrogenase 2 |
| 47 | m6A | K1PPQ1_CRAGI | 14-3-3 protein gamma |
| 48 | m6A | K1Q7A7_CRAGI | Putative tyrosinase-like protein tyr-3 |
| 49 | m6A | K1QHA2_CRAGI | Spectrin beta chain, brain 4 |
| 50 | m6A | K1Q6U0_CRAGI | Coatomer subunit zeta-1 |
| 51 | m6A | K1QU16_CRAGI | Protein polybromo-1 |
| 52 | m6A | K1P7W5_CRAGI | Histone H1-delta |
| 53 | m6A | K1QBL6_CRAGI | Tudor domain-containing protein 1 |
| 54 | m6A | K1QVS1_CRAGI | ER membrane protein complex subunit 3 |
| 55 | m6A | K1Q1L9_CRAGI | Interferon-induced protein 44-like protein |
| 56 | m6A | K1Q109_CRAGI | Neurexin-4 |
| 57 | m6A | K1PJN7_CRAGI | PC3-like endoprotease variant A |
| 58 | m6A | K1RAH1_CRAGI | Uncharacterized protein |
| 59 | m6A | K1R472_CRAGI | Synaptobrevin-like protein YKT6 |
| 60 | m6A | K1QMY9_CRAGI | Uncharacterized protein |
| | m6A | K1QBT8_CRAGI | Uncharacterized protein |
| | m6A | K1Q1R2_CRAGI | Caprin-2 |

| | | | |
|----|-----|--------------|---|
| 1 | | | |
| 2 | | | |
| 3 | m6A | K1R8V1_CRAGI | Puratrophin-1 |
| 4 | m6A | K1PUF0_CRAGI | G-protein coupled receptor moody |
| 5 | m6A | K1Q4R2_CRAGI | Zinc finger protein 26 |
| 6 | m6A | K1QXP9_CRAGI | Uncharacterized protein |
| 7 | m6A | K1P6M6_CRAGI | Cerebellin-1 |
| 8 | A | K1QNA2_CRAGI | Vitellogenin-6 |
| 9 | A | K1PTY5_CRAGI | Protocadherin Fat 4 |
| 10 | A | K1QBR5_CRAGI | Uncharacterized protein |
| 11 | A | K1PFG1_CRAGI | Uncharacterized protein |
| 12 | A | K1P9A4_CRAGI | Beta-1,3-glucan-binding protein |
| 13 | A | K1QHI5_CRAGI | Pyruvate carboxylase, mitochondrial |
| 14 | A | K1R5B4_CRAGI | Proteasome activator complex subunit 4 |
| 15 | A | K1QQ94_CRAGI | Uncharacterized protein |
| 16 | A | K1QXR4_CRAGI | Pancreatic lipase-related protein 2 |
| 17 | A | K1RWS2_CRAGI | Transcriptional activator protein Pur-alpha |
| 18 | A | K1PNI6_CRAGI | Heterogeneous nuclear ribonucleoprotein A/B |
| 19 | A | K1R3U2_CRAGI | Uncharacterized protein |
| 20 | A | K1R7V7_CRAGI | Tubulin beta chain |
| 21 | A | K1QMX5_CRAGI | Uncharacterized protein |
| 22 | A | K1R9B6_CRAGI | H/ACA ribonucleoprotein complex subunit 4 |
| 23 | A | K1QQ68_CRAGI | Tubulin alpha chain |
| 24 | A | K1PQP2_CRAGI | Nucleolin |
| 25 | A | K1RLF8_CRAGI | Splicing factor 3B subunit 3 |
| 26 | A | K1R164_CRAGI | Galectin-4 |
| 27 | A | K1QVJ8_CRAGI | Piwi-like protein 1 |
| 28 | A | K1RGT5_CRAGI | Metalloendopeptidase |
| 29 | A | K1PH76_CRAGI | Y-box factor-like protein (Fragment) |
| 30 | A | K1QII6_CRAGI | Tubulin alpha chain |
| 31 | A | K1QSX8_CRAGI | ATPase family AAA domain-containing protein 2B |
| 32 | A | K1QK56_CRAGI | Uncharacterized protein |
| 33 | A | K1QKB5_CRAGI | Uncharacterized protein |
| 34 | A | K1PE00_CRAGI | Tubulin alpha chain |
| 35 | A | K1QQ27_CRAGI | Pancreatic lipase-related protein 2 |
| 36 | A | K1PVA1_CRAGI | Transitional endoplasmic reticulum ATPase |
| 37 | A | K1PEP0_CRAGI | 40S ribosomal protein S8 |
| 38 | A | K1QXX7_CRAGI | Myosin heavy chain, non-muscle (Fragment) |
| 39 | A | K1RK12_CRAGI | 40S ribosomal protein S23 |
| 40 | A | K1QSQ9_CRAGI | Putative ATP-dependent RNA helicase an3 |
| 41 | A | K1PNR3_CRAGI | Clathrin heavy chain |
| 42 | A | K1QMA4_CRAGI | RRP5-like protein |
| 43 | A | K1QHM2_CRAGI | Dolichyl-diphosphooligosaccharide--protein glycosyltransferase subunit 2 |
| 44 | A | K1QU53_CRAGI | NAD(P) transhydrogenase, mitochondrial |
| 45 | A | K1PJC1_CRAGI | Adipophilin |
| 46 | A | K1RG73_CRAGI | Acetyl-CoA carboxylase |
| 47 | A | K1QFM6_CRAGI | Vitellogenin |
| 48 | A | K1R6Q7_CRAGI | DNA topoisomerase I |
| 49 | A | K1R6Z7_CRAGI | ATP synthase subunit alpha |
| 50 | A | K1QGS8_CRAGI | Elongation factor 1-alpha |
| 51 | A | K1QWZ6_CRAGI | Dolichyl-diphosphooligosaccharide--protein glycosyltransferase subunit 1 |
| 52 | A | K1RD58_CRAGI | Uncharacterized protein |
| 53 | A | K1QLS3_CRAGI | Cytochrome b-c1 complex subunit 2, mitochondrial |
| 54 | A | K1S1S1_CRAGI | Insulin-like growth factor 2 mRNA-binding protein 1 |
| 55 | A | K1R0L4_CRAGI | Sodium/potassium-transporting ATPase subunit alpha |
| 56 | A | K1RWW5_CRAGI | ATP synthase subunit beta |
| 57 | A | K1QA13_CRAGI | Calcium-transporting ATPase |
| 58 | A | K1QFN2_CRAGI | Uncharacterized protein |
| 59 | A | K1R545_CRAGI | Pre-mRNA-processing-splicing factor 8 (Fragment) |
| 60 | A | K1R252_CRAGI | Putative methylmalonate-semialdehyde dehydrogenase [acylating], mitochondrial |
| | A | K1PMT6_CRAGI | Heterogeneous nuclear ribonucleoprotein U-like protein 1 |
| | A | K1RGB7_CRAGI | Epidermal retinal dehydrogenase 2 |

| | | | |
|----|---|--------------|--|
| 1 | | | |
| 2 | | | |
| 3 | A | K1R466_CRAGI | T-complex protein 1 subunit gamma |
| 4 | A | K1R294_CRAGI | T-complex protein 1 subunit beta |
| 5 | A | K1RIT6_CRAGI | NADH-ubiquinone oxidoreductase 75 kDa subunit, mitochondrial |
| 6 | A | K1QIR8_CRAGI | 78 kDa glucose-regulated protein |
| 7 | | | |
| 8 | A | K1RI55_CRAGI | Insulin-like growth factor 2 mRNA-binding protein 3 |
| 9 | A | K1QH74_CRAGI | Splicing factor, arginine/serine-rich 1 |
| 10 | A | K1S2N7_CRAGI | Innexin |
| 11 | A | K1R435_CRAGI | Splicing factor, arginine/serine-rich 4 |
| 12 | A | K1R5U4_CRAGI | Acetyl-CoA carboxylase 1 |
| 13 | A | K1QBK6_CRAGI | Splicing factor 3B subunit 1 |
| 14 | A | K1Q988_CRAGI | Band 4.1-like protein 3 |
| 15 | A | K1R420_CRAGI | Non-specific serine/threonine protein kinase |
| 16 | A | A5LGH1_CRAGI | Voltage-dependent anion channel |
| 17 | A | K1PHW2_CRAGI | Uncharacterized protein |
| 18 | A | K1REG6_CRAGI | DNA helicase |
| 19 | A | K1QAE5_CRAGI | Uncharacterized protein |
| 20 | A | K1QWT8_CRAGI | Uncharacterized protein |
| 21 | A | K1QRL6_CRAGI | Methenyltetrahydrofolate synthetase domain-containing protein |
| 22 | A | K1QYB3_CRAGI | Ig-like and fibronectin type-III domain-containing protein C25G4.10 |
| 23 | A | K1QKD6_CRAGI | Uncharacterized protein |
| 24 | A | K1R115_CRAGI | Succinate dehydrogenase [ubiquinone] flavoprotein subunit, mitochondrial |
| 25 | A | K1S4Q2_CRAGI | T-complex protein 1 subunit delta (Fragment) |
| 26 | A | K1QWK2_CRAGI | MAM domain-containing glycosylphosphatidylinositol anchor protein 2 |
| 27 | A | K1R0S3_CRAGI | T-complex protein 1 subunit theta |
| 28 | A | K1QFW9_CRAGI | Uncharacterized protein |
| 29 | A | K1Q0Z3_CRAGI | Estradiol 17-beta-dehydrogenase 11 |
| 30 | A | K1PNQ5_CRAGI | Heat shock protein HSP 90-alpha 1 |
| 31 | A | K1RBF6_CRAGI | Uncharacterized protein yfeX |
| 32 | A | K1R4D4_CRAGI | 40S ribosomal protein SA |
| 33 | A | K1QJ14_CRAGI | 40S ribosomal protein S3a |
| 34 | A | K1PUL2_CRAGI | Long-chain-fatty-acid--CoA ligase 1 |
| 35 | A | K1RFT1_CRAGI | Band 4.1-like protein 3 |
| 36 | A | K1PJ06_CRAGI | Importin subunit alpha-1 |
| 37 | A | K1QT21_CRAGI | Putative ATP-dependent RNA helicase DDX5 |
| 38 | A | K1QM19_CRAGI | Uncharacterized protein |
| 39 | A | K1QXS6_CRAGI | Heterogeneous nuclear ribonucleoprotein A2-like protein 1 |
| 40 | A | K1QMX8_CRAGI | DNA replication licensing factor MCM7 |
| 41 | A | K1PD57_CRAGI | Constitutive coactivator of PPAR-gamma-like protein 1-like protein |
| 42 | A | K1R953_CRAGI | Acetyl-CoA carboxylase |
| 43 | A | K1RJH5_CRAGI | Polyadenylate-binding protein |
| 44 | A | K1RSZ6_CRAGI | 40S ribosomal protein S7 |
| 45 | A | K1R7A2_CRAGI | Uncharacterized protein |
| 46 | A | K1QUC6_CRAGI | Uncharacterized protein |
| 47 | A | K1QWX2_CRAGI | 60S acidic ribosomal protein P0 |
| 48 | A | K1RNB5_CRAGI | Propionyl-CoA carboxylase beta chain, mitochondrial |
| 49 | A | K1PCS4_CRAGI | Eukaryotic translation initiation factor 2 subunit 3, Y-linked |
| 50 | A | K1Q923_CRAGI | Putative ATP-dependent RNA helicase DDX4 |
| 51 | A | K1QPX8_CRAGI | Alkyl/aryl-sulfatase BDS1 |
| 52 | A | K1R4R9_CRAGI | Mitotic apparatus protein p62 |
| 53 | A | K1RAJ1_CRAGI | T-complex protein 1 subunit alpha |
| 54 | A | K1Q0L1_CRAGI | 60S ribosomal protein L23a |
| 55 | A | K1Q620_CRAGI | Uncharacterized protein |
| 56 | A | K1QG58_CRAGI | Actin |
| 57 | A | K1Q4H2_CRAGI | Nodal modulator 3 |
| 58 | A | K1Q260_CRAGI | Nucleolar protein 58 |
| 59 | A | K1QF01_CRAGI | 40S ribosomal protein S4 |
| 60 | A | K1PUM2_CRAGI | Histone H2A |
| | A | K1QNN9_CRAGI | MICOS complex subunit MIC60 |
| | A | K1RQA0_CRAGI | Dolichyl-diphosphooligosaccharide--protein glycosyltransferase subunit 2 |
| | A | K1QZW0_CRAGI | Polyadenylate-binding protein 2 |

| | | | |
|----|---|--------------|---|
| 1 | | | |
| 2 | | | |
| 3 | A | K1QBN0_CRAGI | Methylcrotonoyl-CoA carboxylase beta chain, mitochondrial |
| 4 | A | K1Q8S0_CRAGI | Nucleolar complex protein 3 homolog |
| 5 | A | K1RH18_CRAGI | Sarcalumenin |
| 6 | A | K1QQ05_CRAGI | Insulin-like growth factor-binding protein complex acid labile chain |
| 7 | A | K1QT04_CRAGI | Uncharacterized protein |
| 8 | A | K1RLC5_CRAGI | T-complex protein 1 subunit epsilon |
| 9 | A | K1Q9K6_CRAGI | Histone H3 |
| 10 | A | K1QBW8_CRAGI | Uncharacterized protein |
| 11 | A | K1Q9W5_CRAGI | T-complex protein 1 subunit eta |
| 12 | A | K1R0Y9_CRAGI | ADP,ATP carrier protein |
| 13 | A | K1QP17_CRAGI | Caprin-1 |
| 14 | A | K1QYB6_CRAGI | Delta-1-pyrroline-5-carboxylate synthetase |
| 15 | A | K1R7I9_CRAGI | Heterogeneous nuclear ribonucleoprotein Q |
| 16 | A | K1QMB9_CRAGI | Eukaryotic translation initiation factor 3 subunit A |
| 17 | A | K1PM50_CRAGI | 40S ribosomal protein S16 |
| 18 | A | K1P8W6_CRAGI | 60S ribosomal protein L4 |
| 19 | A | K1PXH5_CRAGI | Putative saccharopine dehydrogenase |
| 20 | A | K1PBZ4_CRAGI | Regulator of nonsense transcripts 1 |
| 21 | A | K1R4L8_CRAGI | Electron transfer flavoprotein-ubiquinone oxidoreductase, mitochondrial |
| 22 | A | K1QFP5_CRAGI | NADH dehydrogenase [ubiquinone] flavoprotein 1, mitochondrial |
| 23 | A | K1RIG6_CRAGI | LSM14-like protein A |
| 24 | A | K1R591_CRAGI | Inter-alpha-trypsin inhibitor heavy chain H4 |
| 25 | A | K1RSA6_CRAGI | Methylcrotonoyl-CoA carboxylase subunit alpha, mitochondrial |
| 26 | A | K1R1B1_CRAGI | 35 kDa SR repressor protein |
| 27 | A | K1QZU8_CRAGI | Calcium-transporting ATPase |
| 28 | A | K1QX26_CRAGI | Endoplasmic |
| 29 | A | K1Q358_CRAGI | 60S acidic ribosomal protein P2 |
| 30 | A | K1P112_CRAGI | ATP synthase subunit gamma, mitochondrial |
| 31 | A | K1QHS8_CRAGI | Ribonucleoside-diphosphate reductase |
| 32 | A | K1PXN5_CRAGI | T-complex protein 1 subunit zeta |
| 33 | A | K1R7J6_CRAGI | Putative sodium/potassium-transporting ATPase subunit beta-2 |
| 34 | A | K1Q5H6_CRAGI | FACT complex subunit SSRP1 |
| 35 | A | K1QTD9_CRAGI | Nucleolar protein 56 |
| 36 | A | K1QC78_CRAGI | Ras-related protein Rab-14 |
| 37 | A | K1Q9M7_CRAGI | Histone H1-delta |
| 38 | A | K1RNZ6_CRAGI | Eukaryotic translation initiation factor 3 subunit D |
| 39 | A | K1QAH9_CRAGI | H/ACA ribonucleoprotein complex subunit |
| 40 | A | K1RLT4_CRAGI | Signal recognition particle subunit SRP68 |
| 41 | A | K1RWX7_CRAGI | Metabotropic glutamate receptor 3 |
| 42 | A | K1RA35_CRAGI | Splicing factor, arginine/serine-rich 7 |
| 43 | A | K1QE71_CRAGI | DNA helicase |
| 44 | A | K1PS27_CRAGI | DNA helicase |
| 45 | A | K1Q4Y8_CRAGI | Histone H1oo |
| 46 | A | K1PGW7_CRAGI | Transmembrane protein 2 |
| 47 | A | K1RAB9_CRAGI | Epoxide hydrolase 4 |
| 48 | A | K1Q9P5_CRAGI | Mitochondrial-processing peptidase subunit beta |
| 49 | A | K1QL67_CRAGI | 60S ribosomal protein L7a |
| 50 | A | K1PLY1_CRAGI | DNA polymerase |
| 51 | A | K1R996_CRAGI | Long-chain-fatty-acid--CoA ligase 4 |
| 52 | A | K1Q404_CRAGI | DNA topoisomerase 2 |
| 53 | A | K1QBH0_CRAGI | Uncharacterized protein |
| 54 | A | K1R0W4_CRAGI | Signal recognition particle subunit SRP72 |
| 55 | A | K1RN77_CRAGI | Nuclear autoantigenic sperm protein |
| 56 | A | K1PA54_CRAGI | Replication factor C subunit 3 |
| 57 | A | K1Q4S5_CRAGI | Cadherin-87A |
| 58 | A | K1QEF2_CRAGI | ADP-ribosylation factor-like protein 15 |
| 59 | A | K1QYT5_CRAGI | Phosphate carrier protein, mitochondrial |
| 60 | A | K1QDX9_CRAGI | Ribosome biogenesis protein BMS1-like protein |
| | A | K1QB61_CRAGI | Protocadherin Fat 4 |
| | A | K1R0D7_CRAGI | Eukaryotic translation initiation factor 3 subunit M (Fragment) |

| | | | |
|----|---|--------------|---|
| 1 | | | |
| 2 | | | |
| 3 | A | K1PM76_CRAGI | NADH dehydrogenase [ubiquinone] 1 alpha subcomplex subunit 9, mitochondrial |
| 4 | A | K1PRL4_CRAGI | 60S ribosomal protein L38 (Fragment) |
| 5 | A | K1RW85_CRAGI | Adenosylhomocysteinase |
| 6 | A | K1PAY7_CRAGI | Propionyl-CoA carboxylase alpha chain, mitochondrial |
| 7 | A | K1PZ08_CRAGI | Ras-related protein Rab-7a |
| 8 | A | K1QY12_CRAGI | Dynamin-1-like protein |
| 9 | A | K1QFN1_CRAGI | 60S ribosomal protein L23 |
| 10 | A | K1RDW8_CRAGI | Golgi apparatus protein 1 |
| 11 | A | K1RSS3_CRAGI | Myosin heavy chain, striated muscle |
| 12 | A | K1QGK2_CRAGI | Coatomer subunit beta |
| 13 | A | K1PV79_CRAGI | Importin subunit alpha |
| 14 | A | K1QN79_CRAGI | 40S ribosomal protein S11 |
| 15 | A | K1PV49_CRAGI | RuvB-like helicase |
| 16 | A | K1QG65_CRAGI | rRNA 2'-O-methyltransferase fibrillar |
| 17 | A | K1PK85_CRAGI | Cullin-associated NEDD8-dissociated protein 1 |
| 18 | A | K1QVN9_CRAGI | T-complex protein 1 subunit eta |
| 19 | A | K1QGB4_CRAGI | 40S ribosomal protein S17 |
| 20 | A | K1QK18_CRAGI | Cytochrome b5 |
| 21 | A | K1QVW3_CRAGI | Alkylglycerone-phosphate synthase |
| 22 | A | K1QN11_CRAGI | Pre-mRNA-processing-splicing factor 8 |
| 23 | A | K1RJS5_CRAGI | Uncharacterized protein |
| 24 | A | K1Q6W5_CRAGI | FACT complex subunit spt16 |
| 25 | A | K1QQB6_CRAGI | 40S ribosomal protein S14 |
| 26 | A | K1PKF5_CRAGI | Protein-glutamine gamma-glutamyltransferase 4 |
| 27 | A | K1PH66_CRAGI | Fibrinolytic enzyme, isozyme C |
| 28 | A | K1PY89_CRAGI | Extracellular superoxide dismutase [Cu-Zn] |
| 29 | A | K1QUK3_CRAGI | Putative ATP-dependent RNA helicase DDX41 |
| 30 | A | K1R2V1_CRAGI | Importin subunit beta-1 |
| 31 | A | K1PV86_CRAGI | Phosphoglycerate mutase family member 5 |
| 32 | A | K1QJ08_CRAGI | 60S ribosomal protein L26 |
| 33 | A | K1QLU6_CRAGI | Poly [ADP-ribose] polymerase |
| 34 | A | K1QDN1_CRAGI | Heat shock protein 75 kDa, mitochondrial (Fragment) |
| 35 | A | K1QPP2_CRAGI | Elongation factor Tu, mitochondrial |
| 36 | A | K1R834_CRAGI | 60S ribosomal protein L9 |
| 37 | A | K1R005_CRAGI | Filamin-C (Fragment) |
| 38 | A | K1QET2_CRAGI | Coatomer subunit alpha |
| 39 | A | K1RKC1_CRAGI | Far upstream element-binding protein 3 |
| 40 | A | K1RG19_CRAGI | Protein FAM98A |
| 41 | A | K1Q056_CRAGI | Calpain-A |
| 42 | A | K1QKJ0_CRAGI | Aldehyde dehydrogenase family 3 member B1 |
| 43 | A | K1QDZ5_CRAGI | Cytochrome c1, heme protein, mitochondrial |
| 44 | A | K1PPP8_CRAGI | Vigilin |
| 45 | A | K1RHB2_CRAGI | Nucleolar RNA helicase 2 |
| 46 | A | K1PH31_CRAGI | Protein arginine N-methyltransferase 1 |
| 47 | A | K1Q6V6_CRAGI | Replication factor C subunit 4 |
| 48 | A | K1PI50_CRAGI | 40S ribosomal protein S26 |
| 49 | A | K1PX23_CRAGI | Eukaryotic peptide chain release factor subunit 1 |
| 50 | A | K1QFZ8_CRAGI | Ceramide kinase-like protein |
| 51 | A | K1S2S8_CRAGI | Signal recognition particle 54 kDa protein |
| 52 | A | K1R1T8_CRAGI | Nucleolar protein 56 |
| 53 | A | K1QRZ3_CRAGI | 40S ribosomal protein S13 |
| 54 | A | K1PMP3_CRAGI | Protoporphyrinogen oxidase |
| 55 | A | K1P9N7_CRAGI | 14-3-3 protein zeta |
| 56 | A | K1Q0R4_CRAGI | ATP-binding cassette sub-family F member 2 |
| 57 | A | K1QWC3_CRAGI | 40S ribosomal protein S3 |
| 58 | A | K1Q812_CRAGI | NADH dehydrogenase [ubiquinone] iron-sulfur protein 2, mitochondrial |
| 59 | A | K1P5V7_CRAGI | Eukaryotic translation initiation factor 3 subunit C |
| 60 | A | K1R2N0_CRAGI | Histone H4 |
| | A | K1QLK8_CRAGI | GTP-binding protein SAR1b |
| | A | K1QHX2_CRAGI | La-related protein 7 |

| | | | |
|----|---|--------------|---|
| 1 | | | |
| 2 | | | |
| 3 | A | K1S6V7_CRAGI | Serine/threonine-protein phosphatase 2A 65 kDa regulatory subunit A alpha isoform |
| 4 | A | K1Q3W9_CRAGI | FAS-associated factor 2-B |
| 5 | A | K1QG72_CRAGI | Hemagglutinin/amebocyte aggregation factor |
| 6 | A | K1QHQ6_CRAGI | Acyl-CoA dehydrogenase family member 9, mitochondrial |
| 7 | A | K1QFR2_CRAGI | Calnexin |
| 8 | A | K1S1X3_CRAGI | SWI/SNF-related matrix-associated actin-dependent regulator of chromatin subfamily A member 5 |
| 9 | A | K1PWZ3_CRAGI | Guanine nucleotide-binding protein subunit beta |
| 10 | A | K1QW41_CRAGI | Leucine-zipper-like transcriptional regulator 1 |
| 11 | A | K1RK68_CRAGI | Uncharacterized protein |
| 12 | A | K1RA95_CRAGI | Filamin-A |
| 13 | A | K1QMV5_CRAGI | Annexin |
| 14 | A | K1QW72_CRAGI | Catalase |
| 15 | A | K1QXQ8_CRAGI | DNA helicase |
| 16 | A | K1P7L5_CRAGI | Transmembrane 9 superfamily member |
| 17 | A | K1P8G1_CRAGI | Heterogeneous nuclear ribonucleoprotein H |
| 18 | A | K1PZ23_CRAGI | DnaJ-like protein subfamily C member 3 |
| 19 | A | K1RIZ3_CRAGI | Bone morphogenetic protein 7 |
| 20 | A | K1RNN9_CRAGI | Cytoskeleton-associated protein 5 |
| 21 | A | K1R6L5_CRAGI | NADH-cytochrome b5 reductase |
| 22 | A | K1R5F2_CRAGI | 14-3-3 protein epsilon |
| 23 | A | K1P9D0_CRAGI | Stress-70 protein, mitochondrial |
| 24 | A | K1RGJ7_CRAGI | Neogenin |
| 25 | A | K1PZP6_CRAGI | Coatmer subunit gamma |
| 26 | A | K1RJ97_CRAGI | Multifunctional protein ADE2 |
| 27 | A | K1R6F5_CRAGI | Putative ATP-dependent RNA helicase DDX23 |
| 28 | A | K1PS84_CRAGI | Alpha-crystallin B chain |
| 29 | A | K1P9S7_CRAGI | Brix domain-containing protein 2 |
| 30 | A | K1PI40_CRAGI | Uncharacterized protein |
| 31 | A | K1QAI2_CRAGI | Ufm1-specific protease 2 |
| 32 | A | K1REP0_CRAGI | Uncharacterized protein |
| 33 | A | K1QJM1_CRAGI | 60S ribosomal protein L30 |
| 34 | A | K1S3G2_CRAGI | HMGB1 |
| 35 | A | K1PXD4_CRAGI | Putative ATP-dependent RNA helicase DDX6 |
| 36 | A | K1RJ7_CRAGI | Histone H5 |
| 37 | A | K1Q3W3_CRAGI | NADH dehydrogenase [ubiquinone] iron-sulfur protein 3, mitochondrial |
| 38 | A | K1RJW8_CRAGI | Protein DEK |
| 39 | A | K1RN97_CRAGI | Hemagglutinin/amebocyte aggregation factor |
| 40 | A | K1QW36_CRAGI | 60S ribosomal protein L6 |
| 41 | A | K1RA63_CRAGI | Transmembrane protein 2 |
| 42 | A | K1R9T2_CRAGI | Eukaryotic translation initiation factor 3 subunit B |
| 43 | A | K1PM66_CRAGI | 60S ribosomal protein L12 |
| 44 | A | K1Q273_CRAGI | 60S ribosomal protein L14 |
| 45 | A | K1PXG6_CRAGI | Serine/threonine-protein phosphatase |
| 46 | A | K1QPC6_CRAGI | Nucleolar complex protein 2-like protein |
| 47 | A | K1RCW3_CRAGI | Elongation factor 1-beta |
| 48 | A | K1Q324_CRAGI | Heterogeneous nuclear ribonucleoprotein K |
| 49 | A | K1PLA7_CRAGI | Eukaryotic initiation factor 4A-II (Fragment) |
| 50 | A | K1RBI9_CRAGI | Small nuclear ribonucleoprotein Sm D2 |
| 51 | A | K1RCL2_CRAGI | Mitochondrial import inner membrane translocase subunit Tim13-B |
| 52 | A | K1QKV1_CRAGI | Cytochrome b-c1 complex subunit 6 |
| 53 | A | K1QVU0_CRAGI | Synaptojanin-2-binding protein |
| 54 | A | K1QRG9_CRAGI | Uncharacterized protein |
| 55 | A | K1PZ70_CRAGI | NADH dehydrogenase [ubiquinone] iron-sulfur protein 6, mitochondrial |
| 56 | A | K1Q350_CRAGI | Glyceraldehyde-3-phosphate dehydrogenase |
| 57 | A | K1PXU6_CRAGI | 60S ribosomal protein L24 |
| 58 | A | K1QZQ8_CRAGI | Low-density lipoprotein receptor-related protein 8 |
| 59 | A | K1RUM2_CRAGI | Uncharacterized protein |
| 60 | A | K1REY2_CRAGI | Dysferlin |
| | A | K1Q6X5_CRAGI | Protein disulfide-isomerase |
| | A | K1QWK6_CRAGI | Metalloendopeptidase |

| | | | |
|----|---|--------------|--|
| 1 | | | |
| 2 | | | |
| 3 | A | K1QDH9_CRAGI | Myosin-11 |
| 4 | A | K1QQR1_CRAGI | Major vault protein |
| 5 | A | K1RAH2_CRAGI | Superoxide dismutase [Cu-Zn] |
| 6 | A | K1PH13_CRAGI | Dolichyl-diphosphooligosaccharide--protein glycosyltransferase subunit STT3B |
| 7 | A | K1PY73_CRAGI | Basic leucine zipper and W2 domain-containing protein 1 |
| 8 | A | K1Q7T5_CRAGI | Protein disulfide-isomerase |
| 9 | A | K1PFS5_CRAGI | Elongation factor 1-gamma |
| 10 | A | K1PW39_CRAGI | Glycerol-3-phosphate dehydrogenase, mitochondrial |
| 11 | A | K1R1C5_CRAGI | Signal recognition particle receptor subunit beta |
| 12 | A | K1Q1F4_CRAGI | 60S ribosomal protein L3 (Fragment) |
| 13 | A | K1QNS4_CRAGI | DnaJ-like protein subfamily C member 9 |
| 14 | A | K1QNS4_CRAGI | DnaJ-like protein subfamily C member 9 |
| 15 | A | K1QNS4_CRAGI | DnaJ-like protein subfamily C member 9 |
| 16 | A | K1QY85_CRAGI | Transport protein Sec31A |
| 17 | A | K1QWP1_CRAGI | Nucleoporin seh1 |
| 18 | A | K1RAU3_CRAGI | DNA ligase |
| 19 | A | K1R5W3_CRAGI | Uncharacterized protein |
| 20 | A | K1QF31_CRAGI | Serine/threonine-protein kinase PLK |
| 21 | A | K1Q667_CRAGI | tRNA-splicing ligase RtcB homolog |
| 22 | A | K1Q667_CRAGI | tRNA-splicing ligase RtcB homolog |
| 23 | A | K1QRM1_CRAGI | Nuclear pore protein |
| 24 | A | K1R790_CRAGI | Retinol dehydrogenase 13 |
| 25 | A | K1R0M2_CRAGI | Uncharacterized protein |
| 26 | A | K1R0M2_CRAGI | Uncharacterized protein |
| 27 | A | K1QNT7_CRAGI | Aldehyde dehydrogenase, mitochondrial |
| 28 | A | K1QIV3_CRAGI | Uncharacterized protein |
| 29 | A | K1QR48_CRAGI | Calcium-binding mitochondrial carrier protein SCaMC-2 |
| 30 | A | K1R4F7_CRAGI | Ras-related protein Rab-6B |
| 31 | A | K1PIC5_CRAGI | Transmembrane protein 85 |
| 32 | A | K1PIC5_CRAGI | Transmembrane protein 85 |
| 33 | A | K1RKZ5_CRAGI | DNA damage-binding protein 1 |
| 34 | A | K1QW21_CRAGI | 39S ribosomal protein L40, mitochondrial |
| 35 | A | K1PB87_CRAGI | Uncharacterized protein |
| 36 | A | K1R150_CRAGI | Ras-related protein Rab-1A |
| 37 | A | K1PVZ3_CRAGI | Cold shock domain-containing protein E1 |
| 38 | A | K1PVZ3_CRAGI | Cold shock domain-containing protein E1 |
| 39 | A | K1QSD9_CRAGI | Uncharacterized protein |
| 40 | A | K1PPW8_CRAGI | Coatomer subunit beta |
| 41 | A | K1QKG9_CRAGI | Cysteine desulfurase, mitochondrial |
| 42 | A | K1R833_CRAGI | Tyrosine-protein kinase BAZ1B |
| 43 | A | K1R833_CRAGI | Tyrosine-protein kinase BAZ1B |
| 44 | A | K1QE94_CRAGI | Alpha-galactosidase |
| 45 | A | K1RIJ1_CRAGI | Synaptobrevin (Fragment) |
| 46 | A | K1PJB0_CRAGI | Heat shock protein 70 B2 |
| 47 | A | K1R6S5_CRAGI | 40S ribosomal protein S9 |
| 48 | A | K1PAM6_CRAGI | Uncharacterized protein |
| 49 | A | K1QY71_CRAGI | Histone H2B |
| 50 | A | K1QY71_CRAGI | Histone H2B |
| 51 | A | K1P6Y1_CRAGI | Uncharacterized protein |
| 52 | A | K1PNY5_CRAGI | Splicing factor, proline-and glutamine-rich |
| 53 | A | K1PDL3_CRAGI | Ribosomal protein L19 |
| 54 | A | K1RDG4_CRAGI | DNA helicase |
| 55 | A | K1RV41_CRAGI | Guanine nucleotide-binding protein subunit beta-2-like 1 |
| 56 | A | K1RV41_CRAGI | Guanine nucleotide-binding protein subunit beta-2-like 1 |
| 57 | A | K1QMH5_CRAGI | Small nuclear ribonucleoprotein Sm D1 |
| 58 | A | K1R4Z3_CRAGI | Malate dehydrogenase, mitochondrial |
| 59 | A | K1R3T3_CRAGI | Transcription factor BTF3 |
| 60 | A | K1QAB1_CRAGI | AP-2 complex subunit alpha |
| | A | K1QSU3_CRAGI | Protein I(2)37Cc |
| | A | K1PEY4_CRAGI | 26S proteasome non-ATPase regulatory subunit 2 |
| | A | K1PU46_CRAGI | Lethal(2) giant larvae-like protein 1 |
| | A | K1Q0N6_CRAGI | Dolichyl-diphosphooligosaccharide--protein glycosyltransferase subunit STT3A |
| | A | K1QGP1_CRAGI | Replication factor C subunit 2 |
| | A | K1QDV6_CRAGI | Protein argonaute-2 |
| | A | K1S6H7_CRAGI | Vacuolar protein sorting-associated protein 13C |
| | A | K1PF10_CRAGI | PAN2-PAN3 deadenylation complex catalytic subunit PAN2 |
| | A | K1Q1L4_CRAGI | Uncharacterized protein |
| | A | K1PWC3_CRAGI | Tetratricopeptide repeat protein 35 |
| | A | K1QKL8_CRAGI | V-type proton ATPase subunit a |

| | | | |
|----|---|--------------|--|
| 1 | | | |
| 2 | | | |
| 3 | A | K1QT61_CRAGI | NADH dehydrogenase [ubiquinone] flavoprotein 2, mitochondrial (Fragment) |
| 4 | A | K1Q7G8_CRAGI | Fatty acid synthase |
| 5 | A | K1QX44_CRAGI | Ras-related protein Rab-11B |
| 6 | A | K1P7K8_CRAGI | Vesicle-fusing ATPase 1 |
| 7 | A | K1QHK9_CRAGI | Dynein heavy chain, cytoplasmic |
| 8 | A | K1Q7Q2_CRAGI | CCAAT/enhancer-binding protein zeta |
| 9 | A | K1Q880_CRAGI | Transportin-1 |
| 10 | A | K1Q253_CRAGI | Neutral and basic amino acid transport protein rBAT |
| 11 | A | K1QGA7_CRAGI | Kynurenine formamidase |
| 12 | A | K1QAL3_CRAGI | RNA-binding protein 28 |
| 13 | A | K1PXS8_CRAGI | Calreticulin |
| 14 | A | K1QTP6_CRAGI | Cation-transporting ATPase |
| 15 | A | K1PR25_CRAGI | Regulator of differentiation 1 |
| 16 | A | K1PA61_CRAGI | Actin-like protein 6A |
| 17 | A | K1QAA8_CRAGI | CAAX prenyl protease 1-like protein |
| 18 | A | K1PY30_CRAGI | Septin-2 |
| 19 | A | K1R100_CRAGI | Metaxin-2 |
| 20 | A | K1PTL4_CRAGI | Odr-4-like protein |
| 21 | A | K1QA50_CRAGI | V-type proton ATPase subunit H |
| 22 | A | K1PVH5_CRAGI | Centromere/kinetochore protein zw10-like protein |
| 23 | A | K1PUQ5_CRAGI | Histone H2B |
| 24 | A | K1RFB1_CRAGI | Stomatin-like protein 2 (Fragment) |
| 25 | A | K1QAA2_CRAGI | Uncharacterized protein |
| 26 | A | K1PNC7_CRAGI | AFG3-like protein 2 |
| 27 | A | K1PJS7_CRAGI | Poly [ADP-ribose] polymerase |
| 28 | A | K1PLF9_CRAGI | Arginine kinase |
| 29 | A | K1RC37_CRAGI | Uncharacterized protein |
| 30 | A | K1PKD4_CRAGI | 40S ribosomal protein S30 |
| 31 | A | K1RDS1_CRAGI | Splicing factor, arginine/serine-rich 2 |
| 32 | A | K1Q5Z1_CRAGI | Uncharacterized protein |
| 33 | A | K1PF96_CRAGI | Spliceosome RNA helicase BAT1 |
| 34 | A | K1QTW6_CRAGI | Eukaryotic translation initiation factor 3 subunit F |
| 35 | A | K1RAU8_CRAGI | Eukaryotic translation initiation factor 3 subunit E |
| 36 | A | K1RAI3_CRAGI | Annexin |
| 37 | A | K1PUX5_CRAGI | Casein kinase II subunit alpha |
| 38 | A | K1PDF8_CRAGI | Splicing factor, arginine/serine-rich 6 |
| 39 | A | K1QXH3_CRAGI | Translational activator GCN1 |
| 40 | A | K1PQE3_CRAGI | RNA-binding protein Raly |
| 41 | A | K1QWE5_CRAGI | Ras-related protein Rab-18-B |
| 42 | A | K1R5G4_CRAGI | 60S ribosomal protein L31 |
| 43 | A | K1RCT2_CRAGI | Translocon-associated protein subunit delta |
| 44 | A | K1RFU6_CRAGI | Proteasome activator complex subunit 3 |
| 45 | A | K1ROW0_CRAGI | Ferritin |
| 46 | A | K1Q5Z6_CRAGI | Eukaryotic translation initiation factor 2 subunit 2 |
| 47 | A | K1RKE5_CRAGI | IQ and AAA domain-containing protein 1 |
| 48 | A | K1P8G6_CRAGI | Vesicular integral-membrane protein VIP36 |
| 49 | A | K1P3Q5_CRAGI | Programmed cell death 6-interacting protein |
| 50 | A | K1Q615_CRAGI | Peroxiredoxin-1 |
| 51 | A | K1RG04_CRAGI | ALK tyrosine kinase receptor |
| 52 | A | K1QQK5_CRAGI | Metabotropic glutamate receptor 2 |
| 53 | A | K1R3G0_CRAGI | Transformer-2-like protein beta |
| 54 | A | K1QCB0_CRAGI | 40S ribosomal protein S5 |
| 55 | A | K1REQ4_CRAGI | Cytochrome c oxidase subunit 6B |
| 56 | A | K1QHI2_CRAGI | Heterogeneous nuclear ribonucleoprotein L |
| 57 | A | K1PSH2_CRAGI | 28S ribosomal protein S12, mitochondrial |
| 58 | A | K1R9P5_CRAGI | Mitochondrial import receptor subunit TOM70 |
| 59 | A | K1PGK7_CRAGI | Uncharacterized protein |
| 60 | A | K1QPF0_CRAGI | Uncharacterized protein |
| | A | K1QT00_CRAGI | ATP synthase subunit alpha, mitochondrial |
| | A | K1RG28_CRAGI | Kinase C and casein kinase substrate in neurons protein 2 |

| | | | |
|----|---|--------------|---|
| 1 | | | |
| 2 | | | |
| 3 | A | K1PMY9_CRAGI | Calmodulin |
| 4 | A | K1R1Q8_CRAGI | Ras-related protein Rab-5C |
| 5 | A | K1RPP1_CRAGI | Synaptophysin |
| 6 | A | K1RFU8_CRAGI | High mobility group protein DSP1 |
| 7 | A | K1PJ85_CRAGI | 26S protease regulatory subunit 6A |
| 8 | A | K1R2G9_CRAGI | SEC13-like protein |
| 9 | | | |
| 10 | A | K1QJW6_CRAGI | Translocon-associated protein subunit gamma |
| 11 | A | K1R5B9_CRAGI | DNA-directed RNA polymerase, mitochondrial |
| 12 | A | K1R8C6_CRAGI | 40S ribosomal protein S12 |
| 13 | A | K1QSR2_CRAGI | Apoptosis inhibitor 5 |
| 14 | A | K1Q5E0_CRAGI | Dual specificity protein kinase CLK2 |
| 15 | A | K1QBM3_CRAGI | Ras-related protein Rab-2 |
| 16 | A | K1Q8K9_CRAGI | KRR1 small subunit processome component-like protein |
| 17 | A | K1QNU0_CRAGI | Non-specific serine/threonine protein kinase |
| 18 | A | K1RDM2_CRAGI | 60S ribosomal protein L18a |
| 19 | A | K1RD12_CRAGI | Uncharacterized protein |
| 20 | A | K1QGP7_CRAGI | Uncharacterized protein |
| 21 | A | K1PBL2_CRAGI | Eukaryotic initiation factor 4A-III |
| 22 | A | K1QAT9_CRAGI | ATP-dependent RNA helicase DDX1 |
| 23 | A | K1QWJ4_CRAGI | Splicing factor 3B subunit 5 |
| 24 | A | K1Q412_CRAGI | Uncharacterized protein |
| 25 | A | K1R8R6_CRAGI | Fructose-bisphosphate aldolase |
| 26 | A | K1RWP3_CRAGI | Peptidyl-tRNA hydrolase 2, mitochondrial |
| 27 | A | K1PGN0_CRAGI | Fatty-acid amide hydrolase 2 |
| 28 | A | K1PUV4_CRAGI | 40S ribosomal protein S24 |
| 29 | A | K1PJY2_CRAGI | Inositol polyphosphate 1-phosphatase |
| 30 | A | K1QWZ8_CRAGI | Catenin beta |
| 31 | A | K1R1F0_CRAGI | ATP-dependent DNA helicase 2 subunit 1 |
| 32 | A | K1PN47_CRAGI | Succinate dehydrogenase [ubiquinone] iron-sulfur subunit, mitochondrial |
| 33 | A | K1QYQ9_CRAGI | Uncharacterized protein |
| 34 | A | K1PNZ8_CRAGI | Ribosomal protein L37 |
| 35 | A | K1PVD7_CRAGI | Cytochrome c oxidase subunit 5A, mitochondrial |
| 36 | A | K1QEJ0_CRAGI | Ras GTPase-activating protein-binding protein 2 |
| 37 | A | K1PYL5_CRAGI | Uncharacterized protein |
| 38 | A | K1QQQ5_CRAGI | Replication factor C subunit 5 |
| 39 | A | K1RFA3_CRAGI | Lamin Dm0 |
| 40 | A | K1RRH1_CRAGI | Chromodomain-helicase-DNA-binding protein Mi-2-like protein |
| 41 | A | K1Q2Y1_CRAGI | 40S ribosomal protein S15 |
| 42 | A | K1RIZ9_CRAGI | Band 4.1-like protein 5 |
| 43 | A | K1QVI0_CRAGI | Isocitrate dehydrogenase [NAD] subunit, mitochondrial |
| 44 | A | K1PS77_CRAGI | Prostaglandin G/H synthase 1 |
| 45 | A | K1QZK9_CRAGI | Uncharacterized protein |
| 46 | A | K1R9V5_CRAGI | Tetraspanin |
| 47 | A | K1PPV1_CRAGI | Atlastin-2 |
| 48 | A | K1R0Z4_CRAGI | Uncharacterized protein |
| 49 | A | K1R1R9_CRAGI | Pre-mRNA-processing factor 6 |
| 50 | A | K1QKU6_CRAGI | mRNA export factor |
| 51 | A | K1PCR5_CRAGI | KH domain-containing, RNA-binding, signal transduction-associated protein 2 |
| 52 | A | K1R7L4_CRAGI | Neural cell adhesion molecule 1 |
| 53 | A | K1QAL1_CRAGI | Transmembrane emp24 domain-containing protein 7 |
| 54 | A | K1QB65_CRAGI | Dolichyl-diphosphooligosaccharide--protein glycosyltransferase subunit 1 |
| 55 | A | K1QVP6_CRAGI | Developmentally-regulated GTP-binding protein 1 |
| 56 | A | K1QNT4_CRAGI | Anoctamin |
| 57 | A | K1QMT1_CRAGI | DnaJ-like protein subfamily B member 4 |
| 58 | A | K1RCF4_CRAGI | Translocon-associated protein subunit alpha |
| 59 | A | K1QJL6_CRAGI | Microtubule-associated protein RP/EB family member 3 |
| 60 | A | K1QPY8_CRAGI | Extracellular superoxide dismutase [Cu-Zn] |
| | A | K1R5V4_CRAGI | GTP-binding nuclear protein |
| | A | K1RNU5_CRAGI | Pre-mRNA-splicing factor RBM22 |
| | A | K1QK68_CRAGI | Myosin-2 essential light chain |

| | | | |
|----|---|--------------|---|
| 1 | | | |
| 2 | | | |
| 3 | A | K1QED7_CRAGI | Replication protein A subunit |
| 4 | A | K1QPS1_CRAGI | Poly [ADP-ribose] polymerase |
| 5 | A | K1PD36_CRAGI | Ubiquitin |
| 6 | A | K1R4B8_CRAGI | Plexin domain-containing protein 2 |
| 7 | A | K1RHP3_CRAGI | Proliferation-associated protein 2G4 |
| 8 | A | K1QE43_CRAGI | Uncharacterized protein |
| 9 | A | K1R3I6_CRAGI | Nucleolar complex protein 2-like protein (Fragment) |
| 10 | A | K1QMJ8_CRAGI | Transcription initiation factor IIA subunit 1 |
| 11 | A | K1QXF5_CRAGI | Calcyphosin-like protein |
| 12 | A | K1R512_CRAGI | Uncharacterized protein |
| 13 | A | K1QM06_CRAGI | Prohibitin |
| 14 | A | K1R275_CRAGI | Putative ATP-dependent RNA helicase DDX52 |
| 15 | A | K1QSB2_CRAGI | 26S protease regulatory subunit 6B |
| 16 | A | K1QBW6_CRAGI | Tudor domain-containing protein 1 |
| 17 | A | K1PZT2_CRAGI | Cytochrome c oxidase subunit 5B, mitochondrial |
| 18 | A | K1QIZ7_CRAGI | Programmed cell death protein 6 |
| 19 | A | K1QDA7_CRAGI | Uracil phosphoribosyltransferase |
| 20 | A | K1R401_CRAGI | Spectrin alpha chain |
| 21 | A | K1P541_CRAGI | Alpha-soluble NSF attachment protein |
| 22 | A | K1PND7_CRAGI | Fatty acid synthase |
| 23 | A | K1R8L1_CRAGI | Exportin-2 |
| 24 | A | K1QEF9_CRAGI | Protein-glutamine gamma-glutamyltransferase K |
| 25 | A | K1Q2W7_CRAGI | Uncharacterized protein |
| 26 | A | K1RYM7_CRAGI | LAG1 longevity assurance-like protein 6 |
| 27 | A | K1PY09_CRAGI | Uncharacterized protein |
| 28 | A | K1Q105_CRAGI | Ferrochelatase |
| 29 | A | K1PD30_CRAGI | Putative histone-binding protein Caf1 |
| 30 | A | K1QDB9_CRAGI | Transport protein Sec61 subunit alpha isoform 2 (Fragment) |
| 31 | A | K1QTW3_CRAGI | Murinoglobulin-2 |
| 32 | A | K1PVG9_CRAGI | Malectin |
| 33 | A | K1Q3V9_CRAGI | Mitochondrial carnitine/acylcarnitine carrier protein |
| 34 | A | K1QVS0_CRAGI | Ras-like GTP-binding protein Rho1 |
| 35 | A | K1PX68_CRAGI | Tyrosine-protein phosphatase non-receptor type 6 |
| 36 | A | K1RPF7_CRAGI | 60S ribosomal protein L5 |
| 37 | A | K1QZ64_CRAGI | Nuclear pore complex protein Nup98-Nup96 |
| 38 | A | K1QSV1_CRAGI | Uncharacterized protein |
| 39 | A | K1Q2L4_CRAGI | Transmembrane emp24 domain-containing protein 9 |
| 40 | A | K1RMM6_CRAGI | Centromere protein J |
| 41 | A | K1QKK2_CRAGI | NADH dehydrogenase [ubiquinone] 1 beta subcomplex subunit 11, mitochondrial |
| 42 | A | K1PNV6_CRAGI | Dolichyl-diphosphooligosaccharide--protein glycosyltransferase subunit DAD1 |
| 43 | A | K1PNQ1_CRAGI | Ankyrin repeat domain-containing protein 5 |
| 44 | A | K1QKQ8_CRAGI | THO complex subunit 4-A |
| 45 | A | K1QAG9_CRAGI | Ferritin |
| 46 | A | K1QHW8_CRAGI | Ferritin |
| 47 | A | K1RFV5_CRAGI | ATP-dependent RNA helicase DDX1 |
| 48 | A | K1RNH1_CRAGI | 60S ribosomal protein L18 (Fragment) |
| 49 | A | K1PPQ1_CRAGI | 14-3-3 protein gamma |
| 50 | A | K1QQV0_CRAGI | Histone H1.2 |
| 51 | A | K1Q1R1_CRAGI | Exostosin-3 |
| 52 | A | K1QYF5_CRAGI | Apoptosis-inducing factor 1, mitochondrial |
| 53 | A | K1RZE2_CRAGI | Isocitrate dehydrogenase [NADP] |
| 54 | A | K1QL00_CRAGI | Microsomal glutathione S-transferase 1 |
| 55 | A | K1QTV1_CRAGI | Uncharacterized protein |
| 56 | A | K1RZM3_CRAGI | Cartilage acidic protein 1 |
| 57 | A | K1Q0I8_CRAGI | Putative splicing factor, arginine/serine-rich 7 |
| 58 | A | K1RP91_CRAGI | Putative RNA exonuclease NEF-sp |
| 59 | A | K1PG60_CRAGI | 60S ribosomal protein L17 |
| 60 | A | K1QTP4_CRAGI | 5'-3' exoribonuclease |
| | A | K1RG79_CRAGI | Neuronal acetylcholine receptor subunit alpha-6 |
| | A | K1Q947_CRAGI | Dynein light chain |

| | | | |
|----|---|--------------|--|
| 1 | | | |
| 2 | | | |
| 3 | A | K1RJ91_CRAGI | Ubiquitin-associated protein 2 |
| 4 | A | K1Q2Z5_CRAGI | Putative ATP-dependent RNA helicase DDX46 |
| 5 | A | K1PYA0_CRAGI | Cytoplasmic dynein 2 heavy chain 1 |
| 6 | A | K1QAV0_CRAGI | Guanine nucleotide-binding protein G(Q) subunit alpha |
| 7 | A | K1RKR8_CRAGI | Pumilio-like protein 2 |
| 8 | A | K1QZI3_CRAGI | Myosin-le |
| 9 | A | K1R5R4_CRAGI | Dynein heavy chain 10, axonemal |
| 10 | A | K1QKG8_CRAGI | Upstream activation factor subunit spp27 |
| 11 | A | K1P8I1_CRAGI | Pleckstrin-like protein domain-containing family F member 2 (Fragment) |
| 12 | A | K1Q1N1_CRAGI | Alpha-mannosidase |
| 13 | A | K1PXB6_CRAGI | Cadherin-23 |
| 14 | A | K1QXA9_CRAGI | Sortilin-related receptor |
| 15 | A | K1PVG0_CRAGI | Long-chain fatty acid transport protein 4 |
| 16 | A | K1PBG6_CRAGI | Uncharacterized protein |
| 17 | A | K1PP50_CRAGI | Golgi integral membrane protein 4 |
| 18 | A | K1QCQ5_CRAGI | Succinate--CoA ligase [ADP-forming] subunit beta, mitochondrial |
| 19 | A | K1PK87_CRAGI | Putative E3 ubiquitin-protein ligase TRIP12 |
| 20 | A | K1Q373_CRAGI | Splicing factor, arginine/serine-rich 7 |
| 21 | A | K1Q151_CRAGI | 60S ribosomal protein L32 |
| 22 | A | K1QZ95_CRAGI | Nuclear pore complex protein |
| 23 | A | K1PPH0_CRAGI | Gamma-tubulin complex component |
| 24 | A | K1R0R7_CRAGI | Putative ATP-dependent RNA helicase DHX36 |
| 25 | A | K1R247_CRAGI | Condensin complex subunit 1 |
| 26 | A | K1QIB2_CRAGI | Mitogen-activated protein kinase |
| 27 | A | K1QG61_CRAGI | Acetolactate synthase-like protein |
| 28 | A | K1RBC9_CRAGI | Transketolase-like protein 2 |
| 29 | A | K1RCW5_CRAGI | Eukaryotic translation initiation factor 4 gamma 3 |
| 30 | A | K1PQZ3_CRAGI | Armadillo repeat-containing protein 4 |
| 31 | A | K1PYJ8_CRAGI | Uncharacterized protein |
| 32 | A | K1QQP1_CRAGI | Programmed cell death protein 4 |
| 33 | A | K1PQY0_CRAGI | Protein quiver |
| 34 | A | K1PLC6_CRAGI | Nucleolar protein 14 |
| 35 | A | K1QV25_CRAGI | Transcription elongation factor B polypeptide 2 |
| 36 | A | K1QZ50_CRAGI | RNA-dependent RNA polymerase |
| 37 | A | K1QXH7_CRAGI | DNA replication licensing factor mcm4-B |
| 38 | A | K1PDE4_CRAGI | Protein arginine N-methyltransferase |
| 39 | A | K1QT36_CRAGI | Golgi resident protein GCP60 |
| 40 | A | K1PZ89_CRAGI | Mannosyl-oligosaccharide glucosidase |
| 41 | A | K1Q7A7_CRAGI | Putative tyrosinase-like protein tyr-3 |
| 42 | A | K1R481_CRAGI | Epimerase family protein SDR39U1 |
| 43 | A | K1RJ35_CRAGI | All-trans-retinol 13,14-reductase |
| 44 | A | Q70MT4_CRAGI | 40S ribosomal protein S10 |
| 45 | A | K1REV3_CRAGI | DNA polymerase delta subunit 2 |
| 46 | A | K1P9F1_CRAGI | Insulin-like growth factor-binding protein complex acid labile chain |
| 47 | A | K1PJ65_CRAGI | Dual specificity mitogen-activated protein kinase kinase 7 |
| 48 | A | K1Q2T0_CRAGI | ADP-dependent glucokinase |
| 49 | A | K1PZI3_CRAGI | SWI/SNF complex subunit SMARCC2 |
| 50 | A | K1Q8C5_CRAGI | Putative ATP-dependent RNA helicase DDX47 |
| 51 | A | K1QZ58_CRAGI | Splicing factor U2AF 26 kDa subunit |
| 52 | A | K1RR98_CRAGI | NADH dehydrogenase [ubiquinone] 1 alpha subcomplex subunit 4-like 2 |
| 53 | A | K1QMT2_CRAGI | Signal peptidase complex catalytic subunit SEC11 |
| 54 | A | K1PWM3_CRAGI | MICOS complex subunit MIC13 |
| 55 | A | K1QMM4_CRAGI | Leucine zipper transcription factor-like protein 1 |
| 56 | A | K1QMV7_CRAGI | V-type proton ATPase subunit D |
| 57 | A | K1QKI1_CRAGI | Tudor domain-containing protein 1 |
| 58 | A | K1P0H0_CRAGI | Aspartyl/asparaginyl beta-hydroxylase |
| 59 | A | K1PVQ8_CRAGI | Eukaryotic translation initiation factor 3 subunit K |
| 60 | A | K1Q5P0_CRAGI | 60S ribosomal protein L17 |
| | A | K1QJ36_CRAGI | Muscle, skeletal receptor tyrosine protein kinase |
| | A | K1PHS4_CRAGI | Ribosome-binding protein 1 |

| | | | |
|----|---|--------------|---|
| 1 | | | |
| 2 | | | |
| 3 | A | K1QQB4_CRAGI | Long-chain-fatty-acid--CoA ligase 1 |
| 4 | A | K1QYM4_CRAGI | D-beta-hydroxybutyrate dehydrogenase, mitochondrial |
| 5 | A | K1P2G0_CRAGI | Strawberry notch-like protein 1 |
| 6 | A | K1QCT0_CRAGI | Sideroflexin |
| 7 | A | K1QFG2_CRAGI | Telomere-associated protein RIF1 |
| 8 | A | K1Q5J7_CRAGI | Uncharacterized protein |
| 9 | A | K1QKA9_CRAGI | Piwi-like protein 2 |
| 10 | A | K1P7Q6_CRAGI | 40S ribosomal protein S19 |
| 11 | A | K1QYV5_CRAGI | Cytoplasmic polyadenylation element-binding protein 1-B |
| 12 | A | K1QG84_CRAGI | THO complex subunit 2 |
| 13 | A | K1R7G0_CRAGI | Chromobox-like protein 5 |
| 14 | A | K1QHX4_CRAGI | Uncharacterized protein |
| 15 | A | K1QBY6_CRAGI | Transmembrane protein Tmp21 |
| 16 | A | K1PKK7_CRAGI | AP-2 complex subunit mu-1 |
| 17 | A | K1P9V5_CRAGI | General transcription factor IIF subunit 1 |
| 18 | A | K1Q9V2_CRAGI | Antigen KI-67 |
| 19 | A | K1PNU2_CRAGI | Histone-arginine methyltransferase CARM1 |
| 20 | A | K1Q109_CRAGI | Neurexin-4 |
| 21 | A | K1P9Q2_CRAGI | Signal peptidase complex subunit 3 |
| 22 | A | K1QCN0_CRAGI | Signal recognition particle 9 kDa protein |
| 23 | A | K1Q7E4_CRAGI | Ubiquitin-conjugating enzyme E2 N |
| 24 | A | K1Q5G6_CRAGI | 60 kDa heat shock protein, mitochondrial |
| 25 | A | K1RUW0_CRAGI | E3 SUMO-protein ligase RanBP2 |
| 26 | A | K1RB91_CRAGI | Neutral alpha-glucosidase AB |
| 27 | A | K1QGF1_CRAGI | Splicing factor 3B subunit 2 |
| 28 | A | K1Q525_CRAGI | Mechanosensory protein 2 (Fragment) |
| 29 | A | K1RDB3_CRAGI | F-box/WD repeat-containing protein 1A |
| 30 | A | K1QI28_CRAGI | V-type proton ATPase subunit B |
| 31 | A | K1R4J0_CRAGI | MAGUK p55 subfamily member 2 |
| 32 | A | K1Q9T7_CRAGI | Afadin-and alpha-actinin-binding protein |
| 33 | A | K1RNH6_CRAGI | Toll-like receptor 3 |
| 34 | A | K1PZC0_CRAGI | Structural maintenance of chromosomes protein |
| 35 | A | K1PT69_CRAGI | Uncharacterized protein |
| 36 | A | K1RE67_CRAGI | Methylated-DNA--protein-cysteine methyltransferase |
| 37 | A | K1QCX5_CRAGI | Cyclic AMP-dependent transcription factor ATF-2 |
| 38 | A | K1QBT8_CRAGI | Uncharacterized protein |
| 39 | A | K1RFF1_CRAGI | Uncharacterized protein |
| 40 | A | K1RS40_CRAGI | Uncharacterized protein |
| 41 | A | K1R8V1_CRAGI | Puratrophin-1 |
| 42 | | | |
| 43 | | | |
| 44 | | | |
| 45 | | | |
| 46 | | | |
| 47 | | | |
| 48 | | | |
| 49 | | | |
| 50 | | | |
| 51 | | | |
| 52 | | | |
| 53 | | | |
| 54 | | | |
| 55 | | | |
| 56 | | | |
| 57 | | | |
| 58 | | | |
| 59 | | | |
| 60 | | | |

1
2
3 **Data S2:** Identified proteins by RNA pull down coupled with mass spectrometry with m6A or A-oligo, in nuclear or cytosolic protein extracts

4 Proteins identified in cytosolic extracts

| 5 | Oligo | Accession | Description |
|----|--------------|------------------|---|
| 6 | m6A | K1QNA2_CRAGI | Vitellogenin-6 |
| 7 | m6A | K1QVJ8_CRAGI | Piwi-like protein 1 |
| 8 | m6A | K1QQ94_CRAGI | Uncharacterized protein |
| 9 | m6A | K1QHK9_CRAGI | Dynein heavy chain, cytoplasmic |
| 10 | m6A | K1QQ68_CRAGI | Tubulin alpha chain |
| 11 | m6A | K1RLF8_CRAGI | Splicing factor 3B subunit 3 |
| 12 | m6A | K1R473_CRAGI | Tubulin alpha chain |
| 13 | m6A | K1QII6_CRAGI | Tubulin alpha chain |
| 14 | m6A | K1PNR3_CRAGI | Clathrin heavy chain |
| 15 | m6A | K1R7V7_CRAGI | Tubulin beta chain |
| 16 | m6A | K1PNI6_CRAGI | Heterogeneous nuclear ribonucleoprotein A/B |
| 17 | m6A | K1QMX5_CRAGI | Uncharacterized protein |
| 18 | m6A | K1QHI5_CRAGI | Pyruvate carboxylase, mitochondrial |
| 19 | m6A | K1PE00_CRAGI | Tubulin alpha chain |
| 20 | m6A | K1R294_CRAGI | T-complex protein 1 subunit beta |
| 21 | m6A | K1S4Q2_CRAGI | T-complex protein 1 subunit delta (Fragment) |
| 22 | m6A | K1PQP2_CRAGI | Nucleolin |
| 23 | m6A | K1R466_CRAGI | T-complex protein 1 subunit gamma |
| 24 | m6A | K1PN21_CRAGI | Tubulin beta chain |
| 25 | m6A | K1R164_CRAGI | Galectin-4 |
| 26 | m6A | K1S2N7_CRAGI | Innexin |
| 27 | m6A | K1R6Z7_CRAGI | ATP synthase subunit alpha |
| 28 | m6A | K1R5B4_CRAGI | Proteasome activator complex subunit 4 |
| 29 | m6A | K1PVA1_CRAGI | Transitional endoplasmic reticulum ATPase |
| 30 | m6A | K1QFW9_CRAGI | Uncharacterized protein |
| 31 | m6A | K1R0S3_CRAGI | T-complex protein 1 subunit theta |
| 32 | m6A | K1QMA4_CRAGI | RRP5-like protein |
| 33 | m6A | K1R3U2_CRAGI | Uncharacterized protein |
| 34 | m6A | K1Q9W5_CRAGI | T-complex protein 1 subunit eta |
| 35 | m6A | K1QBK6_CRAGI | Splicing factor 3B subunit 1 |
| 36 | m6A | K1R545_CRAGI | Pre-mRNA-processing-splicing factor 8 (Fragment) |
| 37 | m6A | K1RAJ1_CRAGI | T-complex protein 1 subunit alpha |
| 38 | m6A | K1RWS2_CRAGI | Transcriptional activator protein Pur-alpha |
| 39 | m6A | K1Q350_CRAGI | Glyceraldehyde-3-phosphate dehydrogenase |
| 40 | m6A | K1RGT5_CRAGI | Metalloendopeptidase |
| 41 | m6A | K1PJ85_CRAGI | 26S protease regulatory subunit 6A |
| 42 | m6A | K1S6V7_CRAGI | Serine/threonine-protein phosphatase 2A 65 kDa regulatory subunit A alpha isoform |
| 43 | m6A | K1S1S1_CRAGI | Insulin-like growth factor 2 mRNA-binding protein 1 |
| 44 | m6A | K1RZE2_CRAGI | Isocitrate dehydrogenase [NADP] |
| 45 | m6A | K1PNQ5_CRAGI | Heat shock protein HSP 90-alpha 1 |
| 46 | m6A | K1R866_CRAGI | Puromycin-sensitive aminopeptidase |
| 47 | m6A | K1P9D0_CRAGI | Stress-70 protein, mitochondrial |
| 48 | m6A | K1QXX7_CRAGI | Myosin heavy chain, non-muscle (Fragment) |
| 49 | m6A | K1RG73_CRAGI | Acetyl-CoA carboxylase |
| 50 | m6A | K1R420_CRAGI | Non-specific serine/threonine protein kinase |
| 51 | m6A | K1PXN5_CRAGI | T-complex protein 1 subunit zeta |
| 52 | m6A | K1QGS8_CRAGI | Elongation factor 1-alpha |
| 53 | m6A | K1RLC5_CRAGI | T-complex protein 1 subunit epsilon |
| 54 | m6A | K1R6Q7_CRAGI | DNA topoisomerase I |
| 55 | m6A | K1RW85_CRAGI | Adenosylhomocysteinase |
| 56 | m6A | K1QSX8_CRAGI | ATPase family AAA domain-containing protein 2B |
| 57 | m6A | K1R4Z3_CRAGI | Malate dehydrogenase, mitochondrial |
| 58 | m6A | K1PEY4_CRAGI | 26S proteasome non-ATPase regulatory subunit 2 |
| 59 | m6A | K1RI55_CRAGI | Insulin-like growth factor 2 mRNA-binding protein 3 |
| 60 | m6A | K1PK85_CRAGI | Cullin-associated NEDD8-dissociated protein 1 |
| | m6A | K1R9B6_CRAGI | H/ACA ribonucleoprotein complex subunit 4 |
| | m6A | K1R252_CRAGI | Putative methylmalonate-semialdehyde dehydrogenase [acylating], mitochondrial |

| | | | |
|----|-----|--------------|---|
| 1 | | | |
| 2 | | | |
| 3 | m6A | K1RK12_CRAGI | 40S ribosomal protein S23 |
| 4 | m6A | K1QVN9_CRAGI | T-complex protein 1 subunit eta |
| 5 | m6A | K1PLF9_CRAGI | Arginine kinase |
| 6 | m6A | Q8TA69_CRAGI | Actin 2 |
| 7 | m6A | K1QG58_CRAGI | Actin |
| 8 | m6A | K1QSB2_CRAGI | 26S protease regulatory subunit 6B |
| 9 | m6A | K1R401_CRAGI | Spectrin alpha chain |
| 10 | m6A | K1Q112_CRAGI | 26S protease regulatory subunit 7 |
| 11 | m6A | K1Q419_CRAGI | D-3-phosphoglycerate dehydrogenase (Fragment) |
| 12 | m6A | K1R419_CRAGI | D-3-phosphoglycerate dehydrogenase (Fragment) |
| 13 | m6A | K1RJH5_CRAGI | Polyadenylate-binding protein |
| 14 | m6A | K1RWD4_CRAGI | Actin, cytoplasmic |
| 15 | m6A | K1QI14_CRAGI | 40S ribosomal protein S3a |
| 16 | m6A | K1RWW5_CRAGI | ATP synthase subunit beta |
| 17 | m6A | K1QET2_CRAGI | Coatomer subunit alpha |
| 18 | m6A | K1QVS3_CRAGI | Thimet oligopeptidase |
| 19 | m6A | K1QVS3_CRAGI | Thimet oligopeptidase |
| 20 | m6A | K1QVS3_CRAGI | Thimet oligopeptidase |
| 21 | m6A | K1QSQ9_CRAGI | Putative ATP-dependent RNA helicase an3 |
| 22 | m6A | K1Q923_CRAGI | Putative ATP-dependent RNA helicase DDX4 |
| 23 | m6A | K1QXR4_CRAGI | Pancreatic lipase-related protein 2 |
| 24 | m6A | K1R512_CRAGI | Uncharacterized protein |
| 25 | m6A | K1R512_CRAGI | Uncharacterized protein |
| 26 | m6A | K1R8L1_CRAGI | Exportin-2 |
| 27 | m6A | K1PAG1_CRAGI | Dynein beta chain, ciliary |
| 28 | m6A | K1Q988_CRAGI | Band 4.1-like protein 3 |
| 29 | m6A | K1PJ06_CRAGI | Importin subunit alpha-1 |
| 30 | m6A | K1QWX2_CRAGI | 60S acidic ribosomal protein P0 |
| 31 | m6A | K1PH76_CRAGI | Y-box factor-like protein (Fragment) |
| 32 | m6A | K1PH76_CRAGI | Y-box factor-like protein (Fragment) |
| 33 | m6A | K1PW06_CRAGI | Filamin-C |
| 34 | m6A | K1RNB5_CRAGI | Propionyl-CoA carboxylase beta chain, mitochondrial |
| 35 | m6A | K1QWT8_CRAGI | Uncharacterized protein |
| 36 | m6A | K1QWT8_CRAGI | Uncharacterized protein |
| 37 | m6A | K1QNW9_CRAGI | Bifunctional aminoacyl-tRNA synthetase |
| 38 | m6A | K1QCC1_CRAGI | Phosphoglycerate kinase |
| 39 | m6A | K1QBN0_CRAGI | Methylcrotonoyl-CoA carboxylase beta chain, mitochondrial |
| 40 | m6A | K1Q3S7_CRAGI | Cytosolic carboxypeptidase 1 |
| 41 | m6A | K1PMT6_CRAGI | Heterogeneous nuclear ribonucleoprotein U-like protein 1 |
| 42 | m6A | K1Q9Z6_CRAGI | 26S proteasome non-ATPase regulatory subunit 7 |
| 43 | m6A | K1PH66_CRAGI | Fibrinolytic enzyme, isozyme C |
| 44 | m6A | K1PH66_CRAGI | Fibrinolytic enzyme, isozyme C |
| 45 | m6A | K1R1M7_CRAGI | Ubiquitin-like modifier-activating enzyme 1 |
| 46 | m6A | K1Q7G8_CRAGI | Fatty acid synthase |
| 47 | m6A | K1QEA6_CRAGI | Phosphoenolpyruvate carboxykinase [GTP] |
| 48 | m6A | K1QRL4_CRAGI | Importin-5 |
| 49 | m6A | K1RFT1_CRAGI | Band 4.1-like protein 3 |
| 50 | m6A | K1RFT1_CRAGI | Band 4.1-like protein 3 |
| 51 | m6A | K1QR72_CRAGI | Dipeptidyl peptidase 3 |
| 52 | m6A | K1R5R4_CRAGI | Dynein heavy chain 10, axonemal |
| 53 | m6A | K1QLK6_CRAGI | E3 ubiquitin-protein ligase HUWE1 |
| 54 | m6A | K1R5U4_CRAGI | Acetyl-CoA carboxylase 1 |
| 55 | m6A | K1R5U4_CRAGI | Acetyl-CoA carboxylase 1 |
| 56 | m6A | K1QXS6_CRAGI | Heterogeneous nuclear ribonucleoprotein A2-like protein 1 |
| 57 | m6A | K1R953_CRAGI | Acetyl-CoA carboxylase |
| 58 | m6A | K1PCS4_CRAGI | Eukaryotic translation initiation factor 2 subunit 3, Y-linked |
| 59 | m6A | K1QIR8_CRAGI | 78 kDa glucose-regulated protein |
| 60 | m6A | K1RSA6_CRAGI | Methylcrotonoyl-CoA carboxylase subunit alpha, mitochondrial |
| | m6A | K1R2V1_CRAGI | Importin subunit beta-1 |
| | m6A | K1QZW0_CRAGI | Polyadenylate-binding protein 2 |
| | m6A | K1R4R9_CRAGI | Mitotic apparatus protein p62 |
| | m6A | K1QWK2_CRAGI | MAM domain-containing glycosylphosphatidylinositol anchor protein 2 |
| | m6A | K1R2D6_CRAGI | Plastin-3 |
| | m6A | K1QB04_CRAGI | 26S proteasome non-ATPase regulatory subunit 3 |
| | m6A | K1RH70_CRAGI | 6-phosphogluconate dehydrogenase, decarboxylating |
| | m6A | K1QGK2_CRAGI | Coatomer subunit beta |
| | m6A | K1QUE6_CRAGI | 26S proteasome non-ATPase regulatory subunit 6 |
| | m6A | K1R7I9_CRAGI | Heterogeneous nuclear ribonucleoprotein Q |
| | m6A | K1PND7_CRAGI | Fatty acid synthase |

| | | |
|----|-----|---|
| 1 | | |
| 2 | | |
| 3 | m6A | K1QI28_CRAGI V-type proton ATPase subunit B |
| 4 | m6A | K1Q2H5_CRAGI Uncharacterized protein |
| 5 | m6A | K1QLT5_CRAGI 26S protease regulatory subunit 4 |
| 6 | m6A | K1R4I2_CRAGI 26S proteasome non-ATPase regulatory subunit 3 |
| 7 | m6A | K1QQR1_CRAGI Major vault protein |
| 8 | m6A | K1RAU3_CRAGI DNA ligase |
| 9 | m6A | K1PFG1_CRAGI Uncharacterized protein |
| 10 | m6A | K1RBC9_CRAGI Transketolase-like protein 2 |
| 11 | m6A | K1QT21_CRAGI Putative ATP-dependent RNA helicase DDX5 |
| 12 | m6A | K1PKK7_CRAGI AP-2 complex subunit mu-1 |
| 13 | m6A | K1Q358_CRAGI 60S acidic ribosomal protein P2 |
| 14 | m6A | K1PS71_CRAGI Uncharacterized protein |
| 15 | m6A | K1QHA2_CRAGI Spectrin beta chain, brain 4 |
| 16 | m6A | K1REG6_CRAGI DNA helicase |
| 17 | m6A | A7M7T7_CRAGI Non-selenium glutathione peroxidase |
| 18 | m6A | K1QHX2_CRAGI La-related protein 7 |
| 19 | m6A | K1RJ97_CRAGI Multifunctional protein ADE2 |
| 20 | m6A | K1RNZ6_CRAGI Eukaryotic translation initiation factor 3 subunit D |
| 21 | m6A | K1PAY7_CRAGI Propionyl-CoA carboxylase alpha chain, mitochondrial |
| 22 | m6A | K1QQ27_CRAGI Pancreatic lipase-related protein 2 |
| 23 | m6A | K1Q9K6_CRAGI Histone H3 |
| 24 | m6A | K1R083_CRAGI Aspartate aminotransferase, mitochondrial |
| 25 | m6A | K1PEP0_CRAGI 40S ribosomal protein S8 |
| 26 | m6A | K1PU26_CRAGI Malate dehydrogenase (Fragment) |
| 27 | m6A | K1QF01_CRAGI 40S ribosomal protein S4 |
| 28 | m6A | K1QDN1_CRAGI Heat shock protein 75 kDa, mitochondrial (Fragment) |
| 29 | m6A | K1QBH0_CRAGI Uncharacterized protein |
| 30 | m6A | K1Q9V3_CRAGI V-type proton ATPase catalytic subunit A |
| 31 | m6A | K1PJC1_CRAGI Adipophilin |
| 32 | m6A | K1Q330_CRAGI Dihydrolipoyl dehydrogenase |
| 33 | m6A | K1S3Y1_CRAGI 2-amino-3-ketobutyrate coenzyme A ligase, mitochondrial (Fragment) |
| 34 | m6A | K1R2Q9_CRAGI Aspartate aminotransferase |
| 35 | m6A | K1QEF2_CRAGI ADP-ribosylation factor-like protein 15 |
| 36 | m6A | K1PVH5_CRAGI Centromere/kinetochore protein zw10-like protein |
| 37 | m6A | K1PG07_CRAGI Lupus La-like protein |
| 38 | m6A | K1QMX8_CRAGI DNA replication licensing factor MCM7 |
| 39 | m6A | K1P7K8_CRAGI Vesicle-fusing ATPase 1 |
| 40 | m6A | K1QQL6_CRAGI Leucyl-tRNA synthetase, cytoplasmic |
| 41 | m6A | K1PY89_CRAGI Extracellular superoxide dismutase [Cu-Zn] |
| 42 | m6A | K1QKA9_CRAGI Piwi-like protein 2 |
| 43 | m6A | K1QHI6_CRAGI Dynein heavy chain 5, axonemal |
| 44 | m6A | K1QBF7_CRAGI Hypoxia up-regulated protein 1 |
| 45 | m6A | K1RTR1_CRAGI ATP-citrate synthase |
| 46 | m6A | K1PZF2_CRAGI Exportin-7 |
| 47 | m6A | K1PPP8_CRAGI Vigilin |
| 48 | m6A | K1RN77_CRAGI Nuclear autoantigenic sperm protein |
| 49 | m6A | K1PV49_CRAGI RuvB-like helicase |
| 50 | m6A | K1QXQ8_CRAGI DNA helicase |
| 51 | m6A | K1P2G0_CRAGI Strawberry notch-like protein 1 |
| 52 | m6A | K1QRQ2_CRAGI Glutamate dehydrogenase 1, mitochondrial |
| 53 | m6A | K1QHS8_CRAGI Ribonucleoside-diphosphate reductase |
| 54 | m6A | K1QX26_CRAGI Endoplasmic |
| 55 | m6A | K1QGB4_CRAGI 40S ribosomal protein S17 |
| 56 | m6A | K1RJJ7_CRAGI Histone H5 |
| 57 | m6A | K1QY85_CRAGI Transport protein Sec31A |
| 58 | m6A | K1Q6W3_CRAGI Talin-1 |
| 59 | m6A | K1R3V8_CRAGI COP9 signalosome complex subunit 4 |
| 60 | m6A | K1QY12_CRAGI Dynamin-1-like protein |
| | m6A | K1PYA0_CRAGI Cytoplasmic dynein 2 heavy chain 1 |
| | m6A | K1PF10_CRAGI PAN2-PAN3 deadenylation complex catalytic subunit PAN2 |

| | | | |
|----|-----|--------------|--|
| 1 | | | |
| 2 | | | |
| 3 | m6A | K1PNP4_CRAGI | 26S proteasome non-ATPase regulatory subunit 11 |
| 4 | m6A | K1QMB9_CRAGI | Eukaryotic translation initiation factor 3 subunit A |
| 5 | m6A | K1QC10_CRAGI | GTP-binding protein 1 |
| 6 | m6A | K1QK56_CRAGI | Uncharacterized protein |
| 7 | m6A | K1PJP9_CRAGI | 26S proteasome non-ATPase regulatory subunit 1 |
| 8 | m6A | K1PUL2_CRAGI | Long-chain-fatty-acid--CoA ligase 1 |
| 9 | m6A | K1Q7Q2_CRAGI | CCAAT/enhancer-binding protein zeta |
| 10 | m6A | K1Q7Q2_CRAGI | CCAAT/enhancer-binding protein zeta |
| 11 | m6A | K1QQK1_CRAGI | 26S proteasome non-ATPase regulatory subunit 12 |
| 12 | m6A | K1R3T3_CRAGI | Transcription factor BTF3 |
| 13 | m6A | K1PK93_CRAGI | GDP-L-fucose synthetase |
| 14 | m6A | K1PF96_CRAGI | Spliceosome RNA helicase BAT1 |
| 15 | m6A | K1PF96_CRAGI | Spliceosome RNA helicase BAT1 |
| 16 | m6A | K1PM50_CRAGI | 40S ribosomal protein S16 |
| 17 | m6A | K1PX47_CRAGI | Ubiquitin carboxyl-terminal hydrolase |
| 18 | m6A | K1QMV7_CRAGI | V-type proton ATPase subunit D |
| 19 | m6A | K1RAL0_CRAGI | Aspartate aminotransferase, cytoplasmic |
| 20 | m6A | K1P9N7_CRAGI | 14-3-3 protein zeta |
| 21 | m6A | K1P9N7_CRAGI | 14-3-3 protein zeta |
| 22 | m6A | K1QBR5_CRAGI | Uncharacterized protein |
| 23 | m6A | K1PVW0_CRAGI | S-adenosylmethionine synthase |
| 24 | m6A | K1PY73_CRAGI | Basic leucine zipper and W2 domain-containing protein 1 |
| 25 | m6A | K1PY73_CRAGI | Basic leucine zipper and W2 domain-containing protein 1 |
| 26 | m6A | K1QBL6_CRAGI | Tudor domain-containing protein 1 |
| 27 | m6A | K1Q9M7_CRAGI | Histone H1-delta |
| 28 | m6A | K1S151_CRAGI | Rab GDP dissociation inhibitor |
| 29 | m6A | K1RM80_CRAGI | Citrate synthase |
| 30 | m6A | K1R115_CRAGI | Succinate dehydrogenase [ubiquinone] flavoprotein subunit, mitochondrial |
| 31 | m6A | K1R115_CRAGI | Succinate dehydrogenase [ubiquinone] flavoprotein subunit, mitochondrial |
| 32 | m6A | K1R5D5_CRAGI | U3 small nucleolar RNA-associated protein 6-like protein |
| 33 | m6A | K1QSR2_CRAGI | Apoptosis inhibitor 5 |
| 34 | m6A | K1P5D4_CRAGI | Cysteine synthase |
| 35 | m6A | K1PE57_CRAGI | Severin |
| 36 | m6A | K1P8I1_CRAGI | Pleckstrin-like protein domain-containing family F member 2 (Fragment) |
| 37 | m6A | K1P8I1_CRAGI | Pleckstrin-like protein domain-containing family F member 2 (Fragment) |
| 38 | m6A | K1Q5G9_CRAGI | SUMO-activating enzyme subunit 2 |
| 39 | m6A | K1PVZ3_CRAGI | Cold shock domain-containing protein E1 |
| 40 | m6A | K1R4D4_CRAGI | 40S ribosomal protein SA |
| 41 | m6A | K1QXH3_CRAGI | Translational activator GCN1 |
| 42 | m6A | K1PI02_CRAGI | Talin-1 |
| 43 | m6A | K1PI02_CRAGI | Talin-1 |
| 44 | m6A | K1P3Q5_CRAGI | Programmed cell death 6-interacting protein |
| 45 | m6A | K1PKF5_CRAGI | Protein-glutamine gamma-glutamyltransferase 4 |
| 46 | m6A | K1QFZ8_CRAGI | Ceramide kinase-like protein |
| 47 | m6A | K1PJF4_CRAGI | Isoleucyl-tRNA synthetase, cytoplasmic |
| 48 | m6A | K1PV79_CRAGI | Importin subunit alpha |
| 49 | m6A | K1QMD3_CRAGI | Glycerol-3-phosphate dehydrogenase [NAD(+)] |
| 50 | m6A | K1QMD3_CRAGI | Glycerol-3-phosphate dehydrogenase [NAD(+)] |
| 51 | m6A | K1RDV7_CRAGI | Cell division control protein 2-like protein (Fragment) |
| 52 | m6A | K1P8W6_CRAGI | 60S ribosomal protein L4 |
| 53 | m6A | K1P112_CRAGI | ATP synthase subunit gamma, mitochondrial |
| 54 | m6A | K1R5F2_CRAGI | 14-3-3 protein epsilon |
| 55 | m6A | K1R5F2_CRAGI | 14-3-3 protein epsilon |
| 56 | m6A | K1QBW8_CRAGI | Uncharacterized protein |
| 57 | m6A | K1PZP6_CRAGI | Coatomer subunit gamma |
| 58 | m6A | K1PAR4_CRAGI | Unc-45-like protein A |
| 59 | m6A | K1QRZ3_CRAGI | 40S ribosomal protein S13 |
| 60 | m6A | K1QQB6_CRAGI | 40S ribosomal protein S14 |
| | m6A | K1QE71_CRAGI | DNA helicase |
| | m6A | K1RJM8_CRAGI | SAGA-associated factor 11 homolog |
| | m6A | K1RK33_CRAGI | Exportin-1 |
| | m6A | K1PPW8_CRAGI | Coatomer subunit beta |
| | m6A | K1QRK9_CRAGI | Succinyl-CoA ligase [GDP-forming] subunit beta, mitochondrial |
| | m6A | K1Q273_CRAGI | 60S ribosomal protein L14 |
| | m6A | K1PLY1_CRAGI | DNA polymerase |
| | m6A | K1PYR4_CRAGI | 26S proteasome non-ATPase regulatory subunit 1 |
| | m6A | K1QPC6_CRAGI | Nucleolar complex protein 2-like protein |
| | m6A | K1QP17_CRAGI | Caprin-1 |
| | m6A | K1R2N0_CRAGI | Histone H4 |

| | | |
|----|-----|---|
| 1 | | |
| 2 | | |
| 3 | m6A | K1Q5G6_CRAGI 60 kDa heat shock protein, mitochondrial |
| 4 | m6A | K1RIG6_CRAGI LSM14-like protein A |
| 5 | m6A | K1QY71_CRAGI Histone H2B |
| 6 | m6A | K1QAB1_CRAGI AP-2 complex subunit alpha |
| 7 | m6A | K1QAF3_CRAGI Alanine aminotransferase 2 |
| 8 | m6A | K1QI97_CRAGI Adenylyl cyclase-associated protein |
| 9 | m6A | K1PD57_CRAGI Constitutive coactivator of PPAR-gamma-like protein 1-like protein |
| 10 | m6A | K1Q0L1_CRAGI 60S ribosomal protein L23a |
| 11 | m6A | K1R8C6_CRAGI Epidermal retinal dehydrogenase 2 |
| 12 | m6A | K1R8C6_CRAGI Epidermal retinal dehydrogenase 2 |
| 13 | m6A | K1R0Y9_CRAGI ADP,ATP carrier protein |
| 14 | m6A | K1R0Y9_CRAGI ADP,ATP carrier protein |
| 15 | m6A | K1QXF5_CRAGI Calcyphosin-like protein |
| 16 | m6A | K1PA54_CRAGI Replication factor C subunit 3 |
| 17 | m6A | K1PS27_CRAGI DNA helicase |
| 18 | m6A | K1R8C6_CRAGI 40S ribosomal protein S12 |
| 19 | m6A | K1R8C6_CRAGI 40S ribosomal protein S12 |
| 20 | m6A | K1Q880_CRAGI Transportin-1 |
| 21 | m6A | K1PXD4_CRAGI Putative ATP-dependent RNA helicase DDX6 |
| 22 | m6A | K1P421_CRAGI Histone H2A |
| 23 | m6A | K1RL00_CRAGI Proteasome-associated protein ECM29-like protein |
| 24 | m6A | K1PI50_CRAGI 40S ribosomal protein S26 |
| 25 | m6A | K1PI50_CRAGI 40S ribosomal protein S26 |
| 26 | m6A | K1RCW5_CRAGI Eukaryotic translation initiation factor 4 gamma 3 |
| 27 | m6A | K1R0W4_CRAGI Signal recognition particle subunit SRP72 |
| 28 | m6A | K1QN11_CRAGI Pre-mRNA-processing-splicing factor 8 |
| 29 | m6A | K1R8R6_CRAGI Fructose-bisphosphate aldolase |
| 30 | m6A | K1R8R6_CRAGI Fructose-bisphosphate aldolase |
| 31 | m6A | K1QVE8_CRAGI Phosphoacetylglucosamine mutase |
| 32 | m6A | K1R5B9_CRAGI DNA-directed RNA polymerase, mitochondrial |
| 33 | m6A | K1QA50_CRAGI V-type proton ATPase subunit H |
| 34 | m6A | K1Q9J5_CRAGI Importin-4 |
| 35 | m6A | K1R3V0_CRAGI CAD protein |
| 36 | m6A | K1R3V0_CRAGI CAD protein |
| 37 | m6A | K1PFK8_CRAGI Uncharacterized protein |
| 38 | m6A | K1PSN0_CRAGI Pre-mRNA-processing factor 40-like protein A |
| 39 | m6A | K1QL67_CRAGI 60S ribosomal protein L7a |
| 40 | m6A | K1QE32_CRAGI Very long-chain specific acyl-CoA dehydrogenase, mitochondrial |
| 41 | m6A | K1QQ16_CRAGI AP complex subunit beta |
| 42 | m6A | K1QN79_CRAGI 40S ribosomal protein S11 |
| 43 | m6A | K1QN79_CRAGI 40S ribosomal protein S11 |
| 44 | m6A | K1P8B7_CRAGI Ubiquitin-conjugating enzyme E2-17 kDa (Fragment) |
| 45 | m6A | K1RHB2_CRAGI Nucleolar RNA helicase 2 |
| 46 | m6A | K1QWC3_CRAGI 40S ribosomal protein S3 |
| 47 | m6A | K1Q4E1_CRAGI N-acetyl-D-glucosamine kinase |
| 48 | m6A | K1Q6F7_CRAGI V-type proton ATPase subunit C |
| 49 | m6A | K1Q6F7_CRAGI V-type proton ATPase subunit C |
| 50 | m6A | K1R3I6_CRAGI Nucleolar complex protein 2-like protein (Fragment) |
| 51 | m6A | K1PFS5_CRAGI Elongation factor 1-gamma |
| 52 | m6A | K1PBZ4_CRAGI Regulator of nonsense transcripts 1 |
| 53 | m6A | K1RV41_CRAGI Guanine nucleotide-binding protein subunit beta-2-like 1 |
| 54 | m6A | K1QKV1_CRAGI Cytochrome b-c1 complex subunit 6 |
| 55 | m6A | K1QKV1_CRAGI Cytochrome b-c1 complex subunit 6 |
| 56 | m6A | K1S2Y0_CRAGI Uncharacterized protein |
| 57 | m6A | K1QKK5_CRAGI Vacuolar protein sorting-associated protein 4B |
| 58 | m6A | K1Q8S0_CRAGI Nucleolar complex protein 3 homolog |
| 59 | m6A | K1QWK6_CRAGI Metalloendopeptidase |
| 60 | m6A | K1PH31_CRAGI Protein arginine N-methyltransferase 1 |
| | m6A | K1R834_CRAGI 60S ribosomal protein L9 |
| | m6A | K1RDG4_CRAGI DNA helicase |
| | m6A | K1R591_CRAGI Inter-alpha-trypsin inhibitor heavy chain H4 |
| | m6A | K1Q9P5_CRAGI Mitochondrial-processing peptidase subunit beta |
| | m6A | K1QLS3_CRAGI Cytochrome b-c1 complex subunit 2, mitochondrial |
| | m6A | K1QNT7_CRAGI Aldehyde dehydrogenase, mitochondrial |
| | m6A | K1QDX9_CRAGI Ribosome biogenesis protein BMS1-like protein |
| | m6A | K1S6G3_CRAGI Ubiquitin-like modifier-activating enzyme 1 |
| | m6A | K1R8S7_CRAGI Phospholipase A-2-activating protein |
| | m6A | K1QFN1_CRAGI 60S ribosomal protein L23 |
| | m6A | K1Q5Z6_CRAGI Eukaryotic translation initiation factor 2 subunit 2 |

| | | |
|----|-----|--|
| 1 | | |
| 2 | | |
| 3 | m6A | K1R6C2_CRAGI Peroxisomal 3,2-trans-enoyl-CoA isomerase |
| 4 | m6A | K1Q0R4_CRAGI ATP-binding cassette sub-family F member 2 |
| 5 | m6A | K1P5V7_CRAGI Eukaryotic translation initiation factor 3 subunit C |
| 6 | m6A | K1PGW7_CRAGI Transmembrane protein 2 |
| 7 | m6A | K1RKC1_CRAGI Far upstream element-binding protein 3 |
| 8 | m6A | K1QHY1_CRAGI Eosinophil peroxidase |
| 9 | m6A | K1QLK8_CRAGI GTP-binding protein SAR1b |
| 10 | m6A | K1QRG9_CRAGI Uncharacterized protein |
| 11 | m6A | K1QRW4_CRAGI Coronin |
| 12 | m6A | K1QKI1_CRAGI Tudor domain-containing protein 1 |
| 13 | m6A | K1QRM1_CRAGI Nuclear pore protein |
| 14 | m6A | K1RBZ5_CRAGI Ran GTPase-activating protein 1 |
| 15 | m6A | K1RLT4_CRAGI Signal recognition particle subunit SRP68 |
| 16 | m6A | K1R7N6_CRAGI Eukaryotic translation initiation factor 6 |
| 17 | m6A | K1P5F7_CRAGI Metastasis-associated protein MTA1 |
| 18 | m6A | K1RCW3_CRAGI Elongation factor 1-beta |
| 19 | m6A | K1R2H9_CRAGI WD repeat-containing protein 35 |
| 20 | m6A | K1Q1K8_CRAGI Elongation factor 1-beta |
| 21 | m6A | K1QTD9_CRAGI Nucleolar protein 56 |
| 22 | m6A | K1QBW6_CRAGI Tudor domain-containing protein 1 |
| 23 | m6A | K1QFR9_CRAGI Spectrin beta chain |
| 24 | m6A | K1P9S7_CRAGI Brix domain-containing protein 2 |
| 25 | m6A | K1QEK7_CRAGI Ubiquitin carboxyl-terminal hydrolase |
| 26 | m6A | K1PAM6_CRAGI Uncharacterized protein |
| 27 | m6A | K1S3G2_CRAGI HMGB1 |
| 28 | m6A | K1QI11_CRAGI Pyruvate dehydrogenase E1 component subunit alpha type II, mitochondrial |
| 29 | m6A | K1QF31_CRAGI Serine/threonine-protein kinase PLK |
| 30 | m6A | K1QDA7_CRAGI Uracil phosphoribosyltransferase |
| 31 | m6A | K1QKN4_CRAGI Dynein heavy chain 6, axonemal |
| 32 | m6A | K1RNH1_CRAGI 60S ribosomal protein L18 (Fragment) |
| 33 | m6A | K1QK11_CRAGI Dynein heavy chain 7, axonemal |
| 34 | m6A | K1QED7_CRAGI Replication protein A subunit |
| 35 | m6A | K1PB82_CRAGI Electron transfer flavoprotein subunit beta |
| 36 | m6A | K1PPQ1_CRAGI 14-3-3 protein gamma |
| 37 | m6A | K1R8T6_CRAGI Cullin-1 |
| 38 | m6A | K1Q7E4_CRAGI Ubiquitin-conjugating enzyme E2 N |
| 39 | m6A | K1RSZ6_CRAGI 40S ribosomal protein S7 |
| 40 | m6A | K1Q1S3_CRAGI Myosin-VI |
| 41 | m6A | K1QH70_CRAGI Leucine-rich repeat-containing protein 40 |
| 42 | m6A | K1QZ13_CRAGI Myosin-Ie |
| 43 | m6A | K1Q4Z4_CRAGI Bifunctional purine biosynthesis protein PURH |
| 44 | m6A | K1Q5H6_CRAGI FACT complex subunit SSRP1 |
| 45 | m6A | K1PKL8_CRAGI Serine/threonine-protein phosphatase 2A 56 kDa regulatory subunit alpha isoform |
| 46 | m6A | K1QUC6_CRAGI Uncharacterized protein |
| 47 | m6A | K1QPP2_CRAGI Elongation factor Tu, mitochondrial |
| 48 | m6A | K1QMH5_CRAGI Small nuclear ribonucleoprotein Sm D1 |
| 49 | m6A | K1PZD9_CRAGI 26S proteasome non-ATPase regulatory subunit 11 |
| 50 | m6A | K1PBU0_CRAGI L-fucose kinase |
| 51 | m6A | K1QYB6_CRAGI Delta-1-pyrroline-5-carboxylate synthetase |
| 52 | m6A | K1PMP3_CRAGI Protoporphyrinogen oxidase |
| 53 | m6A | K1Q2E0_CRAGI AP-1 complex subunit mu-1 |
| 54 | m6A | K1QEF9_CRAGI Protein-glutamine gamma-glutamyltransferase K |
| 55 | m6A | K1QGE4_CRAGI Proteasome endopeptidase complex (Fragment) |
| 56 | m6A | K1Q6V6_CRAGI Replication factor C subunit 4 |
| 57 | m6A | K1QYT7_CRAGI COP9 signalosome complex subunit 7a |
| 58 | m6A | K1PWP4_CRAGI Phenylalanyl-tRNA synthetase alpha chain |
| 59 | m6A | K1PWD9_CRAGI Uncharacterized protein |
| 60 | m6A | K1QAH9_CRAGI H/ACA ribonucleoprotein complex subunit |
| | m6A | K1PS13_CRAGI Coatomer subunit beta (Fragment) |
| | m6A | K1QJ33_CRAGI Aminoacyl tRNA synthetase complex-interacting multifunctional protein 2 |

| | | |
|----|-----|---|
| 1 | | |
| 2 | | |
| 3 | m6A | K1QRL6_CRAGI Methenyltetrahydrofolate synthetase domain-containing protein |
| 4 | m6A | K1PU46_CRAGI Lethal(2) giant larvae-like protein 1 |
| 5 | m6A | K1R7J6_CRAGI Putative sodium/potassium-transporting ATPase subunit beta-2 |
| 6 | m6A | K1QYV6_CRAGI NMDA receptor-regulated protein 1 |
| 7 | m6A | K1R6E9_CRAGI Dihydrolipoamide acetyltransferase component of pyruvate dehydrogenase complex |
| 8 | m6A | K1P7L9_CRAGI Nucleolar GTP-binding protein 1 |
| 9 | m6A | K1PIB7_CRAGI Phenylalanyl-tRNA synthetase beta chain |
| 10 | m6A | K1PX23_CRAGI Eukaryotic peptide chain release factor subunit 1 |
| 11 | m6A | K1QDV6_CRAGI Protein argonaute-2 |
| 12 | m6A | K1R5G4_CRAGI 60S ribosomal protein L31 |
| 13 | m6A | K1R9T2_CRAGI Eukaryotic translation initiation factor 3 subunit B |
| 14 | m6A | K1PW99_CRAGI Protein OSCP1 |
| 15 | m6A | K1R1F0_CRAGI ATP-dependent DNA helicase 2 subunit 1 |
| 16 | m6A | K1Q260_CRAGI Nucleolar protein 58 |
| 17 | m6A | K1QFS4_CRAGI Actin-related protein 2 |
| 18 | m6A | K1QLZ1_CRAGI Actin-related protein 3 |
| 19 | m6A | K1Q6X5_CRAGI Protein disulfide-isomerase |
| 20 | m6A | K1PJB0_CRAGI Heat shock protein 70 B2 |
| 21 | m6A | K1Q8K2_CRAGI Importin subunit alpha |
| 22 | m6A | K1PKF6_CRAGI 26S proteasome non-ATPase regulatory subunit 13 |
| 23 | m6A | K1QGL9_CRAGI Mannose-1-phosphate guanyltransferase beta |
| 24 | m6A | K1RGJ7_CRAGI Neogenin |
| 25 | m6A | K1PUJ1_CRAGI Radixin |
| 26 | m6A | K1Q811_CRAGI Alpha-centractin |
| 27 | m6A | K1QWZ0_CRAGI Tetratricopeptide repeat protein 38 |
| 28 | m6A | K1PRL4_CRAGI 60S ribosomal protein L38 (Fragment) |
| 29 | m6A | K1Q9I1_CRAGI TRAF2 and NCK-interacting protein kinase |
| 30 | m6A | K1QVR0_CRAGI 26S proteasome non-ATPase regulatory subunit 8 |
| 31 | m6A | K1QK68_CRAGI Myosin-2 essential light chain |
| 32 | m6A | K1QMH2_CRAGI DNA polymerase |
| 33 | m6A | K1PD36_CRAGI Ubiquitin |
| 34 | m6A | K1Q4V0_CRAGI Myosin-VIIa |
| 35 | m6A | K1QBT2_CRAGI Proteasome subunit beta |
| 36 | m6A | K1PXU6_CRAGI 60S ribosomal protein L24 |
| 37 | m6A | K1Q329_CRAGI Pyruvate dehydrogenase E1 component subunit beta, mitochondrial |
| 38 | m6A | K1QDH9_CRAGI Myosin-11 |
| 39 | m6A | K1QW36_CRAGI 60S ribosomal protein L6 |
| 40 | m6A | K1Q4Y8_CRAGI Histone H1oo |
| 41 | m6A | K1PM66_CRAGI 60S ribosomal protein L12 |
| 42 | m6A | K1Q4U7_CRAGI AP-3 complex subunit delta-1 |
| 43 | m6A | K1QPY8_CRAGI Extracellular superoxide dismutase [Cu-Zn] |
| 44 | m6A | K1QIP0_CRAGI 26S proteasome non-ATPase regulatory subunit 5 |
| 45 | m6A | K1QW72_CRAGI Catalase |
| 46 | m6A | K1QMD8_CRAGI Proteasome subunit alpha type |
| 47 | m6A | K1PZC0_CRAGI Structural maintenance of chromosomes protein |
| 48 | m6A | K1RBI9_CRAGI Small nuclear ribonucleoprotein Sm D2 |
| 49 | m6A | K1QCQ5_CRAGI Succinate--CoA ligase [ADP-forming] subunit beta, mitochondrial |
| 50 | m6A | K1ROL4_CRAGI Sodium/potassium-transporting ATPase subunit alpha |
| 51 | m6A | K1QKG9_CRAGI Cysteine desulfurase, mitochondrial |
| 52 | m6A | K1PPK1_CRAGI Actin-related protein 2/3 complex subunit 4 |
| 53 | m6A | K1PUQ5_CRAGI Histone H2B |
| 54 | m6A | K1RFU6_CRAGI Proteasome activator complex subunit 3 |
| 55 | m6A | K1Q615_CRAGI Peroxiredoxin-1 |
| 56 | m6A | K1RIT6_CRAGI NADH-ubiquinone oxidoreductase 75 kDa subunit, mitochondrial |
| 57 | m6A | K1PQZ3_CRAGI Armadillo repeat-containing protein 4 |
| 58 | m6A | K1QW41_CRAGI Leucine-zipper-like transcriptional regulator 1 |
| 59 | m6A | K1PNS2_CRAGI 33 kDa inner dynein arm light chain, axonemal |
| 60 | m6A | K1QQP1_CRAGI Programmed cell death protein 4 |
| | m6A | K1QQC1_CRAGI Dynein light chain roadblock |
| | m6A | K1P6F0_CRAGI HEAT repeat-containing protein 2 |

| | | |
|----|-----|--|
| 1 | | |
| 2 | | |
| 3 | m6A | K1QHM2_CRAGI Dolichyl-diphosphooligosaccharide--protein glycosyltransferase subunit 2 |
| 4 | m6A | K1QY58_CRAGI Eukaryotic translation initiation factor 3 subunit I (Fragment) |
| 5 | m6A | K1PLA7_CRAGI Eukaryotic initiation factor 4A-II (Fragment) |
| 6 | m6A | K1R8I8_CRAGI Acetyltransferase component of pyruvate dehydrogenase complex |
| 7 | m6A | K1R2L7_CRAGI Glutaminyl-tRNA synthetase (Fragment) |
| 8 | m6A | K1QSD9_CRAGI Uncharacterized protein |
| 9 | m6A | K1R008_CRAGI Proteasome subunit alpha type |
| 10 | m6A | K1QBL3_CRAGI Putative phosphoglycerate mutase |
| 11 | m6A | K1R6S5_CRAGI 40S ribosomal protein S9 |
| 12 | m6A | K1R6S5_CRAGI 40S ribosomal protein S9 |
| 13 | m6A | K1QNS4_CRAGI DnaJ-like protein subfamily C member 9 |
| 14 | m6A | K1QNS4_CRAGI DnaJ-like protein subfamily C member 9 |
| 15 | m6A | K1Q7X3_CRAGI Pre-mRNA-splicing factor SYF1 |
| 16 | m6A | K1QG65_CRAGI rRNA 2'-O-methyltransferase fibrillar |
| 17 | m6A | K1QU53_CRAGI NAD(P) transhydrogenase, mitochondrial |
| 18 | m6A | K1RU04_CRAGI Actin, cytoplasmic |
| 19 | m6A | K1RAH6_CRAGI Ubiquitin-conjugating enzyme E2-17 kDa |
| 20 | m6A | K1RAH6_CRAGI Ubiquitin-conjugating enzyme E2-17 kDa |
| 21 | m6A | K1PTV1_CRAGI Splicing factor 3B subunit 4 |
| 22 | m6A | K1PCR5_CRAGI KH domain-containing, RNA-binding, signal transduction-associated protein 2 |
| 23 | m6A | K1QYH6_CRAGI COP9 signalosome complex subunit 3 |
| 24 | m6A | K1QH74_CRAGI Splicing factor, arginine/serine-rich 1 |
| 25 | m6A | K1QH74_CRAGI Splicing factor, arginine/serine-rich 1 |
| 26 | m6A | K1PX83_CRAGI Dynein heavy chain 5, axonemal |
| 27 | m6A | K1QJF7_CRAGI Coronin |
| 28 | m6A | K1PNX0_CRAGI Methionyl-tRNA synthetase, cytoplasmic |
| 29 | m6A | K1Q1L4_CRAGI Uncharacterized protein |
| 30 | m6A | K1PH10_CRAGI Polyadenylate-binding protein-interacting protein 1 |
| 31 | m6A | K1PH10_CRAGI Polyadenylate-binding protein-interacting protein 1 |
| 32 | m6A | K1QCL6_CRAGI Proteasomal ubiquitin receptor ADRM1 |
| 33 | m6A | K1Q1Q9_CRAGI Alpha-aminoacidic semialdehyde synthase, mitochondrial |
| 34 | m6A | K1QVP6_CRAGI Developmentally-regulated GTP-binding protein 1 |
| 35 | m6A | K1QNU0_CRAGI Non-specific serine/threonine protein kinase |
| 36 | m6A | K1Q6U0_CRAGI Coatomer subunit zeta-1 |
| 37 | m6A | K1Q6U0_CRAGI Coatomer subunit zeta-1 |
| 38 | m6A | K1S058_CRAGI Transcription factor RFX3 |
| 39 | m6A | K1R488_CRAGI Actin-related protein 2/3 complex subunit |
| 40 | m6A | K1Q4G7_CRAGI Tubulin gamma chain |
| 41 | m6A | K1PDL3_CRAGI Ribosomal protein L19 |
| 42 | m6A | K1PDL3_CRAGI Ribosomal protein L19 |
| 43 | m6A | K1PBL2_CRAGI Eukaryotic initiation factor 4A-III |
| 44 | m6A | K1QE83_CRAGI CCR4-NOT transcription complex subunit 1 |
| 45 | m6A | K1R1Q8_CRAGI Ras-related protein Rab-5C |
| 46 | m6A | K1ROP8_CRAGI CTP synthase |
| 47 | m6A | K1QJ46_CRAGI Putative methylcrotonoyl-CoA carboxylase beta chain, mitochondrial |
| 48 | m6A | K1QJ46_CRAGI Putative methylcrotonoyl-CoA carboxylase beta chain, mitochondrial |
| 49 | m6A | K1QG70_CRAGI Katanin p60 ATPase-containing subunit A1 |
| 50 | m6A | K1RBF6_CRAGI Uncharacterized protein yfeX |
| 51 | m6A | K1RZM3_CRAGI Cartilage acidic protein 1 |
| 52 | m6A | K1R5V4_CRAGI GTP-binding nuclear protein |
| 53 | m6A | K1QZX9_CRAGI Uncharacterized protein |
| 54 | m6A | K1Q6U7_CRAGI 78 kDa glucose-regulated protein |
| 55 | m6A | K1Q6U7_CRAGI 78 kDa glucose-regulated protein |
| 56 | m6A | K1R195_CRAGI Protein DJ-1 |
| 57 | m6A | K1Q317_CRAGI Serine/threonine-protein kinase SRPK1 |
| 58 | m6A | K1QJE9_CRAGI Uncharacterized protein |
| 59 | m6A | K1PD30_CRAGI Putative histone-binding protein Caf1 |
| 60 | m6A | K1QJM1_CRAGI 60S ribosomal protein L30 |
| | m6A | K1RHP3_CRAGI Proliferation-associated protein 2G4 |
| | m6A | K1PMJ9_CRAGI Cleavage stimulation factor 77 kDa subunit |
| | m6A | K1RAU8_CRAGI Eukaryotic translation initiation factor 3 subunit E |
| | m6A | K1RIS2_CRAGI 3-oxoacyl-[acyl-carrier-protein] reductase |
| | m6A | K1PLM3_CRAGI Hydroxyacyl-coenzyme A dehydrogenase, mitochondrial |
| | m6A | K1PWU5_CRAGI Cytosolic carboxypeptidase 1 |
| | m6A | K1QFF0_CRAGI Vacuolar protein sorting-associated protein 35 (Fragment) |
| | m6A | K1P6C4_CRAGI Poly [ADP-ribose] polymerase |
| | m6A | K1RG19_CRAGI Protein FAM98A |
| | m6A | K1QCB0_CRAGI 40S ribosomal protein S5 |
| | m6A | K1PCH8_CRAGI Nucleoporin p54 |

| | | |
|----|-----|--|
| 1 | | |
| 2 | | |
| 3 | m6A | K1Q2Y1_CRAGI 40S ribosomal protein S15 |
| 4 | m6A | K1QGW4_CRAGI Density-regulated protein |
| 5 | m6A | K1R6H7_CRAGI Uncharacterized protein |
| 6 | m6A | K1R0D7_CRAGI Eukaryotic translation initiation factor 3 subunit M (Fragment) |
| 7 | m6A | K1PPI6_CRAGI Synaptobrevin-like protein YKT6 |
| 8 | m6A | K1RMW3_CRAGI Protein kinase C |
| 9 | m6A | K1QV25_CRAGI Transcription elongation factor B polypeptide 2 |
| 10 | m6A | K1QC27_CRAGI Hydroxysteroid dehydrogenase-like protein 2 |
| 11 | m6A | K1RAT9_CRAGI Tubulin-specific chaperone D |
| 12 | m6A | K1RAT9_CRAGI Tubulin-specific chaperone D |
| 13 | m6A | K1QWJ4_CRAGI Splicing factor 3B subunit 5 |
| 14 | m6A | K1PZ08_CRAGI Ras-related protein Rab-7a |
| 15 | m6A | K1PZ08_CRAGI Ras-related protein Rab-7a |
| 16 | m6A | K1QMQ1_CRAGI TBC1 domain family member 10B |
| 17 | m6A | K1R811_CRAGI Ribonucleoside-diphosphate reductase small chain |
| 18 | m6A | K1P8G1_CRAGI Heterogeneous nuclear ribonucleoprotein H |
| 19 | m6A | K1R983_CRAGI Protein transport protein SEC23 |
| 20 | m6A | K1R983_CRAGI Protein transport protein SEC23 |
| 21 | m6A | K1QDI4_CRAGI Superoxide dismutase [Cu-Zn] |
| 22 | m6A | K1RDM2_CRAGI 60S ribosomal protein L18a |
| 23 | m6A | K1QYI9_CRAGI Arginyl-tRNA synthetase, cytoplasmic (Fragment) |
| 24 | m6A | K1QVS0_CRAGI Ras-like GTP-binding protein Rho1 |
| 25 | m6A | K1QVS0_CRAGI Ras-like GTP-binding protein Rho1 |
| 26 | m6A | K1PJS7_CRAGI Poly [ADP-ribose] polymerase |
| 27 | m6A | K1QRD0_CRAGI Cytoplasmic dynein 1 light intermediate chain 1 |
| 28 | m6A | K1R0R7_CRAGI Putative ATP-dependent RNA helicase DHX36 |
| 29 | m6A | K1Q1F1_CRAGI Serine/threonine-protein kinase 31 |
| 30 | m6A | K1Q1F1_CRAGI Serine/threonine-protein kinase 31 |
| 31 | m6A | K1QI32_CRAGI Synaptotagmin-like protein 5 |
| 32 | m6A | K1PMY9_CRAGI Calmodulin |
| 33 | m6A | K1PXG6_CRAGI Serine/threonine-protein phosphatase |
| 34 | m6A | K1QW61_CRAGI WD repeat-containing protein 19 |
| 35 | m6A | K1P2B8_CRAGI GDP-mannose 4,6 dehydratase |
| 36 | m6A | K1QYT5_CRAGI Phosphate carrier protein, mitochondrial |
| 37 | m6A | K1QYT5_CRAGI Phosphate carrier protein, mitochondrial |
| 38 | m6A | K1RIZ9_CRAGI Band 4.1-like protein 5 |
| 39 | m6A | K1QT97_CRAGI N(G),N(G)-dimethylarginine dimethylaminohydrolase 1 |
| 40 | m6A | K1QKF8_CRAGI S-(hydroxymethyl)glutathione dehydrogenase |
| 41 | m6A | K1REJ2_CRAGI Lon protease homolog, mitochondrial |
| 42 | m6A | K1R1B1_CRAGI 35 kDa SR repressor protein |
| 43 | m6A | K1R1B1_CRAGI 35 kDa SR repressor protein |
| 44 | m6A | K1PRK2_CRAGI Small glutamine-rich tetratricopeptide repeat-containing protein beta |
| 45 | m6A | K1QAT9_CRAGI ATP-dependent RNA helicase DDX1 |
| 46 | m6A | K1PFV9_CRAGI 4-trimethylaminobutyraldehyde dehydrogenase |
| 47 | m6A | K1QLP5_CRAGI Coatomer subunit delta |
| 48 | m6A | K1PIH2_CRAGI V-type proton ATPase subunit E |
| 49 | m6A | K1RBU9_CRAGI Non-specific serine/threonine protein kinase |
| 50 | m6A | K1RBU9_CRAGI Non-specific serine/threonine protein kinase |
| 51 | m6A | K1QGP1_CRAGI Replication factor C subunit 2 |
| 52 | m6A | K1PJ96_CRAGI Uncharacterized protein |
| 53 | m6A | K1QHH0_CRAGI Protein henna |
| 54 | m6A | K1ROW0_CRAGI Ferritin |
| 55 | m6A | K1ROW0_CRAGI Ferritin |
| 56 | m6A | K1Q6W5_CRAGI FACT complex subunit spt16 |
| 57 | m6A | K1QEZ5_CRAGI MON2-like protein |
| 58 | m6A | K1RJW8_CRAGI Protein DEK |
| 59 | m6A | K1P752_CRAGI UPF0195 protein FAM96B |
| 60 | m6A | K1RP91_CRAGI Putative RNA exonuclease NEF-sp |
| | m6A | K1QSZ6_CRAGI Uncharacterized protein |
| | m6A | K1RD83_CRAGI Serine hydroxymethyltransferase |
| | m6A | K1R5W3_CRAGI Uncharacterized protein |
| | m6A | K1S211_CRAGI Poly(A) RNA polymerase gld-2-like protein A |
| | m6A | K1QTW6_CRAGI Eukaryotic translation initiation factor 3 subunit F |
| | m6A | K1QEJ0_CRAGI Ras GTPase-activating protein-binding protein 2 |
| | m6A | K1R1R9_CRAGI Pre-mRNA-processing factor 6 |
| | m6A | K1QJL2_CRAGI CCR4-NOT transcription complex subunit 10 |
| | m6A | K1PUV4_CRAGI 40S ribosomal protein S24 |
| | m6A | K1RH58_CRAGI Alpha-actinin, sarcomeric |
| | m6A | K1PQI4_CRAGI Enolase-phosphatase E1 |

| | | |
|----|-----|---|
| 1 | | |
| 2 | | |
| 3 | m6A | K1R7D7_CRAGI Poly(A)-specific ribonuclease PARN |
| 4 | m6A | K1PS84_CRAGI Alpha-crystallin B chain |
| 5 | m6A | K1QQV0_CRAGI Histone H1.2 |
| 6 | m6A | K1QPJ9_CRAGI Serine/threonine-protein phosphatase 2A 55 kDa regulatory subunit B |
| 7 | m6A | K1QZX3_CRAGI Vacuolar protein sorting-associated protein VTA1-like protein |
| 8 | m6A | K1R517_CRAGI Superkiller viralicidic activity 2-like 2 |
| 9 | m6A | K1RJS5_CRAGI Uncharacterized protein |
| 10 | m6A | K1S3Q9_CRAGI MAK16-like protein (Fragment) |
| 11 | m6A | K1PKD4_CRAGI 40S ribosomal protein S30 |
| 12 | m6A | K1PGZ0_CRAGI Thyroid adenoma-associated protein |
| 13 | m6A | K1REV3_CRAGI DNA polymerase delta subunit 2 |
| 14 | m6A | K1QGF1_CRAGI Splicing factor 3B subunit 2 |
| 15 | m6A | K1R8B2_CRAGI Isovaleryl-CoA dehydrogenase, mitochondrial |
| 16 | m6A | K1PR25_CRAGI Regulator of differentiation 1 |
| 17 | m6A | K1PZ23_CRAGI DnaJ-like protein subfamily C member 3 |
| 18 | m6A | K1PLG1_CRAGI Putative ribosomal RNA methyltransferase NOP2 |
| 19 | m6A | K1PNY5_CRAGI Splicing factor, proline-and glutamine-rich |
| 20 | m6A | K1RG79_CRAGI Neuronal acetylcholine receptor subunit alpha-6 |
| 21 | m6A | K1PRB6_CRAGI Apolipoprotein D |
| 22 | m6A | K1PTR3_CRAGI Oxysterol-binding protein |
| 23 | m6A | K1Q1F4_CRAGI 60S ribosomal protein L3 (Fragment) |
| 24 | m6A | Q70MT4_CRAGI 40S ribosomal protein S10 |
| 25 | m6A | K1Q662_CRAGI Actin-interacting protein 1 |
| 26 | m6A | K1R2G9_CRAGI SEC13-like protein |
| 27 | m6A | K1PRV7_CRAGI Profilin |
| 28 | m6A | K1QWZ6_CRAGI Dolichyl-diphosphooligosaccharide--protein glycosyltransferase subunit 1 |
| 29 | m6A | K1R9S5_CRAGI Cytosolic Fe-S cluster assembly factor NUBP2 homolog |
| 30 | m6A | K1QUK0_CRAGI NEDD8-activating enzyme E1 catalytic subunit |
| 31 | m6A | K1PTE3_CRAGI Uncharacterized protein |
| 32 | m6A | K1Q6M6_CRAGI 6-phosphofructokinase |
| 33 | m6A | K1QZN3_CRAGI Myosin-IId |
| 34 | m6A | K1PB94_CRAGI ATP-binding cassette sub-family E member 1 |
| 35 | m6A | K1RNN9_CRAGI Cytoskeleton-associated protein 5 |
| 36 | m6A | K1PZL0_CRAGI B-box type zinc finger protein ncl-1 |
| 37 | m6A | K1RKZ5_CRAGI DNA damage-binding protein 1 |
| 38 | m6A | K1R138_CRAGI Nuclear pore glycoprotein p62 |
| 39 | m6A | K1Q9D7_CRAGI Sorting nexin-2 |
| 40 | m6A | K1R6F1_CRAGI Proteasome subunit alpha type |
| 41 | m6A | K1QKQ5_CRAGI N-terminal acetyltransferase B complex subunit MDM20 |
| 42 | m6A | K1PDC6_CRAGI Proteasome subunit beta |
| 43 | m6A | A5LGH1_CRAGI Voltage-dependent anion channel |
| 44 | m6A | K1PF60_CRAGI 3-ketoacyl-CoA thiolase, mitochondrial |
| 45 | m6A | K1R924_CRAGI RNA-binding protein 45 |
| 46 | m6A | K1RTQ6_CRAGI Fructose-bisphosphate aldolase |
| 47 | m6A | K1Q888_CRAGI Translin |
| 48 | m6A | K1R255_CRAGI Heterogeneous nuclear ribonucleoprotein L |
| 49 | m6A | K1QIZ7_CRAGI Programmed cell death protein 6 |
| 50 | m6A | K1QI48_CRAGI Inositol hexakisphosphate and diphosphoinositol-pentakisphosphate kinase |
| 51 | m6A | K1PWB9_CRAGI EH domain-containing protein 1 |
| 52 | m6A | K1QZ84_CRAGI Thioredoxin domain-containing protein 3-like protein |
| 53 | m6A | K1PJY4_CRAGI Calcium-binding protein 39 |
| 54 | m6A | K1PBC0_CRAGI Non-neuronal cytoplasmic intermediate filament protein |
| 55 | m6A | K1PRD5_CRAGI Trifunctional purine biosynthetic protein adenosine-3 |
| 56 | m6A | K1QXH7_CRAGI DNA replication licensing factor mcm4-B |
| 57 | m6A | K1Q719_CRAGI Serine/threonine-protein kinase OSR1 |
| 58 | m6A | K1QV87_CRAGI Catenin alpha-2 |
| 59 | m6A | K1PBH3_CRAGI Dynein heavy chain 3, axonemal |
| 60 | m6A | K1R4M7_CRAGI Serine/threonine protein phosphatase 2A regulatory subunit |
| | m6A | K1R3A0_CRAGI Transcription initiation factor IIB |
| | m6A | K1QQQ5_CRAGI Replication factor C subunit 5 |

| | | |
|----|-----|--|
| 1 | | |
| 2 | | |
| 3 | m6A | K1RJ70_CRAGI Cytosolic non-specific dipeptidase |
| 4 | m6A | K1QNY7_CRAGI Transport protein Sec24C |
| 5 | m6A | K1R481_CRAGI Epimerase family protein SDR39U1 |
| 6 | m6A | K1QRE1_CRAGI COP9 signalosome complex subunit 6 |
| 7 | m6A | K1RA63_CRAGI Transmembrane protein 2 |
| 8 | m6A | K1QHT0_CRAGI Deoxyuridine 5'-triphosphate nucleotidohydrolase, mitochondrial |
| 9 | m6A | K1PQA3_CRAGI Pseudouridylate synthase 7-like protein |
| 10 | m6A | K1PII4_CRAGI YTH domain-containing protein 1 |
| 11 | m6A | K1P8S5_CRAGI Condensin complex subunit 3 |
| 12 | m6A | K1QMT1_CRAGI DnaJ-like protein subfamily B member 4 |
| 13 | m6A | K1PN10_CRAGI Intron-binding protein aquarius |
| 14 | m6A | K1PCR9_CRAGI Proteasome endopeptidase complex |
| 15 | m6A | K1PZI3_CRAGI SWI/SNF complex subunit SMARCC2 |
| 16 | m6A | K1RIZ3_CRAGI Bone morphogenetic protein 7 |
| 17 | m6A | K1QMY1_CRAGI Aconitate hydratase, mitochondrial |
| 18 | m6A | K1R3W9_CRAGI Replication protein A 14 kDa subunit |
| 19 | m6A | K1PLD4_CRAGI Dynein heavy chain 2, axonemal |
| 20 | m6A | K1QC78_CRAGI Ras-related protein Rab-14 |
| 21 | m6A | K1PTV5_CRAGI Programmed cell death protein 10 |
| 22 | m6A | K1RGG1_CRAGI Alanyl-tRNA synthetase, cytoplasmic |
| 23 | m6A | K1R3R4_CRAGI Cytosolic Fe-S cluster assembly factor NUBP1 homolog |
| 24 | m6A | K1R266_CRAGI Retinal dehydrogenase 1 |
| 25 | m6A | K1QGC9_CRAGI Acetyl-coenzyme A synthetase |
| 26 | m6A | K1Q7T5_CRAGI Protein disulfide-isomerase |
| 27 | m6A | K1QKQ8_CRAGI THO complex subunit 4-A |
| 28 | m6A | K1QR54_CRAGI Zinc finger RNA-binding protein |
| 29 | m6A | K1PEW1_CRAGI Sorting nexin |
| 30 | m6A | K1PFL3_CRAGI Dihydropteridine reductase |
| 31 | m6A | K1QC11_CRAGI AP-1 complex subunit gamma |
| 32 | m6A | K1QQI3_CRAGI Rab-like protein 5 |
| 33 | m6A | K1R916_CRAGI Structural maintenance of chromosomes protein |
| 34 | m6A | K1PF37_CRAGI Thioredoxin domain-containing protein 9 |
| 35 | m6A | K1PJW0_CRAGI Talin-1 |
| 36 | m6A | K1PUX5_CRAGI Casein kinase II subunit alpha |
| 37 | m6A | K1QB86_CRAGI Dynamin-1 |
| 38 | m6A | K1QWX0_CRAGI 26S proteasome non-ATPase regulatory subunit 14 |
| 39 | m6A | K1QBM3_CRAGI Ras-related protein Rab-2 |
| 40 | m6A | K1RG04_CRAGI ALK tyrosine kinase receptor |
| 41 | m6A | K1PXH5_CRAGI Putative saccharopine dehydrogenase |
| 42 | m6A | K1Q407_CRAGI Ras GTPase-activating protein 1 |
| 43 | m6A | K1PYK7_CRAGI RNA-binding protein 39 |
| 44 | m6A | K1PZR3_CRAGI U2 small nuclear ribonucleoprotein A |
| 45 | m6A | K1RBJ3_CRAGI DnaJ-like protein subfamily C member 13 |
| 46 | m6A | K1Q324_CRAGI Heterogeneous nuclear ribonucleoprotein K |
| 47 | m6A | K1PA61_CRAGI Actin-like protein 6A |
| 48 | m6A | K1PWS8_CRAGI Mitotic spindle assembly checkpoint protein MAD2A |
| 49 | m6A | K1PL64_CRAGI Poly(A) polymerase gamma |
| 50 | m6A | K1RB97_CRAGI Kinetochores-associated protein 1 |
| 51 | m6A | K1R6S7_CRAGI Mannose-1-phosphate guanyltransferase alpha-A |
| 52 | m6A | K1RK83_CRAGI Tyrosine-protein kinase BAZ1B |
| 53 | m6A | K1QSA2_CRAGI Short-chain specific acyl-CoA dehydrogenase, mitochondrial |
| 54 | m6A | K1RFU8_CRAGI High mobility group protein DSP1 |
| 55 | m6A | K1QV46_CRAGI Tetratricopeptide repeat protein 21B |
| 56 | m6A | K1R8W3_CRAGI S-phase kinase-associated protein 1 |
| 57 | m6A | K1RFF7_CRAGI Protein lethal(2)essential for life |
| 58 | m6A | K1R1T8_CRAGI Nucleolar protein 56 |
| 59 | m6A | K1PNG7_CRAGI Sorting nexin-33 |
| 60 | m6A | K1PCV0_CRAGI Severin |
| | m6A | K1QVX4_CRAGI Glycogen synthase kinase-3 beta |
| | m6A | K1P9V5_CRAGI General transcription factor IIF subunit 1 |

| | | |
|----|-----|--|
| 1 | | |
| 2 | | |
| 3 | m6A | K1Q904_CRAGI PAN2-PAN3 deadenylation complex subunit PAN3 |
| 4 | m6A | K1REC3_CRAGI Exportin-5 |
| 5 | m6A | K1P137_CRAGI Actin-related protein 2/3 complex subunit 5 |
| 6 | m6A | K1QBT8_CRAGI Uncharacterized protein |
| 7 | m6A | K1PZN1_CRAGI Calcium/calmodulin-dependent protein kinase type II delta chain |
| 8 | m6A | K1QVZ2_CRAGI Uncharacterized protein |
| 9 | m6A | K1REPO_CRAGI Uncharacterized protein |
| 10 | m6A | K1QHX0_CRAGI Double-stranded RNA-specific editase 1 |
| 11 | m6A | K1PVL5_CRAGI tRNA 2'-phosphotransferase 1 |
| 12 | m6A | K1Q6Y2_CRAGI Uncharacterized protein |
| 13 | m6A | K1Q6Y2_CRAGI Uncharacterized protein |
| 14 | m6A | K1PMQ4_CRAGI Microtubule-associated serine/threonine-protein kinase-like protein |
| 15 | m6A | K1PQR9_CRAGI Squamous cell carcinoma antigen recognized by T-cells 3 |
| 16 | m6A | K1R150_CRAGI Ras-related protein Rab-1A |
| 17 | m6A | K1PNU2_CRAGI Histone-arginine methyltransferase CARM1 |
| 18 | m6A | K1PEX5_CRAGI Protein hu-li tai shao |
| 19 | m6A | K1PDF0_CRAGI Protein disulfide-isomerase A6 |
| 20 | m6A | K1PDF0_CRAGI Protein disulfide-isomerase A6 |
| 21 | m6A | K1QC22_CRAGI 40S ribosomal protein S19 |
| 22 | m6A | K1PUF0_CRAGI G-protein coupled receptor moody |
| 23 | m6A | K1S422_CRAGI Katanin p80 WD40 repeat-containing subunit B1 |
| 24 | m6A | K1S422_CRAGI Katanin p80 WD40 repeat-containing subunit B1 |
| 25 | m6A | K1PI41_CRAGI Flap endonuclease 1 |
| 26 | m6A | K1PI41_CRAGI Flap endonuclease 1 |
| 27 | m6A | K1RON8_CRAGI Flap endonuclease GEN-like protein 1 |
| 28 | m6A | K1RXR4_CRAGI Arrestin domain-containing protein 3 |
| 29 | m6A | K1PXX6_CRAGI Uncharacterized protein |
| 30 | m6A | K1QXP9_CRAGI Uncharacterized protein |
| 31 | m6A | K1QXP9_CRAGI Uncharacterized protein |
| 32 | m6A | K1RJB4_CRAGI Ubiquitin carboxyl-terminal hydrolase 1 |
| 33 | A | K1QNA2_CRAGI Vitellogenin-6 |
| 34 | A | K1QHK9_CRAGI Dynein heavy chain, cytoplasmic |
| 35 | A | K1PNR3_CRAGI Clathrin heavy chain |
| 36 | A | K1QVJ8_CRAGI Piwi-like protein 1 |
| 37 | A | K1QVJ8_CRAGI Piwi-like protein 1 |
| 38 | A | K1R7V7_CRAGI Tubulin beta chain |
| 39 | A | K1QQ94_CRAGI Uncharacterized protein |
| 40 | A | K1RLF8_CRAGI Splicing factor 3B subunit 3 |
| 41 | A | K1QQ68_CRAGI Tubulin alpha chain |
| 42 | A | K1S2N7_CRAGI Innexin |
| 43 | A | K1S2N7_CRAGI Innexin |
| 44 | A | K1R164_CRAGI Galectin-4 |
| 45 | A | K1QMX5_CRAGI Uncharacterized protein |
| 46 | A | K1QHI5_CRAGI Pyruvate carboxylase, mitochondrial |
| 47 | A | K1PQP2_CRAGI Nucleolin |
| 48 | A | K1PN21_CRAGI Tubulin beta chain |
| 49 | A | K1PAG1_CRAGI Dynein beta chain, ciliary |
| 50 | A | K1PAG1_CRAGI Dynein beta chain, ciliary |
| 51 | A | K1QII6_CRAGI Tubulin alpha chain |
| 52 | A | K1R5B4_CRAGI Proteasome activator complex subunit 4 |
| 53 | A | K1QFW9_CRAGI Uncharacterized protein |
| 54 | A | K1R473_CRAGI Tubulin alpha chain |
| 55 | A | K1R473_CRAGI Tubulin alpha chain |
| 56 | A | K1PK85_CRAGI Cullin-associated NEDD8-dissociated protein 1 |
| 57 | A | K1R294_CRAGI T-complex protein 1 subunit beta |
| 58 | A | K1PE00_CRAGI Tubulin alpha chain |
| 59 | A | K1PNI6_CRAGI Heterogeneous nuclear ribonucleoprotein A/B |
| 60 | A | K1PYA0_CRAGI Cytoplasmic dynein 2 heavy chain 1 |
| | A | K1R466_CRAGI T-complex protein 1 subunit gamma |
| | A | K1S4Q2_CRAGI T-complex protein 1 subunit delta (Fragment) |
| | A | K1QMA4_CRAGI RRP5-like protein |
| | A | K1R5R4_CRAGI Dynein heavy chain 10, axonemal |
| | A | K1RZE2_CRAGI Isocitrate dehydrogenase [NADP] |
| | A | K1QGS8_CRAGI Elongation factor 1-alpha |
| | A | K1QXX7_CRAGI Myosin heavy chain, non-muscle (Fragment) |
| | A | K1S6V7_CRAGI Serine/threonine-protein phosphatase 2A 65 kDa regulatory subunit A alpha isoform |
| | A | K1R866_CRAGI Puromycin-sensitive aminopeptidase |
| | A | K1QBK6_CRAGI Splicing factor 3B subunit 1 |
| | A | K1R3U2_CRAGI Uncharacterized protein |

| | | |
|----|---|--|
| 1 | | |
| 2 | | |
| 3 | A | K1QNW9_CRAGI Bifunctional aminoacyl-tRNA synthetase |
| 4 | A | K1R545_CRAGI Pre-mRNA-processing-splicing factor 8 (Fragment) |
| 5 | A | K1R6Z7_CRAGI ATP synthase subunit alpha |
| 6 | A | K1R6Q7_CRAGI DNA topoisomerase I |
| 7 | A | K1R0S3_CRAGI T-complex protein 1 subunit theta |
| 8 | A | K1RAJ1_CRAGI T-complex protein 1 subunit alpha |
| 9 | A | K1PNQ5_CRAGI Heat shock protein HSP 90-alpha 1 |
| 10 | A | K1PVA1_CRAGI Transitional endoplasmic reticulum ATPase |
| 11 | A | K1QHI6_CRAGI Dynein heavy chain 5, axonemal |
| 12 | A | K1Q7G8_CRAGI Fatty acid synthase |
| 13 | A | K1R401_CRAGI Spectrin alpha chain |
| 14 | A | K1PND7_CRAGI Fatty acid synthase |
| 15 | A | K1RGT5_CRAGI Metalloendopeptidase |
| 16 | A | K1PLF9_CRAGI Arginine kinase |
| 17 | A | K1QET2_CRAGI Coatomer subunit alpha |
| 18 | A | K1QSB2_CRAGI 26S protease regulatory subunit 6B |
| 19 | A | K1R9B6_CRAGI H/ACA ribonucleoprotein complex subunit 4 |
| 20 | A | K1R512_CRAGI Uncharacterized protein |
| 21 | A | K1RK12_CRAGI 40S ribosomal protein S23 |
| 22 | A | K1QQR1_CRAGI Major vault protein |
| 23 | A | K1R420_CRAGI Non-specific serine/threonine protein kinase |
| 24 | A | K1Q9W5_CRAGI T-complex protein 1 subunit eta |
| 25 | A | K1QSX8_CRAGI ATPase family AAA domain-containing protein 2B |
| 26 | A | K1Q350_CRAGI Glyceraldehyde-3-phosphate dehydrogenase |
| 27 | A | K1PJ85_CRAGI 26S protease regulatory subunit 6A |
| 28 | A | K1Q923_CRAGI Putative ATP-dependent RNA helicase DDX4 |
| 29 | A | K1PJ06_CRAGI Importin subunit alpha-1 |
| 30 | A | K1RLC5_CRAGI T-complex protein 1 subunit epsilon |
| 31 | A | K1R278_CRAGI Tubulin beta chain |
| 32 | A | K1R8L1_CRAGI Exportin-2 |
| 33 | A | K1PEY4_CRAGI 26S proteasome non-ATPase regulatory subunit 2 |
| 34 | A | K1RWS2_CRAGI Transcriptional activator protein Pur-alpha |
| 35 | A | K1RG73_CRAGI Acetyl-CoA carboxylase |
| 36 | A | K1QLK6_CRAGI E3 ubiquitin-protein ligase HUWE1 |
| 37 | A | K1PXN5_CRAGI T-complex protein 1 subunit zeta |
| 38 | A | K1P9D0_CRAGI Stress-70 protein, mitochondrial |
| 39 | A | K1QR72_CRAGI Dipeptidyl peptidase 3 |
| 40 | A | K1R4Z3_CRAGI Malate dehydrogenase, mitochondrial |
| 41 | A | K1Q988_CRAGI Band 4.1-like protein 3 |
| 42 | A | K1QB04_CRAGI 26S proteasome non-ATPase regulatory subunit 3 |
| 43 | A | K1QRL4_CRAGI Importin-5 |
| 44 | A | K1Q112_CRAGI 26S protease regulatory subunit 7 |
| 45 | A | K1QXR4_CRAGI Pancreatic lipase-related protein 2 |
| 46 | A | K1RH70_CRAGI 6-phosphogluconate dehydrogenase, decarboxylating |
| 47 | A | K1PH66_CRAGI Fibrinolytic enzyme, isozyme C |
| 48 | A | K1PTY5_CRAGI Protocadherin Fat 4 |
| 49 | A | K1Q114_CRAGI 40S ribosomal protein S3a |
| 50 | A | K1QBN0_CRAGI Methylcrotonoyl-CoA carboxylase beta chain, mitochondrial |
| 51 | A | K1QMD3_CRAGI Glycerol-3-phosphate dehydrogenase [NAD(+)] |
| 52 | A | K1QVN9_CRAGI T-complex protein 1 subunit eta |
| 53 | A | K1RN77_CRAGI Nuclear autoantigenic sperm protein |
| 54 | A | K1QSQ9_CRAGI Putative ATP-dependent RNA helicase an3 |
| 55 | A | K1RI55_CRAGI Insulin-like growth factor 2 mRNA-binding protein 3 |
| 56 | A | K1S1S1_CRAGI Insulin-like growth factor 2 mRNA-binding protein 1 |
| 57 | A | K1PH76_CRAGI Y-box factor-like protein (Fragment) |
| 58 | A | K1QWP8_CRAGI Actin-2 |
| 59 | A | K1R252_CRAGI Putative methylmalonate-semialdehyde dehydrogenase [acylating], mitochondrial |
| 60 | A | K1QEA6_CRAGI Phosphoenolpyruvate carboxykinase [GTP] |
| | A | K1RNB5_CRAGI Propionyl-CoA carboxylase beta chain, mitochondrial |
| | A | K1RJH5_CRAGI Polyadenylate-binding protein |

| | | |
|----|---|---|
| 1 | | |
| 2 | | |
| 3 | A | K1PLY1_CRAGI DNA polymerase |
| 4 | A | K1R5U4_CRAGI Acetyl-CoA carboxylase 1 |
| 5 | A | K1PF10_CRAGI PAN2-PAN3 deadenylation complex catalytic subunit PAN2 |
| 6 | A | K1QBR5_CRAGI Uncharacterized protein |
| 7 | A | K1QVS3_CRAGI Thimet oligopeptidase |
| 8 | A | K1RFT1_CRAGI Band 4.1-like protein 3 |
| 9 | A | K1R2V1_CRAGI Importin subunit beta-1 |
| 10 | A | K1RW85_CRAGI Adenosylhomocysteinase |
| 11 | A | K1QWT8_CRAGI Uncharacterized protein |
| 12 | A | K1PFG1_CRAGI Uncharacterized protein |
| 13 | A | K1QWX2_CRAGI 60S acidic ribosomal protein P0 |
| 14 | A | K1R1M7_CRAGI Ubiquitin-like modifier-activating enzyme 1 |
| 15 | A | K1QK11_CRAGI Dynein heavy chain 7, axonemal |
| 16 | A | K1RWW5_CRAGI ATP synthase subunit beta |
| 17 | A | K1RJ97_CRAGI Multifunctional protein ADE2 |
| 18 | A | K1RWD4_CRAGI Actin, cytoplasmic |
| 19 | A | K1R3V0_CRAGI CAD protein |
| 20 | A | K1QHA2_CRAGI Spectrin beta chain, brain 4 |
| 21 | A | K1REG6_CRAGI DNA helicase |
| 22 | A | K1R4I2_CRAGI 26S proteasome non-ATPase regulatory subunit 3 |
| 23 | A | K1RTR1_CRAGI ATP-citrate synthase |
| 24 | A | K1QGK2_CRAGI Coatomer subunit beta |
| 25 | A | K1Q9Z6_CRAGI 26S proteasome non-ATPase regulatory subunit 7 |
| 26 | A | K1QQL6_CRAGI Leucyl-tRNA synthetase, cytoplasmic |
| 27 | A | K1Q330_CRAGI Dihydrolipoyl dehydrogenase |
| 28 | A | K1QUE6_CRAGI 26S proteasome non-ATPase regulatory subunit 6 |
| 29 | A | K1QY12_CRAGI Dynamin-1-like protein |
| 30 | A | K1Q3S7_CRAGI Cytosolic carboxypeptidase 1 |
| 31 | A | K1RSZ6_CRAGI 40S ribosomal protein S7 |
| 32 | A | K1PJF4_CRAGI Isoleucyl-tRNA synthetase, cytoplasmic |
| 33 | A | K1Q9V3_CRAGI V-type proton ATPase catalytic subunit A |
| 34 | A | K1RBC9_CRAGI Transketolase-like protein 2 |
| 35 | A | K1PPP8_CRAGI Vigilin |
| 36 | A | K1PX47_CRAGI Ubiquitin carboxyl-terminal hydrolase |
| 37 | A | K1QX26_CRAGI Endoplasmic |
| 38 | A | K1PZP6_CRAGI Coatomer subunit gamma |
| 39 | A | K1QE71_CRAGI DNA helicase |
| 40 | A | K1QBH0_CRAGI Uncharacterized protein |
| 41 | A | K1QCC1_CRAGI Phosphoglycerate kinase |
| 42 | A | K1PJP9_CRAGI 26S proteasome non-ATPase regulatory subunit 1 |
| 43 | A | K1QIR8_CRAGI 78 kDa glucose-regulated protein |
| 44 | A | K1Q4I9_CRAGI D-3-phosphoglycerate dehydrogenase (Fragment) |
| 45 | A | K1RNZ6_CRAGI Eukaryotic translation initiation factor 3 subunit D |
| 46 | A | K1R3V8_CRAGI COP9 signalosome complex subunit 4 |
| 47 | A | K1PUL2_CRAGI Long-chain-fatty-acid--CoA ligase 1 |
| 48 | A | K1QHX2_CRAGI La-related protein 7 |
| 49 | A | K1QDN1_CRAGI Heat shock protein 75 kDa, mitochondrial (Fragment) |
| 50 | A | K1PZF2_CRAGI Exportin-7 |
| 51 | A | K1PMT6_CRAGI Heterogeneous nuclear ribonucleoprotein U-like protein 1 |
| 52 | A | K1RCW5_CRAGI Eukaryotic translation initiation factor 4 gamma 3 |
| 53 | A | K1R7I9_CRAGI Heterogeneous nuclear ribonucleoprotein Q |
| 54 | A | K1QYB6_CRAGI Delta-1-pyrroline-5-carboxylate synthetase |
| 55 | A | K1P3Q5_CRAGI Programmed cell death 6-interacting protein |
| 56 | A | K1Q2H5_CRAGI Uncharacterized protein |
| 57 | A | K1QBF7_CRAGI Hypoxia up-regulated protein 1 |
| 58 | A | K1PW06_CRAGI Filamin-C |
| 59 | A | K1QHS8_CRAGI Ribonucleoside-diphosphate reductase |
| 60 | A | K1RL00_CRAGI Proteasome-associated protein ECM29-like protein |
| | A | K1QQ16_CRAGI AP complex subunit beta |
| | A | K1R4R9_CRAGI Mitotic apparatus protein p62 |

| | | |
|----|---|--|
| 1 | | |
| 2 | | |
| 3 | A | K1QXH3_CRAGI Translational activator GCN1 |
| 4 | A | K1P5D4_CRAGI Cysteine synthase |
| 5 | A | K1RM80_CRAGI Citrate synthase |
| 6 | A | K1PVH5_CRAGI Centromere/kinetochore protein zw10-like protein |
| 7 | A | K1QQ27_CRAGI Pancreatic lipase-related protein 2 |
| 8 | A | K1QMX8_CRAGI DNA replication licensing factor MCM7 |
| 9 | A | K1QK56_CRAGI Uncharacterized protein |
| 10 | A | K1QMB9_CRAGI Eukaryotic translation initiation factor 3 subunit A |
| 11 | A | K1R0W4_CRAGI Signal recognition particle subunit SRP72 |
| 12 | A | K1QLT5_CRAGI 26S protease regulatory subunit 4 |
| 13 | A | K1QSR2_CRAGI Apoptosis inhibitor 5 |
| 14 | A | K1QKA9_CRAGI Piwi-like protein 2 |
| 15 | A | K1RJM8_CRAGI SAGA-associated factor 11 homolog |
| 16 | A | K1QQB6_CRAGI 40S ribosomal protein S14 |
| 17 | A | K1PE57_CRAGI Severin |
| 18 | A | K1PKK7_CRAGI AP-2 complex subunit mu-1 |
| 19 | A | K1QXS6_CRAGI Heterogeneous nuclear ribonucleoprotein A2-like protein 1 |
| 20 | A | K1R5F2_CRAGI 14-3-3 protein epsilon |
| 21 | A | K1Q4V0_CRAGI Myosin-VIIa |
| 22 | A | K1QA50_CRAGI V-type proton ATPase subunit H |
| 23 | A | K1QWK2_CRAGI MAM domain-containing glycosylphosphatidylinositol anchor protein 2 |
| 24 | A | K1PV49_CRAGI RuvB-like helicase |
| 25 | A | K1QAB1_CRAGI AP-2 complex subunit alpha |
| 26 | A | K1RK33_CRAGI Exportin-1 |
| 27 | A | K1PCS4_CRAGI Eukaryotic translation initiation factor 2 subunit 3, Y-linked |
| 28 | A | K1RSA6_CRAGI Methylcrotonoyl-CoA carboxylase subunit alpha, mitochondrial |
| 29 | A | K1PI02_CRAGI Talin-1 |
| 30 | A | K1PNP4_CRAGI 26S proteasome non-ATPase regulatory subunit 11 |
| 31 | A | K1RAL0_CRAGI Aspartate aminotransferase, cytoplasmic |
| 32 | A | K1QXQ8_CRAGI DNA helicase |
| 33 | A | K1QI28_CRAGI V-type proton ATPase subunit B |
| 34 | A | K1Q9K6_CRAGI Histone H3 |
| 35 | A | K1S151_CRAGI Rab GDP dissociation inhibitor |
| 36 | A | K1P2G0_CRAGI Strawberry notch-like protein 1 |
| 37 | A | K1QI97_CRAGI Adenylyl cyclase-associated protein |
| 38 | A | K1QBW6_CRAGI Tudor domain-containing protein 1 |
| 39 | A | K1PEP0_CRAGI 40S ribosomal protein S8 |
| 40 | A | K1QG84_CRAGI THO complex subunit 2 |
| 41 | A | K1PJM2_CRAGI Histone H2A |
| 42 | A | K1PU26_CRAGI Malate dehydrogenase (Fragment) |
| 43 | A | A7M7T7_CRAGI Non-selenium glutathione peroxidase |
| 44 | A | K1PWW9_CRAGI 26S proteasome non-ATPase regulatory subunit 3 |
| 45 | A | K1QF01_CRAGI 40S ribosomal protein S4 |
| 46 | A | K1QZW0_CRAGI Polyadenylate-binding protein 2 |
| 47 | A | K1RAU3_CRAGI DNA ligase |
| 48 | A | K1PVW0_CRAGI S-adenosylmethionine synthase |
| 49 | A | K1QBL6_CRAGI Tudor domain-containing protein 1 |
| 50 | A | K1QE32_CRAGI Very long-chain specific acyl-CoA dehydrogenase, mitochondrial |
| 51 | A | K1PY73_CRAGI Basic leucine zipper and W2 domain-containing protein 1 |
| 52 | A | K1S2Y0_CRAGI Uncharacterized protein |
| 53 | A | K1QEF2_CRAGI ADP-ribosylation factor-like protein 15 |
| 54 | A | K1PV79_CRAGI Importin subunit alpha |
| 55 | A | K1R083_CRAGI Aspartate aminotransferase, mitochondrial |
| 56 | A | K1QMH2_CRAGI DNA polymerase |
| 57 | A | K1QL67_CRAGI 60S ribosomal protein L7a |
| 58 | A | K1QDV6_CRAGI Protein argonaute-2 |
| 59 | A | K1QU53_CRAGI NAD(P) transhydrogenase, mitochondrial |
| 60 | A | K1RIZ9_CRAGI Band 4.1-like protein 5 |
| | A | K1R2Q9_CRAGI Aspartate aminotransferase |
| | A | K1Q4E1_CRAGI N-acetyl-D-glucosamine kinase |

| | | |
|----|---|---|
| 1 | | |
| 2 | | |
| 3 | A | K1R916_CRAGI Structural maintenance of chromosomes protein |
| 4 | A | K1R2N0_CRAGI Histone H4 |
| 5 | A | K1P7K8_CRAGI Vesicle-fusing ATPase 1 |
| 6 | A | K1PJC1_CRAGI Adipophilin |
| 7 | A | K1QVR0_CRAGI 26S proteasome non-ATPase regulatory subunit 8 |
| 8 | A | K1Q6X5_CRAGI Protein disulfide-isomerase |
| 9 | A | K1Q6X5_CRAGI Protein disulfide-isomerase |
| 10 | A | K1QGB4_CRAGI 40S ribosomal protein S17 |
| 11 | A | K1QT21_CRAGI Putative ATP-dependent RNA helicase DDX5 |
| 12 | A | K1Q7Q2_CRAGI CCAAT/enhancer-binding protein zeta |
| 13 | A | K1Q6W3_CRAGI Talin-1 |
| 14 | A | K1R4D4_CRAGI 40S ribosomal protein SA |
| 15 | A | K1R4D4_CRAGI 40S ribosomal protein SA |
| 16 | A | K1QH70_CRAGI Leucine-rich repeat-containing protein 40 |
| 17 | A | K1Q880_CRAGI Transportin-1 |
| 18 | A | K1PS71_CRAGI Uncharacterized protein |
| 19 | A | K1PAY7_CRAGI Propionyl-CoA carboxylase alpha chain, mitochondrial |
| 20 | A | K1PAY7_CRAGI Propionyl-CoA carboxylase alpha chain, mitochondrial |
| 21 | A | K1QPP2_CRAGI Elongation factor Tu, mitochondrial |
| 22 | A | K1PX23_CRAGI Eukaryotic peptide chain release factor subunit 1 |
| 23 | A | K1QRG9_CRAGI Uncharacterized protein |
| 24 | A | K1PIB7_CRAGI Phenylalanyl-tRNA synthetase beta chain |
| 25 | A | K1R115_CRAGI Succinate dehydrogenase [ubiquinone] flavoprotein subunit, mitochondrial |
| 26 | A | K1R115_CRAGI Succinate dehydrogenase [ubiquinone] flavoprotein subunit, mitochondrial |
| 27 | A | K1PF96_CRAGI Spliceosome RNA helicase BAT1 |
| 28 | A | K1QFN1_CRAGI 60S ribosomal protein L23 |
| 29 | A | K1R0D7_CRAGI Eukaryotic translation initiation factor 3 subunit M (Fragment) |
| 30 | A | K1R0D7_CRAGI Eukaryotic translation initiation factor 3 subunit M (Fragment) |
| 31 | A | K1PK93_CRAGI GDP-L-fucose synthetase |
| 32 | A | K1R2D6_CRAGI Plastin-3 |
| 33 | A | K1Q358_CRAGI 60S acidic ribosomal protein P2 |
| 34 | A | K1QMV7_CRAGI V-type proton ATPase subunit D |
| 35 | A | K1R953_CRAGI Acetyl-CoA carboxylase |
| 36 | A | K1PPQ1_CRAGI 14-3-3 protein gamma |
| 37 | A | K1PPQ1_CRAGI 14-3-3 protein gamma |
| 38 | A | K1QYV6_CRAGI NMDA receptor-regulated protein 1 |
| 39 | A | K1PH31_CRAGI Protein arginine N-methyltransferase 1 |
| 40 | A | K1RDV7_CRAGI Cell division control protein 2-like protein (Fragment) |
| 41 | A | K1PBZ4_CRAGI Regulator of nonsense transcripts 1 |
| 42 | A | K1PD57_CRAGI Constitutive coactivator of PPAR-gamma-like protein 1-like protein |
| 43 | A | K1PD57_CRAGI Constitutive coactivator of PPAR-gamma-like protein 1-like protein |
| 44 | A | K1PVZ3_CRAGI Cold shock domain-containing protein E1 |
| 45 | A | K1PLA7_CRAGI Eukaryotic initiation factor 4A-II (Fragment) |
| 46 | A | K1Q1S3_CRAGI Myosin-VI |
| 47 | A | K1QY85_CRAGI Transport protein Sec31A |
| 48 | A | K1QH74_CRAGI Splicing factor, arginine/serine-rich 1 |
| 49 | A | K1RB97_CRAGI Kinetochores-associated protein 1 |
| 50 | A | K1RB97_CRAGI Kinetochores-associated protein 1 |
| 51 | A | K1REC3_CRAGI Exportin-5 |
| 52 | A | K1R3T3_CRAGI Transcription factor BTF3 |
| 53 | A | K1Q9J5_CRAGI Importin-4 |
| 54 | A | K1Q0R4_CRAGI ATP-binding cassette sub-family F member 2 |
| 55 | A | K1Q0R4_CRAGI ATP-binding cassette sub-family F member 2 |
| 56 | A | K1QD40_CRAGI Importin-7 |
| 57 | A | K1R5B9_CRAGI DNA-directed RNA polymerase, mitochondrial |
| 58 | A | K1PD30_CRAGI Putative histone-binding protein Caf1 |
| 59 | A | K1QRW4_CRAGI Coronin |
| 60 | A | K1RDG4_CRAGI DNA helicase |
| | A | K1QHY1_CRAGI Eosinophil peroxidase |
| | A | K1QLS3_CRAGI Cytochrome b-c1 complex subunit 2, mitochondrial |
| | A | K1Q5G9_CRAGI SUMO-activating enzyme subunit 2 |
| | A | K1QED7_CRAGI Replication protein A subunit |
| | A | K1S3Y1_CRAGI 2-amino-3-ketobutyrate coenzyme A ligase, mitochondrial (Fragment) |
| | A | K1PGW7_CRAGI Transmembrane protein 2 |
| | A | K1R7N6_CRAGI Eukaryotic translation initiation factor 6 |
| | A | K1QRL6_CRAGI Methenyltetrahydrofolate synthetase domain-containing protein |
| | A | K1PN10_CRAGI Intron-binding protein aquarius |
| | A | K1QNT7_CRAGI Aldehyde dehydrogenase, mitochondrial |
| | A | K1QLZ1_CRAGI Actin-related protein 3 |

| | | |
|----|---|---|
| 1 | | |
| 2 | | |
| 3 | A | K1R9T2_CRAGI Eukaryotic translation initiation factor 3 subunit B |
| 4 | A | K1PS27_CRAGI DNA helicase |
| 5 | A | K1Q5G6_CRAGI 60 kDa heat shock protein, mitochondrial |
| 6 | A | K1QRM1_CRAGI Nuclear pore protein |
| 7 | A | K1QGC9_CRAGI Acetyl-coenzyme A synthetase |
| 8 | A | K1RLT4_CRAGI Signal recognition particle subunit SRP68 |
| 9 | A | K1PAR4_CRAGI Unc-45-like protein A |
| 10 | A | K1QVE8_CRAGI Phosphoacetylglucosamine mutase |
| 11 | A | K1Q4Z4_CRAGI Bifunctional purine biosynthesis protein PURH |
| 12 | A | K1P8W6_CRAGI 60S ribosomal protein L4 |
| 13 | A | K1P8W6_CRAGI 60S ribosomal protein L4 |
| 14 | A | K1P8W6_CRAGI 60S ribosomal protein L4 |
| 15 | A | K1QQK1_CRAGI 26S proteasome non-ATPase regulatory subunit 12 |
| 16 | A | K1RIT6_CRAGI NADH-ubiquinone oxidoreductase 75 kDa subunit, mitochondrial |
| 17 | A | K1R2L7_CRAGI Glutaminyl-tRNA synthetase (Fragment) |
| 18 | A | K1QRQ2_CRAGI Glutamate dehydrogenase 1, mitochondrial |
| 19 | A | K1RKZ5_CRAGI DNA damage-binding protein 1 |
| 20 | A | K1QC10_CRAGI GTP-binding protein 1 |
| 21 | A | K1QC10_CRAGI GTP-binding protein 1 |
| 22 | A | K1PGZ0_CRAGI Thyroid adenoma-associated protein |
| 23 | A | K1QUK0_CRAGI NEDD8-activating enzyme E1 catalytic subunit |
| 24 | A | K1QQP1_CRAGI Programmed cell death protein 4 |
| 25 | A | K1PM50_CRAGI 40S ribosomal protein S16 |
| 26 | A | K1PJS7_CRAGI Poly [ADP-ribose] polymerase |
| 27 | A | K1PJS7_CRAGI Poly [ADP-ribose] polymerase |
| 28 | A | K1QX37_CRAGI Enolase |
| 29 | A | K1QCA7_CRAGI Valyl-tRNA synthetase |
| 30 | A | K1Q811_CRAGI Alpha-centractin |
| 31 | A | K1Q811_CRAGI Alpha-centractin |
| 32 | A | K1QRZ3_CRAGI 40S ribosomal protein S13 |
| 33 | A | K1QG70_CRAGI Katanin p60 ATPase-containing subunit A1 |
| 34 | A | K1QW36_CRAGI 60S ribosomal protein L6 |
| 35 | A | K1R8S7_CRAGI Phospholipase A-2-activating protein |
| 36 | A | K1P9N7_CRAGI 14-3-3 protein zeta |
| 37 | A | K1P9N7_CRAGI 14-3-3 protein zeta |
| 38 | A | K1PG07_CRAGI Lupus La-like protein |
| 39 | A | K1QFZ8_CRAGI Ceramide kinase-like protein |
| 40 | A | K1Q1Q9_CRAGI Alpha-amino adipic semialdehyde synthase, mitochondrial |
| 41 | A | K1PX83_CRAGI Dynein heavy chain 5, axonemal |
| 42 | A | K1PCV0_CRAGI Severin |
| 43 | A | K1QP17_CRAGI Caprin-1 |
| 44 | A | K1QP17_CRAGI Caprin-1 |
| 45 | A | K1PS13_CRAGI Coatomer subunit beta (Fragment) |
| 46 | A | K1Q273_CRAGI 60S ribosomal protein L14 |
| 47 | A | K1PBU0_CRAGI L-fucose kinase |
| 48 | A | K1QVV5_CRAGI Periostin |
| 49 | A | K1P112_CRAGI ATP synthase subunit gamma, mitochondrial |
| 50 | A | K1P112_CRAGI ATP synthase subunit gamma, mitochondrial |
| 51 | A | K1QKN4_CRAGI Dynein heavy chain 6, axonemal |
| 52 | A | K1P2B8_CRAGI GDP-mannose 4,6 dehydratase |
| 53 | A | K1QC11_CRAGI AP-1 complex subunit gamma |
| 54 | A | K1QPD6_CRAGI Ubiquitin conjugation factor E4 B |
| 55 | A | K1QPD6_CRAGI Ubiquitin conjugation factor E4 B |
| 56 | A | K1QWZ0_CRAGI Tetratricopeptide repeat protein 38 |
| 57 | A | K1QKF8_CRAGI S-(hydroxymethyl)glutathione dehydrogenase |
| 58 | A | K1RD83_CRAGI Serine hydroxymethyltransferase |
| 59 | A | K1R1F0_CRAGI ATP-dependent DNA helicase 2 subunit 1 |
| 60 | A | K1QMD8_CRAGI Proteasome subunit alpha type |
| | A | K1Q8S0_CRAGI Nucleolar complex protein 3 homolog |
| | A | K1PI50_CRAGI 40S ribosomal protein S26 |
| | A | K1R8T6_CRAGI Cullin-1 |
| | A | K1P6F0_CRAGI HEAT repeat-containing protein 2 |
| | A | K1PXG6_CRAGI Serine/threonine-protein phosphatase |
| | A | K1QG65_CRAGI rRNA 2'-O-methyltransferase fibrillarin |
| | A | K1R5W3_CRAGI Uncharacterized protein |
| | A | K1QB60_CRAGI Uncharacterized protein |
| | A | K1R5D5_CRAGI U3 small nucleolar RNA-associated protein 6-like protein |
| | A | K1REJ2_CRAGI Lon protease homolog, mitochondrial |
| | A | K1PLD4_CRAGI Dynein heavy chain 2, axonemal |

| | | |
|----|---|--|
| 1 | | |
| 2 | | |
| 3 | A | K1QPC6_CRAGI Nucleolar complex protein 2-like protein |
| 4 | A | K1PQZ3_CRAGI Armadillo repeat-containing protein 4 |
| 5 | A | K1Q6F7_CRAGI V-type proton ATPase subunit C |
| 6 | A | K1RPF7_CRAGI 60S ribosomal protein L5 |
| 7 | A | K1QHQ6_CRAGI Acyl-CoA dehydrogenase family member 9, mitochondrial |
| 8 | A | K1PFS5_CRAGI Elongation factor 1-gamma |
| 9 | A | K1PPW8_CRAGI Coatomer subunit beta |
| 10 | A | K1QGE4_CRAGI Proteasome endopeptidase complex (Fragment) |
| 11 | A | K1QDX9_CRAGI Ribosome biogenesis protein BMS1-like protein |
| 12 | A | K1Q8K2_CRAGI Importin subunit alpha |
| 13 | A | K1Q8K2_CRAGI Importin subunit alpha |
| 14 | A | K1Q8K2_CRAGI Importin subunit alpha |
| 15 | A | K1Q8K2_CRAGI Importin subunit alpha |
| 16 | A | K1Q8K2_CRAGI Importin subunit alpha |
| 17 | A | K1Q8K2_CRAGI Importin subunit alpha |
| 18 | A | K1Q8K2_CRAGI Importin subunit alpha |
| 19 | A | K1Q8K2_CRAGI Importin subunit alpha |
| 20 | A | K1Q8K2_CRAGI Importin subunit alpha |
| 21 | A | K1Q8K2_CRAGI Importin subunit alpha |
| 22 | A | K1Q8K2_CRAGI Importin subunit alpha |
| 23 | A | K1Q8K2_CRAGI Importin subunit alpha |
| 24 | A | K1Q8K2_CRAGI Importin subunit alpha |
| 25 | A | K1Q8K2_CRAGI Importin subunit alpha |
| 26 | A | K1Q8K2_CRAGI Importin subunit alpha |
| 27 | A | K1Q8K2_CRAGI Importin subunit alpha |
| 28 | A | K1Q8K2_CRAGI Importin subunit alpha |
| 29 | A | K1Q8K2_CRAGI Importin subunit alpha |
| 30 | A | K1Q8K2_CRAGI Importin subunit alpha |
| 31 | A | K1Q8K2_CRAGI Importin subunit alpha |
| 32 | A | K1Q8K2_CRAGI Importin subunit alpha |
| 33 | A | K1Q8K2_CRAGI Importin subunit alpha |
| 34 | A | K1Q8K2_CRAGI Importin subunit alpha |
| 35 | A | K1Q8K2_CRAGI Importin subunit alpha |
| 36 | A | K1Q8K2_CRAGI Importin subunit alpha |
| 37 | A | K1Q8K2_CRAGI Importin subunit alpha |
| 38 | A | K1Q8K2_CRAGI Importin subunit alpha |
| 39 | A | K1Q8K2_CRAGI Importin subunit alpha |
| 40 | A | K1Q8K2_CRAGI Importin subunit alpha |
| 41 | A | K1Q8K2_CRAGI Importin subunit alpha |
| 42 | A | K1Q8K2_CRAGI Importin subunit alpha |
| 43 | A | K1Q8K2_CRAGI Importin subunit alpha |
| 44 | A | K1Q8K2_CRAGI Importin subunit alpha |
| 45 | A | K1Q8K2_CRAGI Importin subunit alpha |
| 46 | A | K1Q8K2_CRAGI Importin subunit alpha |
| 47 | A | K1Q8K2_CRAGI Importin subunit alpha |
| 48 | A | K1Q8K2_CRAGI Importin subunit alpha |
| 49 | A | K1Q8K2_CRAGI Importin subunit alpha |
| 50 | A | K1Q8K2_CRAGI Importin subunit alpha |
| 51 | A | K1Q8K2_CRAGI Importin subunit alpha |
| 52 | A | K1Q8K2_CRAGI Importin subunit alpha |
| 53 | A | K1Q8K2_CRAGI Importin subunit alpha |
| 54 | A | K1Q8K2_CRAGI Importin subunit alpha |
| 55 | A | K1Q8K2_CRAGI Importin subunit alpha |
| 56 | A | K1Q8K2_CRAGI Importin subunit alpha |
| 57 | A | K1Q8K2_CRAGI Importin subunit alpha |
| 58 | A | K1Q8K2_CRAGI Importin subunit alpha |
| 59 | A | K1Q8K2_CRAGI Importin subunit alpha |
| 60 | A | K1Q8K2_CRAGI Importin subunit alpha |
| | A | K1R3I6_CRAGI Nucleolar complex protein 2-like protein (Fragment) |
| | A | K1QJF7_CRAGI Coronin |
| | A | K1PKF5_CRAGI Protein-glutamine gamma-glutamyltransferase 4 |
| | A | K1R266_CRAGI Retinal dehydrogenase 1 |
| | A | K1Q3F9_CRAGI Armadillo repeat-containing protein 8 |
| | A | K1QSZ6_CRAGI Uncharacterized protein |
| | A | K1P8B7_CRAGI Ubiquitin-conjugating enzyme E2-17 kDa (Fragment) |
| | A | K1QLK8_CRAGI GTP-binding protein SAR1b |
| | A | K1QF31_CRAGI Serine/threonine-protein kinase PLK |
| | A | K1RKC1_CRAGI Far upstream element-binding protein 3 |
| | A | K1PHE1_CRAGI Putative ubiquitin carboxyl-terminal hydrolase FAF-X |
| | A | K1QOL1_CRAGI 60S ribosomal protein L23a |

| | | |
|----|---|---|
| 1 | | |
| 2 | | |
| 3 | A | K1R008_CRAGI Proteasome subunit alpha type |
| 4 | A | K1QBG8_CRAGI Proteasome subunit beta type-4 |
| 5 | A | K1R8B2_CRAGI Isovaleryl-CoA dehydrogenase, mitochondrial |
| 6 | A | K1RNN9_CRAGI Cytoskeleton-associated protein 5 |
| 7 | A | K1QYG7_CRAGI Glucosamine--fructose-6-phosphate aminotransferase [isomerizing] 1 |
| 8 | A | K1PFK8_CRAGI Uncharacterized protein |
| 9 | A | K1PRD5_CRAGI Trifunctional purine biosynthetic protein adenosine-3 |
| 10 | A | K1PBH3_CRAGI Dynein heavy chain 3, axonemal |
| 11 | A | K1QVK0_CRAGI Transaldolase |
| 12 | A | K1PAM6_CRAGI Uncharacterized protein |
| 13 | A | K1Q948_CRAGI Alpha-1,4 glucan phosphorylase |
| 14 | A | K1RGG1_CRAGI Alanyl-tRNA synthetase, cytoplasmic |
| 15 | A | K1Q9P5_CRAGI Mitochondrial-processing peptidase subunit beta |
| 16 | A | K1QTE3_CRAGI ATP-binding cassette sub-family F member 1 |
| 17 | A | K1PZ08_CRAGI Ras-related protein Rab-7a |
| 18 | A | K1RGJ7_CRAGI Neogenin |
| 19 | A | K1RK68_CRAGI Uncharacterized protein |
| 20 | A | K1QEF9_CRAGI Protein-glutamine gamma-glutamyltransferase K |
| 21 | A | K1RHB2_CRAGI Nucleolar RNA helicase 2 |
| 22 | A | K1QAF3_CRAGI Alanine aminotransferase 2 |
| 23 | A | K1PB94_CRAGI ATP-binding cassette sub-family E member 1 |
| 24 | A | K1R488_CRAGI Actin-related protein 2/3 complex subunit |
| 25 | A | K1QC65_CRAGI DNA polymerase alpha subunit B |
| 26 | A | K1PCR9_CRAGI Proteasome endopeptidase complex |
| 27 | A | K1RFU6_CRAGI Proteasome activator complex subunit 3 |
| 28 | A | K1R9R5_CRAGI Proteasome subunit alpha type |
| 29 | A | K1PRQ5_CRAGI Ubiquitin-like modifier-activating enzyme 1 |
| 30 | A | K1Q1L4_CRAGI Uncharacterized protein |
| 31 | A | K1Q982_CRAGI Malignant fibrous histiocytoma-amplified sequence 1 |
| 32 | A | K1PKF6_CRAGI 26S proteasome non-ATPase regulatory subunit 13 |
| 33 | A | K1QBT2_CRAGI Proteasome subunit beta |
| 34 | A | K1P5Z3_CRAGI Lysosomal aspartic protease |
| 35 | A | K1P7L9_CRAGI Nucleolar GTP-binding protein 1 |
| 36 | A | K1Q9M7_CRAGI Histone H1-delta |
| 37 | A | K1PS84_CRAGI Alpha-crystallin B chain |
| 38 | A | K1R6C2_CRAGI Peroxisomal 3,2-trans-enoyl-CoA isomerase |
| 39 | A | K1PZC0_CRAGI Structural maintenance of chromosomes protein |
| 40 | A | K1PMJ9_CRAGI Cleavage stimulation factor 77 kDa subunit |
| 41 | A | K1R4M7_CRAGI Serine/threonine protein phosphatase 2A regulatory subunit |
| 42 | A | K1S3G2_CRAGI HMGB1 |
| 43 | A | K1PB82_CRAGI Electron transfer flavoprotein subunit beta |
| 44 | A | K1PWP4_CRAGI Phenylalanyl-tRNA synthetase alpha chain |
| 45 | A | K1QNS4_CRAGI DnaJ-like protein subfamily C member 9 |
| 46 | A | K1Q7E4_CRAGI Ubiquitin-conjugating enzyme E2 N |
| 47 | A | K1R6F1_CRAGI Proteasome subunit alpha type |
| 48 | A | K1Q667_CRAGI tRNA-splicing ligase RtcB homolog |
| 49 | A | K1QWC3_CRAGI 40S ribosomal protein S3 |
| 50 | A | K1RAH6_CRAGI Ubiquitin-conjugating enzyme E2-17 kDa |
| 51 | A | K1RIM7_CRAGI Methionine aminopeptidase 2 |
| 52 | A | K1PXS8_CRAGI Calreticulin |
| 53 | A | K1RIG6_CRAGI LSM14-like protein A |
| 54 | A | K1R168_CRAGI Dynein heavy chain 2, axonemal |
| 55 | A | K1R591_CRAGI Inter-alpha-trypsin inhibitor heavy chain H4 |
| 56 | A | K1QK11_CRAGI Tudor domain-containing protein 1 |
| 57 | A | K1RNB6_CRAGI Alpha-aminoadipic semialdehyde dehydrogenase |
| 58 | A | K1ROY9_CRAGI ADP,ATP carrier protein |
| 59 | A | K1QE83_CRAGI CCR4-NOT transcription complex subunit 1 |
| 60 | A | K1QFR9_CRAGI Spectrin beta chain |
| | A | K1RAP8_CRAGI Malic enzyme |
| | A | K1PK49_CRAGI Myosin-Ic |

| | | |
|----|---|---|
| 1 | | |
| 2 | | |
| 3 | A | K1QAH9_CRAGI H/ACA ribonucleoprotein complex subunit |
| 4 | A | K1PYR4_CRAGI 26S proteasome non-ATPase regulatory subunit 1 |
| 5 | A | K1R8C6_CRAGI 40S ribosomal protein S12 |
| 6 | A | K1PY89_CRAGI Extracellular superoxide dismutase [Cu-Zn] |
| 7 | A | K1Q662_CRAGI Actin-interacting protein 1 |
| 8 | A | K1Q4G7_CRAGI Tubulin gamma chain |
| 9 | A | K1R472_CRAGI Synaptobrevin-like protein YKT6 |
| 10 | A | K1PS69_CRAGI Importin-9 |
| 11 | A | K1QDU9_CRAGI 3-phosphoinositide-dependent protein kinase 1 |
| 12 | A | K1PFU5_CRAGI Ubiquitin-conjugating enzyme E2 C |
| 13 | A | K1QKG8_CRAGI Upstream activation factor subunit spp27 |
| 14 | A | K1ROP8_CRAGI CTP synthase |
| 15 | A | K1QZX9_CRAGI Uncharacterized protein |
| 16 | A | K1QTD9_CRAGI Nucleolar protein 56 |
| 17 | A | K1PIP8_CRAGI Proteasome subunit beta |
| 18 | A | K1RBF6_CRAGI Uncharacterized protein yfeX |
| 19 | A | K1PW99_CRAGI Protein OSCP1 |
| 20 | A | K1PWB9_CRAGI EH domain-containing protein 1 |
| 21 | A | K1PU46_CRAGI Lethal(2) giant larvae-like protein 1 |
| 22 | A | K1QYH6_CRAGI COP9 signalosome complex subunit 3 |
| 23 | A | K1Q611_CRAGI Ubiquitin-conjugating enzyme E2 L3 |
| 24 | A | K1PF60_CRAGI 3-ketoacyl-CoA thiolase, mitochondrial |
| 25 | A | K1PQD4_CRAGI Phosphoglucomutase-1 |
| 26 | A | K1PSNO_CRAGI Pre-mRNA-processing factor 40-like protein A |
| 27 | A | K1R834_CRAGI 60S ribosomal protein L9 |
| 28 | A | K1RBU9_CRAGI Non-specific serine/threonine protein kinase |
| 29 | A | K1QHM2_CRAGI Dolichyl-diphosphooligosaccharide--protein glycosyltransferase subunit 2 |
| 30 | A | K1QW73_CRAGI Glycoprotein 3-alpha-L-fucosyltransferase A |
| 31 | A | K1Q7X3_CRAGI Pre-mRNA-splicing factor SYF1 |
| 32 | A | K1PUJ1_CRAGI Radixin |
| 33 | A | K1R818_CRAGI Acetyltransferase component of pyruvate dehydrogenase complex |
| 34 | A | K1PRL4_CRAGI 60S ribosomal protein L38 (Fragment) |
| 35 | A | K1Q0G7_CRAGI Developmentally-regulated GTP-binding protein 2 |
| 36 | A | K1PBN1_CRAGI Phospholipase |
| 37 | A | K1QJ33_CRAGI Aminoacyl tRNA synthetase complex-interacting multifunctional protein 2 |
| 38 | A | A5LGH1_CRAGI Voltage-dependent anion channel |
| 39 | A | K1PUV4_CRAGI 40S ribosomal protein S24 |
| 40 | A | K1QJE9_CRAGI Uncharacterized protein |
| 41 | A | K1R005_CRAGI Filamin-C (Fragment) |
| 42 | A | K1RGB7_CRAGI Epidermal retinal dehydrogenase 2 |
| 43 | A | K1PPJ6_CRAGI Nicotinamide phosphoribosyltransferase |
| 44 | A | K1PEW1_CRAGI Sorting nexin |
| 45 | A | K1QDH9_CRAGI Myosin-11 |
| 46 | A | K1QPJ9_CRAGI Serine/threonine-protein phosphatase 2A 55 kDa regulatory subunit B |
| 47 | A | K1R9S5_CRAGI Cytosolic Fe-S cluster assembly factor NUBP2 homolog |
| 48 | A | K1PTV1_CRAGI Splicing factor 3B subunit 4 |
| 49 | A | K1Q5H6_CRAGI FACT complex subunit SSRP1 |
| 50 | A | K1RN05_CRAGI Transportin-3 |
| 51 | A | K1PDE4_CRAGI Protein arginine N-methyltransferase |
| 52 | A | K1Q9G3_CRAGI Isocitrate dehydrogenase [NAD] subunit, mitochondrial |
| 53 | A | K1R2H9_CRAGI WD repeat-containing protein 35 |
| 54 | A | K1PA61_CRAGI Actin-like protein 6A |
| 55 | A | K1QQT2_CRAGI Uncharacterized protein y4x0 |
| 56 | A | K1PJG8_CRAGI Timeless-like protein |
| 57 | A | K1QJM1_CRAGI 60S ribosomal protein L30 |
| 58 | A | K1QK68_CRAGI Myosin-2 essential light chain |
| 59 | A | K1R517_CRAGI Superkiller viralicidic activity 2-like 2 |
| 60 | A | K1Q6V6_CRAGI Replication factor C subunit 4 |
| | A | K1Q888_CRAGI Translin |
| | A | K1QQC1_CRAGI Dynein light chain roadblock |

| | | |
|----|---|--|
| 1 | | |
| 2 | | |
| 3 | A | K1Q1F4_CRAGI 60S ribosomal protein L3 (Fragment) |
| 4 | A | K1Q2E0_CRAGI AP-1 complex subunit mu-1 |
| 5 | A | K1Q155_CRAGI THO complex subunit 1 |
| 6 | A | K1R3M4_CRAGI Ubiquitin-like modifier-activating enzyme 1 |
| 7 | A | K1PML4_CRAGI Pre-mRNA-processing factor 39 |
| 8 | A | K1QEK7_CRAGI Ubiquitin carboxyl-terminal hydrolase |
| 9 | A | K1QDI4_CRAGI Superoxide dismutase [Cu-Zn] |
| 10 | A | K1Q1Z3_CRAGI Seryl-tRNA synthetase, cytoplasmic |
| 11 | A | K1Q4X8_CRAGI DNA mismatch repair protein Msh2 |
| 12 | A | K1Q4X8_CRAGI DNA mismatch repair protein Msh2 |
| 13 | A | K1P5F7_CRAGI Metastasis-associated protein MTA1 |
| 14 | A | K1R7J6_CRAGI Putative sodium/potassium-transporting ATPase subunit beta-2 |
| 15 | A | K1R7J6_CRAGI Putative sodium/potassium-transporting ATPase subunit beta-2 |
| 16 | A | K1QNY7_CRAGI Transport protein Sec24C |
| 17 | A | K1QKQ5_CRAGI N-terminal acetyltransferase B complex subunit MDM20 |
| 18 | A | K1PH10_CRAGI Polyadenylate-binding protein-interacting protein 1 |
| 19 | A | K1Q329_CRAGI Pyruvate dehydrogenase E1 component subunit beta, mitochondrial |
| 20 | A | K1Q329_CRAGI Pyruvate dehydrogenase E1 component subunit beta, mitochondrial |
| 21 | A | K1QI08_CRAGI Ribose-phosphate pyrophosphokinase 1 |
| 22 | A | K1QV87_CRAGI Catenin alpha-2 |
| 23 | A | K1PXD4_CRAGI Putative ATP-dependent RNA helicase DDX6 |
| 24 | A | K1QCQ5_CRAGI Succinate--CoA ligase [ADP-forming] subunit beta, mitochondrial |
| 25 | A | K1QCQ5_CRAGI Succinate--CoA ligase [ADP-forming] subunit beta, mitochondrial |
| 26 | A | K1QCL6_CRAGI Proteasomal ubiquitin receptor ADRM1 |
| 27 | A | K1PFV9_CRAGI 4-trimethylaminobutyraldehyde dehydrogenase |
| 28 | A | K1PTR3_CRAGI Oxysterol-binding protein |
| 29 | A | K1R1T8_CRAGI Nucleolar protein 56 |
| 30 | A | K1QUC6_CRAGI Uncharacterized protein |
| 31 | A | K1QUC6_CRAGI Uncharacterized protein |
| 32 | A | K1QCM0_CRAGI Rho GDP-dissociation inhibitor 1 |
| 33 | A | K1QNZ3_CRAGI Serine/threonine-protein phosphatase |
| 34 | A | K1QKG9_CRAGI Cysteine desulfurase, mitochondrial |
| 35 | A | K1RUW0_CRAGI E3 SUMO-protein ligase RanBP2 |
| 36 | A | K1QPZ1_CRAGI Actin-related protein 2/3 complex subunit 3 |
| 37 | A | K1QHT0_CRAGI Deoxyuridine 5'-triphosphate nucleotidohydrolase, mitochondrial |
| 38 | A | K1QHT0_CRAGI Deoxyuridine 5'-triphosphate nucleotidohydrolase, mitochondrial |
| 39 | A | K1Q5I4_CRAGI COP9 signalosome complex subunit 2 |
| 40 | A | K1PLW6_CRAGI Bifunctional purine biosynthesis protein PURH |
| 41 | A | K1PWU5_CRAGI Cytosolic carboxypeptidase 1 |
| 42 | A | K1P9S7_CRAGI Brix domain-containing protein 2 |
| 43 | A | K1P9S7_CRAGI Brix domain-containing protein 2 |
| 44 | A | K1Q260_CRAGI Nucleolar protein 58 |
| 45 | A | K1PKL8_CRAGI Serine/threonine-protein phosphatase 2A 56 kDa regulatory subunit alpha isoform |
| 46 | A | K1S1X3_CRAGI SWI/SNF-related matrix-associated actin-dependent regulator of chromatin subfamily A member 5 |
| 47 | A | K1Q3F4_CRAGI Inorganic pyrophosphatase |
| 48 | A | K1P7J8_CRAGI 6-phosphofructokinase |
| 49 | A | K1QXR6_CRAGI Protein farnesyltransferase/geranylgeranyltransferase type-1 subunit alpha |
| 50 | A | K1QXR6_CRAGI Protein farnesyltransferase/geranylgeranyltransferase type-1 subunit alpha |
| 51 | A | K1Q4Q8_CRAGI Pyruvate dehydrogenase E1 component subunit alpha, somatic form, mitochondrial |
| 52 | A | K1RA63_CRAGI Transmembrane protein 2 |
| 53 | A | K1Q8T3_CRAGI Importin subunit alpha |
| 54 | A | K1QMT1_CRAGI DnaJ-like protein subfamily B member 4 |
| 55 | A | K1RBT5_CRAGI Ran GTPase-activating protein 1 |
| 56 | A | K1RBT5_CRAGI Ran GTPase-activating protein 1 |
| 57 | A | K1PST9_CRAGI Brefeldin A-inhibited guanine nucleotide-exchange protein 1 |
| 58 | A | K1QWJ4_CRAGI Splicing factor 3B subunit 5 |
| 59 | A | K1QYT7_CRAGI COP9 signalosome complex subunit 7a |
| 60 | A | K1R7D7_CRAGI Poly(A)-specific ribonuclease PARN |
| | A | K1QZI3_CRAGI Myosin-1e |
| | A | K1PNX0_CRAGI Methionyl-tRNA synthetase, cytoplasmic |
| | A | K1Q324_CRAGI Heterogeneous nuclear ribonucleoprotein K |
| | A | K1QY71_CRAGI Histone H2B |
| | A | K1QDA7_CRAGI Uracil phosphoribosyltransferase |
| | A | K1RAU8_CRAGI Eukaryotic translation initiation factor 3 subunit E |
| | A | K1QRD0_CRAGI Cytoplasmic dynein 1 light intermediate chain 1 |
| | A | K1Q719_CRAGI Serine/threonine-protein kinase OSR1 |
| | A | K1RJJ7_CRAGI Histone H5 |
| | A | K1P8Y3_CRAGI Sulfotransferase 1C4 |
| | A | K1QMY1_CRAGI Aconitate hydratase, mitochondrial |

| | | |
|----|---|---|
| 1 | | |
| 2 | | |
| 3 | A | K1RBI9_CRAGI Small nuclear ribonucleoprotein Sm D2 |
| 4 | A | K1QEJ0_CRAGI Ras GTPase-activating protein-binding protein 2 |
| 5 | A | K1Q5Z6_CRAGI Eukaryotic translation initiation factor 2 subunit 2 |
| 6 | A | K1RGS1_CRAGI WD repeat-containing protein 19 |
| 7 | A | K1R195_CRAGI Protein DJ-1 |
| 8 | A | K1R8Y1_CRAGI Obg-like ATPase 1 |
| 10 | A | K1RRH1_CRAGI Chromodomain-helicase-DNA-binding protein Mi-2-like protein |
| 11 | A | K1PM66_CRAGI 60S ribosomal protein L12 |
| 12 | A | K1PKQ3_CRAGI Uncharacterized protein |
| 13 | A | K1QIB2_CRAGI Mitogen-activated protein kinase |
| 14 | A | K1PSN4_CRAGI Tetratricopeptide repeat protein 39C |
| 15 | A | K1PT09_CRAGI Uncharacterized protein |
| 17 | A | K1S0I4_CRAGI Methylthioribose-1-phosphate isomerase |
| 18 | A | K1Q9I1_CRAGI TRAF2 and NCK-interacting protein kinase |
| 19 | A | K1R5G4_CRAGI 60S ribosomal protein L31 |
| 20 | A | K1R7F6_CRAGI Cystathionine gamma-lyase |
| 21 | A | K1QGP1_CRAGI Replication factor C subunit 2 |
| 22 | A | K1Q4S7_CRAGI Calreticulin |
| 23 | A | K1RTQ6_CRAGI Fructose-bisphosphate aldolase |
| 24 | A | K1QN79_CRAGI 40S ribosomal protein S11 |
| 25 | A | K1R6E9_CRAGI Dihydrolipoamide acetyltransferase component of pyruvate dehydrogenase complex |
| 26 | A | K1PXU6_CRAGI 60S ribosomal protein L24 |
| 27 | A | K1PVA0_CRAGI Cullin-5 |
| 28 | A | K1QSZ4_CRAGI Serine--pyruvate aminotransferase |
| 29 | A | K1RNH1_CRAGI 60S ribosomal protein L18 (Fragment) |
| 30 | A | K1PIH2_CRAGI V-type proton ATPase subunit E |
| 31 | A | K1QG08_CRAGI Phosphatidylinositol-binding clathrin assembly protein LAP |
| 32 | A | K1RVR1_CRAGI Telomerase protein component 1 |
| 33 | A | K1Q9D7_CRAGI Sorting nexin-2 |
| 34 | A | K1PDC6_CRAGI Proteasome subunit beta |
| 35 | A | K1R1E2_CRAGI Arp2/3 complex 34 kDa subunit |
| 36 | A | K1PCR5_CRAGI KH domain-containing, RNA-binding, signal transduction-associated protein 2 |
| 37 | A | K1P8S5_CRAGI Condensin complex subunit 3 |
| 38 | A | K1PCH8_CRAGI Nucleoporin p54 |
| 39 | A | K1QY58_CRAGI Eukaryotic translation initiation factor 3 subunit I (Fragment) |
| 40 | A | K1Q947_CRAGI Dynein light chain |
| 41 | A | K1Q615_CRAGI Peroxiredoxin-1 |
| 42 | A | K1QC78_CRAGI Ras-related protein Rab-14 |
| 43 | A | K1QET6_CRAGI Neurobeachin |
| 44 | A | K1PG48_CRAGI Dynein-1-beta heavy chain, flagellar inner arm I1 complex |
| 45 | A | K1R9P5_CRAGI Mitochondrial import receptor subunit TOM70 |
| 46 | A | K1PGV8_CRAGI Nucleoprotein TPR |
| 47 | A | K1PRV7_CRAGI Profilin |
| 48 | A | K1QIZ7_CRAGI Programmed cell death protein 6 |
| 49 | A | K1Q4U7_CRAGI AP-3 complex subunit delta-1 |
| 50 | A | K1QGL9_CRAGI Mannose-1-phosphate guanyltransferase beta |
| 51 | A | K1PBL2_CRAGI Eukaryotic initiation factor 4A-III |
| 52 | A | K1R3A0_CRAGI Transcription initiation factor IIB |
| 53 | A | K1P7Q2_CRAGI Elongation factor 1-gamma |
| 54 | A | K1PNU2_CRAGI Histone-arginine methyltransferase CARM1 |
| 55 | A | K1PWP8_CRAGI Echinoderm microtubule-associated protein-like 1 |
| 56 | A | K1QV46_CRAGI Tetratricopeptide repeat protein 21B |
| 57 | A | K1QKQ9_CRAGI Dynein heavy chain 7, axonemal |
| 58 | A | K1PR47_CRAGI Eukaryotic translation initiation factor 2A |
| 59 | A | K1S058_CRAGI Transcription factor RFX3 |
| 60 | A | K1QEG3_CRAGI Heat shock 70 kDa protein 12B |
| | A | K1R481_CRAGI Epimerase family protein SDR39U1 |
| | A | K1QBF3_CRAGI Trpc4-associated protein |
| | A | K1PUX5_CRAGI Casein kinase II subunit alpha |
| | A | K1QK98_CRAGI IST1-like protein |

| | | |
|----|---|---|
| 1 | | |
| 2 | | |
| 3 | A | K1RDV2_CRAGI Myotrophin-like protein |
| 4 | A | K1PDL3_CRAGI Ribosomal protein L19 |
| 5 | A | K1S2S8_CRAGI Signal recognition particle 54 kDa protein |
| 6 | A | K1QZ11_CRAGI Geranylgeranyl transferase type-2 subunit alpha |
| 7 | A | K1QU47_CRAGI Dual oxidase 2 |
| 8 | A | K1QXF9_CRAGI Acyl-protein thioesterase 2 |
| 9 | A | K1PL64_CRAGI Poly(A) polymerase gamma |
| 10 | A | K1RQJ6_CRAGI Enhancer of mRNA-decapping protein 4 |
| 11 | A | K1QLP5_CRAGI Coatomer subunit delta |
| 12 | A | K1PJB0_CRAGI Heat shock protein 70 B2 |
| 13 | A | K1Q404_CRAGI DNA topoisomerase 2 |
| 14 | A | K1QJA7_CRAGI Histone chaperone asf1-B |
| 15 | A | K1RP91_CRAGI Putative RNA exonuclease NEF-sp |
| 16 | A | K1PZD9_CRAGI 26S proteasome non-ATPase regulatory subunit 11 |
| 17 | A | K1QI32_CRAGI Synaptotagmin-like protein 5 |
| 18 | A | K1RK83_CRAGI Tyrosine-protein kinase BAZ1B |
| 19 | A | K1QQG2_CRAGI ATP-dependent RNA helicase DHX8 |
| 20 | A | K1PUQ5_CRAGI Histone H2B |
| 21 | A | K1QW72_CRAGI Catalase |
| 22 | A | K1R2U8_CRAGI Universal stress protein A-like protein |
| 23 | A | K1PY30_CRAGI Septin-2 |
| 24 | A | K1Q8C5_CRAGI Putative ATP-dependent RNA helicase DDX47 |
| 25 | A | K1QNP9_CRAGI Putative deoxyribose-phosphate aldolase |
| 26 | A | K1PDF0_CRAGI Protein disulfide-isomerase A6 |
| 27 | A | K1R1R9_CRAGI Pre-mRNA-processing factor 6 |
| 28 | A | K1Q3G8_CRAGI Chaperone activity of bc1 complex-like, mitochondrial |
| 29 | A | K1QBH4_CRAGI ATP-dependent RNA helicase DDX42 |
| 30 | A | K1PEM0_CRAGI Ubiquitin-like modifier-activating enzyme 5 |
| 31 | A | K1QD23_CRAGI Acetyl-CoA acetyltransferase B, mitochondrial |
| 32 | A | K1RJ96_CRAGI Sphere organelles protein SPH-1 |
| 33 | A | K1R1B1_CRAGI 35 kDa SR repressor protein |
| 34 | A | K1QCB0_CRAGI 40S ribosomal protein S5 |
| 35 | A | K1RGZ8_CRAGI Wings apart-like protein |
| 36 | A | K1Q107_CRAGI Histidine triad nucleotide-binding protein 1 |
| 37 | A | K1QYM1_CRAGI Thymidylate synthase |
| 38 | A | K1QYT5_CRAGI Phosphate carrier protein, mitochondrial |
| 39 | A | K1QJT3_CRAGI COP9 signalosome complex subunit 1 |
| 40 | A | K1QAU8_CRAGI Peptidyl-prolyl cis-trans isomerase E |
| 41 | A | K1RG28_CRAGI Kinase C and casein kinase substrate in neurons protein 2 |
| 42 | A | K1R2S4_CRAGI NEDD8-activating enzyme E1 regulatory subunit (Fragment) |
| 43 | A | K1Q4Y8_CRAGI Histone H1oo |
| 44 | A | K1PYQ1_CRAGI Protein phosphatase 1 regulatory subunit 7 |
| 45 | A | K1RWE5_CRAGI Thioredoxin-like protein 1 |
| 46 | A | K1QJL2_CRAGI CCR4-NOT transcription complex subunit 10 |
| 47 | A | K1P6C4_CRAGI Poly [ADP-ribose] polymerase |
| 48 | A | K1PNL0_CRAGI Microtubule-associated protein futsch |
| 49 | A | K1QSA2_CRAGI Short-chain specific acyl-CoA dehydrogenase, mitochondrial |
| 50 | A | K1QU30_CRAGI MON2-like protein |
| 51 | A | K1Q317_CRAGI Serine/threonine-protein kinase SRPK1 |
| 52 | A | K1RGE2_CRAGI Prostaglandin reductase 1 |
| 53 | A | K1RIB1_CRAGI Arginyl-tRNA synthetase, cytoplasmic |
| 54 | A | K1ROW0_CRAGI Ferritin |
| 55 | A | K1P8T5_CRAGI Glycerol-3-phosphate dehydrogenase [NAD(+)] |
| 56 | A | K1QQD8_CRAGI Putative ATP-dependent RNA helicase DDX43 |
| 57 | A | K1QMH5_CRAGI Small nuclear ribonucleoprotein Sm D1 |
| 58 | A | K1QS22_CRAGI UPF0160 protein MYG1, mitochondrial (Fragment) |
| 59 | A | K1QHP8_CRAGI Uncharacterized protein |
| 60 | A | K1PXM3_CRAGI Chromatin assembly factor 1 subunit A |
| | A | K1QF45_CRAGI Alpha-tocopherol transfer-like protein |
| | A | K1QC27_CRAGI Hydroxysteroid dehydrogenase-like protein 2 |

| | | |
|----|---|--|
| 1 | | |
| 2 | | |
| 3 | A | Q70MT4_CRAGI 40S ribosomal protein S10 |
| 4 | A | K1PQB4_CRAGI Acyl-CoA dehydrogenase family member 10 |
| 5 | A | K1PZI3_CRAGI SWI/SNF complex subunit SMARCC2 |
| 6 | A | K1PNS2_CRAGI 33 kDa inner dynein arm light chain, axonemal |
| 7 | A | K1RG36_CRAGI Phosphoribosylformylglycinamide synthase (Fragment) |
| 8 | A | K1R366_CRAGI Putative exonuclease mut-7-like protein |
| 9 | A | K1QMQ0_CRAGI Putative exonuclease mut-7-like protein |
| 10 | A | K1QD80_CRAGI Protein quaking-B |
| 11 | A | K1ROM2_CRAGI Uncharacterized protein |
| 12 | A | K1QKI4_CRAGI Lysine--tRNA ligase |
| 13 | A | K1PPH6_CRAGI Kelch domain-containing protein 8B |
| 14 | A | K1QBE2_CRAGI Syntaxin-5 |
| 15 | A | K1RHP3_CRAGI Proliferation-associated protein 2G4 |
| 16 | A | K1PZU1_CRAGI Hsc70-interacting protein |
| 17 | A | K1RMW3_CRAGI Protein kinase C |
| 18 | A | K1R1Q8_CRAGI Ras-related protein Rab-5C |
| 19 | A | K1PPK1_CRAGI Actin-related protein 2/3 complex subunit 4 |
| 20 | A | K1R8Y9_CRAGI Translin-associated protein X |
| 21 | A | K1QW41_CRAGI Leucine-zipper-like transcriptional regulator 1 |
| 22 | A | K1Q1G2_CRAGI Elongator complex protein 1 |
| 23 | A | K1RA79_CRAGI E3 ubiquitin-protein ligase HECTD1 |
| 24 | A | K1RZM3_CRAGI Cartilage acidic protein 1 |
| 25 | A | K1QD81_CRAGI Ubiquitin conjugation factor E4 A |
| 26 | A | K1PMY9_CRAGI Calmodulin |
| 27 | A | K1RU04_CRAGI Actin, cytoplasmic |
| 28 | A | K1QND2_CRAGI Septin-2 |
| 29 | A | K1PR25_CRAGI Regulator of differentiation 1 |
| 30 | A | K1QV25_CRAGI Transcription elongation factor B polypeptide 2 |
| 31 | A | K1RJ70_CRAGI Cytosolic non-specific dipeptidase |
| 32 | A | K1R751_CRAGI Nuclear pore complex protein Nup88 |
| 33 | A | K1QDK0_CRAGI Engulfment and cell motility protein 2 |
| 34 | A | K1PLV6_CRAGI F-actin-capping protein subunit alpha |
| 35 | A | K1QWN2_CRAGI Elongation factor 1-delta |
| 36 | A | K1RRP7_CRAGI Uncharacterized protein |
| 37 | A | K1R6H7_CRAGI Uncharacterized protein |
| 38 | A | K1REP0_CRAGI Uncharacterized protein |
| 39 | A | K1R0L4_CRAGI Sodium/potassium-transporting ATPase subunit alpha |
| 40 | A | K1R0V5_CRAGI Cell differentiation protein RCD1-like protein |
| 41 | A | K1R2N1_CRAGI Glutathione reductase |
| 42 | A | K1PRB6_CRAGI Apolipoprotein D |
| 43 | A | K1QMF1_CRAGI Isocitrate dehydrogenase [NAD] subunit gamma, mitochondrial |
| 44 | A | K1R5E7_CRAGI Cathepsin L |
| 45 | A | K1PMI0_CRAGI Charged multivesicular body protein 4b |
| 46 | A | K1QZN3_CRAGI Myosin-IId |
| 47 | A | K1S0N3_CRAGI Glutamate receptor-interacting protein 1 |
| 48 | A | K1RDM2_CRAGI 60S ribosomal protein L18a |
| 49 | A | K1R0R7_CRAGI Putative ATP-dependent RNA helicase DHX36 |
| 50 | A | K1QWX0_CRAGI 26S proteasome non-ATPase regulatory subunit 14 |
| 51 | A | K1PQA3_CRAGI Pseudouridylate synthase 7-like protein |
| 52 | A | K1Q7K0_CRAGI Putative serine carboxypeptidase CPVL |
| 53 | A | K1R7N8_CRAGI Proteasome endopeptidase complex |
| 54 | A | K1QCL7_CRAGI Uncharacterized protein |
| 55 | A | K1QQB3_CRAGI Glycyl-tRNA synthetase |
| 56 | A | K1RFU8_CRAGI High mobility group protein DSP1 |
| 57 | A | K1PJW0_CRAGI Talin-1 |
| 58 | A | K1RBJ3_CRAGI DnaJ-like protein subfamily C member 13 |
| 59 | A | K1PRV2_CRAGI Threonine synthase-like 1 |
| 60 | A | K1R347_CRAGI Tetratricopeptide repeat protein 38 |
| | A | K1S422_CRAGI Katanin p80 WD40 repeat-containing subunit B1 |
| | A | K1QK18_CRAGI Cytochrome b5 |
| | A | K1QJU3_CRAGI Cell division cycle protein 20-like protein |

| | | |
|----|---|---|
| 1 | | |
| 2 | | |
| 3 | A | K1QRM9_CRAGI Acidic leucine-rich nuclear phosphoprotein 32 family member A |
| 4 | A | K1R373_CRAGI ATP-binding cassette sub-family F member 3 |
| 5 | A | K1RE81_CRAGI Transport protein Sec24B |
| 6 | A | K1QW21_CRAGI 39S ribosomal protein L40, mitochondrial |
| 7 | A | K1PLG1_CRAGI Putative ribosomal RNA methyltransferase NOP2 |
| 8 | A | K1R712_CRAGI Transforming growth factor-beta receptor-associated protein 1 |
| 9 | A | K1R712_CRAGI Transforming growth factor-beta receptor-associated protein 1 |
| 10 | A | K1Q1K8_CRAGI Elongation factor 1-beta |
| 11 | A | K1PNK5_CRAGI Ras GTPase-activating-like protein IQGAP1 |
| 12 | A | K1Q1F1_CRAGI Serine/threonine-protein kinase 31 |
| 13 | A | K1QFS4_CRAGI Actin-related protein 2 |
| 14 | A | K1PUK3_CRAGI Armadillo repeat-containing protein 6 |
| 15 | A | K1PI41_CRAGI Flap endonuclease 1 |
| 16 | A | K1PI41_CRAGI Flap endonuclease 1 |
| 17 | A | K1QU96_CRAGI Pre-rRNA-processing protein TSR1-like protein |
| 18 | A | K1QFK8_CRAGI Target of Myb protein 1 |
| 19 | A | K1R4Q3_CRAGI Spectrin beta chain, brain 1 |
| 20 | A | K1R4Q3_CRAGI Spectrin beta chain, brain 1 |
| 21 | A | K1QMS7_CRAGI Malonyl CoA-acyl carrier protein transacylase, mitochondrial |
| 22 | A | K1P8Q1_CRAGI Putative methyltransferase TARBP1 |
| 23 | A | K1RXV8_CRAGI PAT1-like protein 1 |
| 24 | A | K1PXH5_CRAGI Putative saccharopine dehydrogenase |
| 25 | A | K1PXH5_CRAGI Putative saccharopine dehydrogenase |
| 26 | A | K1QWP1_CRAGI Nucleoporin seh1 |
| 27 | A | K1RDF6_CRAGI Long-chain specific acyl-CoA dehydrogenase, mitochondrial |
| 28 | A | K1QYH5_CRAGI Ubiquitin carboxyl-terminal hydrolase 14 |
| 29 | A | K1S0J9_CRAGI Uncharacterized protein |
| 30 | A | K1R247_CRAGI Condensin complex subunit 1 |
| 31 | A | K1R247_CRAGI Condensin complex subunit 1 |
| 32 | A | K1QKZ6_CRAGI Inosine-5'-monophosphate dehydrogenase |
| 33 | A | K1QQ48_CRAGI Serine/threonine-protein kinase N2 |
| 34 | A | K1RIZ3_CRAGI Bone morphogenetic protein 7 |
| 35 | A | K1PVQ8_CRAGI Eukaryotic translation initiation factor 3 subunit K |
| 36 | A | K1QMQ1_CRAGI TBC1 domain family member 10B |
| 37 | A | K1QMQ1_CRAGI TBC1 domain family member 10B |
| 38 | A | K1QFF0_CRAGI Vacuolar protein sorting-associated protein 35 (Fragment) |
| 39 | A | K1Q435_CRAGI Eukaryotic translation initiation factor 2 subunit 1 |
| 40 | A | K1Q435_CRAGI Eukaryotic translation initiation factor 2 subunit 1 |
| 41 | A | K1QNZ7_CRAGI Ubiquilin-1 |
| 42 | A | K1QYI6_CRAGI Cullin-3-B |
| 43 | A | K1PFV4_CRAGI Eukaryotic translation initiation factor 4E |
| 44 | A | K1QVV1_CRAGI Ribose-5-phosphate isomerase |
| 45 | A | K1RT39_CRAGI Glutaredoxin-3 |
| 46 | A | K1PNG7_CRAGI Sorting nexin-33 |
| 47 | A | K1PYK7_CRAGI RNA-binding protein 39 |
| 48 | A | K1QCP3_CRAGI Crooked neck-like protein 1 |
| 49 | A | K1QSV4_CRAGI RNA helicase |
| 50 | A | K1QSV4_CRAGI RNA helicase |
| 51 | A | K1R811_CRAGI Ribonucleoside-diphosphate reductase small chain |
| 52 | A | K1R944_CRAGI Tetratricopeptide repeat protein 37 |
| 53 | A | K1QS07_CRAGI Proteasome subunit beta type-3 |
| 54 | A | K1PZV3_CRAGI Guanine nucleotide-binding protein-like 3-like protein (Fragment) |
| 55 | A | K1PZV3_CRAGI Guanine nucleotide-binding protein-like 3-like protein (Fragment) |
| 56 | A | K1QNU0_CRAGI Non-specific serine/threonine protein kinase |
| 57 | A | K1R3R4_CRAGI Cytosolic Fe-S cluster assembly factor NUBP1 homolog |
| 58 | A | K1R3R4_CRAGI Cytosolic Fe-S cluster assembly factor NUBP1 homolog |
| 59 | A | K1RJS5_CRAGI Uncharacterized protein |
| 60 | A | K1RNK8_CRAGI Rho GTPase-activating protein 17 |
| | A | K1RG79_CRAGI Neuronal acetylcholine receptor subunit alpha-6 |
| | A | K1QVF8_CRAGI Uncharacterized protein in QAH/OAS sulfhydrylase 3'region (Fragment) |
| | A | K1Q4C3_CRAGI Fumarylacetoacetase |
| | A | K1R7T0_CRAGI GMP synthase [glutamine-hydrolyzing] |
| | A | K1QX22_CRAGI 4-hydroxyphenylpyruvate dioxygenase |
| | A | K1RIS2_CRAGI 3-oxoacyl-[acyl-carrier-protein] reductase |
| | A | K1Q407_CRAGI Ras GTPase-activating protein 1 |
| | A | K1R9I0_CRAGI Myosin-VIIa |
| | A | K1Q0N9_CRAGI Uncharacterized protein |
| | A | K1PUE8_CRAGI Serine/threonine-protein phosphatase 4 regulatory subunit 3 |
| | A | K1PSY2_CRAGI Fragile X mental retardation syndrome-related protein 1 |
| | A | K1RA35_CRAGI Splicing factor, arginine/serine-rich 7 |

| | | |
|----|---|---|
| 1 | | |
| 2 | | |
| 3 | A | K1QW39_CRAGI Neurobeachin |
| 4 | A | K1QJ19_CRAGI Importin-13 |
| 5 | A | K1R3M6_CRAGI Ubiquitin-conjugating enzyme E2-22 kDa |
| 6 | A | K1RCR8_CRAGI Carbonyl reductase [NADPH] 1 |
| 7 | A | K1RJW8_CRAGI Protein DEK |
| 8 | A | K1R2G9_CRAGI SEC13-like protein |
| 9 | A | K1PLF8_CRAGI Diacylglycerol kinase |
| 10 | A | K1PWV7_CRAGI Uncharacterized protein |
| 11 | A | K1R3W9_CRAGI Replication protein A 14 kDa subunit |
| 12 | A | K1P8G1_CRAGI Heterogeneous nuclear ribonucleoprotein H |
| 13 | A | K1R2S2_CRAGI Peptidylprolyl isomerase |
| 14 | A | K1PNY5_CRAGI Splicing factor, proline-and glutamine-rich |
| 15 | A | K1P7Q6_CRAGI 40S ribosomal protein S19 |
| 16 | A | K1PZN1_CRAGI Calcium/calmodulin-dependent protein kinase type II delta chain |
| 17 | A | K1PBC0_CRAGI Non-neuronal cytoplasmic intermediate filament protein |
| 18 | A | K1QNN9_CRAGI MICOS complex subunit MIC60 |
| 19 | A | K1QJ46_CRAGI Putative methylcrotonoyl-CoA carboxylase beta chain, mitochondrial |
| 20 | A | K1R2G7_CRAGI Ran-binding protein 3 |
| 21 | A | K1RJG6_CRAGI Heterogeneous nuclear ribonucleoprotein 27C |
| 22 | A | K1QZ58_CRAGI Splicing factor U2AF 26 kDa subunit |
| 23 | A | K1QCU0_CRAGI Eukaryotic translation initiation factor 3 subunit G |
| 24 | A | K1PH25_CRAGI Methionyl-tRNA synthetase, cytoplasmic |
| 25 | A | K1RN97_CRAGI Hemagglutinin/amebocyte aggregation factor |
| 26 | A | K1Q6M6_CRAGI 6-phosphofructokinase |
| 27 | A | K1PPL6_CRAGI Malonyl-CoA decarboxylase, mitochondrial |
| 28 | A | K1R9Q4_CRAGI Uncharacterized protein |
| 29 | A | K1QPX8_CRAGI Alkyl/aryl-sulfatase BDS1 |
| 30 | A | K1PJP2_CRAGI Putative pre-mRNA-splicing factor ATP-dependent RNA helicase DHX15 |
| 31 | A | K1RRZ9_CRAGI MKI67 FHA domain-interacting nucleolar phosphoprotein-like protein |
| 32 | A | K1S6R2_CRAGI N-acetyltransferase 11 |
| 33 | A | K1PJY4_CRAGI Calcium-binding protein 39 |
| 34 | A | K1Q1G9_CRAGI Putative ATP-dependent RNA helicase DHX37 |
| 35 | A | K1RA95_CRAGI Filamin-A |
| 36 | A | K1Q865_CRAGI Trafficking protein particle complex subunit 4 |
| 37 | A | K1RFQ4_CRAGI Tetratricopeptide repeat protein 27 |
| 38 | A | K1QRD4_CRAGI S-formylglutathione hydrolase |
| 39 | A | K1Q9Z4_CRAGI Aldehyde dehydrogenase |
| 40 | A | K1QB76_CRAGI Uncharacterized protein |
| 41 | A | K1Q2Y1_CRAGI 40S ribosomal protein S15 |
| 42 | A | K1S3Q9_CRAGI MAK16-like protein (Fragment) |
| 43 | A | K1RAF8_CRAGI Uncharacterized protein |
| 44 | A | K1QE44_CRAGI UPF0663 transmembrane protein C17orf28 |
| 45 | A | K1PN44_CRAGI Casein kinase II subunit beta |
| 46 | A | K1PWR4_CRAGI Signal recognition particle receptor subunit alpha |
| 47 | A | K1QDS1_CRAGI 3-hydroxyacyl-CoA dehydrogenase type-2 |
| 48 | A | K1R924_CRAGI RNA-binding protein 45 |
| 49 | A | K1QWZ6_CRAGI Dolichyl-diphosphooligosaccharide--protein glycosyltransferase subunit 1 |
| 50 | A | K1PSH2_CRAGI 28S ribosomal protein S12, mitochondrial |
| 51 | A | K1QKL1_CRAGI DNA-directed RNA polymerases I, II, and III subunit RPABC3 |
| 52 | A | K1RCY7_CRAGI Eukaryotic peptide chain release factor GTP-binding subunit ERF3B |
| 53 | A | K1Q6U7_CRAGI 78 kDa glucose-regulated protein |
| 54 | A | K1R2E8_CRAGI Prolyl endopeptidase |
| 55 | A | K1R4M1_CRAGI Intraflagellar transport protein 52-like protein |
| 56 | A | K1RB91_CRAGI Neutral alpha-glucosidase AB |
| 57 | A | K1Q056_CRAGI Calpain-A |
| 58 | A | K1REW8_CRAGI Ribosomal protein L15 |
| 59 | A | K1QQQ5_CRAGI Replication factor C subunit 5 |
| 60 | A | K1QLC6_CRAGI JmjC domain-containing protein 8 |
| | A | K1QFP5_CRAGI NADH dehydrogenase [ubiquinone] flavoprotein 1, mitochondrial |
| | A | K1Q7H0_CRAGI ATP-dependent DNA helicase II subunit 2 |

| | | |
|----|---|---|
| 1 | | |
| 2 | | |
| 3 | A | K1PYW7_CRAGI CDK5 regulatory subunit-associated protein 3 |
| 4 | A | K1QVD0_CRAGI Small nuclear ribonucleoprotein Sm D3 |
| 5 | A | K1QAT9_CRAGI ATP-dependent RNA helicase DDX1 |
| 6 | A | K1R920_CRAGI Eukaryotic translation initiation factor 1A, X-chromosomal |
| 7 | A | K1QQG7_CRAGI DNA-directed RNA polymerase subunit |
| 8 | A | K1R0T1_CRAGI V-type proton ATPase subunit G |
| 9 | A | K1PD36_CRAGI Ubiquitin |
| 10 | A | K1QHI2_CRAGI Heterogeneous nuclear ribonucleoprotein L |
| 11 | A | K1RED7_CRAGI Poly(RC)-binding protein 3 |
| 12 | A | K1QRE1_CRAGI COP9 signalosome complex subunit 6 |
| 13 | A | K1QHS9_CRAGI Tubulin polyglutamylase TTLL13 |
| 14 | A | K1R6Y8_CRAGI Uncharacterized protein |
| 15 | A | K1RC37_CRAGI Uncharacterized protein |
| 16 | A | K1PBG6_CRAGI Uncharacterized protein |
| 17 | A | K1R150_CRAGI Ras-related protein Rab-1A |
| 18 | A | K1QVS0_CRAGI Ras-like GTP-binding protein Rho1 |
| 19 | A | K1R716_CRAGI Putative isovaleryl-CoA dehydrogenase |
| 20 | A | K1Q1I3_CRAGI Ornithine aminotransferase |
| 21 | A | K1Q151_CRAGI 60S ribosomal protein L32 |
| 22 | A | K1QMY8_CRAGI Dedicator of cytokinesis protein 9 |
| 23 | A | K1PR93_CRAGI 3-hydroxyisobutyrate dehydrogenase |
| 24 | A | K1QZX3_CRAGI Vacuolar protein sorting-associated protein VTA1-like protein |
| 25 | A | K1Q3W3_CRAGI NADH dehydrogenase [ubiquinone] iron-sulfur protein 3, mitochondrial |
| 26 | A | K1RHA5_CRAGI Nucleoside diphosphate kinase |
| 27 | A | K1RG61_CRAGI Cytosolic carboxypeptidase 2 |
| 28 | A | K1RSK5_CRAGI Kelch-like protein 6 |
| 29 | A | K1Q105_CRAGI Ferrochelatase |
| 30 | A | K1QCS7_CRAGI Leucine-rich repeat-containing protein 16A |
| 31 | A | K1PWR0_CRAGI Protein SET |
| 32 | A | K1RIA0_CRAGI Molybdopterin molybdenumtransferase |
| 33 | A | K1RC43_CRAGI U4/U6 small nuclear ribonucleoprotein Prp31 |
| 34 | A | K1S185_CRAGI Counting factor associated protein D |
| 35 | A | K1PFL3_CRAGI Dihydropteridine reductase |
| 36 | A | K1QIU2_CRAGI Putative tRNA (cytidine(32)/guanosine(34)-2'-O)-methyltransferase |
| 37 | A | K1S6H7_CRAGI Vacuolar protein sorting-associated protein 13C |
| 38 | A | K1QMM4_CRAGI Leucine zipper transcription factor-like protein 1 |
| 39 | A | K1PEX5_CRAGI Protein hu-li tai shao |
| 40 | A | K1PUM5_CRAGI Cytoplasmic aconitate hydratase |
| 41 | A | K1QE49_CRAGI DnaJ-like protein subfamily A member 1 |
| 42 | A | K1QGF1_CRAGI Splicing factor 3B subunit 2 |
| 43 | A | K1P8Z2_CRAGI Histidyl-tRNA synthetase, cytoplasmic |
| 44 | A | K1QFN2_CRAGI Uncharacterized protein |
| 45 | A | K1QI48_CRAGI Inositol hexakisphosphate and diphosphoinositol-pentakisphosphate kinase |
| 46 | A | K1PZ93_CRAGI Dihydropyrimidine dehydrogenase [NADP(+)] |
| 47 | A | K1QN99_CRAGI Regulator of nonsense transcripts 2 |
| 48 | A | K1QXX2_CRAGI Ubiquitin-conjugating enzyme E2 Q2 |
| 49 | A | K1Q6U0_CRAGI Coatamer subunit zeta-1 |
| 50 | A | K1P8F1_CRAGI Uncharacterized protein |
| 51 | A | K1RTD6_CRAGI UDP-glucose:glycoprotein glucosyltransferase 1 |
| 52 | A | K1RKE5_CRAGI IQ and AAA domain-containing protein 1 |
| 53 | A | K1QKD6_CRAGI Uncharacterized protein |
| 54 | A | K1QN55_CRAGI 60S acidic ribosomal protein P1 |
| 55 | A | K1RGT9_CRAGI 60S ribosomal protein L13a |
| 56 | A | K1PZ23_CRAGI DnaJ-like protein subfamily C member 3 |
| 57 | A | K1PCC8_CRAGI Serine/threonine-protein kinase 25 |
| 58 | A | K1PKD4_CRAGI 40S ribosomal protein S30 |
| 59 | A | K1RXA0_CRAGI cAMP-dependent protein kinase regulatory subunit |
| 60 | A | K1QAL3_CRAGI RNA-binding protein 28 |
| | A | K1Q6J3_CRAGI Eukaryotic translation initiation factor 2-alpha kinase 4 |
| | A | K1S049_CRAGI Putative RNA-binding protein 16 |

| | | |
|----|---|--|
| 1 | | |
| 2 | | |
| 3 | A | K1RBT3_CRAGI ATP-dependent RNA helicase SUV3-like protein, mitochondrial |
| 4 | A | K1QFS8_CRAGI Importin-9 |
| 5 | A | K1QVF4_CRAGI Heterogeneous nuclear ribonucleoprotein L |
| 6 | A | K1PGD2_CRAGI Putative aminopeptidase NPEPL1 |
| 7 | A | K1QUT5_CRAGI Amine oxidase |
| 8 | A | K1QAG0_CRAGI Serine-threonine kinase receptor-associated protein |
| 9 | A | K1PHS4_CRAGI Ribosome-binding protein 1 |
| 10 | A | K1RMS0_CRAGI Translation initiation factor eIF-2B subunit beta |
| 11 | A | K1R604_CRAGI DCC-interacting protein 13-alpha |
| 12 | A | K1PQE3_CRAGI RNA-binding protein Raly |
| 13 | A | K1PQH6_CRAGI Cullin-4A |
| 14 | A | K1PM29_CRAGI Glucose-6-phosphate 1-dehydrogenase |
| 15 | A | K1QNK4_CRAGI 3-oxoacyl-[acyl-carrier-protein] reductase |
| 16 | A | K1PD41_CRAGI DNA primase |
| 17 | A | K1PTV5_CRAGI Programmed cell death protein 10 |
| 18 | A | K1PV35_CRAGI Kyphoscoliosis peptidase |
| 19 | A | K1Q4J3_CRAGI Nuclear cap-binding protein subunit 1 |
| 20 | A | K1RJV3_CRAGI TRS85-like protein |
| 21 | A | K1QM61_CRAGI Uncharacterized protein |
| 22 | A | K1PKI9_CRAGI Uncharacterized protein |
| 23 | A | K1QPB0_CRAGI U3 small nucleolar RNA-associated protein 6-like protein |
| 24 | A | K1PF70_CRAGI MON2-like protein (Fragment) |
| 25 | A | K1RFF7_CRAGI Protein lethal(2)essential for life |
| 26 | A | K1PG60_CRAGI 60S ribosomal protein L17 |
| 27 | A | K1Q189_CRAGI F-box/WD repeat-containing protein 9 |
| 28 | A | K1QBM3_CRAGI Ras-related protein Rab-2 |
| 29 | A | K1PNP9_CRAGI Bullous pemphigoid antigen 1, isoforms 1/2/3/4 |
| 30 | A | K1QIJ3_CRAGI Nuclear pore complex protein Nup85 |
| 31 | A | K1QX44_CRAGI Ras-related protein Rab-11B |
| 32 | A | K1QLD7_CRAGI Kinetochores protein NDC80-like protein |
| 33 | A | K1QUD7_CRAGI Conserved oligomeric Golgi complex subunit 3 (Fragment) |
| 34 | A | K1Q9Z5_CRAGI Peptidyl-prolyl cis-trans isomerase |
| 35 | A | K1RLT0_CRAGI D-erythrulose reductase |
| 36 | A | K1PG98_CRAGI rRNA-processing protein FCF1-like protein |
| 37 | A | K1QKQ8_CRAGI THO complex subunit 4-A |
| 38 | A | K1RB07_CRAGI 60S ribosomal protein L27a |
| 39 | A | K1PEZ6_CRAGI Kyphoscoliosis peptidase |
| 40 | A | D7EZH1_CRAGI Cystatin B-like protein |
| 41 | A | K1RJ53_CRAGI Tetratricopeptide repeat protein 12 |
| 42 | A | K1QQH9_CRAGI DNA (Cytosine-5)-methyltransferase 1 (Fragment) |
| 43 | A | K1PL63_CRAGI TBC1 domain family member 15 |
| 44 | A | K1PG17_CRAGI 60S ribosomal protein L21 |
| 45 | A | K1QQ99_CRAGI Uncharacterized protein |
| 46 | A | K1RG04_CRAGI ALK tyrosine kinase receptor |
| 47 | A | K1PZP3_CRAGI Conserved oligomeric Golgi complex subunit 2 |
| 48 | A | K1QH68_CRAGI Syntenin-1 |
| 49 | A | K1S4H5_CRAGI Adenosylhomocysteinase |
| 50 | A | K1R4L8_CRAGI Electron transfer flavoprotein-ubiquinone oxidoreductase, mitochondrial |
| 51 | A | K1RFD2_CRAGI Adenylate kinase |
| 52 | A | K1PB87_CRAGI Uncharacterized protein |
| 53 | A | K1PM74_CRAGI DNA mismatch repair protein Msh6 |
| 54 | A | K1RR99_CRAGI Rho guanine nucleotide exchange factor 12 |
| 55 | A | K1QGQ5_CRAGI Superoxide dismutase |
| 56 | A | K1PBB1_CRAGI Stress-induced-phosphoprotein 1 |
| 57 | A | K1Q681_CRAGI Clustered mitochondria protein homolog |
| 58 | A | K1PQR9_CRAGI Squamous cell carcinoma antigen recognized by T-cells 3 |
| 59 | A | K1QSV1_CRAGI Uncharacterized protein |
| 60 | A | K1QKY7_CRAGI Uncharacterized protein |
| | A | K1QBJ7_CRAGI Uncharacterized protein |
| | A | K1S5H7_CRAGI Cell division cycle 5-related protein |

| | | | |
|----|---|--------------|--|
| 1 | | | |
| 2 | | | |
| 3 | A | K1RHJ9_CRAGI | Suppressor of G2 allele of SKP1-like protein |
| 4 | A | K1R2Z2_CRAGI | Methyltransferase-like protein 13 |
| 5 | A | K1QHY6_CRAGI | Rap1 GTPase-GDP dissociation stimulator 1-A |
| 6 | A | K1Q1L1_CRAGI | Kinesin-associated protein 3 |
| 7 | A | K1R3Z4_CRAGI | 5'-3' exoribonuclease 1 |
| 8 | A | K1P951_CRAGI | Fanconi anemia group D2 protein |
| 9 | A | K1PKD7_CRAGI | 6-phosphogluconolactonase |
| 10 | A | K1QN54_CRAGI | Brain protein 16 |
| 11 | A | K1QYD0_CRAGI | UBX domain-containing protein 1 |
| 12 | A | K1QCY6_CRAGI | 40S ribosomal protein S28 |
| 13 | A | K1QZ29_CRAGI | Uncharacterized protein |
| 14 | A | K1R136_CRAGI | Phosphatidylinositol transfer protein alpha isoform |
| 15 | A | K1R969_CRAGI | Uncharacterized protein |
| 16 | A | K1R1E4_CRAGI | Serine/threonine-protein kinase Chk2 |
| 17 | A | K1QVL1_CRAGI | Serine/threonine-protein phosphatase 4 regulatory subunit 4 |
| 18 | A | K1QYD8_CRAGI | Trans-1,2-dihydrobenzene-1,2-diol dehydrogenase |
| 19 | A | K1Q927_CRAGI | Neurofibromin |
| 20 | A | K1QAU3_CRAGI | WD repeat-containing protein 63 |
| 21 | A | K1Q8P7_CRAGI | Aspartyl aminopeptidase |
| 22 | A | K1QZ64_CRAGI | Nuclear pore complex protein Nup98-Nup96 |
| 23 | A | K1PLR8_CRAGI | Chromosome transmission fidelity protein 18-like protein (Fragment) |
| 24 | A | K1P752_CRAGI | UPF0195 protein FAM96B |
| 25 | A | K1QAY3_CRAGI | Dipeptidyl-peptidase 1 (Fragment) |
| 26 | A | K1R669_CRAGI | Uncharacterized protein |
| 27 | A | K1PWS8_CRAGI | Mitotic spindle assembly checkpoint protein MAD2A |
| 28 | A | K1PK87_CRAGI | Putative E3 ubiquitin-protein ligase TRIP12 |
| 29 | A | K1QKU6_CRAGI | mRNA export factor |
| 30 | A | K1QQV0_CRAGI | Histone H1.2 |
| 31 | A | K1QR54_CRAGI | Zinc finger RNA-binding protein |
| 32 | A | K1PE13_CRAGI | Uncharacterized protein |
| 33 | A | K1QUW5_CRAGI | U2 snRNP auxiliary factor large subunit |
| 34 | A | K1PTH4_CRAGI | ADP-ribosylation factor |
| 35 | A | K1Q3C3_CRAGI | Lambda-crystallin-like protein |
| 36 | A | K1RE82_CRAGI | Uncharacterized protein |
| 37 | A | K1P486_CRAGI | Heat shock 70 kDa protein 12A |
| 38 | A | K1R7A4_CRAGI | Peptidylprolyl isomerase |
| 39 | A | K1PEC8_CRAGI | Actin-related protein 8 |
| 40 | A | K1RAR8_CRAGI | Protein FAM49B |
| 41 | A | K1QZD2_CRAGI | Tudor domain-containing protein 7 |
| 42 | A | K1QM54_CRAGI | Activator of 90 kDa heat shock protein ATPase-like protein 1 |
| 43 | A | K1Q904_CRAGI | PAN2-PAN3 deadenylation complex subunit PAN3 |
| 44 | A | K1P6N8_CRAGI | Ubiquitin carboxyl-terminal hydrolase 7 |
| 45 | A | K1RBM7_CRAGI | Ubiquitin-conjugating enzyme E2 variant 1 |
| 46 | A | K1PV92_CRAGI | Hsp90 co-chaperone Cdc37 |
| 47 | A | K1PQU8_CRAGI | Sperm-associated antigen 6 |
| 48 | A | K1QUK4_CRAGI | Protein SET |
| 49 | A | K1QJ85_CRAGI | Glutathione S-transferase A |
| 50 | A | K1QJW3_CRAGI | Heat shock 70 kDa protein 12B |
| 51 | A | K1QNW5_CRAGI | MAK10-like protein |
| 52 | A | K1QZ84_CRAGI | Thioredoxin domain-containing protein 3-like protein |
| 53 | A | K1QXH7_CRAGI | DNA replication licensing factor mcm4-B |
| 54 | A | K1Q1L9_CRAGI | Interferon-induced protein 44-like protein |
| 55 | A | K1RGD5_CRAGI | F-box only protein 36 |
| 56 | A | K1Q3B4_CRAGI | DNA topoisomerase |
| 57 | A | K1P8Z1_CRAGI | Uncharacterized protein |
| 58 | A | K1PYA2_CRAGI | Host cell factor |
| 59 | A | K1PZR3_CRAGI | U2 small nuclear ribonucleoprotein A |
| 60 | A | K1QB69_CRAGI | Uncharacterized protein |
| | A | K1PI78_CRAGI | Golgi-specific brefeldin A-resistance guanine nucleotide exchange factor 1 |
| | A | K1RKK2_CRAGI | Phosphatidylinositol-4-phosphate 5-kinase type-1 alpha |

| | | | |
|----|---|--------------|--|
| 1 | | | |
| 2 | | | |
| 3 | A | K1QLS5_CRAGI | Uncharacterized protein |
| 4 | A | K1QFI3_CRAGI | Apoptosis-inducing factor 3 |
| 5 | A | K1QKB1_CRAGI | Tryptophanyl-tRNA synthetase, cytoplasmic |
| 6 | A | K1REU2_CRAGI | WD repeat and HMG-box DNA-binding protein 1 |
| 7 | A | K1QUK3_CRAGI | Putative ATP-dependent RNA helicase DDX41 |
| 8 | A | K1QBT8_CRAGI | Uncharacterized protein |
| 9 | A | K1QBT8_CRAGI | Uncharacterized protein |
| 10 | A | K1QVX4_CRAGI | Glycogen synthase kinase-3 beta |
| 11 | A | K1PF20_CRAGI | Gamma-tubulin complex component |
| 12 | A | K1RFG1_CRAGI | Lipoxygenase-like protein domain-containing protein 1 |
| 13 | A | K1PCI8_CRAGI | Cullin-2 |
| 14 | A | K1PC18_CRAGI | Cullin-2 |
| 15 | A | K1QS27_CRAGI | UBX domain-containing protein 6 |
| 16 | A | K1RFF1_CRAGI | Uncharacterized protein |
| 17 | A | K1Q4N9_CRAGI | Uncharacterized protein |
| 18 | A | K1QJN8_CRAGI | AP-3 complex subunit beta |
| 19 | A | K1PXA0_CRAGI | Uncharacterized protein |
| 20 | A | K1PXA0_CRAGI | Uncharacterized protein |
| 21 | A | K1QA13_CRAGI | Calcium-transporting ATPase |
| 22 | A | K1QXY4_CRAGI | Kinase |
| 23 | A | K1PBW4_CRAGI | Uncharacterized protein |
| 24 | A | K1PUF0_CRAGI | G-protein coupled receptor moody |
| 25 | A | K1QMY9_CRAGI | Uncharacterized protein |
| 26 | A | K1QMY9_CRAGI | Uncharacterized protein |
| 27 | A | K1QZ54_CRAGI | Coiled-coil domain-containing protein 39 |
| 28 | A | K1QWU8_CRAGI | Uncharacterized protein |
| 29 | A | K1Q3L1_CRAGI | Kielin/chordin-like protein |
| 30 | A | K1PGR2_CRAGI | G patch domain-containing protein 1 |
| 31 | A | K1PGR2_CRAGI | G patch domain-containing protein 1 |
| 32 | A | K1RXP9_CRAGI | Ventricular zone-expressed PH domain-containing-like protein 1 |
| 33 | A | K1PIB2_CRAGI | Uncharacterized protein |
| 34 | A | K1R4U3_CRAGI | Uncharacterized protein |
| 35 | | | |
| 36 | | | |
| 37 | | | |
| 38 | | | |
| 39 | | | |
| 40 | | | |
| 41 | | | |
| 42 | | | |
| 43 | | | |
| 44 | | | |
| 45 | | | |
| 46 | | | |
| 47 | | | |
| 48 | | | |
| 49 | | | |
| 50 | | | |
| 51 | | | |
| 52 | | | |
| 53 | | | |
| 54 | | | |
| 55 | | | |
| 56 | | | |
| 57 | | | |
| 58 | | | |
| 59 | | | |
| 60 | | | |

Data S3: Complete list of GO terms of clustered genes of m6A interacting proteins (p-value<0,05)

| | Cluster | term_ID | description | log10 p-value | Class |
|----|----------------|----------------|---|----------------------|--------------------|
| 6 | cluster1 | GO:0006172 | ADP biosynthetic process | -2,848 | Biological process |
| 7 | cluster1 | GO:0006886 | intracellular protein transport | -6,1176 | Biological process |
| 8 | cluster1 | GO:0015031 | protein transport | -1,6944 | Biological process |
| 9 | cluster1 | GO:0006511 | ubiquitin-dependent protein catabolic process | -1,8071 | Biological process |
| 10 | cluster1 | GO:0030833 | regulation of actin filament polymerization | -2,5256 | Biological process |
| 11 | cluster1 | GO:0006563 | L-serine metabolic process | -2,3716 | Biological process |
| 12 | cluster1 | GO:0006544 | glycine metabolic process | -2,0706 | Biological process |
| 13 | cluster1 | GO:0016192 | vesicle-mediated transport | -3,119 | Biological process |
| 14 | cluster1 | GO:0006429 | leucyl-tRNA aminoacylation | -2,1763 | Biological process |
| 15 | cluster1 | GO:0006413 | translational initiation | -1,3708 | Biological process |
| 16 | cluster1 | GO:0006122 | mitochondrial electron transport, ubiquinol to cytochrome c | -1,9328 | Biological process |
| 17 | cluster1 | GO:0048280 | vesicle fusion with Golgi apparatus | -2,3699 | Biological process |
| 18 | cluster1 | GO:0006888 | ER to Golgi vesicle-mediated transport | -1,4737 | Biological process |
| 19 | cluster1 | GO:0030117 | membrane coat | -3,0546 | Cellular component |
| 20 | cluster1 | GO:0030127 | COPII vesicle coat | -1,6994 | Cellular component |
| 21 | cluster1 | GO:0030131 | clathrin adaptor complex | -1,5595 | Cellular component |
| 22 | cluster1 | GO:0005737 | cytoplasm | -2,3551 | Cellular component |
| 23 | cluster1 | GO:0031105 | septin complex | -2,0349 | Cellular component |
| 24 | cluster1 | GO:0005850 | eukaryotic translation initiation factor 2 complex | -2,6924 | Cellular component |
| 25 | cluster1 | GO:0005856 | cytoskeleton | -1,6967 | Cellular component |
| 26 | cluster1 | GO:0005750 | mitochondrial respiratory chain complex III | -1,9328 | Cellular component |
| 27 | cluster1 | GO:0000139 | Golgi membrane | -1,4267 | Cellular component |
| 28 | cluster1 | GO:0003743 | translation initiation factor activity | -2,6564 | Molecular function |
| 29 | cluster1 | GO:0004372 | glycine hydroxymethyltransferase activity | -2,3716 | Molecular function |
| 30 | cluster1 | GO:0005488 | binding | -1,66 | Molecular function |
| 31 | cluster1 | GO:0008565 | protein transporter activity | -2,7964 | Molecular function |
| 32 | cluster1 | GO:0004823 | leucine-tRNA ligase activity | -2,1763 | Molecular function |
| 33 | cluster1 | GO:0008242 | omega peptidase activity | -2,0158 | Molecular function |
| 34 | cluster1 | GO:0008536 | Ran GTPase binding | -1,4396 | Molecular function |
| 35 | cluster1 | GO:0005525 | GTP binding | -1,9855 | Molecular function |
| 36 | cluster1 | GO:0016813 | hydrolase activity, acting on carbon-nitrogen (but not peptide) bonds, in linear amidines | -1,9675 | Molecular function |
| 37 | cluster1 | GO:0002161 | aminoacyl-tRNA editing activity | -1,4387 | Molecular function |
| 38 | cluster1 | GO:0016776 | phosphotransferase activity, phosphate group as acceptor | -2,0567 | Molecular function |
| 39 | cluster1 | GO:0005543 | phospholipid binding | -1,3689 | Molecular function |
| 40 | cluster1 | GO:0004017 | adenylate kinase activity | -2,2504 | Molecular function |
| 41 | cluster1 | GO:0019205 | nucleobase-containing compound kinase activity | -1,9387 | Molecular function |
| 42 | cluster1 | GO:0019904 | protein domain specific binding | -1,4245 | Molecular function |
| 43 | cluster1 | GO:0004843 | thiol-dependent ubiquitin-specific protease activity | -1,6596 | Molecular function |
| 44 | cluster1 | GO:0003779 | actin binding | -1,33 | Molecular function |
| 45 | cluster 2 | GO:0006376 | mRNA splice site selection | -2,2802 | Biological process |
| 46 | cluster 2 | GO:0016192 | vesicle-mediated transport | -1,9467 | Biological process |
| 47 | cluster 2 | GO:0006511 | ubiquitin-dependent protein catabolic process | -1,895 | Biological process |
| 48 | cluster 2 | GO:0051603 | proteolysis involved in cellular protein catabolic process | -1,4434 | Biological process |
| 49 | cluster 2 | GO:0006281 | DNA repair | -1,946 | Biological process |
| 50 | cluster 2 | GO:0006164 | purine nucleotide biosynthetic process | -1,9132 | Biological process |
| 51 | cluster 2 | GO:0006606 | protein import into nucleus | -1,6687 | Biological process |
| 52 | cluster 2 | GO:0006367 | transcription initiation from RNA polymerase II promoter | -1,8729 | Biological process |
| 53 | cluster 2 | GO:0045893 | positive regulation of transcription, DNA-templated | -1,8902 | Biological process |
| 54 | cluster 2 | GO:0051276 | chromosome organization | -1,9322 | Biological process |
| 55 | cluster 2 | GO:0005685 | U1 snRNP | -2,0889 | Cellular component |
| 56 | cluster 2 | GO:0005694 | chromosome | -1,6569 | Cellular component |
| 57 | cluster 2 | GO:0019773 | proteasome core complex, alpha-subunit complex | -1,7608 | Cellular component |
| 58 | cluster 2 | GO:0005839 | proteasome core complex | -1,4434 | Cellular component |
| 59 | cluster 2 | GO:0005643 | nuclear pore | -1,5471 | Cellular component |
| 60 | cluster 2 | GO:0003938 | IMP dehydrogenase activity | -2,5964 | Molecular function |
| | cluster 2 | GO:0005488 | binding | -5,6024 | Molecular function |
| | cluster 2 | GO:0008536 | Ran GTPase binding | -3,3815 | Molecular function |
| | cluster 2 | GO:0008565 | protein transporter activity | -1,3099 | Molecular function |
| | cluster 2 | GO:0017056 | structural constituent of nuclear pore | -2,5981 | Molecular function |
| | cluster 2 | GO:0016844 | strictosidine synthase activity | -2,4472 | Molecular function |
| | cluster 2 | GO:0042578 | phosphoric ester hydrolase activity | -2,0068 | Molecular function |
| | cluster 2 | GO:0008641 | small protein activating enzyme activity | -1,8257 | Molecular function |
| | cluster 2 | GO:0003729 | mRNA binding | -1,9507 | Molecular function |
| | cluster 2 | GO:0000166 | nucleotide binding | -1,9175 | Molecular function |
| | cluster 2 | GO:0030554 | adenyl nucleotide binding | -1,4276 | Molecular function |
| | cluster 2 | GO:0004175 | endopeptidase activity | -1,4434 | Molecular function |
| | cluster 2 | GO:0004298 | threonine-type endopeptidase activity | -1,4434 | Molecular function |
| | cluster 3 | GO:0006184 | (obsolete) GTP catabolic process | -1,3497 | Biological process |
| | cluster 3 | GO:0007156 | homophilic cell adhesion via plasma membrane adhesion molecules | -1,6645 | Biological process |
| | cluster 3 | GO:0008152 | metabolic process | -1,9382 | Biological process |

| | | | | | |
|----|-----------|------------|---|---------|--------------------|
| 1 | | | | | |
| 2 | | | | | |
| 3 | | | | | |
| 4 | cluster 3 | GO:0015986 | ATP synthesis coupled proton transport | -4,8627 | Biological process |
| 5 | cluster 3 | GO:0006096 | glycolytic process | -1,4156 | Biological process |
| 6 | cluster 3 | GO:0051258 | protein polymerization | -2,6757 | Biological process |
| 7 | cluster 3 | GO:0044262 | cellular carbohydrate metabolic process | -2,0966 | Biological process |
| 8 | cluster 3 | GO:0006388 | tRNA splicing, via endonucleolytic cleavage and ligation | -1,523 | Biological process |
| 9 | cluster 3 | GO:0006879 | cellular iron ion homeostasis | -1,4857 | Biological process |
| 10 | cluster 3 | GO:0007017 | microtubule-based process | -2,4915 | Biological process |
| 11 | cluster 3 | GO:0006412 | translation | -2,0331 | Biological process |
| 12 | cluster 3 | GO:0006122 | mitochondrial electron transport, ubiquinol to cytochrome c | -2,0662 | Biological process |
| 13 | cluster 3 | GO:0000276 | mitochondrial proton-transporting ATP synthase complex, coupling factor F(o) | -4,1068 | Cellular component |
| 14 | cluster 3 | GO:0005750 | mitochondrial respiratory chain complex III | -2,0662 | Cellular component |
| 15 | cluster 3 | GO:0045261 | proton-transporting ATP synthase complex, catalytic core F(1) | -2,0025 | Cellular component |
| 16 | cluster 3 | GO:0005874 | microtubule | -2,2282 | Cellular component |
| 17 | cluster 3 | GO:0005882 | intermediate filament | -1,9067 | Cellular component |
| 18 | cluster 3 | GO:0043231 | intracellular membrane-bounded organelle | -2,1492 | Cellular component |
| 19 | cluster 3 | GO:0005852 | eukaryotic translation initiation factor 3 complex | -1,6821 | Cellular component |
| 20 | cluster 3 | GO:0005737 | cytoplasm | -1,9776 | Cellular component |
| 21 | cluster 3 | GO:0005840 | ribosome | -2,0503 | Cellular component |
| 22 | cluster 3 | GO:0043234 | protein complex | -2,6757 | Cellular component |
| 23 | cluster 3 | GO:0004739 | pyruvate dehydrogenase (acetyl-transferring) activity | -2,8179 | Molecular function |
| 24 | cluster 3 | GO:0016624 | oxidoreductase activity, acting on the aldehyde or oxo group of donors, disulfide as acceptor | -2,0554 | Molecular function |
| 25 | cluster 3 | GO:0005200 | structural constituent of cytoskeleton | -2,3865 | Molecular function |
| 26 | cluster 3 | GO:0005525 | GTP binding | -1,9304 | Molecular function |
| 27 | cluster 3 | GO:0015078 | hydrogen ion transmembrane transporter activity | -3,0193 | Molecular function |
| 28 | cluster 3 | GO:0046961 | proton-transporting ATPase activity, rotational mechanism | -1,6263 | Molecular function |
| 29 | cluster 3 | GO:0046933 | proton-transporting ATP synthase activity, rotational mechanism | -1,7326 | Molecular function |
| 30 | cluster 3 | GO:0004775 | succinate-CoA ligase (ADP-forming) activity | -2,3995 | Molecular function |
| 31 | cluster 3 | GO:0046912 | transferase activity, transferring acyl groups, acyl groups converted into alkyl on transfer | -2,3982 | Molecular function |
| 32 | cluster 3 | GO:0016874 | ligase activity | -1,4798 | Molecular function |
| 33 | cluster 3 | GO:0048037 | cofactor binding | -1,6628 | Molecular function |
| 34 | cluster 3 | GO:0008199 | ferric iron binding | -1,4607 | Molecular function |
| 35 | cluster 3 | GO:0005544 | calcium-dependent phospholipid binding | -1,6049 | Molecular function |
| 36 | cluster 3 | GO:0003878 | ATP citrate synthase activity | -2,3995 | Molecular function |
| 37 | cluster 3 | GO:0003735 | structural constituent of ribosome | -1,9881 | Molecular function |
| 38 | | | | | |
| 39 | | | | | |
| 40 | | | | | |
| 41 | | | | | |
| 42 | | | | | |
| 43 | | | | | |
| 44 | | | | | |
| 45 | | | | | |
| 46 | | | | | |
| 47 | | | | | |
| 48 | | | | | |
| 49 | | | | | |
| 50 | | | | | |
| 51 | | | | | |
| 52 | | | | | |
| 53 | | | | | |
| 54 | | | | | |
| 55 | | | | | |
| 56 | | | | | |
| 57 | | | | | |
| 58 | | | | | |
| 59 | | | | | |
| 60 | | | | | |

Table S1: Transitions used for each compound. A: first transition, B: second transition

| Nucleoside | Retention time (min) | MRM precursor (m/z) | MRM product (m/z) | | Collision Energy (V) | |
|-----------------------|----------------------|---------------------|-------------------|-------|----------------------|-----|
| | | | A | B | A | B |
| A | 3.07 | 268.0 | 135.9 | 119.0 | -30 | -12 |
| m⁶A | 2.12 | 282.0 | 150.1 | 123.1 | -17 | -46 |

For Review Only

1
2
3
4
5
6
7
8
9
10
11
12
13
14
15
16
17
18
19
20
21
22
23
24
25
26
27
28
29
30
31
32
33
34
35
36
37
38
39
40
41
42
43
44
45
46
47
48
49
50
51
52
53
54
55
56
57
58
59
60

Table S2: Correspondence between development stages in our study, and the GigaTON database.

| Development stages : This Study | Development stages : GigaTON [53] |
|--|--|
| Oocytes | E (Eggs) |
| 2/8 Cells | TC (Two Cell embryos) |
| | FC (Four Cell embryos) |
| | EM (Early Morula) |
| Morula | M (Morula) |
| Blastula | B (Blastula) |
| | RM (Rotary Movement) |
| | FS (Free Swimming) |
| Gastrula | EG (Early Gastrula) |
| | G (Gastrula) |
| | T (Trochophore) 1 |
| | T2 |
| Trochophore | T3 |
| | T4 |
| | T5 |
| | ED (Early D larvae) 1 |
| | ED2 |
| D larvae | D (D larvae)1 |
| | D2 |
| | D3 |
| | D4 |
| | D5 |
| Spat | S (Spat) |
| Juvenile | J (Juvenile) |